PhD Thesis UTh/MIE No. 23

Development and Application of a Computer Aided Engineering Methodology Supporting the Design Optimization of Automotive Exhaust Treatment Systems

THESIS

submitted in partial fulfillment of the requirements

for the degree of

Doctor of Philosophy in Mechanical Engineering

of the

Department of Mechanical and Industrial Engineering

University of Thessaly

BY

GEORGIOS S. KONSTANTAS

Dipl. Mechanical Engineer,
University of Thessaly

Born on 29th May 1977

in Athens

Advisory Committee:

Prof. A. M. Stamatelos, supervisor
Assoc. Prof. H. Stapountzis
Prof. N. S. Vlachos

Volos, June 2006

U N I V E R S I T Y O F T H E S S A L Y
DEPARTMENT OF MECHANICAL AND INDUSTRIAL ENGINEERING

Development and Application of a Computer Aided Engineering Methodology Supporting the Design Optimization of Automotive Exhaust Treatment Systems

By G E O R G I O S S . K O N S T A N T A S

A thesis presented on the field of automotive catalysis, covering the current and near future exhaust aftertreatment systems for automobiles and presenting a systematic approach towards the optimum design and accurate engineering modelling of such systems.

Approved by:

Professor	Anastassios Stamatelos MIE/UTh	Supervisor
Associate Professor	HerricosStapountzis MIE/UTh	Advisor Commitee
Professor	Nikolaos Vlachos MIE/UTh	Advisor Commitee
Professor	Vasileios Bontozoglou MIE/UTh	Indermediate examination Commitee
Assistant Professor	Nikolaos Pelekasis MIE/UTh	Indermediate examination Commitee
Professor	Costas Papadimitriou MIE/UTh	Final examination Commitee
Assistant Professor	Anastassios Stamatis MIE/UTh	Final examination Commitee

PREFACE

Motivated by increasing stringent legislation, automotive industry has lowered tailpipe pollutant emissions down to the order of centigrams per kilometer, mainly as a result of higher than 95% average efficiency of exhaust treatment devices. Such levels of efficiency are not yet sufficient, however. Although great improvements have been made in catalytic converter technology, engine design and control systems, there still remains a lot to be done in several fields of automotive exhaust aftertreatment, in order to further reduce the emitted pollutants, especially in urban areas.

Since the core of almost every automotive exhaust aftertreatment system is some kind of catalytic converter, intensive research activity is devoted to the various scientific and technical aspects of catalytic technology. These aspects vary from practical research on new materials and novel techniques to improve catalyst microstructure, to theoretical contributions of detailed descriptions of chemical phenomena inside the converters and proposals of mechanistic reaction schemes.

Nevertheless, the extremely high efficiencies that are expected from any modern catalyst cannot be attained without simultaneously optimizing aftertreatment device performance, engine design and the control system that drives the whole system. Thus, from a mechanical engineer's point of view, the exhaust treatment complexity is expressed as a strong interaction between these three fields: powertrain operation, engine management characteristics and exhaust treatment device operation.

In general, the composition of exhaust gas depends on the engine type, the operating point of the engine, the ambient temperature, the transmission system and miscellaneous characteristics of each system. Thus, the engine management holds a key role in the behavior of the catalytic converter, since it affects both its input as well as the temperature range under which it operates. Moreover, exhaust line design, involving exhaust manifold heat capacity, insulated pipes and positioning of the devices, is strongly connected with the catalytic converter operation. Furthermore, catalysts with the same chemical composition may behave quite differently, depending on the actual procedures that were employed during catalyst preparation.

The complexity of the automotive exhaust treatment systems quickly became apparent in the industry. Mathematical modeling tools are continuously developed, in order to complement the experimental efforts and provide guidance for areas that needed improvement. In the last 30 years, many models have appeared in the literature [2]. Their approaches and their scope were diverse, but in general they were rather focused on the individual devices than on the whole aftertreatment system.

Specifically for the catalytic converter modeling: most kinetic studies so far resulted in models that are valid for the specific combination of engine and catalyst status at that moment (usually fresh catalysts). Although valuable for a specific engineering problem, such modeling results could only partially be extended in different systems, and only with great caution. Indeed, successful extension of the results of a specific case to another one is rare in the literature [1]. As a characteristic example, consider that testing the same catalyst after some period of operation, e.g. a few months later, can yield quite different results [2].

As a response to this shortcoming, several different attempts have been made to tackle the exhaust treatment design problem in its more general form. The recent PhD thesis of Pontikakis [3] presented a group of semi-empirical models and CAE tools for supporting the design of engine exhaust lines. A schematic of the principles of interaction of each model or activity is depicted in the diagram of Figure 1

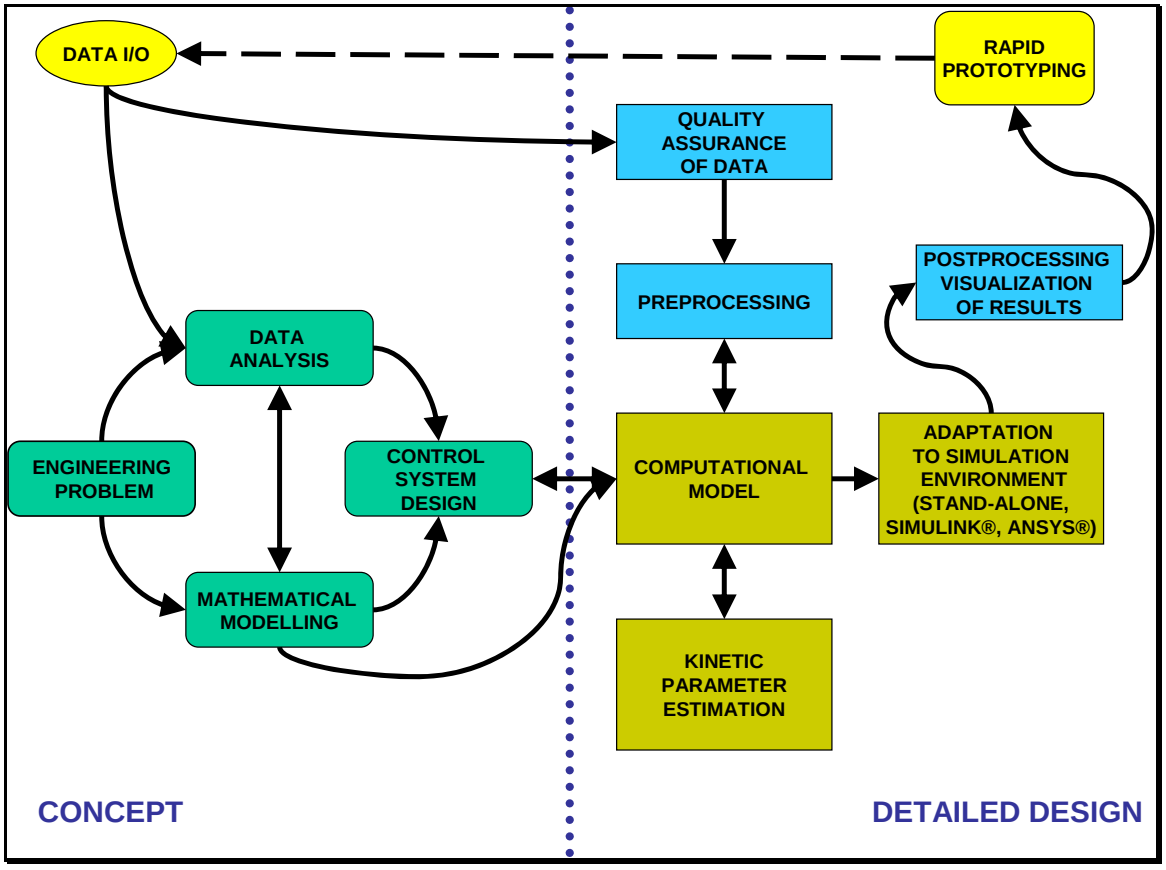

Figure 1 An emerging paradigm for exhaust aftertreatment systems engineering modeling (adapted from [3])

Pontikakis [3] had studied the concepts of mathematical modeling of the catalytic converter and further developed the computational codes required in the fields of

computational modeling, automated kinetic parameter estimation and adaptation to simulation environment of commercial software packages (denoted with dark yellow color Figure 1). However, a number of questions remained to be answered:

- Why the model, in some cases, fails to match the experimental data? Can this be attributed to the quality of experimental data or to the weakness of the model?
- Which principal directions have to be considered for the reaction scheme and the kinetic parameters with washcoat formulation changes?
- How can the individual core models assist the design optimization of the system engine-control-device?

Answering to these questions was the motivation to develop a workable approach to the study of the overall system based on three groups of Figure 1. Formulation and engineering analysis of the problem (green color group) and inlet/outlet data processing (blue color group) are the main fields of study in this thesis. To a lesser extent, the study and the further improvement of the computational cores (dark yellow group) was necessary to support the structure of the thesis. Consequently, current work is a synthesis of the following fields of study:

- Real engine test data analysis, which focuses to the issues affecting the operation of the exhaust aftertreatment devices, mainly directed by the specific engineering problem.
- Study of the control system design concepts and investigation of advanced engine control strategies.
- Automation of the preprocess and development of a quality assurance methodology for input data, in order to identify and correct possible perturbations that stem from the experimental procedure
- Improvements in postprocessing and visualization of modeling results in the direction of rapid prototyping assistance
- Minor improvements of computational cores, which subsequently improved the modeling of the exhaust gas aftertreatment devices

Initially, a review of the literature of catalytic converters in their thirty years of evolution was essential to understand the phenomena involved and the interactions of the numerous variables affecting the operation of the converter. The literature study focused on the following aspects of the catalytic converter's business:

(a) recent progress on washcoat technology and the interactions between washcoat components,

(b) several kinetic considerations and fundamental chemical studies, and mostly

(c) engineering design of commercial catalysts with simple, approximate rules and apparent reaction rates for the description of the catalyst chemistry.

An automated and standardized treatment of experimental datasets was necessary in order to improve both models and comprehension of the phenomena in the entire system. The first step to this direction was the creation of a standardized spreadsheet format that enabled better communication between the members of the laboratory. As will be shown in this thesis, the need for faster, error-free and easy processing of the experimental datasets has lead to the creation of a large set of macros and MS-EXCEL spreadsheets, which analyze raw experimental data, create input files for the computational models, and compare the modeling results with experimental data. The choice to implement the above tools in the environment of MS-EXCEL instead of developing some stand-alone software, was made on the grounds that these were just support tool for the main purposes of this thesis.

The successful implementation of automated processes for data treatment offered the motivation to develop a quality assurance methodology for experimental data of internal combustion engines, in order to support the optimum design of the exhaust line [5]. Although quality assurance has been extensively applied in chemical engineering and biological studies, its important impact to the study of exhaust aftertreatment devices, considering the increased number of interacting variables affecting their operation, is supported herein.

As a next step, the study of the interactions of the global system was needed for a detailed analysis of the engine operation. For these purposes, experimental data has been analysed during the individual modes of engine operation. The requirement for direct comparison of different engines, tested under different conditions, addressed the use and extension of several ideas found in the literature.

Several improvements have been made in the direction of computational modeling. The starting point of this thesis was the version of the catalytic converter model presented by Pontikakis [3]. Improvements towards the better visualization of the modeling results enabled us to concentrate on the poorly performed modes of catalytic converter model. Through a systematic study of the literature the dominant phenomena were identified while superfluous degrees of freedom of the model were eliminated. Thus, further development of the model was better focused and the model was more accurately tuned. The most important result of this approach was the dramatic decrease of the number of the tunable parameters of the model, with simultaneous small improvements of the quality of

the results. This approach also enabled the easy application of the model to several different design studies with success.

In addition to the main improvements at the core model, peripheral changes enabled its adaptation to a general-purpose optimization algorithm (GenOpt ®), developed by the Laurence Berkeley National Laboratory of U.S.A [4]. The choice to use this general-purpose optimization algorithm (as an alternative to the in-house optimization algorithm of Pontikakis) has shown the great challenges in the use of advanced engineering tools in complex real world applications. Although the optimization time was initially increased, the systematic reduction of the model's tunable parameters in conjunction with the improvements made in the core model and the more rationalized use of these engineering tools, enabled the reduction of the optimization time needed, up to two orders of magnitude.

Further, the updated version of the CATRAN model that is presented in this study, in combination with the Genopt ® and other widespread commercial software (MS-EXCEL, MATLAB/SIMULINK, LabView) enabled the engineering study and simultaneous optimization of complex exhaust systems equipped with more than one aftertreatment devices. We believe that this approach can be easily extended to the optimization of engineering systems including engine characteristics, optimum control and aftertreatment devices design.

Improvements in both the computational modeling and the kinetic parameter estimation procedure have also enabled the extraction of approximate trends regarding the effect of the catalytic converter's design parameters [5]. The results of such studies are expected to aim towards the fundamental understanding of the catalytic converter operation by focusing on the dominant phenomena that take place therein. It is shown that a simplified but well-targeted modeling approach is sufficient to model complex physicochemical phenomena within good accuracy and assist fundamental studies by suggesting promising directions for further research.

For the study of the control system design the models were adapted to Matlab/Simulink environment, which is a widely accepted standard in the automotive and aerospace industry as a powerful tool for signal management and complex systems' simulation. The use of built-in modules of this commercial software enables advanced computational study of the transient behavior of the device under the influence of various realistic, on-line perturbations or bifurcation of models' input data.

The laboratory facilities of LTTE enable the experimental validation of such a methodology, which was also extended in other exhaust aftertreatment devices, such as the Diesel Particulate Filter (DPF), which targets diesel-fueled vehicles to control their particulate emissions. Using the experimental observations of the recent PhD thesis of Stratakis [6], a control-oriented model was built in Matlab/Simulink environment for the study of the regeneration of the DPF using fuel post-injection [7]. A respective supervisor model is being developed for the NO_x trap adsorber that uses a concept of engine control-assisted regeneration through fuel enrichments.

Extensive validation of the above family of models in numerous real world application case studies enabled an increased insight and assessment of a number of important patents in automotive exhaust aftertreatment.

Overview of the Thesis

In what follows, a short review of legislation and recent advances in engine and catalytic converter technology are presented in chapter one, aiming at the better comprehension of the objective of this thesis and the effort exerted at all fields of vehicle engineering. In addition, a literature review in the field of automotive catalytic converter modeling and experimental study is presented, which reflects the various fields of research, directions followed and modeling approaches of several research groups.

Chapter two presents the catalytic converter simulation model. This chapter is primarily focused on (a) the improvements that were made in the core and the shell of the source code and (b) the systematic approach towards the minimization of the model's unnecessary degrees of freedom, which is reflected on the elimination of redundant tunable parameters. The principles of the optimization algorithm that was used are also presented in this chapter, as well as a higher programming level, which targets to the development of user friendly GUIs and the improvement of the models usability, which is necessary for the transformation of this kind of mathematical models into robust CAE tools.

Chapter three presents the quality assurance methodology of experimental data that was developed in the frame of this thesis. Quality assurance procedures were first applied to the catalytic converter inlet test data, which are prerequisite as input for the model. Application of this kind of procedures has revealed erroneous experimental data that could practically ruin the modeling effort. The development of the quality assurance methodology necessitated the creation of several data cross-checking tools, which are presented in

chapter 3. Finally, the quality assurance methodology was extended to the test data at converter's exit and also the model's output data.

Chapter four presents the study of engine management characteristics as they are revealed from the study of legislated test data. In this chapter the engine management of five vehicles, equipped with exhaust aftertreatment systems of varying type, size and position at the exhaust line, is studied through modal analysis. The role of optimized engine tuning to the performance of the exhaust system is demonstrated. The results of this study assisted the choice of a proper reaction scheme (consisting of the dominant reactions per case) for use in the model.

Chapters five, six, seven and eight present a matrix of catalytic converter case studies modeled with the updated version of CATRAN model. They form an extensive database both for the model validation and the analysis of the different exhaust aftertreament systems. The role of mathematical modeling as an indispensable tool for the exhaust treatment system design becomes apparent through the extraction of simplified rules regarding important design parameters.

Chapter nine is a review of the methodology developed in this thesis and an extended discussion on the advantages, the disadvantages and the limits of the current modeling approach. The cases that were successfully modeled and those that were not, are equally weighted in this discussion, in order to have an overview of the current status. Also, perspectives and future paths for research and development are briefly discussed.

Finally, several Graphical User Interfaces that were developed during this thesis are presented and a few cases for CAE design of complex exhaust aftertreatment systems are referenced.

TABLE OF CONTENTS

LIST OF FIGURES

LIST OF TABLES

Acknowledgements

Although several people supported me in a variety of ways in the course of my PhD studies, I would like to express my special thanks to the following:

My advisor Dr. Tassos Stamatelos for his support in every aspect of this work and beyond. Always considered as one of the most important persons I have met in my lifetime, he inspired me and affected in many ways my thought and daily action.

The other members of my supervising committee: Dr. E. Stapountzis for helpful discussions and cooperation in the frame and beyond the subject of this Thesis, and Dr. N. Vlachos for his help and motivation, starting from my undergraduate studies.

The other members of my examination committee, Dr. Vassilios Bontozoglou, Dr. N. Pelekasis, Dr. Tassos Stamatis and Dr. Costas Papadimitriou, for helpful suggestions for improvements in this Thesis.

Dr. George Pontikakis, for the long hours he devoted to teach me the secrets of CATRAN code, and his close cooperation during the last four hears. This Thesis could be considered, in many aspects, as a continuation of his own Thesis.

Mr. Herve Colas of PSA for his very interesting experimental input, information, discussions and overall research collaboration.

Mr. Sungtae Hong, IBIDEN Co. Ltd. for helpful cooperation with respect to Diesel exhaust aftertreatment systems.

Dr. Martin Votsmeier, of OMG, for the supply of interesting case studies, useful discussions and suggestions regarding NOx storage catalyst modeling. Mr. Dietmar Ernst of OMG for interesting feedback on NOx trap modeling.

Dr. Marcus Frey and Dr. Guenter Wenninger, of DaimlerChrysler, Stuttgart, for useful discussions regarding kinetic modeling of DPF and NOx traps. Dr. Yoshihide Watanabe, Toyota Central R&D Labs, for useful discussions.

Dr. Michael Wetter/ Lawrence Berkeley Laboratory for the GenOpt®

My senior colleague in LTTE, Dr. George Stratakis (currently in SIELMAN S.A.)

Dr. Grigorios Koltsakis, assist. Professor, LAT/ Aristotle University Thessaloniki.

Dr. Panagiotis Konstantinidis, of MELONWEB/ Knowledge Solutions.

My other colleagues in the University of Thessaly, Olympia Zogou, Dimitris Felekis, Loucas Demetriades, for the smooth collaboration, fruitful discussions and valuable feedback in the validation of modeling tools for the gasoline and diesel exhaust aftertreatment devices and systems. Special thanks to Dimitri Felekis for his valuable work on the validation of the NOx-traps submodel in his diploma thesis.

Financial support for this study was provided by

PSA Peugeot Citroën

and the

Greek State Scholarship Foundation

Dedication

Several people supported me and inspired me during the period of this thesis elaboration. Their contribution is beyond the scientific part of this work and it was determinative both for the initiation and the completion of this dissertation. Although their names are not mentioned here, they share an important part of my good and bad memories, at least during this period, and they are always considered to be close to me. I hope some day to meet again those that I have lost contact. For those still in touch, a great thanks for their continuous support during the most stressed period of this thesis. Special thanks to Joanna for her memorable patience, the love and the calm she offered me during the last hours and her contribution to the aesthetics and the final retouch of the text. I would like to dedicate this work to my father, my mother, my brother and his wife and the new member of our family.

ABBREVIATIONS

NOx	Nitrogen Oxides ($NO+NO_2+N_2O$)
W	apparent mass transfer coefficient
x	chemical specie molar fraction
R	reaction rate, resistance
T	Temperature
D	diffusivity
L	length
P	transverse Peclet number
k_b	boltzmann constant
E	apparent activation energy
A	apparent frequency factor
F	objective function
w	weight factor

Acronyms

THC	total hydrocarbons
NEDC	new European driving cycle
PGM	platinum group metals
PML	precious metal loading
PME	precious metal exposed
3WCC	3-way catalytic converter
TWC	three way catalysis
NVH	noise, vibration&harshness

Greek letters

ψ	ceria oxidation state
η	efficiency

Subscripts

g	gas
s	solid
i	node, chemical specie
j	chemical specie
eo	engine out
tp	tailpipe

Symbols

^	apparent

CHAPTER1

INTRODUCTION

This chapter presents an overview of automotive catalytic converter technology. The reader is introduced to the research and development effort given at every field of automotive pollution control systems. The driving force for the continuously developing exhaust treatment systems is the need to deliver "clean vehicles" as indicated by the legislation directives. The compliance with current and future legislation has driven the manufacturers to implement complex systems that vary according to the specific design target (described in a short in this chapter and studied later at chapters 5, 6, 7 and 8). The complexity of the problem necessitated the cooperation of several disciplines in achieving an optimum solution. The autocatalyst technology principles presented here are essential to the understanding of the currently used aftretreatment devices' behavior and to the engineering modeling thereof that will be presented in chapters 2 and 3.

1 INTRODUCTION

1.1 AUTOMOBILES-THE MAIN SOURCE OF URBAN POLLUTION?

Automobiles are considered as the main pollutant source in the urban environment. In general, vehicles' mobility is a widespread, partially uncontrolled emitting source depended primarily on the characteristics and the condition of vehicle and on the driving behavior of each driver. In fact, there are numerous sociopolitical factors that are affecting global emission from transportation, such as per capita vehicle distance of travel, auto ownership, person trips, and fraction of single occupant vehicles (SOV) that have increased disproportionally to population growth in the western civilization [8]. Internal combustion engines, that are responsible for the pollutants, are practically the only power generation unit for automobiles and are expected to stay for the next two decades in intensive production, considering their high power density and recent great improvements in emissions control [9, 10].

The air pollutants of concern emitted by the automobiles are carbon monoxide (CO), several hydrocarbons species (THC), oxides of nitrogen (NOx), particulate matter (PM-10), sulfur dioxide (SO_2) and lead (Pb). The implementation of recent standards in the fuels technology practically eliminates the emissions of lead and sulfur dioxide. Presently, the overriding concern is shifting to the reduction of carbon dioxide (CO_2), an unavoidable product of carbonaceous fossil fuels combustion, and fuel consumption, that is the main factor for emissions production [11]. The health effects of automotive pollution are more or less known and can be summarized to respiratory and heart diseases, cancers and increase in mortality, while they are implicated in the "global warming" trend through the greenhouse effect [12].

In ideal combustion, oxygen and fuel (mixture of HC) are combusted and produce carbon dioxide (CO_2) and water (H_2O). Air, however, contains, among other chemical species, nitrogen (N2) and, as a consequent of incomplete combustion, toxic byproducts of HC, CO and NOx are always present [13]. The air to fuel (A/F) ratio is an important factor in determining the quantity of pollutants produced by combustion. Generally, rich fuel mixtures (low A/F ratios) produce high amounts of CO and HC because of incomplete combustion. Lean fuel mixtures (high A/F ratios)

will typically produce higher amounts of NOx (especially during very hot, lean conditions) and lower amounts of CO and HC, due to excess of reacting oxygen and thus better combustion. When considering the vehicle activity, high power demands (sharp accelerations, heavy loads, etc.) require combustion mixture fuel enrichments that results in elevated CO and HC emission rates while NOx generally decreases. At high speeds with low acceleration rates, a lean fuel mixture develops which increases NOx emission rates [13].

Car manufacturers design automobile engines to provide power in order to meet consumer demands, to maximize fuel efficiency and to comply with legislation standards in certification tests (Federal Test Procedure (FTP) for USA, New European Driving Cycle NEDC for EU, Japanese stationary driving modes, and other standardized tests in respect to the local legislation). Practically, this is translated to a balance of the A/F ratio through computerized engine controls to its optimum point according to the operation mode of engine (idle, acceleration, etc.). Characteristic examples of variable engine control are the recently developed direct injection engines where the A/F ratio varies from the extremely lean 60:1 to slightly rich 14:1, in respect to the power demands and the driving mode [14].

The emission rates of the modern vehicles show an obvious trend towards significant reduction of the pollutants. Vehicle technology has changed dramatically over the last thirty years and great strides have been made in reducing emissions. The improvements have been attributed to legislatively induced emission controls for new vehicles, which include both advanced engine management and improved exhaust aftertreatment devices.

The published exhaust-gas results of modern vehicles with optimized exhaust-gas aftertreatment systems, exhibit ever more frequently negative exhaust-gas results, in the condition warm from operation, even in the case of comparatively low ambient air pollution. This fact means that, with an active catalyst system, such vehicles are in a position, to contribute a positive (i.e. cleaning) effect to the problems associated with emissions, primarily in urban areas with relatively high emissions [9].

1.2 LEGISLATION

Legislation is the driving force for automotive and catalytic systems manufacturers for continuous improvements of the automotive systems in production in order to comply with current and future emission limits. To acquire a certification, the vehicles are tested into legislated test cycles, which are specific driving patterns, simulating different driving conditions. The accumulated emissions at the end of the test must be below the legislation limit. While several countries have legislated their own driving cycles, EU and US legislation is the more important because of the large vehicle market share in these regions. They also remain the most demanding, considering current, future emission limits and catalyst performance monitoring with on-board diagnostics (OBD). European Union has affiliated the NEDC shown in Figure 2, which includes a cold start, an urban driving and an extra-urban driving phase.

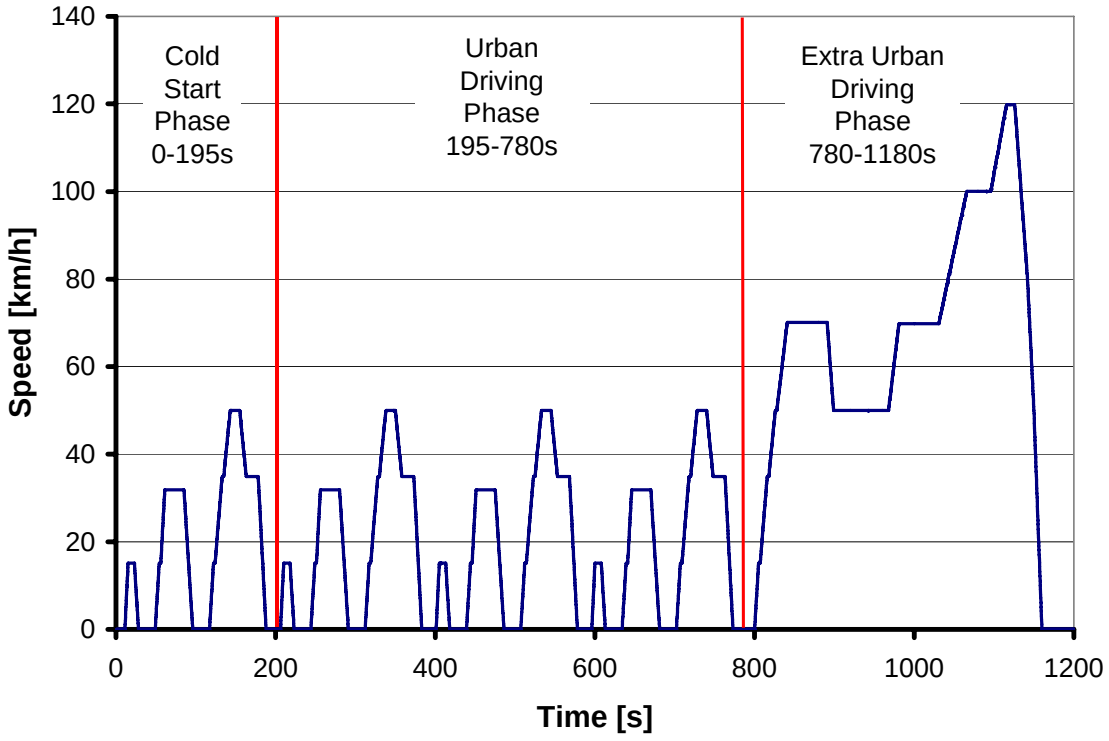

Figure 2 New European Driving Cycle. The vehicle is tested upon the driving pattern that includes idling, smooth and sharp accelerations, cruising at 15, 30, 50, 70, 100 and 120 km/h and decelerations. Emissions sampling starts immediately after engine ignition

US legislation tests are accomplishing over the FTP-75 driving cycle shown in Figure 3 that includes a cold start, a hot transient and a hot start phase where the engine starts again after a 10 minutes stop.

Comparing the two driving cycles, we see that FTP-75 has sharper accelerations and decelerations (e.g more transient driving) but lower maximum speed compared to the NEDC. Both cycles have similar average speeds at about 33 km/h.

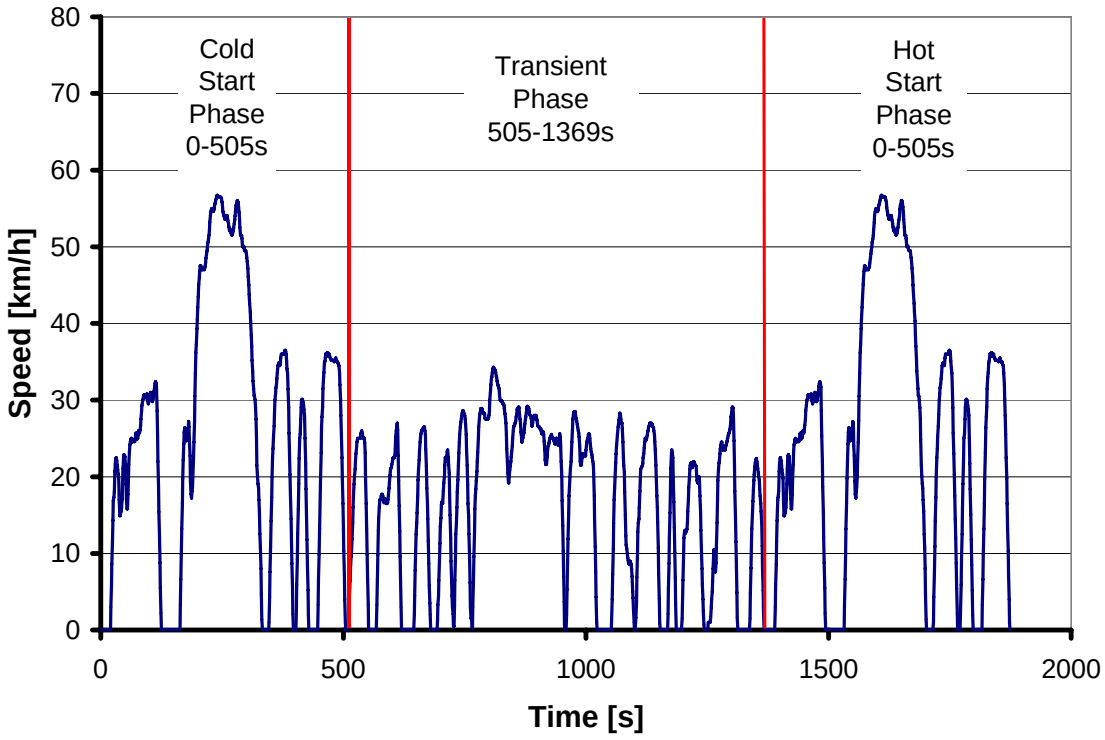

Figure 3 Federal Test Procedure (FTP-75) for the US legislation vehicle testing. After the transient phase (1368s) the catalyst is soaked for ten minutes and immediately after the hot start phase begins, that is identical to the first part of the cycle (Cold start phase)

Engine exhaust is a complex mixture of combustion products that contains thousands of different compounds. Three of these are considered by legislators to warrant special attention. These are carbon monoxide (CO), total unburned hydrocarbons (THC) and oxides of nitrogen (NO_x) emissions. Figure 4 shows a comparison between emission limits for previous and current legislation for both US and EU. Even more stringent standards to be initiated in EU from 2008 are currently under discussion [15, 16], which will include particulate matter emissions monitoring for SI engines and cold start operation at temperatures below zero.

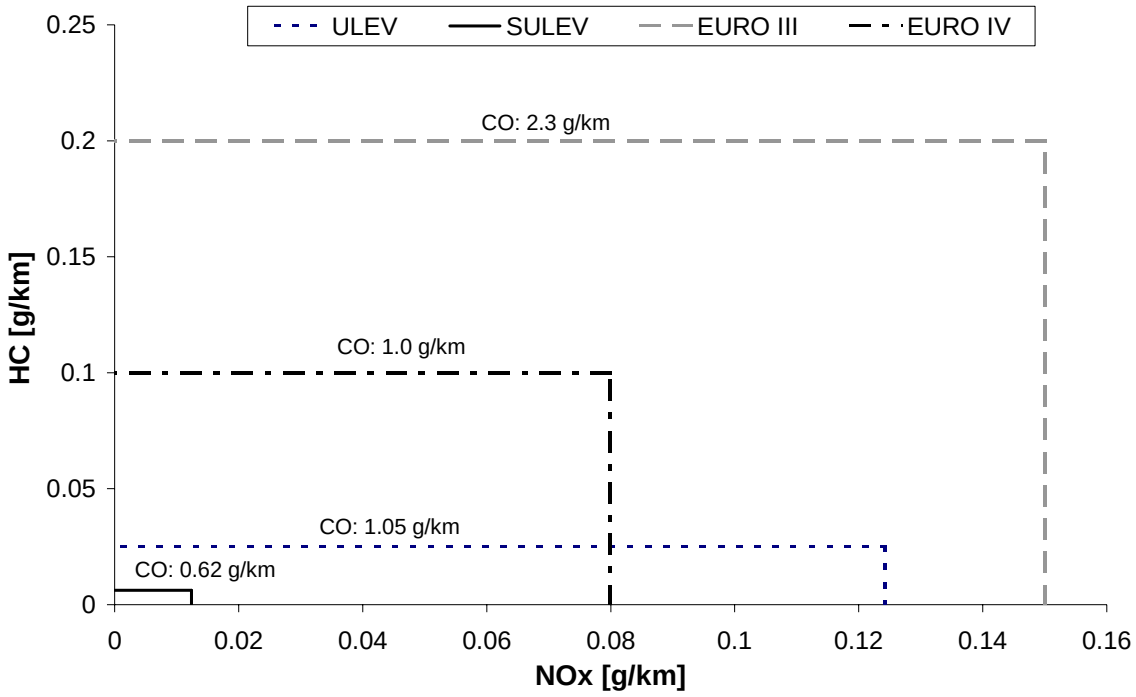

Figure 4 Comparison of current and next emission limits for United States and European Union. It must be considered that the accumulated emissions at the end of the test are strictly correlated with the driving pattern, so a direct comparison is not right. The trends concerning exhaust aftertreatment is focusing mainly on NOx emissions for U.S., while E.U. concerns are for simultaneous HC and NOx reduction

By this time Euro 3 cars on average already fulfill Euro 4 standards in the homologation tests [17]. Several research studies have also shown that vehicles complying with current legislation in both EU and US, are able to certificate with future emission limits (Euro IV and SULEV) using current aftertreatment technology status, with special focal given to NOx emissions [9,11]. Of course, in order to achieve this goal, the complete system of engine, engine management and aftertreatment devices have to be optimized [18,19]. At the same time, there is an increasing interest and study in "off-cycle" emissions [20,21] as there are evidences that starting in lower temperatures or operating at higher speeds result in higher emission levels for vehicles that comply with legislation [17]. It should be mentioned that compliance with new emissions standards and application of new technologies requires the delivery of improved "clean" fuels [22].

1.3 TECHNOLOGY REVIEW

Design and integration of exhaust gas aftertreatment systems is a part of a systems engineering approach, with strong interactions between engine operation, engine management and aftertreatment devices. The optimization of the overall system is a strong prerequisite for effective automotive pollution control, as catalytic emission control is in many ways linked to the engine combustion process and engine management system [11].

The exploitation of current exhaust gas aftertreatment technology in new propulsion systems or combinations of them (e.g. hybrid vehicles) will be a future challenge, as new demands are rising for better control, new sensors and advanced modeling of the entire system. The use of advanced technology for SI engines with the combination of a common 3WCC and optimized heat management of the exhaust line resulted in compliance with ULEV emission limits [23]. The capacity of further improvements is obvious, considering the technological advances that can be achieved in the near future over the entire system design.

ENGINE IMPROVEMENTS

Current engines are using state-of-the-art technology that enables them to handle strict emissions regulations. The compliance with future emissions legislation, the challenge to reduce CO_2 emissions and increasing customer demands for more power, comfort and fuel economy, configure the landscape of research for the next years. Some directions and recently developed technologies can be summed up to the following [10]

As regards spark-ignition engine, current status and future challenges are:

- Direct injection engines that introduce the advantages of diesel engines for lean burn combustion in SI.
- Fully variable valve train systems for optimum control of engine operation in the full operation range.
- Downsizing, highly boosted, with variable compression, that results in fuel economy advantages without loss of power.
- Homogeneous lean combustion at high loads.
- Diesel engine design has greatly improved during last years with:

- Improved injection systems with higher pressures for better atomization of diesel fuel injected in cylinder
- High (cooled/uncooled) EGR, for in cylinder control of NO_x emissions
- Further improved, partly homogeneous combustion.

In the near future downsized, turbocharged, direct injected and lean engine concepts will enter the market [24]. This will present a new challenge for exhaust aftertreatment systems with respect to temperature and sulphur loading as well as lean operation capability.

It is expected that NO_x-aftertreatment systems will probably be in production in the future, while combinations of exhaust aftertreatment devices are tested and optimized. Additionally, On Board Diagnosis (OBD) is becoming a major issue for reliable monitoring of exhaust aftertreatment systems during lifetime. Most stringent emission limits can also be achieved, however effort, cost and fuel efficiency penalty has to be considered.

SENSORS TECHNOLOGY IMPROVEMENTS

Great activity in development of sensors used in automotive industry is observed in recent years, focused in sensitivity and faster response [25]. Several requests of engine management were covered by new sensors, such as NOx sensor [26] and in-cylinder piezoelectric pressure sensors [27]. Lambda and UEGO sensors equip commercial cars, whereas laboratory measurement devices and faster gas analyzers aim the research and the better understanding of the engine behavior. Algorithm improvements have enabled tighter control of A/F mixtures using existing oxygen sensors. Current sensor needs can be summarized up to the following [28]

- wider range of operation
- cheaper designs
- improved robustness
- faster response time
- improved signal processing and feedback control

MODELLING IMPROVEMENTS

The great cost of experiments and the increasing need for predicting new integrated systems effects in tailpipe emissions, has established a great activity in modeling of engine operation and exhaust systems during the past 15 years. The improvements in computer science, which reduced the computational times, had great contribution to this.

By this time, several of the models that exist in the market predict the engine operation [29] or components of it, exhaust aftertreatment devices [30], even the whole vehicle behavior during the driving cycle [31]. Today's requests of a computational model used for industrial designing are accuracy, low computational time and suppleness regarding the latest technology improvements.

Obviously, the stringent legislation has pushed the automotive and fuel industry into strides of technological improvements. Moreover, it has pushed research to all directions regarding vehicle technology. The new vehicles are heavier (due to improvements in the safety and higher level of equipment), equipped with downsized engines with increased power density and improved fuel economy and at the same time, they deliver ultra-low tailpipe emissions. The assembly of the technological advances has leaded to a great reduction of in-cylinder emissions, but it is not able of a practical elimination of them. The key role to the ultra low emissions delivery is attributed to the recent technological advances of the exhaust aftertreatment systems and especially to the catalytic converters.

1.4 EXHAUST AFTERTREATMENT SYSTEMS

The exhaust line of modern vehicles consists of various combinations of one or more exhaust aftertreatment devices, regarding their position at the exhaust line and the individual characteristics of each device. Each type of application has several characteristics and restrictions that define the type and the position in exhaust line of an exhaust gas aftertreatment device, depending primarily on the characteristics of the engine, the electronic control and the aftertreatment.

In general, the design of a vehicle exhaust line is a multi-parametric optimization problem that includes at least the following parameters:

- Engine operation characteristics: temperature range, mass flow rate range, engine out gas chemical composition
- Engine management: strategy followed during the different modes of engine operation and especially during cold start
- Catalytic converter's characteristics: dimensions, mass, thermal response, channel density, channel shape and of course washcoat formulation, in respect to the storage characteristics and the precious metal type, content and ratio.
- Exhaust line characteristics: insulation, thermal response, position of the devices and piping bifurcations.
- Assistance techniques: injection of secondary air, heating elements, elements for temporal storage of chemical species, flow reversing techniques and others.

The main issues of the exhaust aftertreatment research, as regards the more stringent future emissions legislation (EU-V and SULEV), are [11]

- Exhaust treatment for ultra - low emission concepts
- Nitrogen oxides for lean engines
- Particulate emissions of diesel engines

The extent of this thesis is limited to gasoline-powered vehicles and thus the discussion hereafter is focused on the developments made in 3WCC technology and NO_x adsorbers.

Typical arrangements that are met frequently at the exhaust line of commercial vehicles are shown in Figure 5

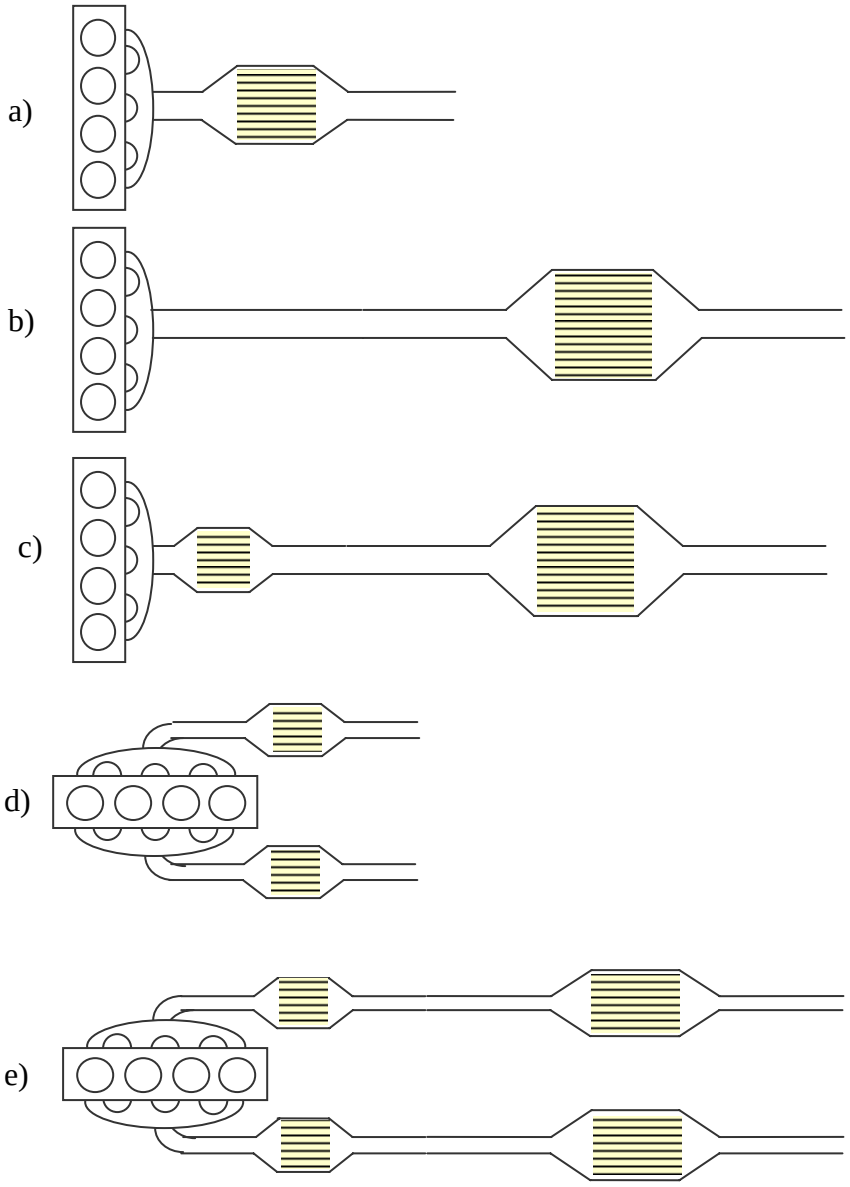

Figure 5 Typical exhaust line arrangements of commercial vehicles. a) close coupled position, b) underfloor position, c) two devices in serial, d) two devices in parallel and e) devices in parallel and serial position.

1.5 MONOLITH CATALYTIC CONVERTERS PRINCIPLES

The first catalytic device for purifying exhaust gas from internal combustion engines was implemented in 1976 in the US. Following the positive experience of US, Japan and EU manufacturers adopted the use of automotive catalysts in 1986.

New material requirements, along with a more fundamental understanding of the function of various components, allows more precisely defined washcoats with less expensive metals and enhanced performance for a lifetime. Future needs for meeting ULEV standards and on-board diagnostics will continue to be a challenge into the 21st century [32]. The needs of a catalytic converter are [33]:

- Proper functionality of emissions systems for 100000km
- Combined requirements for compactness, high volumetric flow rates and low backpressure
- Survivability of the catalysts in the field (poisoning, sintering, leeching)
- High efficiency under extremely oscillating chemical environment
- Low initial cost and null service cost

Early research and development in automotive catalysts was devoted to non-noble metal catalysts (so-called base metal catalysts), largely due to concerns over the cost and availability of noble metals. However, it quickly became obvious that the base metals lacked the intrinsic reactivity, durability, and poison resistance required for automotive applications. The recognition that the rest candidate platinum group metals formed volatile oxides was the key factor to leave Pt and Pd as clear choices for the oxidation catalysts employed. Rh was selected as the best NO_x reduction catalyst due to its high NO_x conversion in the lean regime of engine operation and the significant lower selectivity for NH_3 production under rich conditions [34]

Worldwide high demands and mining rates affect the prices of the noble metals through the years and thus the optimum cost solutions for efficient washcoat formulations. The prices of noble metals over the years are a driving force for testing alternative washcoat formulations, searching substitute metals for catalysts and lowering the precious metal loading of the catalytic converter. This effort aims at reducing the demand for noble metals and at finding alternative design that could possibly push off the pressure of feedstock prices.

Figure 6 presents the prices of noble metals for the period July 1992 to March 2006. Obviously, the breakthroughs in the stock market prices coincide with specific events related to the auto catalyst industry, considering that it is the major consumer of these metals. As of year 2000, when both EURO III and LEV standards where implemented, the prices of all three metals (Pt, Pd, Rh) rapidly increased and the use of palladium as alternatives to platinum catalyst formulations, nearly tripled its price. Nowadays, the constant increase of the platinum prices is attributed to both auto catalyst industry and jewelry, which are competitive consumers of the majority of the platinum world production. The increase of rhodium prices is correlated to the increased interest to reduce NOx emissions, as indicated by current and near-future legislation.

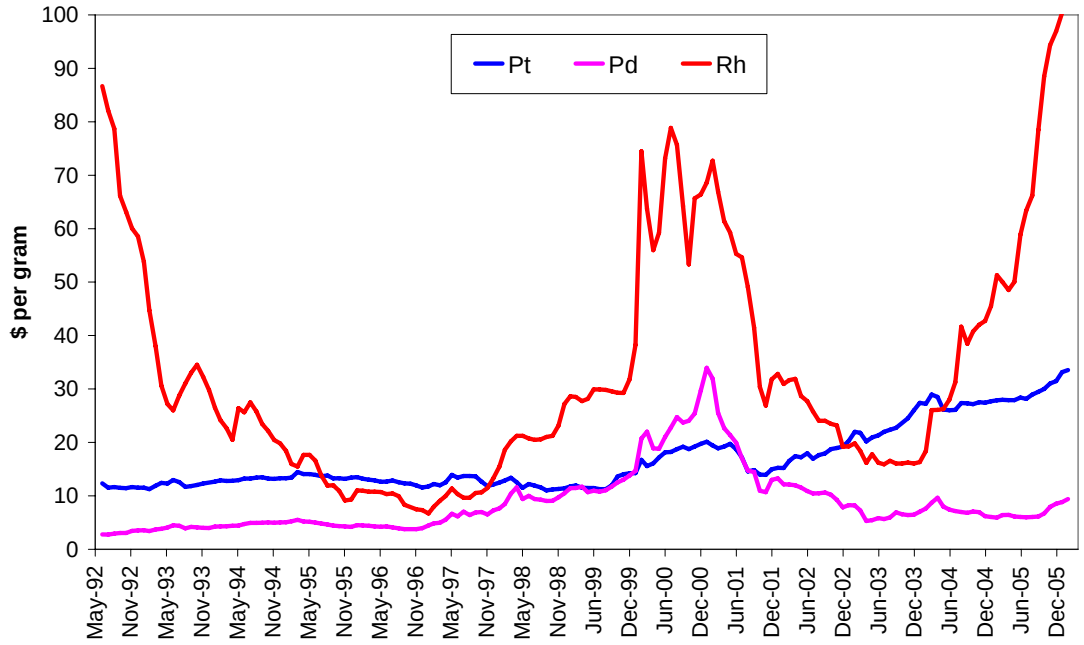

Figure 6 Evolution of market prices of precious metals used in automotive applications since July 1992. Adopted from data by Johnsson-Matthey website

The great majority of the catalytic converters share the same principles regarding their macroscopic characteristics. Monolithic converters may be considered as a batch of parallel channels running the axial direction providing high geometric surface area for contacting the gas phase, which flows through the channels.

The most common catalytic converter design is illustrated in Figure 7. It utilizes a ceramic or metallic honeycomb monolithic substrate, usually cylindrical or oval shaped. The substrate features many small parallel channels running in the axial direction, which are orthogonal, triangular, sinusoidal or hexagonal, depending

on the manufacturer choices. Parts that have been commercially used for automotive applications have a typical cell density range from 400 cpsi to 1200 cpsi for ceramic substrates and even higher for the metallic ones.

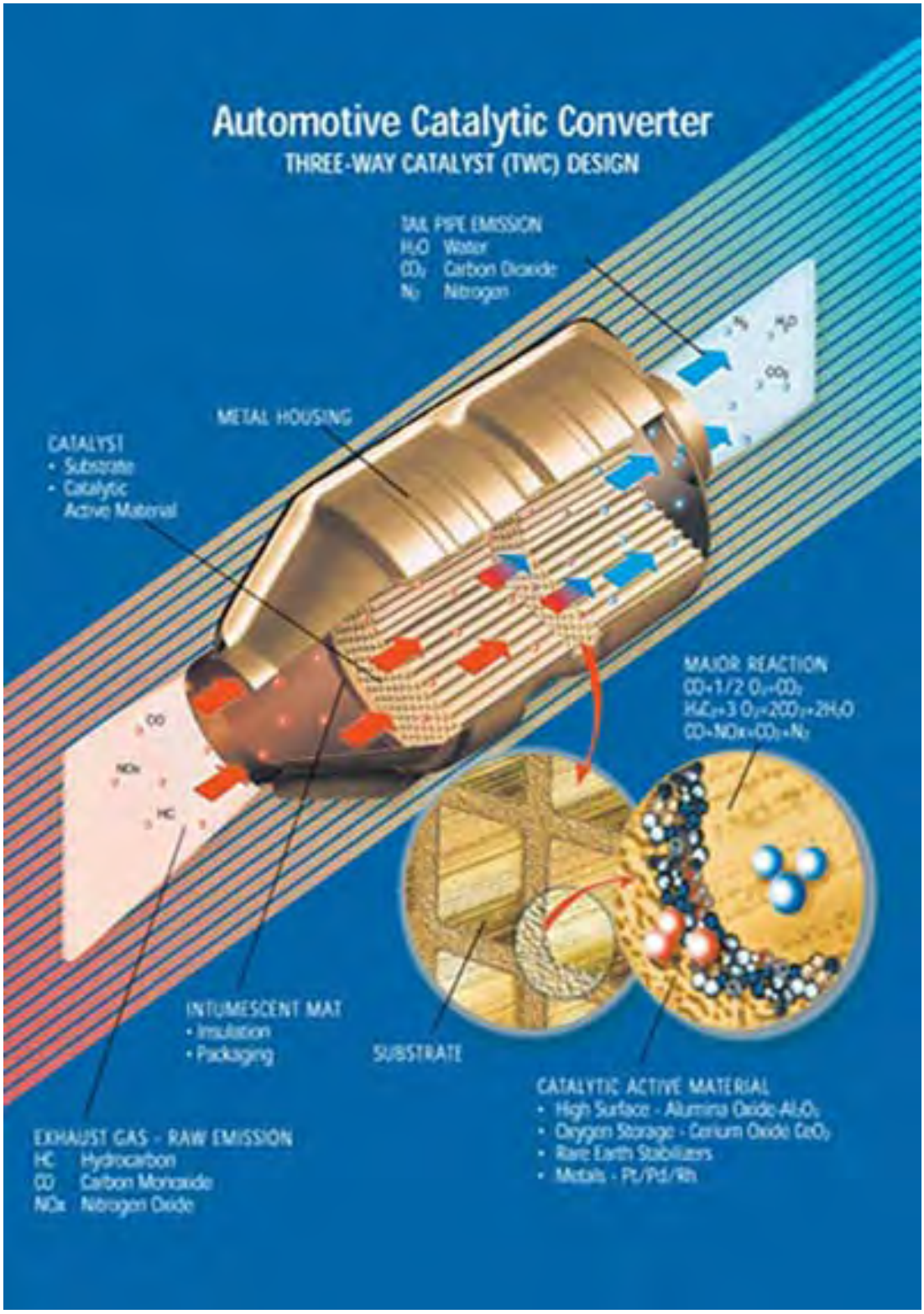

Figure 7 Concepts of the monolithic catalytic converter design

The ceramic or metallic substrate of the monolithic catalytic converter does not have any catalytic activity of its own. The function of the monolith substrate is to provide high geometric surface area for contacting the gas phase that flows through the channels, with the catalyst, which is coated on the channel walls. The active catalyst layer has to be coated on the monolith walls. That coating, called the washcoat, is composed of porous, high surface area inorganic oxides and platinum group metals that are deposited on the surface and within the pores of the washcoat. Exhaust gas flowing in a catalytic converter diffuses through the washcoat pore structure to the catalytic sites, where heterogeneous catalytic reactions occur.

There are several processes to prepare a monolithic catalyst, as shown in Figure 8. A schematic representation is that the active catalysts are supported (washcoated) onto the monolith by dipping it into slurry that contains the catalyst precursors. The excess of the deposited material (washcoat) is then blown out with hot air and the honeycomb is calcinated to obtain the finished catalyst. The exact method of deposition and catalyst composition is therefore highly proprietary and specific for every washcoating company [69].

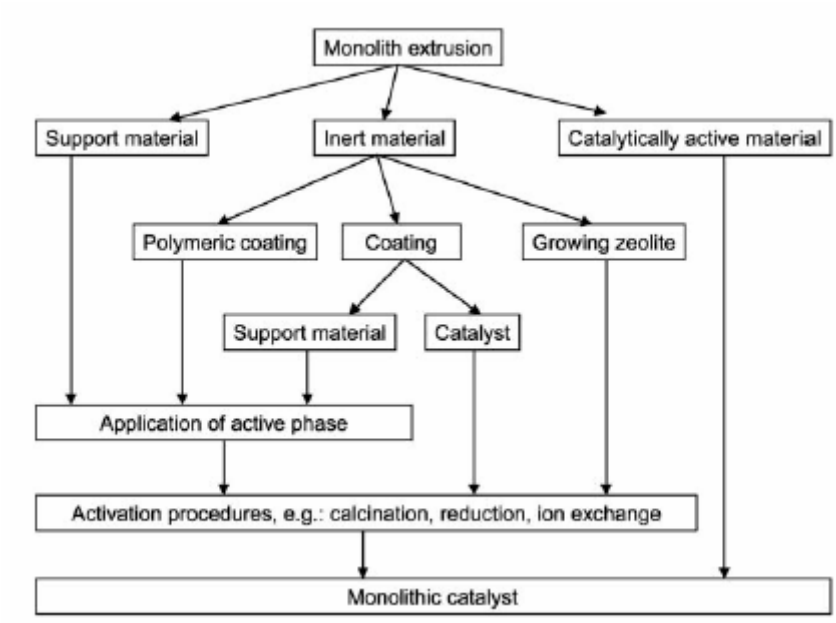

Figure 8 Paths leading to a monolithic catalyst (adopted from [35]).

Pontikakis [3] has examined the field of monolithic catalytic converters' study by addressing it into four distinct levels:

Reactor level: At this level, the individual channels interact with heat transfer and the converter is exchanging heat with the ambient. Flow maldistributions at the front of the converter and any other macroscopic 3-D phenomena are objects of this level of study.

Channel level: The interactions between the catalytic washcoat and bulk gas are studied. The gas flowing into each channel, transports heat and mass to the catalytically active washcoat, where the chemical reactions are taking place, and vice versa. The most prominent phenomenon at this level is the boundary layer heat and mass diffusion.

Washcoat level: This level refers to the phenomena that take place into the solid washcoat. These are summarized up to adsorption/desorption of chemical reactants, chemical species temporal storage and diffusion concepts into the solid washcoat.

Kinetic level: At this level of study, the expressions of the reaction rates are defined and proper reaction schemes for the converters function are selected.

The description of the reactor and the channel level characteristics is the same for both the 3WCC and the NOx absorber. The mathematical equations that describe any type of monolithic channel reactor at these levels are trivial and are presented later in chapter 2. The different function of the various types of catalytic converters is traced to the concepts of the washcoat and the kinetic level, considering that specific types of washcoats are used in each application and are described by different reactions mechanisms.

The macroscopic design concepts of the monolithic catalytic converters have been extensively discussed in literature [32, 33, 69]. Of course, the physical and the geometrical properties, the position of the catalytic converter in exhaust line and specific interactions with other devices and engine management affect the performance of the catalytic converter and consequently the tailpipe emissions. An indicative set of studies in this direction [18,73,36,37,38,39] pointed out the following optimization problems (washcoating excluded):

- Low thermal mass results fast light-off, while enough heat inertia is needed to maintain operation temperature.

- Best converter performance comes with increased cell density, which increases backpressure and thus reduces engine power output.
- Location closer to engine reduces heat losses (faster catalyst heat-up), while temperature excursions shall be below 1100^{o}C, to avoid hot spots and sintering.
- The high hydraulic diameter maintains low backpressure, but has a strong effect in flow maldistribution and consequent reduction in catalyst 's efficiency
- Substrate cell shape affects the mass transfer coefficient but there are material and fabrication limitations
- Combination of different devices in exhaust line results in better tailpipe emissions but it is very common to operate at different temperature windows (e.g. NO_x adsorber temperature window is up to 450^{o}C) and different chemical environment.

The rest of this chapter is a literature research into the properties and the functions of the materials used in the washcoat, in order to assist better understanding of the major concepts of the autocatalysts operation.

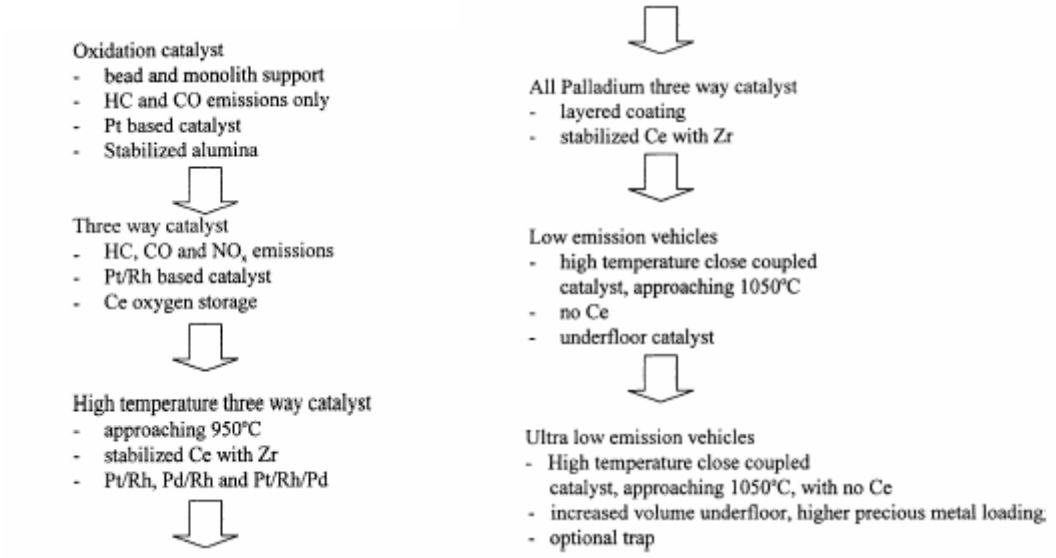

Figure 9 The evolution of the design and the materials used in TWC technology through the last thirty years of application. Adapted from [164]

The evolution of the catalytic converters aftertreatment systems through the years, is shown in Figure 9. Obviously, the design of the catalytic converters is

strongly correlated with the stringent legislation limits, prices of the noble metals market and changes in engine design and calibration.

Washcoat formulation and technology continuously changes due to the new findings from fundamental research and the use of new materials and deposition techniques that are covered by industrial secrecy frequently. Indicative studies are those from Degussa and Johnson Matthey [40, 68] where new formulations of washcoats with similar precious metal loading and ratios tested on vehicles. The results varied significantly regarding to the catalytic activity, while no information for the special washcoat characteristics is given, considered that is covered by industrial secrecy.

Fundamental understanding of new technologies lacks in several ways [41], accounted that:

- Detailed knowledge of the chemical processes and their relative importance is limited.
- Laboratory and on-engine data are often different and not applicable for comparisons.
- Black-box measurements are often insufficient to understand the processes.

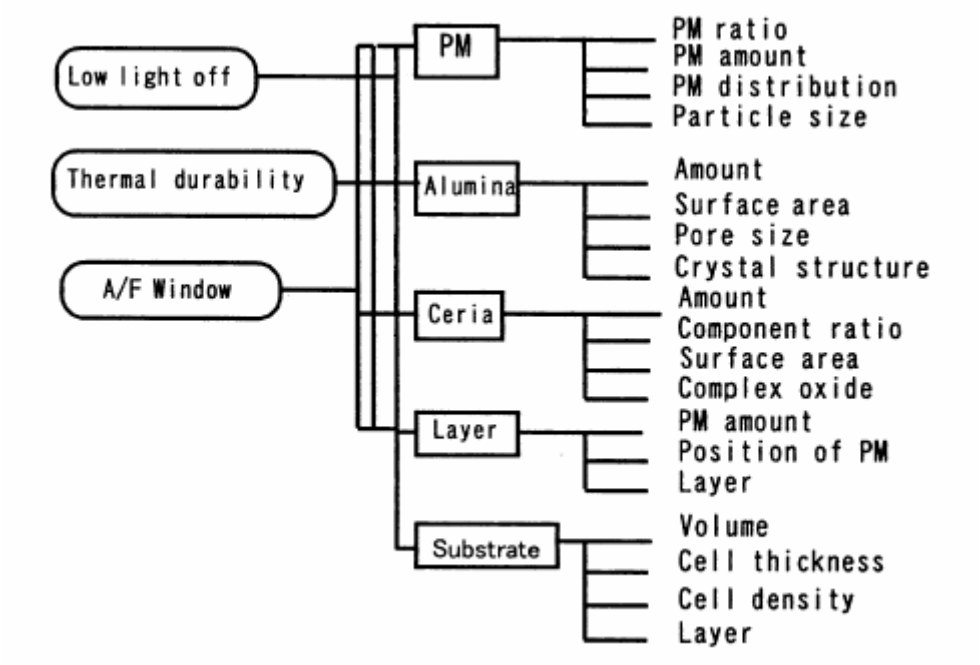

Figure 10 Relationships of TWC materials with catalytic performance. Adapted from [42]

Ishikawa et al. [42] presented a table with the relationships between materials used and catalytic performance characteristics (Figure 10). As shown in Figure 10 the key role to the performance of a catalytic converter, is attributed primarily to the catalytically active washcoat.

It should be mentioned at this point that strong metal support interactions have been reported for several washcoat formulations [43, 44], and it is therefore essential to study the effect of each washcoat component to the catalytic performance. This section is an attempt to clear out the major contribution of each component to the catalytic function, through several, apparently contradictory, literature results. Any confusion in the analysis of the literature results derives from the fact that numerous types of catalytic formulations have been used under a variety of conditions, including binary gas mixtures, synthetic gases or real exhaust gas and a wide range of temperatures and mass flow rates. Studies under constant composition or oscillations of the feed gas are also present and address different catalytic behavior.

At this point, the literature study aims at the fundamental understanding of catalytic washcoat basics and the identification of any existing trends between the chemical components of the washcoat, in order to categorize the major phenomena between the different types of washcoats. The study is organized according to the components of each washcoat composition, which belong in three main groups:

- High surface area support admixed with stabilisers
- Storage promoters.
- Noble metals as catalytically active phases.

Later in this chapter, an attempt to clear out the field of autocatalysis, through a literature review oriented primarily to the study of the chemical processes inside the converter will be presented.

1.6 WASHCOATING MATERIALS

SUPPORT-STABILISERS

The composition of the support for the catalytic active phases is based on γ-alumina (γ-Al_2O_3). Alumina is considered a great choice due to its high surface area that is necessary to increase the effectiveness of the catalyst. The relatively good thermal stability under the hydrothermal conditions of the exhausts comes through alloy formation with a number of stabilising agents that have been reported in the literature, lanthanum, barium, strontium, cerium, and more recently, zirconium oxides [69]. These additives are impregnated onto γ-Al2O3 or, sometimes, sol–gel techniques are employed to improve the stability of the surface area and the selectivity towards a process [45,46].

Both La_2O_3 and CeO_2 confer remarkable stability to the alumina surface on Al_2O_3, as they prevent the formation of α-Al_2O_3, which is associated with a drastic loss of specific area. The formation of Ce^{3+} as $CeAlO_3$, inhibits the surface diffusion of species responsible for sintering under reducing conditions in a manner similar to La^{+3} formation as $LaAlO_3$ under oxidizing conditions [47].

The use of ZrO2 has also been reported to effectively stabilise γ-Al2O3 at high temperatures. The high dispersion and the formation of a very thin monolayer of zirconia over alumina suppress the phase transformation of alumina [48]. The γ-Al2O3 is stabilized with 1±2% of La2O3 and/or BaO [32], while weight fractions of cerium and zirconium oxides admixed with the γ-Al2O3 washcoat, vary significantly among different washcoats, considering that they affect the OSC.

A stabilizer commonly used is also BaO. Ba addition to the Pt catalyst weakens the adsorption strength of hydrocarbons and therefore allows the catalytic reaction to proceed smoothly. On the other hand, the Ba addition to the Rh catalyst causes such a strong oxygen adsorption on Rh that rejects the hydrocarbon adsorptions and therefore suppresses the reaction. The above conclusions suggest that Ba should be located with Pt and separated from Rh in the three-way catalyst for high catalytic activity [49]. An additional function of the Ba implementation is its property to store NO_2 under lean conditions ($\lambda>1$) in the form of $Ba(NO_3)_2$ and to release them under rich chemical environment ($\lambda<1$).

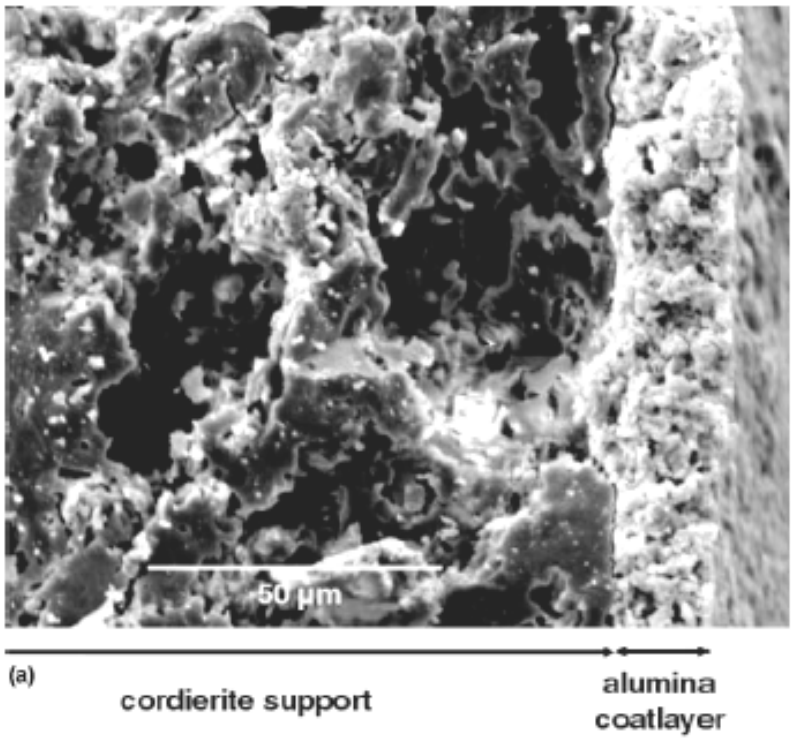

Figure 11 SEM micrographs of g-alumina-slurry-coated cordierite monolith (400 cpsi) (adopted from [35]).

STORAGE COMPONENTS

Cerium oxides are known as good oxygen storage promoters because of its facile redox cycling between the trivalent and tetravalent oxidation states of the Ce ions. They function under lean conditions as an oxygen buffer that release it when there is oxygen deficit, i.e. in a rich environment. It was firstly used as a stabilizer to the alumina supports, because of its good thermal stability at the temperature range of engine operation, ease of impregnation into alumina and compatibility with noble metals [33]. These oxides are found to have O_2 storage capabilities and enhance catalytic activity, especially at low temperatures. Although OSC increases with the increase of CeO_2 content in the washcoat [50], instabilities of structure at elevated temperatures are correlated with the thermal sintering of the noble metals. OSC of cerium oxides is affected by temperature [51] and the conjunction of other oxides, like Zr, used in advanced TWC formulations. It also seems to promote water-gas shift and steam reforming reactions at elevated temperatures and in a rich environment [52].

The phenomenon of OSC dependence of temperature can be possibly attributed to SMSI, where, at increased reduction temperatures, there is a significant loss of the metal chemisorption capability, which can be partly recovered by further reoxidation [43]. Very recent research work [53] claim that at elevated temperatures, oxygen of cerium oxides diffuse into the lattice of the washcoat, leaving by this way oxygen vacancies at the surface.

Zr is recently used in 3WCC to improve durability through stabilization of OSC after ageing [69], but also enhances OSC through participation of oxygen from the bulk of ceria-zirconia oxides compared to pure ceria [54, 63, 55]. Catalysts having the composition $Ce_xZr_{1-x}O_2$ with $0.5<_x<0.8$ show an increased catalytic effectiveness, attributed to their oxygen storage capacity and redox activity [55]. Finally, Christou et al. [56] reported that about 90% of the total OSC comes from CeO_2 or CeO_2-ZrO_2 on aged Pd-Rh commercial TWC, while the rest is due to the storage of oxygen in the noble metals (Pd and Rh). The review by Zhdanov et al. [57] on several mechanisms and models for Cerium oxides storage function is a good guide to the better understanding of these processes.

Barium (Ba) that is used as a support stabilizer in three way catalytic converters, has been found to have a NOx storage functionality under specific conditions, which is directly applicable to the NOx absorbers technology. By adding this specific storage compound to the catalyst, NOx can be stored, mainly as nitrates, in the catalyst under relatively long lean intervals. During subsequent short periods of net reducing conditions, the nitrates are forced to decompose and be reduced to nitrogen. In general, alkaline and alkaline earth compounds are proven effective for NOx storage at elevated temperatures, i.e., about 250–450 ^oC, that lies in the temperature range of automotive applications. This specific function of the barium requires that the operation temperatures lie in a narrow window, as the barium nitrates (the form of the stored NOx fraction) tend to decompose at elevated temperatures.

CATALYTICALLY ACTIVE PHASES

The role of the platinum group metals that are used as catalysts is well established [58]. Pt catalyses CO and HC oxidation, but it is essential for paraffin oxidation. Pd is an active CO, olefin and oxygenates catalyst and Rh improve the NO

reduction ability of the catalyst. In addition to that, several other phenomena are attributed to these components. Combinations at different ratios and loading levels show significant variability in their catalytic activity.

Platinum ages badly [59] and has poor high temperature stability [60], but shows high resistance in sulfur and lead poisoning. Pt form surface PtO and PtO_2 (by oxygen adsorption) that decompose at temperatures higher than 700K [61], leading to thermal deactivation of the catalyst.

Pd is known to enhance in a small portion OSC through formation of PdO in the bulk of the catalyst [33, 62, 63]. Similarly to Pt, Pd segregates as PdO on the surface of Pd/Rh alloys under oxidizing conditions up to temperatures ca. 1000 K, where PdO decomposes and leads to catalyst deactivation [61, 34]. It shows light-off at lower temperatures than Pt, [64] and great resistance in thermal ageing [65], but it is sensitive to poisoning by sulfur and lead compounds [69].

Several studies have shown that excellent NOx reduction could be achieved with Pd formulations, when suitably promoted and deployed at loadings higher than those for Pt/Rh [34].

However, the development of those catalysts could be restricted since Pd is known to be less selective than Rh and Pt for the transformation of NO into N2, in particular during the cold start [66].

Rh is effective for NOx reduction in the rich side of engine operation. Rh undergoes a strong deactivating interaction with alumina at temperatures ca. 600 ◦C and above. Ideally, Rh should be supported on ceria for best CO and NOx performance [34].

The activity of the monometallic catalysts is affected when mixed with other noble metals. In general, their basic characteristics are upholded in mixtures and alloys of them. For example, the effect of Pd advanced resistance to thermal ageing, can also be found in the bimetallic formulations containing palladium. It has been shown that Pd–Pt and Pd–Rh formulations are being much more resistant than the Pt–Rh catalyst, although the latter is the most active (at similar PML), even after subjected to the thermal aging treatment [65].

In aged Pt–Rh/CeO2/Al2O3 catalysts an important alloyed phase is observed between Pt and Rh, next to monometallic Pt and Rh, which are also present but in lower contribution. This means that the activity of these systems is mainly due to the

alloyed phase [67]. Similarities are also present in Pd-Rh and trimetallic catalysts [34,43]. Furthermore, all the reactions are controlled by the presence of the active sites, which consist of a mix between the metal and the oxides and the relative rates to pass from the reduced to the oxidised state and vice versa [67].

From a phenomenological point of view, a crucial point is to define some trends in each catalytic washcoat formulation regarding catalytic activity, chemical species storage behavior and light-off temperatures. Commercial catalytic converters for automotive applications commonly use Pd only, Pd/Rh, Pt/Rh and Pt/Pd/Rh noble metal formulations, CeO_2 and CeO_2-ZrO_2 as oxygen storage promoters or BaO and $Ba(CO_3)_2$ as nitrogen oxides storage promoters, over advanced γ-Al_2O_3 alloys supports.

1.7 THREE-WAY CATALYTIC CONVERTERS WASHCOATS

The three-way washcoat formulation is primarily used in stoichiometric SI engines, as it benefits from the operation close to stoichiometry. Such formulations can also be used as supporting catalysts in exhaust systems of lean burn engines, but they function as oxidation only catalysts. The main purpose of the three-way catalytic washcoating is the simultaneous elimination of the CO, THC and NOx contained into the engine-out exhaust gas, during vehicle operation. The three-way catalytic converter has a bimodal function of catalytic reduction and oxidation (RedOx) of chemical species. CO and THC emissions are oxidized and NOx are reduced inside the catalytic converter. The conversion efficiency is strictly correlated to the RedOx index of the exhaust gas, also known as λ index or simply lambda. The RedOx index is controlled by engine management and is affecting both engine out emissions and three-way catalytic converter efficiency as is shown in Figure 12. The highest overall efficiency of the converter is achieved within a narrow lambda window, very close to stoichiometry (λ=1). In practice, this is achieved by an active closed-loop tight lambda control around stoichiometry during operation, which results to an oscillating pattern of exhaust gas close to stoichiometry.

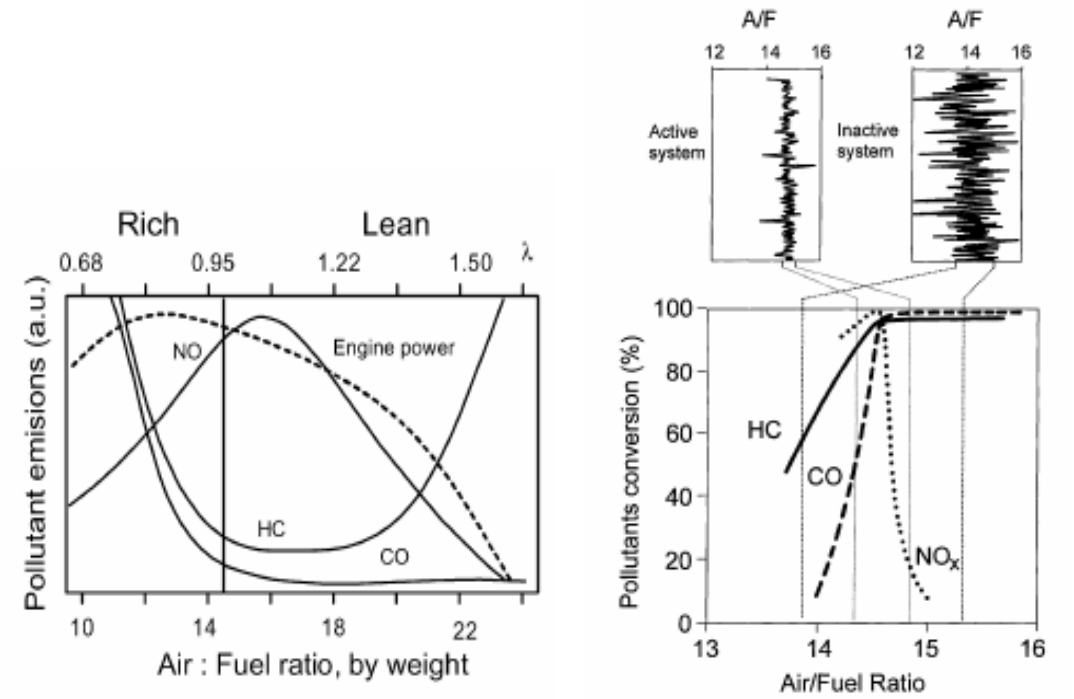

Figure 12 The effect of lambda control on engine out emissions and three way catalytic converter efficiency

Currently, three way washcoat formulations, in commercial use, contain Pt/Rh, Pt/Pd/Rh (trimetalic), Pd-only and Pd/Rh noble metal combinations and more frequently two kinds of washcoat formulations exist in the same exhaust line (e.g Pd-only as light-off catalyst and Pd/Rh as downstream underbody catalyst). Different precious metals ratios [68], various loading levels [1] and/or double- layered formulations are used, in respect to the specific application. Significant benefits appeared by advances in oxygen storage, thermal stability and durability, with the promotion of rare earth oxides in washcoat formulations [69]. Lately, interactions at the metal-oxide interface are under study, as it seems to affect sintering process during catalyst lifetime [70].

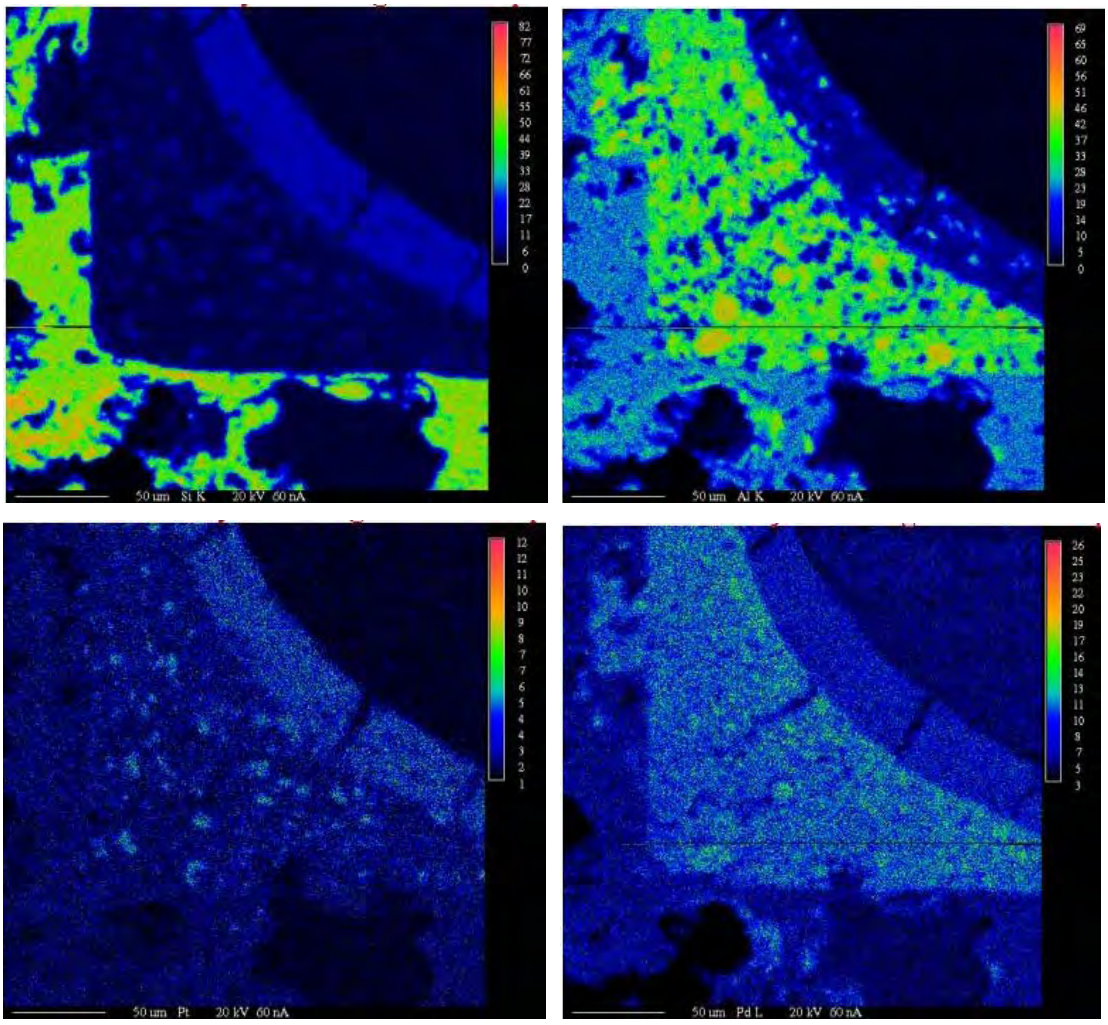

Figure 13 Concentration maps for a double-layer catalyst, where the two consecutive coatings become apparent. (1) Silica, (2) Alumina, (3) Platinum and (4) Palladium (adopted from [71])

The exact process and the paths of reactions are still a field of study in catalysis and will be discussed later. A simple, but not definite, apparent reaction scheme, can

describe the three-way operation. During lean operation (λ>1) the oxidation reactions are dominating due to excess of oxygen, e.g.

$$2CO + O_2 \xrightarrow{Pt\ or\ Pd} CO_2$$

$$THC + O_2 \xrightarrow{Pt\ or\ Pd} CO_2 + H_2O\,(unbalanced)$$

During rich operation (λ<1) the reductive function dominates, e.g.

$$CO + NO \xrightarrow{Rh} CO_2 + \tfrac{1}{2} N_2$$

Modern three-way catalytic washcoats, make use of the ceria property to temporarily store and release oxygen. Ceria functions as oxygen buffer that supports oxygen during rich gas environment and stores oxygen during lean conditions, making by this way the lambda operation window wider.

$$CO\,/\,THC + CeO_2 \longrightarrow CO_2 + H_2O + Ce_2O_3 \quad (unbalanced)$$

$$O_2\,/\,NO + Ce_2O_3 \longrightarrow CeO_2 + N_2 \quad (unbalanced)$$

Under steady, warm operation conditions, modern TWCs achieve about 99% efficiency. However, there are three circumstances, which may lead to undesirably high levels of emissions breakthrough:

1. During the warm-up period before the catalyst is hot enough to work effectively. During this first 30-60 second period up to 80% of the total HC emissions are produced [72]. The proven methods of reducing the warm-up emissions are to heat the catalyst faster by locating it closer to the engine (close-coupling), increase of cell density or decrease of washcoat mass or to formulate catalysts that become effective (light-off) at lower temperatures [69, 73].

2. After chemical or thermal deactivation of the catalyst. This may be due to poisoning (deactivating active sites) with sulphur or phosphorus, high temperature sintering of precious metals leading to decrease of active sites, sintering of the OSC promoter leading to loss of OSC and sintering of Al_2O_3 and deactivation of Rh due to Rh^{3+} migration in alumina lattice [69].

3. During transient operation such as acceleration and braking. Significant fractions of drive-cycle emissions occur during vehicle acceleration, with the effect being more pronounced as the TWC ages. Time lags inherent in current feedback systems due to slow sensor response mean that the AFR is not well controlled during unsteady driving. As a consequence,it is possible for breakthrough of emissions (CO and NO) to occur [74].

1.8 NO_X ADSORBERS WASHCOATS

Increasing awareness of the need to reduce emissions of carbon dioxide into the atmosphere has led to great pressure on automobile manufacturers to reduce the fuel consumption of their products. The most recent approach to improve the fuel economy of gasoline-internal combustion engines is to use engines that operate at lean conditions, rather than at the normal stoichiometric air/fuel ratios.

In this kind of application, the use of a three-way catalytic washcoat is improper, considering that the oxidative chemical environment of the exhaust gases inhibits its reductive function. On the other hand, lean engine operation minimizes engine out CO and THC emissions with significant increase in engine out NOx emissions.

This fact has led automotive industry and catalyst manufacturers to the development of special washcoats, used in the NOx adsorbers (also known as NOx traps or NOx storage catalysts). Practically, this washcoat formulation is a three-way catalytic washcoat with an advanced NOx storage function. The catalytic washcoat combines three active components:

- an oxidation catalyst, usually Pt,
- an adsorbant, for example barium oxide (BaO) or barium anthracite ($Ba(CO_3)_2$)
- a reduction catalyst, usually Rh.

The nitric oxide, contained in exhaust gas, reacts in lean chemical environment with the oxygen on active oxidation catalyst sites (e.g. platinum, Pt) to form NO_2. The storage material then adsorbs nitric dioxide, in the form of an inorganic nitrate.

$$NO + \tfrac{1}{2} O_2 \xrightarrow{Pt} NO_2$$

$$BaO + NO_2 + \tfrac{1}{2} O_2 \rightarrow Ba(NO_3)_2$$

When the engine runs under excessive fuel conditions or at elevated temperatures the nitrate species become thermodynamically unstable and decompose, producing NO or NO_2 (regeneration process). Under rich conditions, the produced nitrogen oxides are reduced by exhaust gas reductants (e.g. carbon monoxide, hydrogen, and hydrocarbons) to N_2 over the reduction catalyst, in a conventional three-way catalyst process.

$$Ba(NO_3)_2 \longrightarrow BaO + NO_2 / NO + O_2 \quad (unbalanced)$$

$$CO + NO \xrightarrow{Rh} CO_2 + \tfrac{1}{2} N_2$$

In practice, regeneration of NOx traps is achieved by shifting the engine operation to the rich side for a short period of 1-2 secs, with proper changes in the engine management.

The activity of NO_x adsorbers covers a fairly wide catalyst temperature window, extending from about 200°C to 450-500°C (Figure 14). The lower end of the temperature window, T_1, is determined by the catalyst activity in regards to the oxidation of NO to NO_2, as well as NO_x release and reduction (3-way function). The upper temperature, T_2, is related to the thermodynamic stability of nitrates, which undergo thermal decomposition at higher exhaust temperatures, even under lean conditions

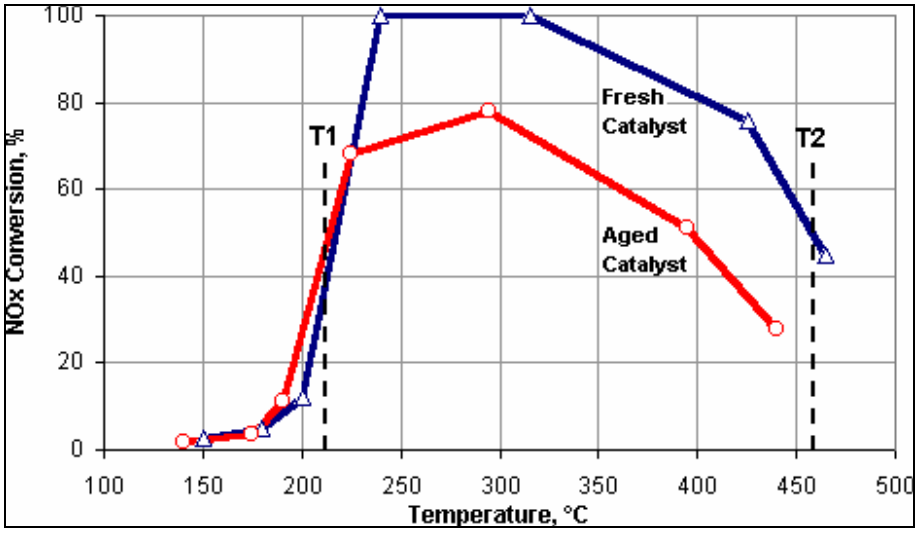

Figure 14 Temperature window of a typical NOx adsorber

An important aspect for the optimum operation of a NOx adsorber washcoat is the gas phase thermodynamic equilibrium of NOx. The NO_2 is thermodynamically stable at temperatures below 150°C, while at higher temperatures the equilibrium is shifted towards NO_2 dissociation to form NO and O_2. This reaction goes to completion at about 650°C.

The optimum NOx trap operation is a complex optimization problem that sums up to the following:

Match of the engine, NOx trap and NOx equilibrium temperature windows. Engine out exhaust gas reaches up to 850^{o}C for lean burn engines, NOx trap operation window lies in the range 200-450^{o}C and NO_2 is thermodynamically unstable practically over 300^{o}C.

Optimum definition of the lean and rich operation periods. The engine management must continuously monitor the status of the NOx trap, with regards to the stored NOx, establish the proper engine operation and control the regeneration rich spikes, regarding their frequency and their duration, accurately.

The required, regular regeneration of the storage catalyst limits the maximum saving on fuel consumption which can be achieved with a lean-burn engine.

The quantity of nitrogen oxides which has been stored by the storage catalyst is described by the nitrogen oxide filling level. The filling level is the ratio of the quantity of nitrogen oxides actually stored to the maximum quantity of nitrogen oxides which can be stored in the catalyst under the prevailing exhaust-gas conditions.

For the reduction in nitrogen oxide emissions which can be achieved with a NOx storage catalyst, it is important for the regeneration to be initiated in good time before the storage capacity of the storage catalyst is exceeded. For this purpose, it is customary to define a limit filling level, which is below the storage capacity of the catalyst. The prevailing, current filling level is determined while the storage catalyst is operating. If the current filling level exceeds the limit filling level, regeneration of the storage catalyst is initiated. If the limit filling level is selected to be a low one, the residual emissions of nitrogen oxides which still remain are low, but the fuel consumption is undesirably increased as a result of the frequent regeneration. If the limit filling level is close to the storage capacity, the proportion of nitrogen oxides which cannot be converted rises. Moreover, there is a risk of the defined limit filling level being exceeded more frequently on account of inaccurate determination of the current filling level, which further increases the remaining nitrogen oxide emissions.

The nitrogen oxide filling level which is present during the storage phase is generally determined continuously by integration of the nitrogen oxide mass stored per unit time at each instant. A mathematical model of the storage process is frequently used for this purpose. For example, [75] describes a method

for operating a NOx storage catalyst, in which the start of the second operating phase is determined on the basis of a nitrogen oxide filling level which is modeled on the basis of a nitrogen oxide storage model. To allow the start and end of the regeneration phase to be determined as accurately and reliably as possible, the nitrogen oxide mass flow is recorded downstream of the storage catalyst and corrected as a function of the recorded value. In addition to the problem of determining the optimum instant to switch from the storage phase to the regeneration phase, it is also necessary to monitor the increasing storage capacity with increasing operating time (aging) of the storage catalyst. The aging of the storage catalyst is composed of a temporary component and a permanent component. The temporary component is related to poisoning by the sulfur compounds contained in the exhaust gas. These compounds, with the basic components of the storage catalyst, form sulfates which compete with the nitrates. The sulfates are significantly more stable than the nitrates and cannot be removed during normal regeneration of the storage catalyst. Therefore, they reduce the nitrate storage capacity to an increasing extent. However, the sulfate loading of the storage catalyst can be reduced again. This process is known as desulfating. For this purpose, the catalyst has to be heated to approximately 650°C and the fuel content of the exhaust gas has to be increased (enrichment) . The normalized air/fuel ratio A during desulfating is typically in the range between 0.7 and 0.98. The permanent aging of a storage catalyst is related to thermal damage to the component of the storage catalyst. Overheating causes the storage materials themselves and also the catalytically active precious metals to sinter together, so that they lose active surface area. This process cannot be reversed.

It is necessary to monitor the aging of the storage catalyst in order to initiate desulfating on demand, to switch the vehicle to stoichiometric operation or if appropriate to trigger a signal that the catalyst needs to be replaced. (On Board Diagnosis). A suitable method for testing the efficiency of a nitrogen oxide storage catalyst which is arranged in the exhaust section of an internal combustion engine operated with a lean mix is described, for example, in [76]. For this purpose, the current storage capacity of the nitrogen oxide storage catalyst is determined, and a defective nitrogen oxide storage catalyst is diagnosed if the capacity drops below a predetermined minimum capacity.

Mathematical modeling plays a crucial role in improving the accuracy with which the instant at which a nitrogen oxide storage catalyst is switched from the storage phase to the regeneration phase.

Finally, the NOx trap is required to operate in series with another aftertreatment device, usually a three-way catalytic converter, in order to treat the rest of the emissions. This indicates the need of an advanced exhaust line design, with regards to the special operation characteristics of each device. Modeling plays a significant role in this process.

1.9 Literature Review on Experiments and Modeling Approaches in Monolithic Catalytic Converters

The function of each component used in automotive catalysts and its properties are well known theoretically. From an engineering point of view, with respect to catalytic converter modeling issues, a remarkable question that remains is the way of exploitation of the existing experimental data. This aims at the improvement of the overall exhaust line design in a time efficient way, to be in line with the current and future technology that will be commercialized.

The majority of current modeling approaches have concluded to very similar mechanisms for the description of the processes inside each monolithic catalytic converter. The most discussed issue is the definition of the reaction scheme used in each case and the determination of appropriate kinetic rate expressions. The reaction mechanism and the catalytic activity are strictly related to the washcoat formulation and the special manufacturing techniques followed. Alignment with this realistic assumption has leaded to the development of tunable models, with a tunable parameters set that is valid in most of the cases only for the specific catalytic converter for which the parameters are determined.

In practice, it has been shown that even approaches with increased number of reactions that use tunable parameters [77, 78,79], thus increased degrees of freedom for the model, were not able to accurate predict the catalyst operation under real engine conditions. On the other hand, detailed kinetics models have shown great potential in laboratory experiments [80, 81, 82] but there is still a lot of work to do for the determination of appropriate rate parameters [2].

However, do extended reactions schemes improve the modeling of 3WCC operation? What are the dominant chemical phenomena and how are they correlated with the manufacturing of the converter?

An effort to answer these questions will be made hereafter through an extended literature review firstly on experiments and secondarily on the various modeling approaches. The available experimental data varies from laboratory experiments to engine tests in legislated driving cycles, aiming both at the understanding of catalyst operation and the catalyst design guidance. Models, on the other hand, assume a valid mechanism in order to assist the design. Considering the incomplete knowledge of the exact mechanisms several models have been developed that focus to specific aspects. Catalytic converters models vary from simple

approximate models to very complex analytical models. An important question that arises is at which extent and under what assumptions could each model be used in order to find the golden section between accuracy and computational cost?

WHAT EACH COMPONENT CONTRIBUTES?

It is very difficult to compare the results of the numerous experiments that have been published during the thirty years of the commercialization of 3WCC, considering the variety of the washcoat formulations[a] used and the experimental conditions[b] of each test. This matrix of experiments constitutes a large database of autocatalysis that assists semi-empirical catalyst design and has to be translated in modeling terms.

Each of these experiments aims at studying a part of the catalyst's function and most of the times the results that come out are not directly applicable under real operation. On the other hand, results for commercial catalysts under real engine operation, that are applicable in practice, show small potential to be adapted in other cases and to extract generalized rules. A schematic representation of the placement of each type of catalytic activity experiment with respect to the commercialization is shown in Figure 15. Modeling needs to handle the modern catalytic converter design migration from "trial and error" methods to "engineering"[83], with the successful adaptation of the experimental findings into engineering models.

An indicative guide of selected published experimental data, where several catalytic converter data was given, is shown in Table 1. Obviously, the catalyst type varies significantly in each case and the experimental conditions range from model gas tests to vehicle engine testing in legislated driving cycles. What is expected, is that such a database would have determine the reaction rates and would have conclude in a proper reaction scheme and mechanism. Silveston [84] claimed that the experiments with integral reactors, conversion and mixing in the exhaust, operation at greater than 90% conversion and under engine exhaust gas oscillations, simultaneous and probably competing reactions could possibly differentiate the reaction rates determined in laboratory experiments.

[a] Regarding the support materials, the storage characteristics, the catalytically active components and their loading, ratio and special impregnation techniques. In general, the term "washcoat formulation" includes all these parameters each time it is referred in this thesis

[b] Regarding the temperature, mass flow rate, chemical species concentrations and dynamic or steady state nature of the test

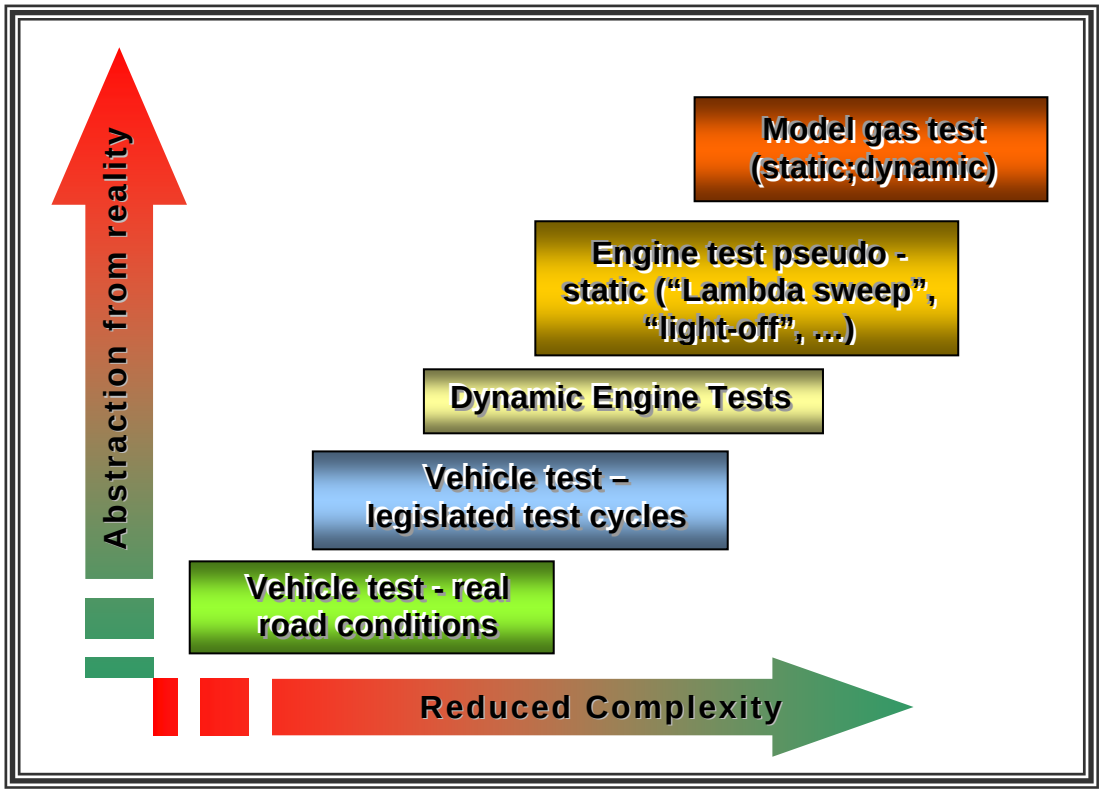

Figure 15 Typical tests of activity measurements of catalytic converters (adapted from [83]).

This thesis is in line with this conjecture; the experimental data derived from laboratory experiments are used to derive trends among the several design parameters of the converter and assist the development of a simple, robust, and flexible engineering model with filtering the dominant and the side effects in autocatalysis.

Despite the fact that the experimental results are strictly depended on the specific type of catalyst studied, general rules and orders of catalytic activity can be extracted from the literature, which aim at the derivation of valid assumptions for catalytic converters modeling.

Maillet et al. [85] have reported that the activity of the three metals commonly used in TWC is:

Pt > Pd > Rh for propane oxidation

Rh > Pd > Pt for propane SR

Table 1 Indicative studies for several types of catalyst and variable parameters under study

Type	Support	PM ratio			PML (g/l)	Feed gas	Temperature range	Parameter studied	Ref.
		Pt	Pd	Rh					
Laboratory	Ce-Zr-Y	Unknown			Unknown	N_2, H_2O, CO_2 CO, O_2, H_2	25-800 °C	OSC vs. PM	[86]
laboratory	CeO_2-Al_2O_3	Unknown			Unknown	HC, CO, NO, CO_2, O_2, H_2, H_2O, N_2	400 °C	PM - CeO_2 interaction	[87]
						engine			
Commercial	Unknown	0	1	0	2.2, 3.9, 5.3, 7, 10.5, 3.3	engine	FTP	light-off, efficiency, vehicle caliration	[68]
		0	9	1	1.4, 2.2				
		0	14	1	3.5, 5.3				
		5	0	1	1.4				
		3	0	2	1.8				
		4.5	0	2	3.3				
		9	0	2	3.9				
commercial	Unknown	0	14	1	5.5	engine	NEDC	cpsi, PML, washcoat type	[88]
		0	11	1	2.8				
		0	14	1	3.9, 2.5				
laboratory commercial	CeO2, CeO2-ZrO2	0	0	1	2.8, 1.2	HC, CO, NO, CO_2, O_2, H_2, H_2O, N_2	25 - 500 °C	light-off, efficiency, OSC	[89]
		0	11	1			400 °C		
		5	0	1		engine			
laboratory	CeO_2-Alumina	5	0	1	1.6	HC, CO, NO, CO_2, O_2, H_2, H_2O, N_2	100-500 °C	light-off, efficiency, A/F window	[42]
		0	1	0	1.3				
		0	1	0	1.6				
Commercial	Unknown	5	0	1	1.41	engine	FTP	light-off, efficiency, A/F window	[40]
	Unknown	5	0	1					
	Unknown	0	9	1	2.12				
		0	5	1	1.41l				
		0	2	1	0.64				
		0	0	1	0.21				
Commercial	CeO_2-Al_2O_3	0	1	0	2.4	engine, CO,HC,H_2O,CO_2,H_2, O_2	NEDC	light-off, efficiency, A/F window, position	[91]
		0	11	1	2.61				
		0	1	0	3		FTP		
		0	9	1	2.1				

Gragner et. al.[66] pointed out, for catalysts with similar precious metal loading, that according to the light-off temperature, T50, the catalytic activity of Pd-based catalysts varies according to the following sequence:

$Pd/Al_2O_3 < Pd/ZrO_2 < Pd/Zr_{0.75}Ce_{0.25}O_2 < Pd/Zr_{0.50}Ce_{0.50}O_2 < Pd/Zr_{0.25}Ce_{0.75}O_2 < Pd/CeO_2$

Dupez et al [90], using step experiments with laboratory gas classified a set of catalyst with respect to the OSC values in descending order as follows

$Rh/CeO_2\text{-}Al_2O_3 > PtRh/CeO_2\text{-}Al_2O_3 > PdRh/CeO_2\text{-}Al_2O_3 > Pd/CeO_2\text{-}Al2O_3 > Pt/CeO_2\text{-}Al_2O_3 > Rh/Al_2O_3 \approx PtRh/Al_2O_3 > PdRh/Al_2O_3 > Pt/Al_2O_3 \approx Pd/Al2O_3$.

Williamson et. al. [64] reported that Pt is more effective than Pd for saturated HC oxidation, however Pd shows light-off at lower temperatures than Pt.

Lafyatis et. al. [91] tested commercial catalyst upon real driving conditions and concluded that at increased temperatures (during the last part of the EUDC or during the majority of the FTP), Pd-Rh catalyst performance continues to improve while the Pd-only catalyst suffers a drop in NOx conversion.

Finally, Andersen et. al. [40] have shown that Pd:Rh and Pt:Rh catalysts show similar performance when Pd:Rh loading is increased compared to that of Pt:Rh. At similar levels of PML Pt:Rh shows a wider a/F window of operation

In conclusion, this type of experimental results could be classified in an indicative sequential order in respect to the catalytic converter design parameters of interest as shown in

Table 2 Classification of the catalytic activity of each component in respect to the commercial converters design parameters

Design parameter	Activity order	Notes
CO activity	$Pt \geq Pd > Rh$	Supported on $Al_2O_3\text{-}Ce_xZrO_{1-x}$
THC activity	$Pt \geq Pd > Rh$	
NOx activity	$Rh >> Pd \approx Pt$	
Light-off temperature	$Pd \geq Pt > Rh$	
Inhibition at high temperatures	$Pt > Rh > Pd$	
A/F window	Pt:Rh > Pd:Rh	
O_2 storage capacity	$Ce_xZrO_{1-x} > Ce_yZrO_{1-y} > CeO_2$	$x\epsilon(0.5, 0.8)$, $y\epsilon[0,1]\cap(0.5, 0.8)$
NO_2 storage capacity	$K^{+1} > Ba^{+2} > Sr^{+2} \geq Na^{+1} > Ca^{+2} > Li^{+1} > Mg^{+2}$	

1.10 DISCUSSION OF REACTION SCHEMES

Several reaction schemes with increased number of catalytic reactions have been proposed to take place inside a 3WCC. For example, Depckick [92] summarises more than 30 reactions that can be used in a TWC model. A reaction scheme can be reduced or increased accordingly to the assumptions and the objective of the study. A summary of the most important models has already published by Olsson [2] that summarises both apparent and detailed kinetic models. It is important to mention that the number of reactions in the published models varies from 2 [93] (for primitive oxidation catalysts) to 23 [77] reactions. In general, the trend is to increase the number of reactions and consequently the model's degrees of freedom, in real engine tests or complicated mixtures modeling, primarily due to the intrinsic complexity of this type of experiments.

The discussion in this chapter will be closed with a literature based systematic reduction of the reaction scheme, in order to facilitate the formulation of a reaction scheme that will be presented in the next chapter. This is a coupled problem of the competition between reactions, the properties of the exhaust gas (presence of chemical species and temperature ranges) and the type of the catalyst used. There are numerous reactions occurring in the components of an automotive catalyst in literature and almost every reaction that is proposed has been crosschecked under specific operation conditions. What is however their relative activity in automotive catalysis conditions?

To answer this question, the discussion hereafter will present the main reactions that have been proposed in the literature for each one of the main pollutants, that is CO, HC and NO.

CO REACTIONS

CO is known to be oxidized by oxygen over Pt and Pd and by NO over Rh. The latter reaction will be discussed later in this section. CO oxidation with pure oxygen

$$CO + \tfrac{1}{2} O_2 \rightarrow CO_2 \qquad (0.1)$$

has been studied extensively in the past over several catalyst formulations [94] and is considered to proceed according L-H mechanism, where adsorbed CO and oxygen react in a rate-determining surface step [95]. The detailed reaction mechanism

is not part of this study and can be found elsewhere [96]. At high CO concentrations the reaction is being self-inhibited by blocking the active sites for O_2 surface dissociation. Further inhibition comes in increased NO concentrations since the strongest chemisorption of NO hinders the subsequent adsorption of either CO or O2 [96].

CO is also reported to react with water through the water gas shift reaction

$$CO + H_2O \rightarrow CO_2 + H_2 \qquad (0.2)$$

This reaction takes place under deficient oxygen conditions and at elevated temperatures significantly higher than those needed to facilitate direct oxidation [52]. In general, precious metals like Pt, Rh, and Pd are not good shift catalysts because they can not be easily oxidized by water [97]. Palladium based catalysts are known to be more active to this reaction, while Cerium oxide supports enhance the reaction rate. Ceria-supported, transition metals are active catalysts for the water-gas-shift reaction. The mechanism for the reaction involves a RedOx process, with Ceria being oxidized by water and then transferring oxygen to the transition metal to react with adsorbed CO [98].

HC REACTIONS

The large variation of hydrocarbon species in exhaust gas practically hinders a clear definition of the exact path of the hydrocarbons oxidation with oxygen. Literature studies are frequently limited to methane [99], propane and propylene studies as characteristic species of fast and slow oxidizing hydrocarbons. Reaction over the metallic surface likely occurs through a Langmuir–Hinshelwood type with competitive adsorption of methane and oxygen [96]. In most of the studies, two reactions describe the oxidation of hydrocarbons, addressed to the fast and the slow oxidizing HCs. The respective reaction rates differentiate to the kinetic parameters and the chemical properties of the reacting hydrocarbons.

$$C_aH_b + \left(a + \tfrac{b}{4}\right)O_2 \rightarrow aCO_2 + \tfrac{b}{2}H_2O \qquad fast,\ slow \qquad (0.3)$$

Hydrocarbons are also reacting with water under conditions described for the water gas shift reaction. The mechanism of the so-called steam reforming comprises three main steps: (i) dissociative adsorption of the hydrocarbon on the metal, (ii) dissociative adsorption of water on the support and (iii) migration of the OH groups from the support to the metal particles where the surface reaction between a CH,

fragment and a hydroxyl group can occur [85]. Similar to the case of water gas shift, ceria enhances the rate of reaction and palladium seems to be the more active catalyst.

$$C_aH_b + aH_2O \rightarrow aCO + \left(a + \tfrac{b}{2}\right)H_2 \quad (0.4)$$

In general, there is not a clear knowledge about possible inhibition of other HC species in oxidation of HC, both with oxygen and water. NO is known to inhibit both reactions, while the role of water is doubtful as it is also reported to promote conversion of reactants by releasing the surface blocking of the catalyst active sites of CO and C_3H_6.

NO REACTIONS

The reduction of NOx is more complicated. Its existence in exhaust gas at low fractions, complicates the conclusion to a confident reaction mechanism. NOx is known to dissociate over Rh and further be reduced into molecular nitrogen. The basic overall reaction is the reduction of NO by CO (also mentioned and as oxidation of CO by NO).

$$CO + NO \rightarrow CO_2 + \tfrac{1}{2}N_2 \quad (0.5)$$

Several other reactions have been proposed in the literature but do not seem to have a great effect in automotive catalysis [100] [101].

Hydrogen is known to react with NO through the following reactions

$$NO + H_2 \rightarrow H_2O + \tfrac{1}{2}N_2 \quad (0.6)$$

$$NO + 2.5H_2 \rightarrow NH_3 + H_2O \quad (0.7)$$

In general, only traces of NH_3 have been found in exhaust gas downstream the catalytic converter under specific conditions, which means that there is low selectivity of TWC to this reaction. Of course, the high capacity of Rh supported catalysts to decompose NH_3 into its elements [100] plays a key role in this phenomenon.

The competitive reactions of NO with CO and H2 with O2 practically diminishes the rate of H2+NO reaction, as CO and O2 are known to be in larger concentrations in exhaust gas, and move the selectivity of catalytic converter towards the reactions

$$CO + NO \longrightarrow CO_2 + \tfrac{1}{2}N_2$$

$$H_2 + \tfrac{1}{2}O_2 \longrightarrow H_2O$$

NO has also been proposed to react with oxygen to form NO_2 (an important mechanism for NOx traps). This reaction is promoted under specifically designed washcoats and the products are unstable at increased temperatures as determined by the thermodynamical equilibrium. The NO oxidation could be considered negligible in the operation window of 3WCC, but remains an important reaction for the NOx trap modeling.

$$NO + \tfrac{1}{2}O_2 \longleftrightarrow NO_2$$

Other nitrogen oxides (NO_2 and N_2O) are found at very low concentrations in spark ignition engines and could be ignored. Any traces that have been detected, especially during transients, can be considered as intermediate steps of the overall reaction. For example CO + N2O reaction is known to be a very fast intermediate step of CO+NO reaction [102], while it has been pointed that CO+NO reaction dominates in all cases over CO+N2O, except that of low temperatures outside the converter's operation window [103]. A recent review on the mechanisms for catalytical removal of NO [100] pointed out the following:

- For the reduction of NO both with CO or H_2, the best catalysts are those containing Rh. Pd only catalysts has also reported to promote this reaction
- For the reduction of NO with hydrocarbons, the best catalysts are metal zeolites, namely Cu, Co, Ce or even Pt. However, these catalysts exhibit catalytic activity only in a very limited range of temperature, and in addition are extremely sensible to water and different poisons, sulphur again being the principal one. Significant activity of this reaction in TWC under similar to engine compositions of exhaust gas was not reported in other studies (e.g [104])
- The oxygen presence in exhaust gas inhibits the reduction rate of NO

Hydrogen reacts on platinum and palladium through the reaction

$$H_2 + \tfrac{1}{2}O_2 \rightarrow H_2O \qquad (0.8)$$

The oxidation rate of hydrogen is inhibited by CO to approximately the same extent as the oxidation of CO itself [105]

Oxygen storage promoters have a principal role in performance of three way catalytic converters. The oxygen storage-release mechanism is described by Cerium

oxide reduction-oxidation cycling between trivalent and four valent state. Trivalent cerium oxide is oxidized into its four valent state through the reaction commonly accepted by all the researchers

$$Ce_2O_3 + \tfrac{1}{2}O_2 \rightarrow 2CeO_2 \quad (0.9)$$

Several studies [79, [106]] has shown proofs for the significant existence of the further oxidation of ceria by nitrogen monoxide through the reaction

$$Ce_2O_3 + NO \rightarrow 2CeO_2 + \tfrac{1}{2}N_2 \quad (0.10)$$

Nakajutsi et al. [[107]] reported that NO reduction on Rh/OSC material proceeds during the lean operation in two kinds of reaction mechanism: NO decomposition on Rh and NO adsorption on an OSC material, with the contribution of the two mechanisms to the NO removal likely depended on the OSC material.

Oxidised ceria is reduced by CO, a reaction that is present in the majority of the literature models but there is not clear evidence for the existence of this reaction considering the possible co-existence of water gas shift reaction

$$2CeO_2 + CO \rightarrow Ce_2O_3 + CO_2 \quad (0.11)$$

Hydrocarbons are well known to reduce ceria, but this reaction too is coupled with the mechanism of the steam reforming.

$$\left(4a+b\right)CeO_2 + C_aH_b \rightarrow \left(2a+\tfrac{b}{2}\right)Ce_2O_3 + aCO_2 + \tfrac{b}{2}H_2O \quad (0.12)$$

Other components that have been proposed to react with ceria are water and molecular hydrogen. Reaction of ceria with water can be considered as an intermediate step for water gas shift [97, 98] and hydrogen oxidation by ceria can be neglected due to the low activity of the reaction at the temperature range of engines [[108]] and the practical domination of the oxidation of hydrogen over noble metals with oxygen.

Kinetic parameters in respect to the catalyst type can be found in several studies. For example [103, [109], [110], 96] give kinetic values for the set of reactions that are dominant in TWC.

Botas et. Al. [[111]] pointed out that a detailed kinetic scheme for the full exhaust gas mixture is difficult to be proposed, as the composition of the environment by the presence or absence of components provokes important changes in the reaction mechanisms. Taking into account the fact that collection of data reported in literature obtained at a great variety of conditions and with very different reaction mixtures, makes impossible to analyze them kinetically in an accurate way. Kinetic expressions

obtained with binary mixtures, as often reported in literature, have very limited validity to build the whole kinetics occurring in the real automobile converters.

1.11 CONCLUSIONS

In this chapter, a literature review of the principal concepts related with automotive catalysis was carried out. Starting from the current and future legislation, the recent advances in the vehicle technology in the fields of engine, engine management, and exhaust treatment devices were briefly presented. Special attention was given to the washcoat components used in catalytic converters for spark ignition engines. The review of the properties of these materials and the investigation of their behavior when they co-exist in a catalytic washcoat, was the first step in the determination of their major characteristics regarding catalytic converter operation.

This literature review resulted in a ranking of the most common catalytic and storage components impregnated in typical washcoat formulations according to their activity. In addition, it demonstrated the dominant reactions taking place inside the converter. This type of classification of the literature claims is an important step for the support of several assumptions regarding the definition of a proper reaction scheme to model the operation of catalytic converters. The assumptions made in the model employed in this thesis, which are discussed in the next chapter, aim to improve the model robustness, flexibility and applicability over a range of design concepts of modern catalytic converters.

CHAPTER 2

MODEL PRESENTATION

This chapter presents the model that was used in this thesis. The model is an improved version of the CATRAN model [3] that is under continuous development for the last ten years[78]. In this thesis, the most important updates made are at the definition of the effective diffusion of gas to the catalytically active sites and the definition of the reaction rates. Significant progress was made at the clear definition of the reaction schemes and the novel approach for the tuning of the rate expressions coefficients, as a result of the literature study presented here and in chapter 1. Further the use of a general-purpose optimization algorithm and a new definition of the tailor made objective function, which are presented in this chapter (along with the quality assured experimental data (see chapter 3), improved the modeling results. As will be shown in the application of the case studies (chapters 5, 6, 7, 8) current modeling methodology delivers at least equal quality of modeling results, using only three tunable parameters (threefold reduction) and needs about half an hour for the automated tuning of the variables (about 50 times less than the previous version). The development of user friendly GUIs, which are presented in chapter 3 and discussed here, reduced dramatically the time needed to process a case and assured error free data.

2 MODEL PRESENTATION

2.1 INTRODUCTION

In theory, heterogeneous catalysis can be described as a seven-step process:

Step 1: Transport of reactants from the bulk fluid to the fluid-solid interface.

Step 2: Intraparticle transport of reactants into the catalyst particle.

Step 3: Adsorption of reactants at interior of the catalyst particle

Step 4: Chemical reaction of adsorbed reactants to adsorbed products

Step 5: Desorption of adsorbed products

Step 6: Transport of products from the interior sites to the outer surface of the catalyst particle

Step 7: Transport of products from the fluid-solid interface to the bulk fluid stream

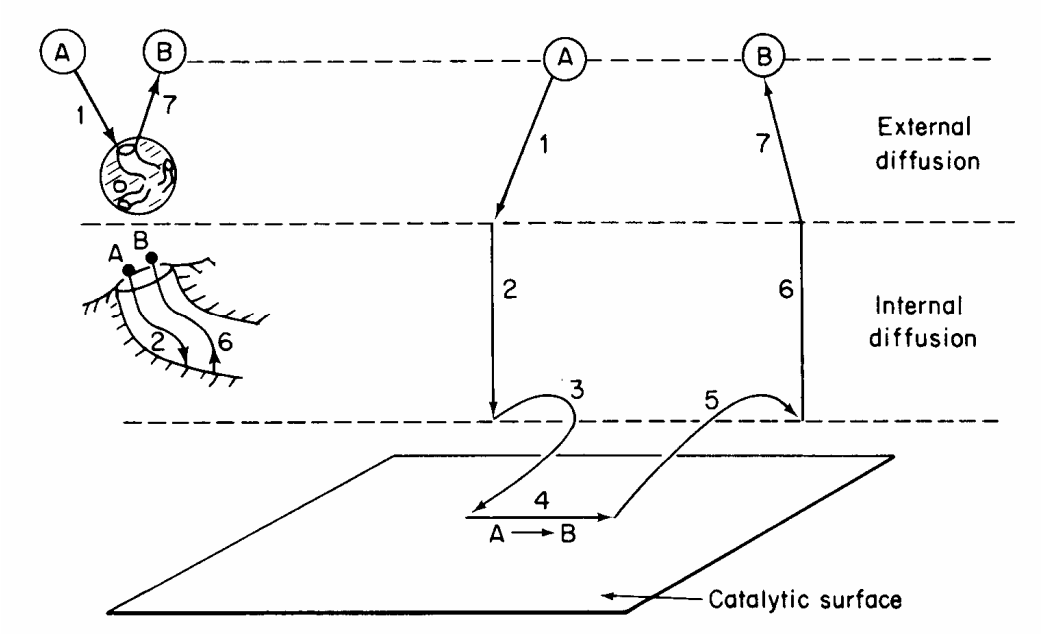

Figure 16 Steps in heterogeneous catalysis

However, this fundamental mechanism, of inherently transient nature, is very difficult to be modeled accurately due to a number of reasons related with the characteristics of both the specific catalyst and washcoat employed and the dynamic characteristics of the gas flow. In general, each automotive catalytic converter is tailor-made to fit the specific characteristics of the associated engine and its position in the exhaust line [88]. This is necessary because the system, comprising the engine, the catalytic converter and the electronic control has to be optimised so as to

minimize negative effects to the engine performance and maximise converter's efficiency [112].

Regarding catalytic converter technologies, several theoretical aspects and design features have to be taken into account in order to model the operation of the catalyst in detail:

- The mechanism of adsorption (direct or precursor mediated), adsorbed molecules characteristics like translation, vibration and rotation and probability of reaction completeness
- Metal-support interactions, catalytic surface orientation, elementary steps of reactions and their relative importance
- Precious metal content, type and ratio, catalyst dispersion into the washcoat.
- Washcoat characteristics like non-uniformities, impurities, exposed area percentage of the impregnated catalyst, type and history of ageing and special manufacturing techniques.
- Oxygen storage characteristics and the role of the promoters implemented into the catalytic washcoat

Most of these aspects are either covered by industrial secrecy (e.g. the exact washcoat formulation of commercial catalysts), or are very difficult to be estimated because of ignorance of the history of catalyst operation (Olsson *et. al.* [2]).

In the last 20 years modeling of catalytic converters has received great attention by a several researchers. The pioneering successful model of Oh and Cavendish [94], based on the apparent kinetics formulated by Voltz [93], has been widely used as the basis of several models and it has been further developed to follow changes in the catalytic technology [77, 78, 113]. The most common modeling approach is 1-D, uses simple balance equations to model the transport phenomena and apparent kinetics expressions for the description of the catalytic reactions.

The more demanding emissions legislation has increased the need to deliver evermore-accurate models for the prediction of the catalytic converter behavior. In the recent years, modeling of catalytic converter has been oriented towards different directions depending on the modeling purpose; research effort has been directed towards the development of very simple and fast control oriented models [62, 114], full scale, accurate but slow models to predict 3-D phenomena [82] and chemistry oriented models to clarify the chemical processes of automotive catalysis [115]. A summary of

them is shown elsewhere [2, 116]. However, if one looks at the main features of the most popular mathematical modeling approaches destined for engineering design of three-way catalytic converters, the following points could be made:

- The gas entering the converter interacts with the solid phase through heat and mass transfer.
- The extent of these interactions is determined by the diffusion or chemical reaction limitations that vary in respect to the dynamics of the exhaust gas and the catalytic converter.
- The modeling of diffusion and/or reaction is made with simplified global mathematical equations and/or complex submodels based in both cases on valid assumptions.
- Models are using tunable parameters to fit the specific system peculiarities.

The detailed review of these models is beyond the scope of this thesis, thus the discussion will be limited in a short comparison of the dominant approaches. Table 3 provides a comparison of an analytical versus a simplified single channel model. Both models can be coupled with a CFD code in order to predict complex flow phenomena, like existing flow maldistribution at the converter's face and channel shape effects [117]. The most important difference between these modeling approaches is their primary scope of their use. Models with analytical solutions for the transport phenomena and complex elementary reactions aim at the understanding of the mechanisms of the catalysis and the precise design of the catalyst particles deposition into the washcoat. The scope of the latter models is completely different; such models aim at the prediction of the operation of the catalytic converter, within a certain good accuracy, in order to assist the engineering design of the exhaust line. Roughly, it can be noted that detailed models are "fundamental research" oriented, while simplified are "engineering" oriented, although this distinction is not always clear and accurate.

At the reactor level modeling, both 1D and multidimensional models have been tested. Nowadays, 1d models are generally preferred because of the simplicity and small sacrifice in accuracy [116]. Thus, the major differences between the engineering and the fundamental research approach appear mainly at the washcoat

and the kinetics level[a]. At the washcoat level, detailed models solve complex coupled differential equations of heat and mass transfer at a great computational cost. Extra computational cost is needed for the solution of the complex reaction scheme with the elementary steps and -in most cases- with "memory" properties for the catalytic surface coverage[b]. It is indicative that in order to model a scheme of three global (apparent) reactions, about 40 elementary reactions are required.

On the other hand, simplified models solve heat and mass transport using the Nusselt and Sherwood approach and assuming no accumulation of species in the solid phase -that is, every mole transported from the exhaust gas to washcoat reacts and desorbs back to the gas flow. The complex chemistry of the autocatalysis is modeled with global apparent reactions, in reduced or extended reaction schemes. For example, Shamim [77] used an extended hybrid reaction scheme of 22 reactions (13 for RedOx and 9 for storage), while Aimard [118] only five.

Both of these approaches use tunable parameters, at least for the reaction scheme. Usually, the reactions' tunable parameters are the pre-exponential factor and the activation energy in the reactions rates expressions. An increase in the number of reactions in a global reaction scheme results in a proportional increase of the tunable parameters, while in a detailed reaction scheme the increase of the tunable parameters is several times greater. The complex nature of autocatalysis model necessitates the tuning of the model for each catalytic converter. The main drawback of this unavoidable procedure is the existing uncertainty when adapting the tuned values of one case to another. The model's flexibility is reduced by this way.

The model that is used in this work belongs to the category of simplified engineering models and features a reduced reaction scheme. This simplification is based on a set of plausible assumptions, which are supported by the results of fundamental studies. In what follows in this chapter, the improvements made in the model are presented along with a methodology for the prediction of the tunable parameters.

[a] See in chapter 1, pp. 46
[b] the term "memory" implies that the model accounts the previous status of the coverage of the catalytically active sites for the calculation of current reaction rates.

Table 3 Comparison of single channel model with detailed kinetics versus simplified model with L-H kinetics

	Single Channel Model	Simplified Model
Kinetics	Extensive/elementary reactions	Reduced pragmatic net reaction rates
Diffusion with reaction	Solving coupled differential equations of reactive mass transport	Weisz (Thiele) modulus approach
Activity profiles	Included	Lumped into net reaction rates
Layers	Included	Lumped into net reaction rates
Heat and Mass transfer	Solving coupled differential equations for heat and mass in the boundary layer of the flow	Nu/Sh approach for the calculation of heat & mass transfer rates at the solid – gas interface.
Cell shape	Included by CFD	Lumped into effectiveness
WC shape	Included by CFD	Lumped into effectiveness
Canning	-	Included
Piping	-	Included
Brick shape	-	Included
Gas distribution	-	Included
Input data	Simple well defined cycles	Typical test cycle modal data (>2Hz)

These improvements aim at the increase of the model's flexibility and robustness[a] as well as applicability to real world case studies. The improvements made in this thesis, which will be discussed hereafter, are focused to the following points:

- Analytical definition of gas properties
- Modified diffusion mechanism
- Definition of reaction schemes and reactions rate expressions
- Extension to model NOx storage converters

[a] The model's usability is promoted through the development of a user friendly GUI.

2.2 OVERVIEW OF THE MODELING LEVELS

The model used in this study is being continuously developed for the last 10 years. Based on the milestone work of Oh and Cavendish [94], the model has been extensively validated [1, 119] and recently extended with an analytical oxygen storage submodel [3]. In a short, the model is a one-dimensional catalytic converter model, which uses semi-empirical coupled equations and simple mechanisms for the gas properties, the heat and the mass transfer. At the washcoat level, it uses an effective diffusion approximation and the storage processes are solved analytically. At the kinetic level, it uses global reactions with apparent rates of Arrhenius and Langmuir-Hinshelwood type. The basic features of the model are listed below [3]:

– Transient, one-dimensional temperature profile for the solid phase of the converter.

– Quasi-steady, 1D computation of temperature and concentration axial distributions for the gaseous phase

– Simplified reaction scheme featuring a minimum set of redox reactions

– Use of simple submodels for oxygen and NOx storage processes.

The model accounts for a gas flow consisted of the species N_2, CO, O_2, CO_2, H_2O, H_2, THC, NO, NO_2 .

Below, the detailed description of model formulation is given for the four modelling levels:

- Reactor Level
- Channel Level
- Washcoat Level
- Kinetics Level

REACTOR LEVEL MODELLING

At the reactor level modeling, heat transfer between channels and between the reactor and its surrounding are modeled. The principal issue here is to decide if one-, two- or three-dimensional modeling of the heat transfer should be employed.

The reactor model presented in this work is a one-dimensional heat transfer model for the transient heat conduction in the monolith. Heat losses to the environment via convection and radiation are also taken into account. Its primary assumptions are the following:

– Heat losses from the front and the rear face of the monolith are neglected. (To our knowledge, this is the case with all models that have appeared in the literature.)

– Since the catalytic converter is always insulated, simpler models approximate the convert as adiabatic. Heat losses to the surrounding are taken into account but, owing to the model's 1D nature, they are inevitably distributed uniformly in each monolith's cross-section.

– Flow rate and temperature profiles of the exhaust gas at the inlet of the filter are considered uniform. An average value for flow rate and temperature is measured, and gas flow is distributed uniformly to each channel.

The temperature field in the converter is described by the equation of transient heat conduction in one-dimension, with heat sources being convection from the exhaust gas, the enthalpy released from the reactions and convection to ambient air.

$$\rho_s c_{p,s} \frac{\partial T_s}{\partial t} = k_{s,z} \frac{\partial^2 T_s}{\partial z^2} + hS\left(T_g - T_s\right) + \sum_{k=1}^{N_R} \left(-\Delta H_k\right) r_k + Q_{amb} \qquad (1)$$

Finally, the boundary condition needed for the solution of the heat conduction equation refers to the heat losses to ambient air:

$$Q_{amb} = S_{mon}\left[h_{amb}\left(T_s - T_{amb}\right) + \varepsilon\sigma\left(T_s^4 - T_{amb}^4\right)\right] \qquad (2)$$

Two- and three- dimensional reactor models have also appeared in the literature, e.g. the models of Heck et al. [120]; Chen et al. [121]; Zygourakis [122]; Jahn et al. [123]. These models are indispensable if the exhaust gas at the converter inlet exhibits a severely non-uniform flow profile but also require mass flow rate and temperature profiles at the inlet of the catalytic converter. Such data are not usually available in routine engine-bench or driving cycle converter tests, which are the main application field for our model. Therefore, the 1D approach is preferred, since

its modeling detail matches routine input data quality, provides sufficient accuracy and has low computational power requirements.

CHANNEL LEVEL MODELLING

For the formulation of the channel-level model, two usual simplifications are employed [124, 125], namely:

- The axial diffusion of mass and heat in the gas phase is negligible.
- The mass and heat accumulation in the gas phase is negligible. (This comprises the assumption for the quasi-steady state nature of the problem.)

The first assumption is generally accepted and is employed in most models, e.g. those of Chen et al. [121] and Siemund et al. [125]. Bulk flow is approximated with plug flow with uniform temperature T_g and species concentrations c_j. The velocity of the flow readily results from the mass flow rate: $u_z = 4\dot{m}/\left(\rho\pi d_h^2\right)$. An effective boundary layer mass transfer is accounted for, using a mass transfer coefficient k_m, which is a function of the Sherwood number. The definition of the effective diffusion and an updated calculation of the Sherwood number are presented later in this chapter (section 2.3).

The second assumption is more controversial and both the quasi-steady and the transient approach have been tested in the literature. Shamim et al. [77] have presented a model that incorporates transient terms at channel level modeling. On the other hand, Young & Finlayson [126] and Oh & Cavendish [94] argue about the validity of the quasi-steady approximation. They provide justification on the basis of the large ratio of thermal to mass time constants of the problem. Following this line of thought, the quasi-steady approach is used here as well, for simplicity and low computational cost.

In order to write the mass balance for the exhaust gas, a mean bulk value c_j is employed for the gas–phase concentration of each species. Likewise, a value $c_{s,j}$ is considered for the concentration of each species at the solid-gas interface. Using the quasi-steady state approximation and neglecting diffusion and accumulation terms, the mass balance for the gas phase becomes:

$$\rho_g u_z \frac{\partial c_j(z)}{\partial z} = \rho_g k_{m,j} S\left(c_j(z) - c_{s,j}(z)\right) \tag{3}$$

Similarly to the above, a mean bulk value T_g is used for the exhaust gas temperature, and a solid phase temperature T_s is introduced for the monolith and the solid–gas interface. Energy is transferred to and from the exhaust gas only due to convection with the channel walls. Thus, the energy balance for the gas phase becomes:

$$\rho_s c_p u_z \frac{\partial T_g(z)}{\partial z} = hS\left(T_s(z) - T_g(z)\right) \tag{4}$$

Parameter h is the heat transfer coefficient and is calculated as a function of the Nusselt dimensionless number.

Finally, the boundary conditions for the temperature, mass flow rate and concentrations are given from measurement at the converter's inlet:

$$\begin{aligned} c_j(t, z=0) &= c_{j,in}(t) \\ T_g(t, z=0) &= T_{g,in}(t) \\ \dot{m}(t, z=0) &= \dot{m}_{in}(t) \end{aligned} \tag{5}$$

WASHCOAT LEVEL MODELLING

The first task of washcoat modelling is to define how the simultaneous phenomena of diffusion and reaction in the washcoat will be taken into account. What will be adopted in this work is the "film model" approach, which approximates the washcoat with a solid–gas interface, where it is assumed that all reactions occur. This approximation essentially neglects diffusion effects completely, and assumes that all catalytically active cites are directly available to gaseous-phase species at this solid–gas interface.

This has been questioned by Zygourakis & Aris [105] and Hayes & Kolaczkowski [127]. They provide evidence that concentration gradients in the washcoat are present and may significantly affect the operation of the monolithic converter, especially in high temperatures. Nevertheless, significant complexity is introduced in the models in order to explicitly consider diffusion in the washcoat. Therefore, washcoat diffusion is not implemented here and its effect is lumped into the kinetic parameters of the model.

The approximation for the solid–gas interface states that all species that diffuse to it through the boundary layer, are removed from the gas phase due to reactions:

$$\frac{\rho_g}{M_g} k_{m,j} S\left(c_j - c_{j,s}\right) = R_j \qquad (6)$$

The left hand side of the above equation describes mass transfer through the boundary layer of the gas flow. Parameter k_m is the mass transfer coefficient in the boundary layer, c_j denotes species concentration at the gaseous phase and $c_{s,j}$ is corresponding concentration at the gas–solid interface. S is the geometrical surface area of the washcoat, i.e. channel wall area per channel volume. For a channel with hydraulic diameter d_h, we readily find: $S = 4/d_h$.

On the right hand side of (6), the rate R_j refers to the production or consumption of each species at the solid–gas interface. For N_R reactions, each taking place with a rate r_k, the rate of consumption or production of a species j is:

$$R_{rea,j} = \delta \gamma S \sum_{k=1}^{N_R} \left(a_{j,k}\, r_k\right) \qquad (7)$$

where $a_{j,k}$ is the stoichiometric coefficient of species j in reaction k, δ is the washcoat thickness and γ is the specific catalyst area, i.e. catalytically active area per washcoat volume.

Adsorption and desorption of chemical species in the catalytic surface are dealing with the surface coverage, that can be either promoting or inhibiting for the reaction. This effect is modeled in a simple way by the inhibition factors of Voltz [93], that are derived from experimental data on Pt – alumina catalysts that were prepared in such a way to minimize intraparticle diffusion. In lack of any similar data for the case of Rh or Pd, we are not using any inhibition term for the reactions on these noble metals.

As regards as oxygen and nitrogen oxides storage dynamics (reactions on Ceria and Barium Oxides respectively) we use a first order differential equation defined by Pontikakis [3] with updated kinetic terms for reactions

$$\frac{d\psi}{dt} = aox\left(1-\psi\right) - ared\,\psi$$

This approximation is valid if we assume that the role of the bulk layers is negligible in oxygen storage compared to the surface layer [57] that is in accordance with the film model approach we use in our model. Recent researches have shown the importance of the oxygen diffusion in ceria lattice from the surface to the solid bulk under several cases [90, 128]. Evidences of this have been expressed in the past by expressing the total oxygen capacity as a function of temperature e.g. [56, 54]. There are

also strong indications that the activity of the ceria is strongly affected by the position of ceria particles in relevance to the PGM particles [90, 34].

The second task of washcoat modelling is to choose a reaction scheme and the appropriate expressions for the reaction rates r_k. We opt for overall reactions, because they provide the user with a more compact and comprehensible reaction scheme and they are computationally less expensive. Here, the three-way catalytic converter and NOx trap will be considered, which are designed for spark-ignition engines exhaust. Below, we briefly discuss what we choose to implement in these cases.

KINETICS LEVEL MODELLING - THREE WAY CATALYTIC CONVERTER

In the present model, the oxidation reactions rates of CO and HC are based on the expressions by Voltz et al. [93]. It is interesting to note that the expressions developed by Voltz et al about 30 years ago for a Pt oxidation catalyst, continue to be successful, with little variation, in describing the performance of Pt:Rh, Pd, Pd:Rh and even tri-metal catalysts. For the HC oxidation, we have to note the real exhaust gas contains a very complex mixture of several hundreds of different hydrocarbon species with variability in composition depending on the driving conditions [129]. In practice, the diversity of the HC mixture is usually taken into account by considering two categories of hydrocarbons, each being oxidized in different temperature: an easily oxidizing HC ("fast" HC), and a less-easily oxidizing HC ("slow" HC) [ ]. Here, the "fast" HC is represented by propene (C_3H_6) and the "slow" HC is represented by propane (C_3H_8). In practice, only the total hydrocarbon content of the exhaust is measured. Throughout this work, considering the ignorance of the exact data for THC mixture and in order to avoid any superfluous complexity, we have chosen to model the THC using a single artificial species (C_7H_{13}), which has a ratio of hydrogen to carbon atoms equal to the overall ratio measured in typical exhaust gas. This choice does not introduce significant errors, as will be shown in the application's part of this thesis.

For the reaction between CO and NO we select a simple Arrhenius type expression, considering the lack of a systematic work towards the definition of possible inhibition terms. Of course, the results of Koberstein and Wannemacher [130] for example, predict that the reaction order for CO in the CO–NO reaction tends to unity as the reactants' concentrations tend to vanish. In this thesis, it is assumed that all catalytic reactions are first order reactions. Finally, hydrogen oxidation is also included in the model.

Apart from the RedOx reactions, oxygen storage phenomena have a key role in the efficiency of the 3WCC. Oxygen storage occurs on the Ceria (Ce), which is contained in large quantities in the catalyst's washcoat (at the order of 30% wt). Under net oxidizing conditions, 3-valent Ce oxide (Ce_2O_3) may react with O_2, NO or H_2O and oxidize to its 4-valent state (CeO_2). Under net reducing conditions, CeO_2 may function as an oxidizing agent for CO, HC and H_2. This redOx function of Ceria

practically smooths the intense variation of the oxygen concentration in the exhaust gas.

Oxygen storage is taken into account by a reaction scheme that consists of four reactions, which account for a) Ce_2O_3 oxidation by O_2 and NO, and b) CeO_2 reduction by CO and hydrocarbons. The model uses the auxiliary quantity ψ_{O2} to express the fractional extent of oxidation of the oxygen storage component. It is defined as:

$$\psi_{O_2} = \frac{2 \times \text{moles } CeO_2}{2 \times \text{moles } CeO_2 + \text{moles } Ce_2O_3} \tag{8}$$

The extent of oxidation ψ_{O2} is continuously changing during the transient converter operation. Its value is affected by the relative reaction rates of reactions 5-8. The rates of reactions, also given in Table 4, are expected to be linear functions of ψ_{O2}. Specifically, the oxidation rate of the oxygen storage component is assumed proportional to the active sites of Ce_2O_3, i.e. to $\Psi_{cap}(1-\psi_{O2})$. On the other hand, the oxidation rate of CO and HC by CeO_2 is assumed proportional to ($\Psi_{cap}\ \psi_{O2}$). Moreover, the rates of these reactions should be linearly dependent on the local concentration of the corresponding gaseous phase reactant.

The rate of variation of ψ_{O2} is the difference between the rate that Ce_2O_3 is oxidized and reduced:

$$\frac{d\psi}{dt} = -\frac{r_5 + r_6}{\Psi_{cap}} + \frac{r_7 + r_8}{\Psi_{cap}} \tag{9}$$

The updated model includes an analytical solution for equation (4) for ψ_{O2} at each node along the catalyst channels.

We assume that these reactions are the dominant ones and, although several other catalytic reactions exist (as it has been noted for example by Olsson [2]), they have negligible effects or are too slow to compete with the dominant reactions. The reactions and the definition of the respective rates are shown in Table 4 and discussed in section 2.4.

We also assume a constant value of 600 mol/m^3 washcoat as the standard oxygen storage capacity of a typical converter in this study. This value is consistent with the given values in literature [34].

Finally, we standardize the values of activation energies that are shown in Table 4 and tune only the three pre-exponential factors A_{Pt}, A_{Rh} and A_{Ce}, one per

each precious metal implemented in the catalytic washcoat. The rationale for this choice is explained in section 2.4. We just note here that the values of the activation energies are selected in a somehow arbitrary way, taking into account that for heterogeneous catalysis over platinum group metals the activation energies are known to be about 90000 J/kmol [131].

Table 4 Reaction scheme and rate expressions of the 3WCC model

		Reaction	Rate expression
Reduction - Oxidation reactions	1	$CO + \frac{1}{2}O_2 \longrightarrow CO_2$	$r_{Pt} = \frac{A_{Pt} T e^{-E_{Pt}/R_g T} c_{CO} c_{O_2}}{G}$
	2	$H_2 + \frac{1}{2}O_2 \longrightarrow H_2O$	$r_{Pt} = \frac{A_{Pt} T e^{-E_{Pt}/R_g T} c_{H_2} c_{O_2}}{G}$
	3	$C_\alpha H_\beta + (\alpha + 0.25\beta)O_2 \longrightarrow \alpha CO_2 + 0.5\beta H_2O$	$r_{Pt} = \frac{A_{Pt} T e^{-E_{Pt}/R_g T} c_{C_\alpha H_\beta} c_{O_2}}{G}$
	4	$2CO + 2NO \longrightarrow 2CO_2 + N_2$	$r_{Rh} = A_{Rh} T e^{-E_{Rh}/R_g T} c_{CO} c_{NO}$
Oxygen storage reactions	5	$2CeO_2 + CO \longrightarrow Ce_2O_3 + CO_2$	$r_{Ce} = A_{Ce} T e^{-E_{Ce}/R_g T} c_{CO} \psi \Psi_{cap}$
	6	$C_\alpha H_\beta + (2\alpha + \beta)CeO_2 \longrightarrow \longrightarrow (\alpha + 0.5\beta)Ce_2O_3 + \alpha CO_2 + 0.5\beta H_2O$	$r_{Ce} = A_{Ce} T e^{-E_{Ce}/R_g T} c_{C_a H_\beta} \psi \Psi_{cap}$
	7	$Ce_2O_3 + \frac{1}{2}O_2 \longrightarrow 2CeO_2$	$r_{Ce} = A_{Ce} T e^{-E_{Ce}/R_g T} c_{O_2} (1-\psi) \Psi_{cap}$
	8	$Ce_2O_3 + NO \longrightarrow 2CeO_2 + \frac{1}{2}N_2$	$r_{Ce} = A_{Ce} T e^{-E_{Ce}/R_g T} c_{NO} (1-\psi) \Psi_{cap}$
Inhibition term		$G = T(1 + K_1 c_{CO} + K_2 c_{CxHy})^2 (1 + K_3 c_{CO}^2 c_{CxHy}^2)(1 + K_4 c_{NO}^{0.7}),\ K_i = k_i \exp(-E_i / R_g T)$	
		k1 = 65.5	k2 = 2080	k3 = 3.98	k4 = 4.79·105
		E1 = −7990	E2 = −3000	E3 = −96534	E4 = 31036
Auxiliary quantities		$\psi_{O_2} = \frac{2 \times \text{moles } CeO_2}{2 \times \text{moles } CeO_2 + \text{moles } Ce_2O_3}$, $\frac{d\psi_{O_2}}{dt} = -\frac{r_5 + r_6}{\Psi_{O_2}} + \frac{r_7 + r_8}{\Psi_{O_2}}$	
		$E_{Pt} = 90000 KJ/kmol$, $E_{Rh} = 95000 KJ/kmol$, $E_{Ce} = 120000 KJ/kmol$	

KINETICS LEVEL MODELLING - NOX ADSORBERS

The operation of the NOx trap is well described by a RedOx reaction scheme extended with proper reactions for the NOx storage processes and the oxidation of NO to NO_2. The selected reaction scheme includes seven reactions; five for the description of the RedOx chemical scheme and two for the nitrogen dioxide storage processes. The reactions and the definition of the respective rates, as already discussed in the previous sections, are shown in Table 5.

Special attention must be paid at the reactions 4 and 6. These reactions are modeled as reversible reactions, in order to predict the thermodynamic equilibrium of NO-NO_2 and the $Ba(NO_3)_2$ decomposition. The NO_2 decomposition occurs via homogeneous gas phase reaction due to thermodynamic instabilities of NO_2 at increased temperatures. The choice of a single reversible reaction was made in order to avoid any superfluous complexity. Figure 17 shows the experimentally studied behavior of this reaction over Pt versus temperature and the successful match of our model. The NO oxidation is a crucial reaction for the efficient operation of the NOx traps, considering that NO storage at Barium oxides is almost negligible. Obviously, the narrow temperature window of this reaction has to be matched with the temperature window of gas at inlet.

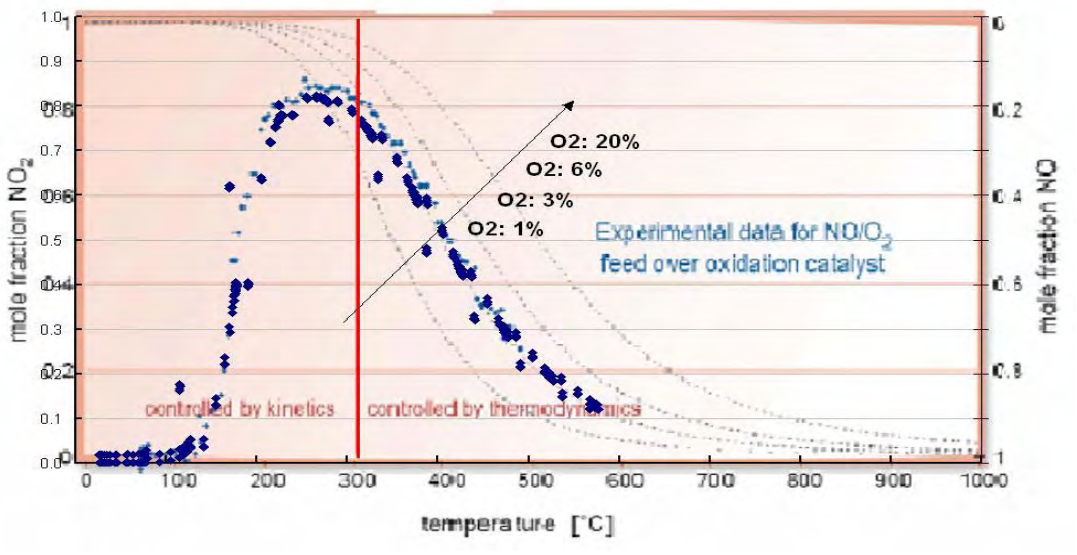

Figure 17 Temperature ramp experiments for the reaction NO+O2<->NO2 over Pt catalyst. The data of the figure adopted by [132] (light –blue squares) is matched by our model (green squares). The model assumed an elementary Pt catalyst with N_2(balance) - O_2(3%) - NO(various) inlet composition.

The $Ba(NO_3)_2$ thermal decomposition due to thermodynamic instabilities of barium nitrates at increased temperatures is modeled by means of a reversible reaction for the storage process. The rate of the reverse reaction is defined by means of the equilibrium term, which practically determines the temperature of initiation of barium nitrates' decomposition.

Finally, a constant value of 250 mol/m^3 washcoat is assumed as the standard nitrogen oxides storage capacity of a typical converter in this study. This value is consistent with the values reported in the literature [133].

The NO_2 storage submodel is adopted from the oxygen storage submodel that was presented above for the three-way catalytic converter. The reaction scheme consists of two reactions which account for a) BaO oxidation by O_2 and NO_2, and b) $Ba(NO_3)_2$ reduction by CO. The model uses the auxiliary quantity ψ_{NO} to express the fractional extent of oxidation of the barium oxides. It is defined as:

$$\psi_{NO} = \frac{\text{moles Ba}\left(\text{NO}_3\right)_2}{\text{moles Ba}\left(\text{NO}_3\right)_2 + \text{moles BaO}} \tag{10}$$

The extent of oxidation ψ_{NO} is continuously changing during transient converter operation. Its value is affected by the relative reaction rates of reactions 6 and 7. The rates of reactions, also given in Table 5, are expected to be linear functions of ψ_{NO}. As described for the oxygen storage model the storage rate is assumed proportional to the $\Psi_{cap}(1-\psi_{NO})$ product and the release rate to the $\Psi_{cap}\psi_{NO}$. The rate of variation of ψ_{NO} is the difference between the rate that BaO is oxidized and reduced:

$$\frac{d\psi_{NO}}{dt} = \frac{r_6}{\Psi_{NO}} - \frac{r_7}{\Psi_{NO}} \tag{11}$$

The updated model includes an analytical solution for equation (4) for ψ_{NO} at each node along the catalyst channels.

Similar to the three way applications, the values of activation energies, shown in Table 5, are fixed and only the three pre-exponential factors A_{Pt}, A_{Rh} and A_{Ba}, one per each precious metal implemented in the catalytic washcoat, are tuned.

Table 5 Reaction scheme and rate expressions of the NOx adsorber catalyst model

		Reaction	Rate expression
Reduction - Oxidation reactions	4	$CO+\frac{1}{2}O_2 \xrightarrow{Pt} CO_2$	$r_{Pt}=\frac{A_{Pt}T\,e^{-E_{Pt}/R_gT}c_{CO}c_{O_2}}{G}$
	5	$H_2+\frac{1}{2}O_2 \xrightarrow{Pt} H_2O$	$r_{Pt}=\frac{A_{Pt}Te^{-E_{Pt}/R_gT}c_{H_2}c_{O_2}}{G}$
	6	$C_\alpha H_\beta+(\alpha+0.25\beta)O_2 \xrightarrow{Pt} \alpha\ CO_2+0.5\beta\ H_2O$	$r_{Pt}=\frac{A_{Pt}Te^{-E_{Pt}/R_gT}c_{C_\alpha H_\beta}c_{O_2}}{G}$
	4	$NO+\frac{1}{2}O_2 \underset{homo}{\overset{Pt}{\rightleftharpoons}} NO_2$	$r_{Pt}=\frac{A_{Pt}Te^{-E_{Pt}/R_gT}c_{NO}c_{O_2}}{G}\left(1-\frac{1}{K_{eq,4}}\right)$
	5	$2CO+2NO \xrightarrow{Rh} 2CO_2+N_2$	$r_{Rh}=A_{Rh}Te^{-E_{Rh}/R_gT}c_{CO}c_{NO}$
NO storage reactions	6	$BaO+2NO_2+\frac{1}{2}O_2 \rightarrow Ba(NO_3)_2$	$r_{Ba}=ATe^{-E_{Ba}/R_cT}c_{NO_2}c_{O_2}\psi_{NO}\Psi_{NO}$
	7	$Ba(NO_3)_2 \rightarrow BaO+2NO_2+\frac{1}{2}O_2$	$r_{Ba}=ATe^{-E_{Ba}/R_cT}\psi_{NO}\Psi_{NO}$
	8	$Ba(NO_3)_2+3CO \longrightarrow BaO+2NO+3CO_2$	$r_{Ba}=ATe^{-E_{Ba}/R_cT}c_{CO}(1-\psi_{NO})\Psi_{NO}$
Inhibition term		$G=T(1+K_1c_{CO}+K_2c_{CxHy})^2(1+K_3c_{CO}^2c_{CxHy}^2)(1+K_4c_{NO}^{0.7}),\ K_i=k_i\exp(-E_i/R_gT)$	
		k1 = 65.5	k2 = 2080	k3 = 3.98	k4 = 4.79·105
		E1 = −7990	E2 = −3000	E3 = −96534	E4 = 31036
Auxiliary quantities		$\psi_{NO}=\frac{\text{moles Ba}(NO_3)_2}{\text{moles Ba}(NO_3)_2+\text{moles BaO}}$,	$\frac{d\psi_{NO}}{dt}=\frac{r_6}{\Psi_{NO}}-\frac{r_7}{\Psi_{NO}}$	$K_{eq,i}=-\frac{\Delta G_i}{RT}$
		$E_{Pt}=90000KJ/kmol$, $E_{Rh}=95000KJ/kmol$, $E_{Ba}=120000KJ/kmol$		

2.3 UPDATES – DEFINITIONS OF GAS SPECIES PROPERTIES

The use of semiempirical expressions based on temperature for gas properties is introducing significant errors if we consider the dynamic variation of the gas composition at the catalyst inlet, as well as the variations along the catalytic converter due to chemical reactions. The equations used in the updated model are based on temperature, pressure and gas composition at each node and are coming from the well known kinetic theory of gases. Their main advantage is that they incorporate the concentration at each node, instead of semi-empirical relations that are precise functions of pressure and temperature only.

For a species i diffusion in a gas mixture, the effective diffusivity can be calculated from a knowledge of all of the relevant binary diffusion coefficients D_{ij} governing encounters with species j (j≠i), where [134]

$$D_{ij} = \frac{3k_B T}{8p} \cdot \left[\frac{k_B T}{2\pi} \left(\frac{1}{m_i} + \frac{1}{m_j} \right) \right]^{1/2} \cdot \frac{1}{\sigma_{ij}^2 \Omega_D \left\{ k_B T / \varepsilon_{ij} \right\}}$$

and the diffusivity into mixture [134]

$$D_{i-mix} \approx (1 - y_i) \cdot \left[\sum_{\substack{j=1, \\ j \neq i}}^{N} \frac{y_j}{D_{ij}} \right]^{-1} \qquad for\ N \geq 3$$

The kinetic theory of gases provides the following explicit expression for the dynamic viscosity of a pure gas [134]

$$\mu_i = \frac{5(\pi m_i k_B T)^{1/2}}{16\pi\sigma_i^2 \Omega_\mu \left\{ k_B T / \varepsilon_{ij} \right\}}$$

The specific heat of each species is calculated as a polynomial function of temperature

$$C_{p,i} = A_{i,1} + A_{i,2} T^2 + A_{i,3} T^3 + A_{i,4} T^4$$

Kinetic theory also provides a reliable theoretical formalism for pure gases conductivity

$$k_i \approx \frac{15}{4} \cdot \frac{R}{M_i} \mu_i \left[1 + \frac{4}{15} \left(\frac{C_p}{R} - \frac{5}{2} \right) \right]$$

and the mixture properties are calculated using a "square-root rule"

2.4 UPDATES – SIMPLIFIED MODEL FOR EFFECTIVE MASS TRANSFER

Conversion in catalytic reactors is practically a complex competition among mass transport of the chemical species from gas phase to catalytically active sites and reaction speed. The complete catalytic conversion of chemical specie, present in a gas flow inside a catalytic reactor, into specific products (e.g. CO to CO_2) could be limited because of:

- The coexistence of a side homogeneous reaction leading to different products (for example reaction of NO with O_2 over Pt that will be discussed later)
- Limitation from boundary layer mass transfer, which occurring at increased flow rates and/or temperatures
- Significant pore diffusion limitations, which stands for deep bed catalysis
- Limitations due to insufficient reaction rate primarily due to low temperature or species inhibition

Of course, a surface reaction includes several elementary steps that define the intrinsic rate of a global reaction and are depended on surface coverage also. The theoretical extent of these cases versus temperatures is schematically presented in the Arrhenius plot shown in Figure 18

The problem of diffusion of gas phase in catalytically active washcoats has been extensively discussed [135, 136]. Several approaches vary from the development of more complex, but precise diffusion models [137], to the total omittance of the diffusion into the washcoat, assuming small solid diffusion length (washcoat thickness) compared to the bulk diffusion length (internal channel radius).

For a gas mixture flowing through a channel the mass transfer from the bulk phase to the solid is described by the following mechanisms

a) External mass transfer through boundary layer from gas phase to the solid-gas interphase

b) Intraphase diffusion of species into the porous solid that includes macropore, mesopore and micropore diffusion.

Micropore diffusion or surface diffusion occurs for pore diameter less than 2nm and has exponential temperature dependence.

Mesopore diffusion occurs for pore diameters 2<dp<50nm and is described by Knudsen diffusion through porous solids.

Macropore diffusion occurs in large pores typically greater than 50nm and is described by the same principles as bulk diffusion.

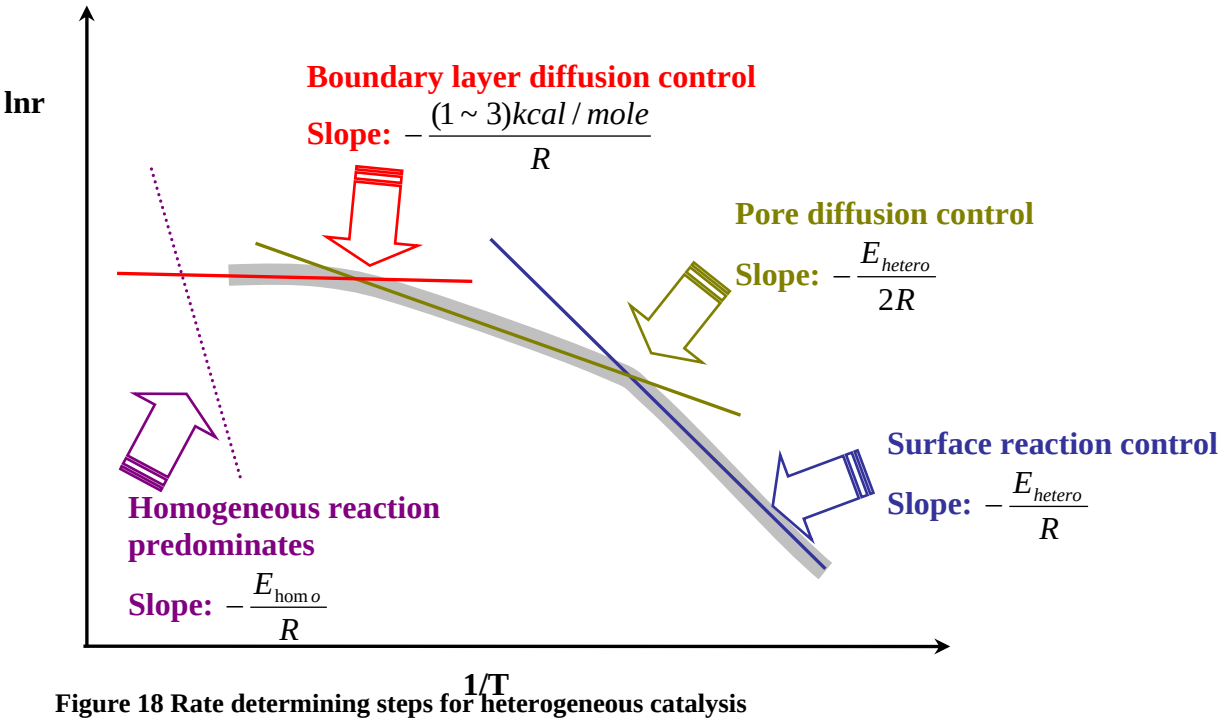

Figure 18 Rate determining steps for heterogeneous catalysis

Typical sizes of pore diameter in commercial 3WCC are ranging from 6.5nm to 200nm [[138]], thus micropore diffusion can be neglected. Macropore and mesopore diffusion can be assumed as parallel mechanisms weighted by the pore diameter distribution of the washcoat. This parallel mechanism can be described by an electrical equivalent of one resistance for the convective mass transfer from gas to solid-gas interface connected in serial with a system of parallel resistances for macropore and mesopore diffusion into solid phase.

The overall resistance per specie j of the circuit is equal to

$$R_{tot,j} = R_{gas,j} + \frac{R_{macro,j} + R_{meso,j}}{R_{macro,j} R_{meso,j}}$$

In each case, diffusion resistance is calculated by the definition of Sherwood number

$$R_{ij} = \frac{L_j}{Sh_{ij} \cdot D_{ij,eff}}$$

where Sh the Sherwood number, D_{eff} the effective diffusivity and L the characteristic length, i=1,2,…15 the chemical species, j=1,2,3 stands for gas, macroporous and mesoporous diffusion respectively.

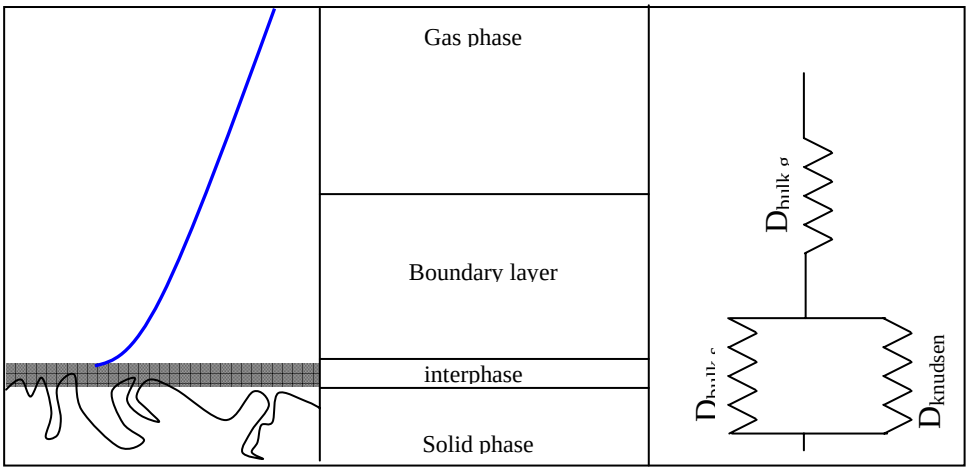

Figure 19 Schematic representation of the modes of gas diffusion in the solid phase for commercial 3WCC.

It is definitely clear that the solid phase diffusion becomes important when compared to the bulk diffusion, when the washcoat thickness is similar to the channel internal diameter. This stands for two cases; the case of intraphase diffusion to the corners of the channel and the case of high channel density (thin-walled catalytic converters).

The relationship of Hawthorn defines an average Sherwood number for the entire converter's length and is not recommended for the estimation of local Sherwood number [139]. The model presented here employs a more accurate local Sherwood number calculation. The local Sherwood number can be expressed explicitly as function of the transverse Peclet number and the channel shape [140]. Considering that the researchers are giving shape constants for the two limiting cases of Sc=0 and Sc=∞ [141], local Sherwood number is calculated by linear interpolation between these two cases.

$$Sh(P) = 4\frac{\sum_{i=1}^{\infty} a_i \phi_i \exp(-\phi_i / P)}{\sum_{i=1}^{\infty} a_i \exp(-\phi_i / P)}$$

where a_i and ϕ_i are constants for fully developed laminar in respect to the channel shape. This correlation shows good agreement with experimental results of several researchers and is more flexible for other channel geometries compared to the previously used correlation of Hawthorn [142]

An important aspect is the definition of the rate determining step in a catalytic process, among the diffusion limitation and the reaction limitation. The diffusion limitation is depended primarily on the washcoat characteristics (exchange area, pore diameter distribution, etc.), the channel density and the converter's volume, while a reaction limitation is depended primarily on temperature, gas chemical composition and catalytic component characteristics (loading, dispersion, deposition, etc.). In both cases, the parameters involved are crucial design parameters of the entire exhaust aftertreatment system (engine - engine management – catalytic converter). A calculation based on catalytic converter utilization factors is presented in Appendix A

2.5 UPDATES - REACTION RATE EXPRESSIONS

A crucial issue of catalytic converters modelling is the definition of the reaction rates. Considering the ignorance of the catalytic surface structure, the history of the catalyst (ageing and pretreatment), the exact preparation procedure and of course the lack of a confident detailed reaction mechanism, it is impossible to define an accurate reaction scheme describing exactly the phenomena. From an engineering point of view, CATRAN models the catalytic reactions with a global reaction scheme that uses tunable parameters. This approach aims to compensate this lack of knowledge at the kinetic level of modeling.

Previous studies have shown that such an approach is able to predict the function of a specific catalyst under real engine conditions [3], while it has been reported that global reactions allow a satisfying fit compared to a detailed reaction scheme [143]. CATRAN uses Arrhenius and Langmuir-Hinshelwood type expressions for the definition of the reaction rates of global reactions, setting as tunable parameters the apparent pre-exponential factor and the apparent activation energy of each reaction. In what follows, a systematic effort is presented to reduce the number of tunable parameters.

In the present model, the expressions of the apparent pre-exponential factors have been changed to conform to the Eyring theory. Both the Eyring and the collision theory predict a temperature dependence of the re-exponential factor with temperature [145]. Eyring theory states that the reaction of adsorbed species, on a catalytic surface, occurs via the production of an activated complex. The reaction proceeds only in the forward direction over the energy barrier and the step of the activated complex production can be assumed as the rate determining step. The rate of the reaction is a function of the temperature and the partition functions of molecular characteristics (translation, vibration, rotation)

$$R = \frac{k_B T}{h} \cdot \frac{q^{\#}}{q} \cdot e^{\left(-\frac{E_b}{k_B T}\right)}$$

This rate equation can be rewritten in Arrhenius type form with apparent pre-exponential factor and apparent activation energy as

$$R = ATe^{-E/RT}$$

The apparent pre-exponential factor lumps all the molecular characteristics. In this apparent rate definition, we have two unknown adjustable variables, the

apparent pre-exponential factor A and the apparent activation energy E. These factors have to be tuned in order to fit the behavior of the catalyst under test.

In the current approach, the washcoat is treated as a black-box with complete ignorance of the special characteristics and the details of the phenomena taking place there. All the unknown characteristics are lumped into the parameters A and E.

As a principle, we consider that the catalytic reaction is instantaneous and that the rate determining step of the process is the adsorption of the reactants at the catalytic surface. The latter is related to the washcoat characteristics and the type of catalyst only. If we account that the washcoat is the same for all the reactants but the reactions are taking place over specific catalysts, we can separate the reaction scheme into groups of reactions with similar characteristics, like the catalyst type over which they occur and the individual reaction mechanism (for example oxidation reactions over platinum or palladium). Certainly, there are several side effects and side reactions of minor importance, which are neglected in order to reduce any superfluous complexity. These groups of reaction will share the same tunable parameters, considering that they share the same washcoat characteristics per type of catalyst (PML, dispersion, metal support interactions, etc.)

According to the principle of Sabatier, the metal – adsorbate bond strength must be neither too strong nor too weak to allow the catalytic reaction to proceed. Catalysis by transition-metal surfaces exhibit trends across the periodic table, resulting to volcano type curves for specific reactions over a range of catalysts [144], like the one shown in Figure 20 for the r.

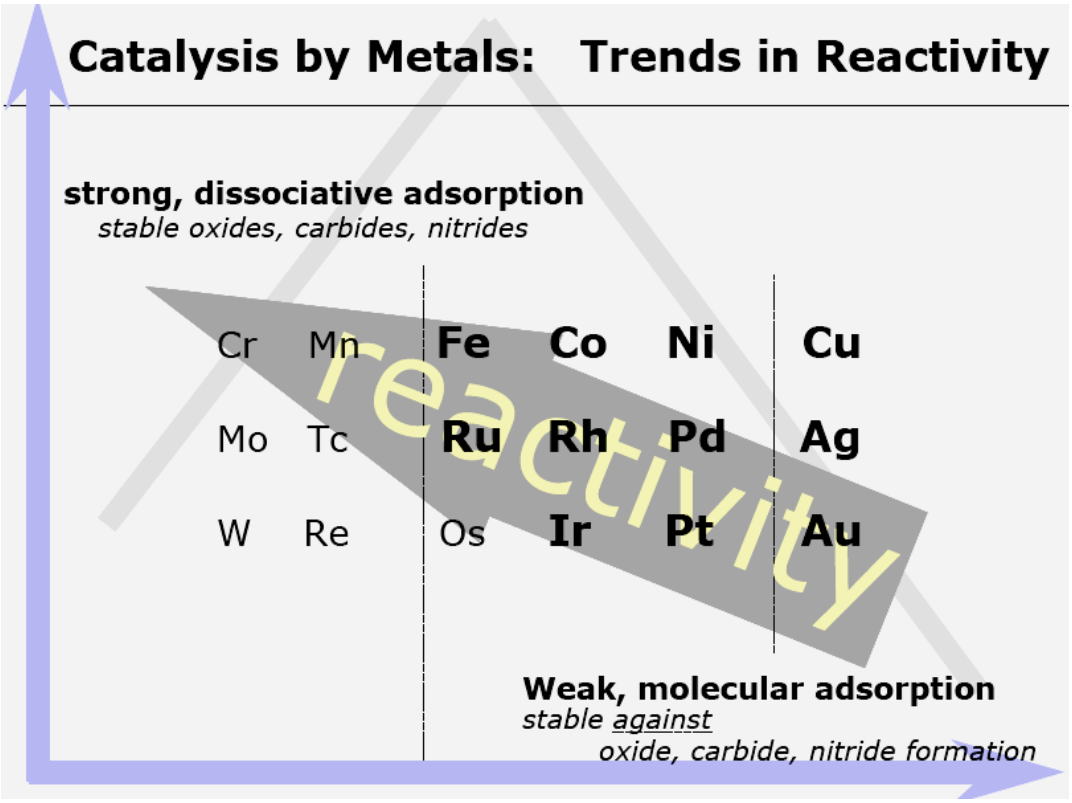

Figure 20 Periodic trends in catalytic activity (adapted from [[145]]). These trends are known to produce volcano type curves in plots of chemical element position in periodic table versus catalytic activity for specific reactions

The catalysts used in automotive catalysis applications (Pt, Pd, Rh) are positioned in the periodic table to the Platinum Metal Group, and the Ceria belongs to Lanthanides. To make a simple translation of the Sabatier effect, for use in engineer models of catalytic converters with apparent global chemical reactions, we assume that the activation energies of the reactions taking place over them can be ranked in an ascending order as follows.

$$E_{Pd} < E_{Pt} < E_{Rh} < E_{Ce}$$

Of course, this ranking is not definite. As it has been shown in Chapter 1, special manufacturing techniques are known to enhance the catalytic activity. This classification is made to provide a simplified approach in the determination of the kinetic parameters for the model of this thesis in order to decouple the complex chemistry of catalytic converters. In fact, application of this approach to cases studied in the past [3] returned at least equal quality for the modeling results as will be shown in the chapters 5 to 9. The accuracy and the extent of this approach have to be checked further. The discussion hereafter is towards this direction.

The subject in this approach is not the absolute definition of activation energies, but the correct sorting and the estimation of the correct order of magnitude. Additionally, the specific order is just proposed for convenience in engineering modeling of 3WCC with apparent reactions that conform to the assumptions made in this thesis. Any inaccuracies in the assumptions made will be compensated in the Arrhenius type expressions, because of the existing, logarithmic correlation between A and E [146, 147].

The correlation between A and E is well described by the compensation effect according to the linear relationship, where a and b are constants.

$$\ln A = a \cdot E + b$$

Compensation may extend over a range of E values differing by as much as 200kJ/mol. Recently, Gonsalez-Velasco *et. al.* [148] shown that the intrinsic activity of catalytic oxides is related to a single parameter derived from linear regression in constable plot. The literature shows strong evidences for the extent of the compensation effect as shown in the constable plot of Figure 21. The data of this figure comes from

- experiments on small-scale catalysts with various feed gas compositions [149, 111],
- tuned data of detailed kinetic models [150, 151]
- tuned data of models with apparent global reactions and with or without inhibition terms [3, 92, 152, 153, 154].

The kinetic data of these indicative studies conforms to the compensation effect, considering that there is an obvious linear trend among lnA and E. Any deviations that are present in the graph could be assigned to either experimental error or different A definition or the existence or not of inhibition terms. This becomes clearer if one accounts only for the data of each single publication where the same principles are followed. Obviously, the kinetic parameters in each publication follow their own linear trend, as a result of the different assumptions, definitions and experimental conditions of each work.

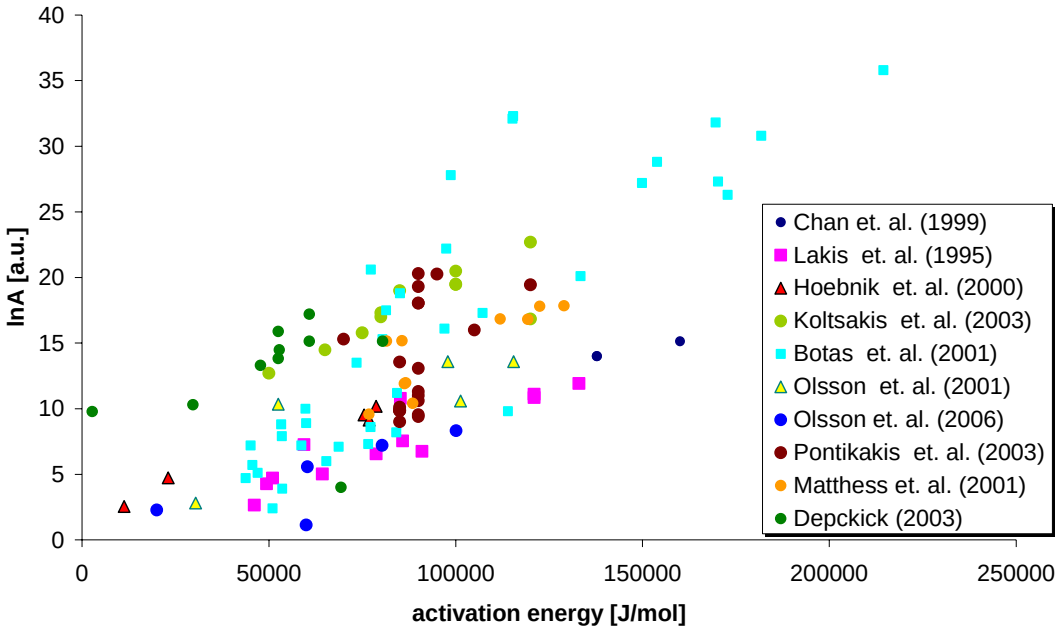

Figure 21 Constable plot for the pre-exponential factors and the activation energies for various autocatalysis reactions found in literature.

Making use of this property, we can assume standard apparent activation energy for each reaction and tune the apparent pre-exponential factor only. Further, if we assume that there is a single tunable parameter per group of reactions, that is a pre-exponential factor per catalytic active component, we can reduce the number of the model tunable parameters dramatically. Each catalytic converter would be modelled with only three tunable parameters (oxidation, reduction and storage). The successful implementation of this approach will be presented in real world case studies in the next chapters. It is assumed that any real deviations at the kinetic terms of each reaction can be compensated without significant error over the temperature range of the catalyst

At this point, it has to be noted that according to the Eyring theory each reaction has its own rate depended primarily on the reactants properties. This fact adds extra complexity without any significant benefit for the engineering scope of modeling. The calculation of the relative differences in the reaction rates of the same reaction group over specific catalyst type is a subject of fundamental research and beyond the purpose of engineering modeling. Although this fact reduces the accuracy of the modeling, it will be shown in the results that it is of minor importance.

The objective here is not to define explicitly the values of the tunable parameters but to indicate robust ranges of values that will return similar quality of modeling results over a range of catalytic converters and will be able to predict the trends of the design characteristics of the catalysts. Small deviations in these ranges of parameters are reasonable, considering that even between catalysts that share the same washcoat technology and manufacturing process small differences in the special characteristics (e.g. exposed precious metal, dispersion) may still exist.

2.6 Use of Global Apparent Reactions instead of Detailed Mechanistic Reactions

Until now, the usual approach for the determination of the reaction rates was to tune one or two parameters for each reaction (the pre-exponential factor and/or the activation energy). In this work, we switch to another approach: We consider that certain reactions occur on certain noble metals. For example, CO and HC oxidation occurs over Pt. Therefore, we speculate that they must share the same values for the pre-exponential factor and the activation energy. In other words, we speculate that the values of A and E do not depend on the reaction per se; they depend on the catalyst where the reaction happens.

Each of these reactions includes several elementary steps. Only one of these elementary steps could be regarded as the rate determining at each temperature and under specific conditions, according to the Bodenstein Approximation[a]. This is valid if we consider the narrow temperature range of the catalytic converter during the most of the warmed operation (about 350-500^{o}C). In effect, this tuning approach implies that the rate-determining step of each heterogeneous catalytic reaction depends on the adsorption, reaction or desorption step of the reaction onto the catalytic particle. According to the literature [131], this is true for heterogeneous catalytic reactions.

Let us assume a hypothetical reaction of four rate determining steps like the one shown in Figure 22. The elementary steps are shown with solid lines. If we assume a fixed activation energy for the apparent global reaction, then the true rate can be fitted by tuning the apparent pre-exponential factor. The assumption of fixed activation energy gives a constant slope for the apparent rate in Arrhenius plots like the one shown in Figure 22. Any tuning of the apparent prexponential factor, do not affects the slope of the rate curve versus temperature. If we assume a range of values for the pre-exponential factor then any value within this range will result in a rate curve within the green shadow zone of Figure 22

There is an optimum value for the apparent pre-exponential factor, which minimizes the error between true rate and tuned apparent rate, within the narrow temperature range of catalytic converter warm operation. This value is estimated by tuning the model for each type of catalyst. Of course, for temperatures outside this

[a] The Bodenstein Approximation assumes that the intermediate products of elementary reactions are short-lived and only one step could be considered as the rate determining.

range introduce significant error. It could be assumed that this error is negligible considering the short transition period of the converter from the cold inactive phase to the warmed up operation.

Let us assume that we tune the model for the warm operation for catalyst temperature ranging within 400-600°C (e.g. during urban driving of NEDC). The error[a] for temperatures higher or lower than this range should be significantly higher than the error within this range. For temperatures higher than this range, other effects independent to the reaction rate, as for example external mass limitations and contribution of bulk storage component, have significant contribution for the catalytic efficiency. During cold phase, the catalyst is inactive and the rates (true and tuned apparent) are close to zero. The reactions are initiated only after the washcoat temperature is higher than the light-off point. The short transition period during light-off is characterized by the rapid switching of the solid boundary condition from constant wall temperature to constant wall heat flux. The accurate prediction of the phenomena during the light-off transition requires the use of analytical models [for example [155]] with significant computational cost.

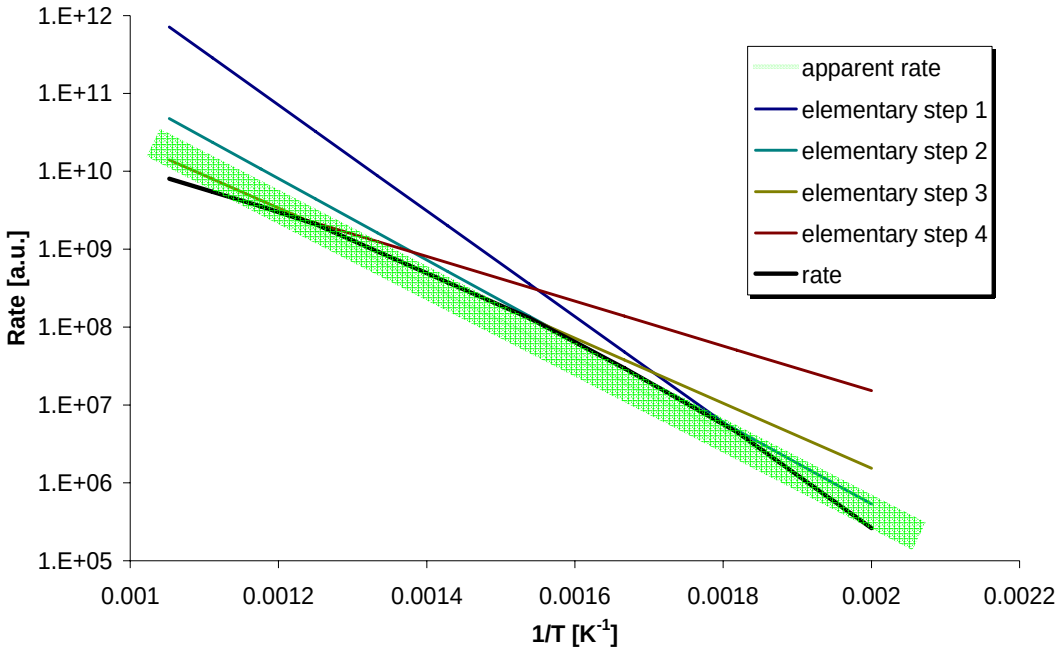

Figure 22 The fitness of an hypothetical reaction of four RDS with a global apparent reaction. The results of keeping a constant activation energy and tune only the pre-exponential factor are lying in the shadowed region.

[a] The term "error" here refers to the error between the true rate and the rate estimated from the model (tuned apparent rate)

2.7 Estimation of the Tunable Parameters of the Model Using A General Purpose Optimisation Algorithm

The variables of the model are tuned with GenOpt, a general purpose optimization algorithm freely distributed from the University of Berkeley. Our case is considered as an optimization problem with independent continuous variables (n=3), without any constraints, where the objective function is been calculated by CATRAN and is not continuously differentiated. According to the GenOpt documentation the Hybrid Generalised Pattern Search with Particle Swarm Optimisation algorithm is a good choice for this case.

This hybrid global optimization algorithm starts by doing a Particle Swarm Optimization (PSO) on a mesh for a user specified number of generations. Afterwards, it initializes the Hooke-Jeeves Generalized Pattern Search (GPS) algorithm, using the continuous independent variables of the particle with the lowest cost function value. The algorithm can be used with both discrete and continuous variables and there is no need of knowledge regarding the properties of the objective function [4]. The characteristics of the algorithm are summarised in Table 6 and the optimisation parameters data is shown in Table 7.

Table 6 Hybrid Particle Swarm Optimization – Generalized Pattern Search optimization algorithm characteristics

NeighborhoodTopology	vonNeumann
NeighborhoodSize	1
NumberOfParticle	50
NumberOfGeneration	30
Seed	0
CognitiveAcceleration	2.8
SocialAcceleration	1.3
MaxVelocityGainContinuous	0.5
MaxVelocityDiscrete	4
ConstrictionGain	0.5
MeshSizeDivider	5
InitialMeshSizeExponent	0
MeshSizeExponentIncrement	1
NumberOfStepReduction	3

On a PC Pentium4 at 3.0GHz with 1.0GB RAM, the hybrid algorithm needs about 30 minutes to converge. The global search algorithm (PSO) needs about 10 generations and 100 simulations and the local search algorithm (GPS) about 40 simulations to complete three step reductions search.

Table 7 Optimization Parameters characteristics

Parameter	MIN	MAX	Step	Type
A_Ox	1e10	1e14	10	CONTINUOUS;
A_Red	1e10	1e14	10	CONTINUOUS;
A_Ce	1e6	1e12	10	CONTINUOUS;

OBJECTIVE FUNCTION FORMULATION

The quality of the computed aided tuning of variables with an optimization algorithm is proportional to the objective function formulation. It has been already stated by Pontikakis [3] that in these types of applications the implementation of common cost functions, such as the absolute or relative differences between experimental and computed data, is not proper. What we need is a custom cost function, tailored for the specific problem. The formulation of the cost function for this type of applications must be in line with the prerequisites already labeled elsewhere [3]. In a short, the objective function should be normalized, range between two extreme values, incorporate as much information as possible, be proper for use in optimization procedures and focus on regions where the measurement is not near extreme values. The last property of the cost function is the most important for achieving "good conversion" of the optimisation algorithm.

By means of "good conversion" we mean that the results of the optimization should be as close as possible to the expected ones by our physical sense. Previous in house experience has shown that several optimization algorithms tend to converge at local minima in the specific applications frequently. This behavior can be easily explained by the coupled reactions inside the converter and the degrees of freedom (tunable parameters) that are allowed by the model. In such cases, the tuned variables are very sensitive to perturbations or usually lie far from reality and are not applicable in other cases. The quality of the optimization results has to be checked out extensively and be validated with other cases qualitatively.

The correct definition of the objective function has to be based upon the characteristics of the application; in this case, the behavior of the measured conversion efficiency during the legislated driving cycle, which is applicable to any similar case. The operation of the automotive catalytic converters is characterized by two periods; a short, initial period when the catalytic converter has not been warmed up and is inactive (0% conversion efficiency) and the period after the light-off when the catalyst temperature has risen and the conversion efficiency of the catalyst is close to 100%. Taking into account the fact that the tunable parameters are the kinetic terms of chemical reactions, there is a range of values below a low limit for the first case, where any value results 0% conversion. On the other hand, there is a range of values above a high limit where any value results 100% efficiency.

This type of behavior is shown in Figure 23 that represents the THC measured efficiency of a medium loaded catalytic converter over the NEDC. The catalytic converter operates for about 35% of the total time at over 99% conversion efficiency and for about 23% of the time at less than 90%. Although it is possible to define the low limit theoretically, the way of definition of the apparent kinetic terms makes the determination of a high limit for the tunable parameters depended on the catalyst characteristics.

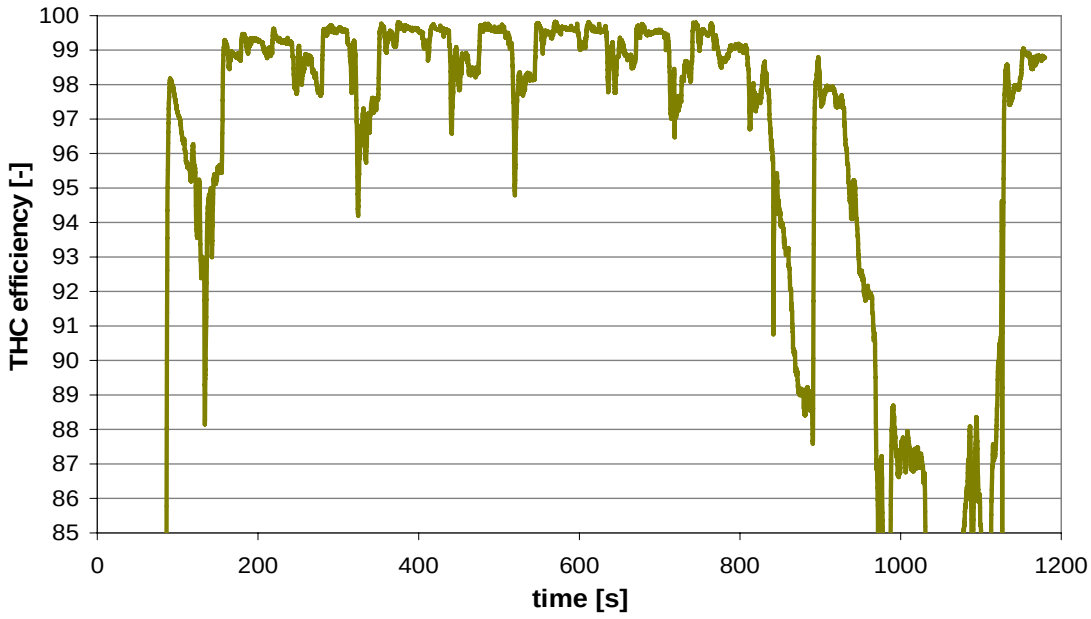

Figure 23 measured THC efficiency of a medium loaded catalyst (50gr/ft^3 Pt:Rh) over the NEDC. For about 25% of the operation time the conversion efficiency is less than 90% and for the 35% of the time is higher than 99%.

Consequently, in addition to the previously discussed characteristics, an objective function tailored for the specific application must be able to:

- provide equally weighted calculations over the complete range of operation,
- avoid attraction by extreme values during tuning and
- focus very close to the measurement

In this work, we define a new objective function for the cases of catalytic converters test that is based on the lever law. This objective function accounts for the deviation of the computation and the measurement in relevance to the extreme values. It identifies two cases for the calculation; the case when computed efficiency is lower than the measured one and the reciprocal one. In both cases, objective function has a linear behavior versus absolute difference between computed and measured efficiencies, but uses a different definition for the slope of the function in each case. Each time the slope is defined as the difference between measured efficiency and its respective extreme value (0 or 100%).

For each chemical species under investigation it is defined as

$$F_j^{'} = MAX\left(\frac{\eta_{j,cmptd} - \eta_{j,meas}}{(1+a)\cdot(100-\eta_{j,meas})}; \frac{\eta_{j,meas} - \eta_{j,cmptd}}{(1-a)\cdot\eta_{j,meas}} \right)$$

where 0≤α<1 is a factor that tunes the slope and consequently weights the focus of the objective function. For example, for α = 0, at regions close to 100% measured efficiency and when the computed efficiency is higher than the measured one, the objective function will return higher value than in the case of α = 1. This is used in the cases of very active catalytic converters when the overestimation of the tunable parameters has little or no effect to the value of the objective function. In these cases the optimization algorithm is attracted to regions of wrong solutions and it is very difficult to converge, so it is desirable to produce high costs for small deviations from the optimum solution. A common value that we have concluded for catalysts with overall efficiency higher than 90% that is met frequently in commercial applications is 0.8. Figure 24 shows a plot of the objective function versus computed and measured efficiencies for the three cases of α.

For the usual case where the responses of CO, THC and NOx are of concern, the objective function is defined as

$$F^{'} = w_{CO}F_{CO}^{'} + w_{THC}F_{THC}^{'} + w_{NOx}F_{NOx}^{'}$$

The three chemical species are equally weighted for simplicity, but in the case we want to focus in one specific pollutant, for example in the case of NOx traps modelling, we adjust properly the weight factors.

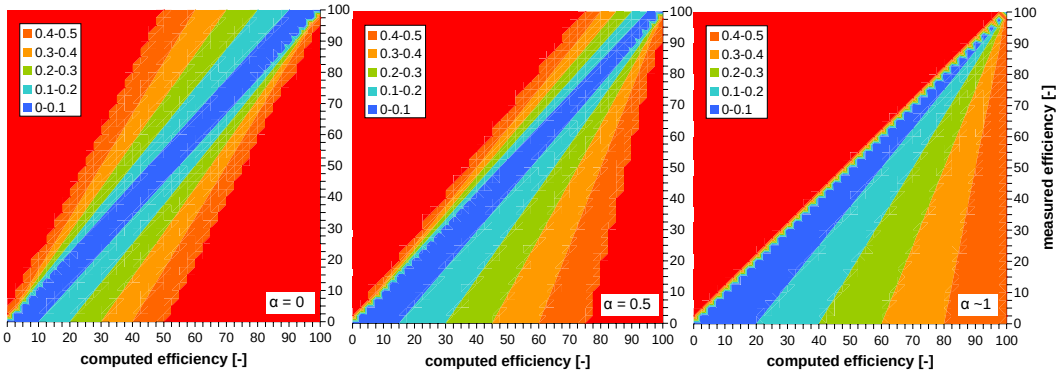

Figure 24 Objective Function plot versus measured and computed efficiencies. The new

2.8 METHODOLOGY OVERVIEW

Up to this point, the model was presented and a systematic effort to reduce the tunable parameters was shown. In the following, the discussion refers to the methodology employed, which is summarized in three steps.

1. Preprocess of the experimental data through a quality assurance system [112]. At this step the experimental data is checked for consistency and validity. The data is cross-checked and we prepare the input files of the model using a minimum set of experimental data that is commonly acquired in routine experiments of legislated driving cycles [112].
2. Tuning of the model variables with an optimisation algorithm [3, 4] that will be discussed in the following.
3. Postprocess and analysis of the results

The minimum possible number of parameters is essential both for the fast and accurate convergence of the optimisation algorithm and for increasing the model 's flexibility. The applicability of the model is an important aspect also. During this thesis it was established a user friendly graphical user interface based on MS-EXCEL. The principal operations of the steps 1 and 3 have been transferred to other environments (Labview, Simulink) enabling indirect adaptation of the model to engineering oriented commercial software.

The basic GUI is comprised by a large set of macros in MS-EXCEL. The choice of MS-EXCEL use instead of the development of a stand-alone application was made to retain compatibility with widespread commercial software and to take advantage of the advanced spreadsheet operation of the parent software. The macros are incorporated into a single toolbar, shown in Figure 25, which is inserted in MS-EXCEL and are accompanied by several workbooks destined for specific operation. The establishment of the graphical user interfaces of the model is shown in appendix B.

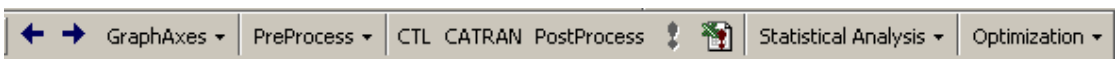

Figure 25 The toolbar that incorporates the sets of macros developed to preprocess experimental data, run the model and postprocess and visualize the results.

2.9 SYNOPSIS

In this chapter, the model that was used in this thesis was presented. The current model is an improved version of the model developed by Pontikakis [3]. The updated features can be summed up to the following:

- Updated definition of the diffusion problem with a simplified mechanism
- Updated definition of the reaction rates expressions
- Updated analytical calculations for the gas properties
- Updated output files to enable crosscheckings and in-depth view of processes
- Minor changes to establish compatibility with external applications (GenOpt)

In addition to these, the overall methodology was reviewed and updated. Firstly, we were systematically concluded to a reduced reaction scheme, featuring the dominant reactions and reacting species. Based on literature findings, the number of tunable parameters was dramatically reduced from ten to three, while it was shown a strong correlation between apparent pre-exponential factor and apparent activation energy of reaction rate expressions. A new optimization tool was used and a new objective function was formulated that is less attractive to the upper limit of tunable variables. The reviewed methodology and the evolutions in computer technology enabled a 50-fold time reduction for the optimization runs in each case. Finally, the established GUI in MS-EXCEL increased the usability of the core program and enabled the fast and error-free input files construction and results postprocessing. The latter dramatically reduced the total time need to process and simulate a raw data format case study.

The discussion in this chapter has shown the way that engineering models are benefited by the findings of fundamental research and how they return a precious feedback to this level of study. A schematic representation is shown in Figure 26. The design strategy of catalytic converters is a cyclic procedure [83] that can take place at many different levels of complexity assisted by experiments and modelling. The most fundamental level corresponds to the study of washcoat processes and the full scale level studies the overall performance of the final product. The approach described in this thesis studies and simulates full-scale engine tests, assisting the engineering design of the final product, but also, at the same time, giving feedback to the fundamental level referenced above. At the full-scale level, due to the overall system complexity, a quality assurance methodology is essential for a systematic

study of experimental data. The transient operation of the engine, lambda oscillations and the associated variations in exhaust gas composition, limitations of instrumentation measurability and different instrumentation measuring responses affect the desirable quality of experimental data. The use of low quality experimental data can drive to misunderstanding of coupled phenomena inside the converter and possibly misleading design suggestions.

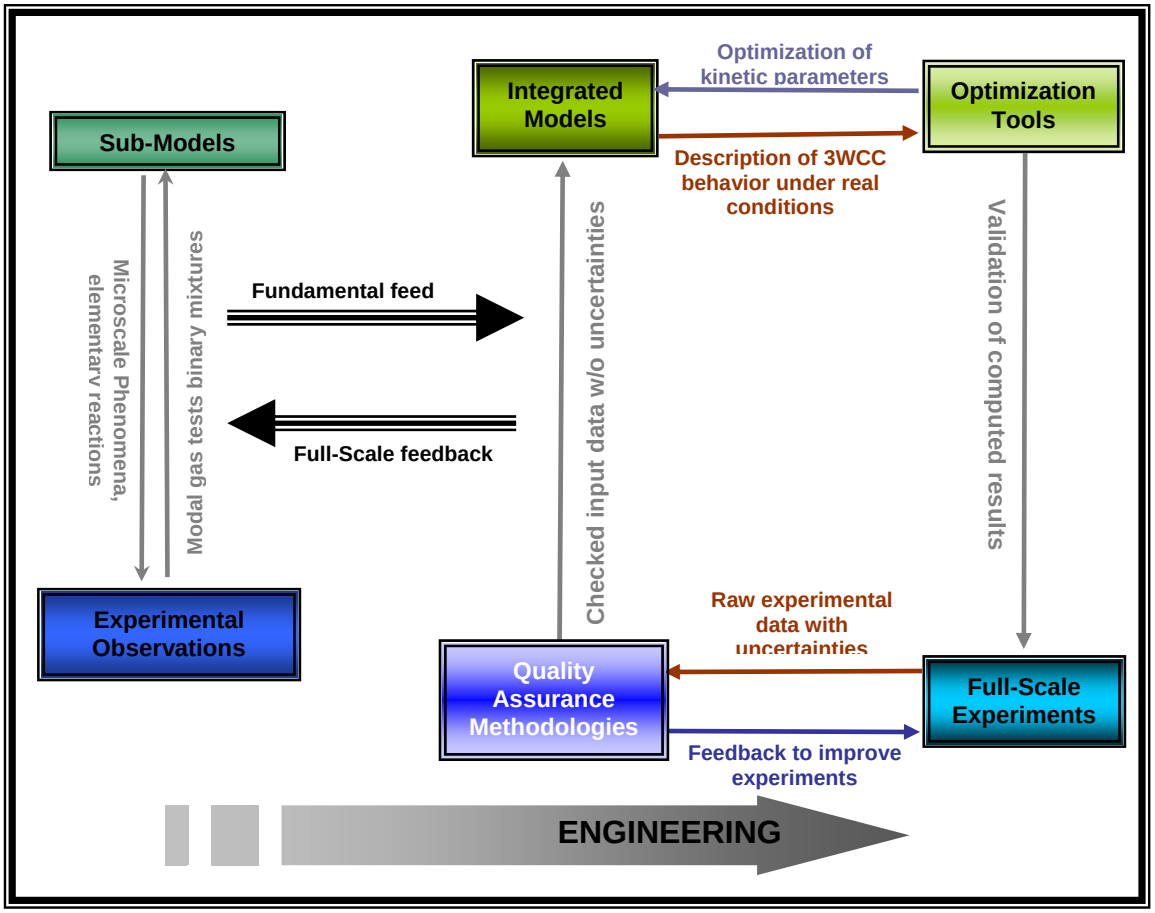

Figure 26 Schematic representation of the 3WCC design strategy with the coupling of experiments and modelling at two levels of study

Moreover, the simulation models must be fast enough for engineering design optimization (significantly faster than realtime). On the other hand, fundamental level catalyst experiments (e.g. [95]), can only be fitted with complex elementary reaction schemes, with a complicated tuning procedure. However, the tuning is useless if we shift even to a slightly different catalyst – washcoat formulation or even loading.

Thus, it was preferable to minimize as much as possible the reaction scheme in order to gain the full control of the model and uncouple somehow the chemical reactions. Primary and secondary effects inside the catalytic converter must be studied and weighted respectively to the contribution they have in the overall performance of the converter.

The way that raw data is treated through a quality assurance procedure will be discussed in the next chapter. The validation of the current approach followed in this chapter will be shown in the successful application to real world case studies presented in chapters 5, 6, 7 and 8.

CHAPTER3

DEVELOPMENT OF A TEST DATA QUALITY ASSURANCE METHODOLOGY

The engineering approach of current work faces the computed aided design of the exhaust line of the vehicles by introducing experimental data from engine field tests as input to the models. On the other hand, the transient operation of the engine itself, the different responses of the devices and the sensors used (as already discussed in chapter 1), and the variability of the engine exhaust data from cycle-to-cycle [13], even between identical tests, requires quality assurance techniques to be implemented before the use of any experimental dataset. Additionally, the required robustness and flexibility of the models (see chapter 2) indicates the necessity of statistical analysis of the experimental datasets. Quality assurance techniques secure that experimental datasets are of equal good quality in general and not someway excellent quality. The motivation for the work in this chapter has arisen when validated model predictions were found to be strongly depended on the differentiated data pre-processing made by each user. As will be shown in the chapters 5, 6, 7, and 8 this novel approach for automotive datasets contributed to the improvement of the modeling results greatly. An extended use of this methodology reveals the behavior of the system engine-engine management-catalyst at a glance (presented in chapter 4) with obvious advantages, which are discussed later at chapter 9.

3 DEVELOPMENT OF A TEST DATA QUALITY ASSURANCE METHODOLOGY

3.1 INTRODUCTION

From the exhaust viewpoint, one could visualize the overall powertrain to comprise three main sections; the engine itself, the exhaust aftertreatment devices and the integrated management system (sensors and ECU). These sections are bound together by the flow of information contained in the exhaust gas, which can be coded in terms of mass flow rate, temperature and species composition.

Obviously, the design and optimisation of exhaust systems must be based on the processing of large quantities of transient exhaust gas data of the above type. For example, Figure 27 presents a typical exhaust system measurement layout for the assessment of a simple catalytic exhaust system of an SI engine.

The specific layout usually involves the following types of measurement devices:

- Thermocouples for the measurement of upstream, downstream and inside catalyst temperatures.
- Accurate flow sensors (i.e. hot wires, hot films, etc) for the reliable measurement of inlet mass flowrate.
- Infrared exhaust gas analyzers for CO, CO2
- FID exhaust analyzers for HC
- Paramagnetic exhaust gas analyzers for O2
- Chemiluminescence exhaust gas analyzers for NOx.
- Accurate electrochemical lambda (or even NOx, CO etc) sensors

The transient character of the engine operation, because of the variable operation points and existing lambda oscillations, usually necessitates faster than 1Hz acquisition of the above data. This can be clearly shown in the exhaust gas species composition datasets, which fluctuate between lean and rich environment, in a stoichiometric SI engine. Thus, it is not surprising that there exists a significant variation in the attainable quality of acquisition of test data between different test labs [156, 157].

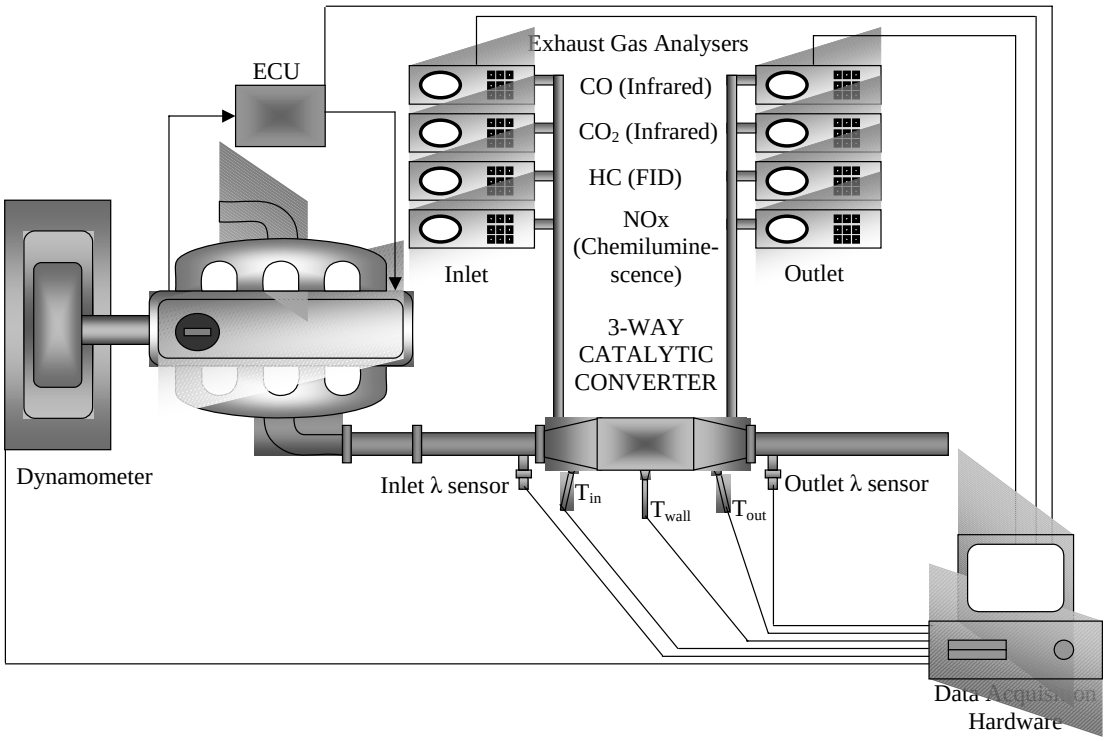

Figure 27 A typical experimental setup of SI engine exhaust emissions tests. Exhaust gas is directly sampled from exhaust line, (HC through heated line). Several thermocouples are measuring temperature upstream, downstream and inside catalyst, and a number of sensors are used for auxiliary measurements. Data is acquired through computerized acquisition systems.

The shift to advanced exhaust treatment systems for use in ultra low emitting vehicles, means that the emissions are so low that, measured according to the legislation, emitted exhaust gas is cleaner than the urban air. The ultra low emissions concentrations are generating losses in accuracy of data, because of the limitations of both instrumentation measurability and the experimental setup itself. Various laboratories are already investigating alternative layouts for more accurate measurements or are developing very precise analytical instruments [158]. Others are implementing methodologies to control the quality of measurement data employed in design optimization of exhaust systems. The adoption of quality assurance procedures, such as statistical quality control and total quality management of the experimental data, supports the optimized engineering design of complex exhaust treatment systems and hints to further improvement in measurement layouts and components. A test data quality assurance procedure must be able to process the acquired test data, spot acquisition problems or experimental errors, accept or reject an experimental data acquisition file and extract further information concerning the overall system's operation, through standardized processes. The procedure consists of four steps, as listed below:

- Data phasing and preprocessing
- Analysis of driving cycle modes
- Mass balance calculations
- Statistical comparative analysis of different systems

These four steps comprise a number of qualitative (graphical methods and flowcharts) and quantitative (statistical analysis, cross checking calculations, database entries) processes.

The quality of the datasets affects the accuracy of the exhaust system design. Exhaust aftertreatment modeling is based on instantaneous transient data, considering that the phenomena inside the converter are extremely fast regarding mass transfer and chemical reactions. It is important to investigate the possible sources that decrease the quality in a dataset and develop techniques and methodologies for managing the total quality in order to ensure that experimental data used in modelling is error free.

3.2 TYPICAL ERRORS OF RAW EXPERIMENTAL DATA

The nature of the exhaust emissions test procedures and instrumentation usually generates several types of errors and common problems in experimental datasets. The transient nature of engine operation and the large duration of the experiments often obscure these dislocations of experimental data that can become clear through the standardized processes of a quality assurance methodology. These errors can be summarized as follows:

- Unphased datasets
- Inconsistent measurement scales and response between analysers
- Condensation of gas phases in the measurement lines
- Noisy lambda signal or bad sensing system calibration

UNPHASED DATASETS

Earlier experimental observations [93, 159] suggested that, in exhaust gas sampling layouts, the data measured by the analysers is found to be significantly distorted between the sampling point and the analyzer input. The nonidealities are usually associated with concentration measurements and can be described by two time delays: pure time delay (e.g. the transportation lag in the pipeline connecting the converter and the analysers) and mixing chamber distortion (e.g. signal dispersion due to gas-phase mixing in the pipeline as well as within the analyzer). The analyzer output signal $y(t)$ can be related to the actual concentration at the sampling points $x(t)$ by the following simple differential equation

$$\theta \frac{dy(t)}{dt} + y(t) = x(t - \tau) \qquad (0.13)$$

where first order constant θ and time lag τ are functions of pipeline and analyzers characteristics and pipeline length and sampling flow rate of each analyzer respectively. Both are determined from composition step changes experiments.

Figure 28 shows raw experimental data for the case of a SI engine. Raw data is usually unphased, a fact that is shown in this figure by studying the peak or valley values of the emissions after a step change in engine operation that is indicated by lambda signal at about 280s.

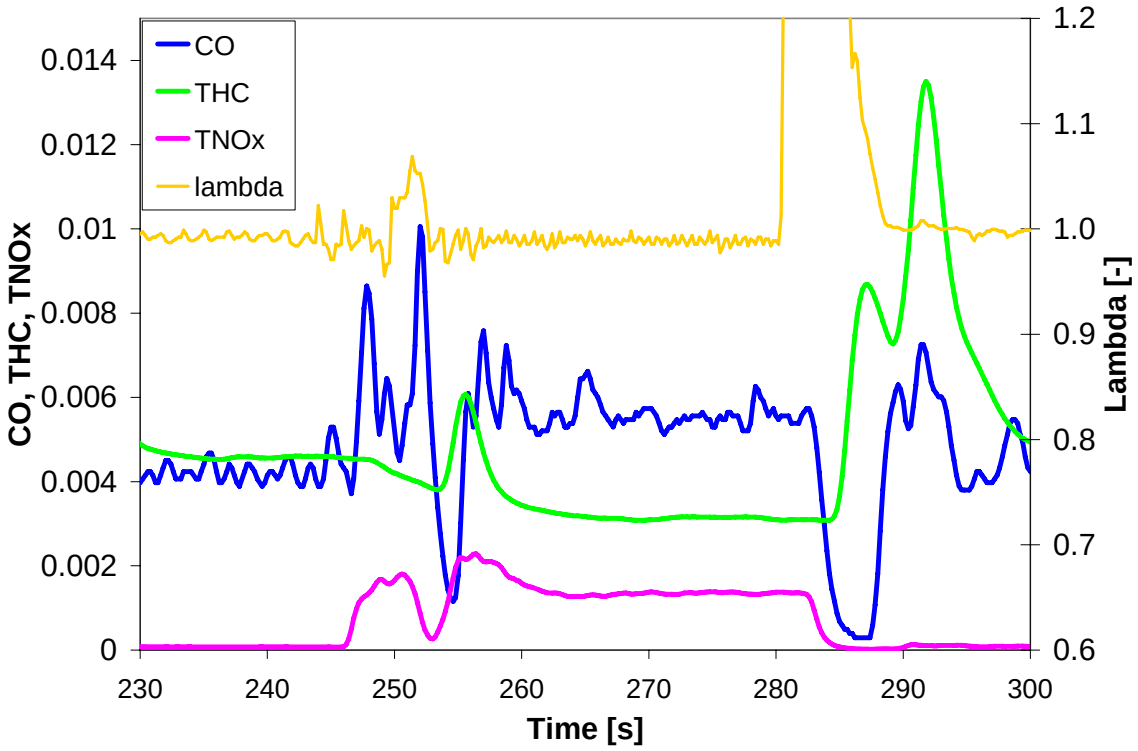

Figure 28 Raw emissions concentrations data. Raw data is incorrectly phased, as becomes apparent by comparing the peak values of the emissions.

The phasing of the datasets is essential to the study of chemical reactions inside catalytic converters, as they are strongly dependent on the instantaneous molar fractions of species in the exhaust gas.

MEASUREMENT SCALES AND RESPONSES

The transient operation of the engine during the several phases of the experiments (e.g. cold start, urban and extra urban driving) results in a wide measurement range of emissions. During cold start engine out exhaust gas is rich in CO and HC and the catalytic converter is inactive resulting in increased emissions downstream. The same stands during accelerations, when mixture enrichment is needed for the additional power supply resulting in at least two orders of magnitude higher emissions. The sum of exhaust gas oxygen and the respective stored in washcoat is not enough to fully oxidize CO and HC during long accelerations (e.g. extra-urban driving) and emissions downstream the catalytic converter are multiple times higher than under normal operation.

Increased accuracy in ultra low emissions systems indicates low scale measurements according to the instrumentation capabilities. A common technique to

measure in the full range is the automatic changing of scales through analyzers hardware, otherwise the use of a constant measuring scale results in reduced accuracy or "flat-top peaks". On the other hand, analyzers' characteristic response time T_{90} (time needed to move from zero to 90% of the measuring scale) is about 1sec for fast instruments while can reach 10secs for lower response instruments (e.g. CO, CO2). This time is an analysis principle (FID, NDIR, etc.) constraint and is far away from less than 1Hz acquisition needed.

Figure 29 shows a typical example of errors produced by changing scale in a SI engine during FTP driving cycle. The noted points on the graph show some characteristic peaks in CO measurement downstream the catalytic converter when lambda signal and CO measurement upstream the converter indicates no reason for this.

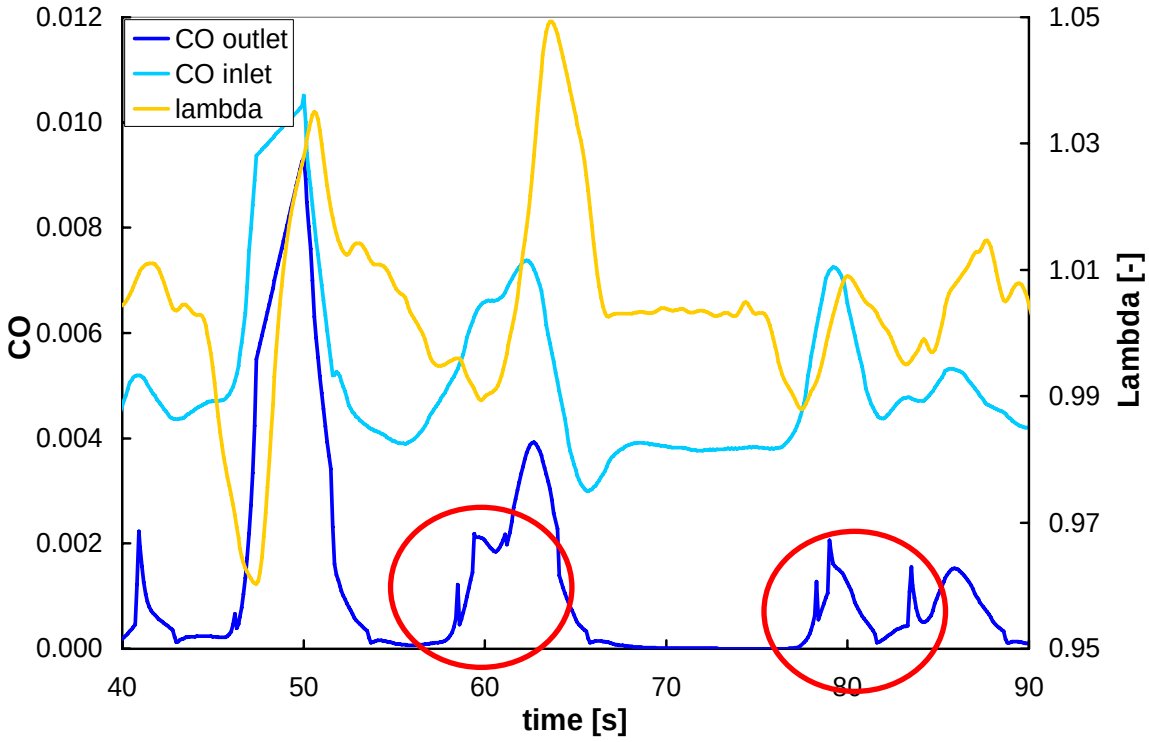

Figure 29 During hot operation of the catalytic converter the tailpipe emissions are only a few ppm. In sharp accelerations emissions breakthroughs and insufficient catalyst operation force the analysers to change their measuring scale introducing in the datasets significant deviations with the shape of the spikes noted in circles in the graph

Figure 30 shows "flat-top peaks" in HC emission downstream the catalytic converter (SI engine operated on NEDC) as result of constant analyzer measuring

scale. This is the period during cold start when the catalytic converter is inactive and the emissions upstream and downstream the converter should be identical.

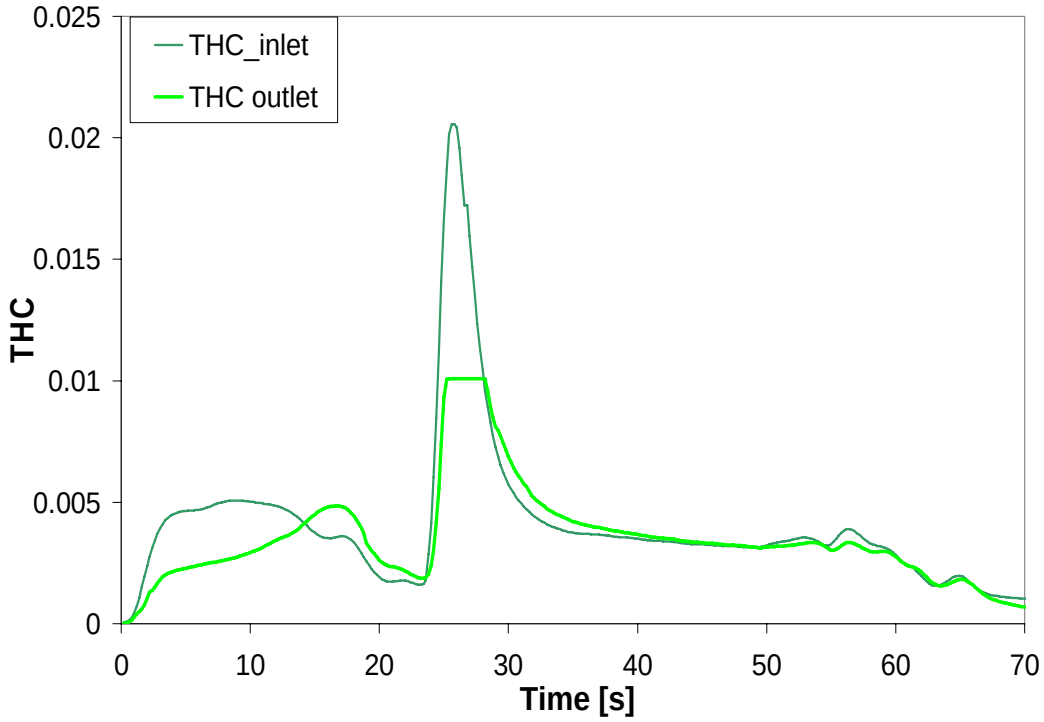

Figure 30 During cold catalyst operation it is very common the analyser used for dwnstream measurements not to be capable of measuring the increased emissions resulting in "flat-top peaks"

NOISY LAMBDA SIGNAL OR BAD SENSING SYSTEM CALIBRATION

Generally, the lambda sensor signal has a faster response (order of ms) than the analyzers' signals and is more sensitive to external sources of noise. This fact gives the impression of a noisy signal with unequal quality compared to the rest of the measurements that affect calculations based on lambda measurements. Additionally, sensors are calibrated in a narrow window of operation (e.g. lambda sensor close to stoichiometry) and measurements out of this window are not very accurate (e.g. lambda sensor signal in extremely rich or extremely lean engine operation).

Figure 31 shows deviations in oxygen signal measured with an analyzer and the respective one calculated by lambda sensor signal upstream the catalytic converter. Operation in rich environment means that we have low concentrations of

oxygen in the exhaust gas. This is affecting both analyzer, which is measuring in its lower limit resulting in misshaping of the output signal, and UEGO where we have low signal to noise ratio. Operation in extremely lean environment results strong differences between the oxygen measured by the analyzer and the respective that was calculated by the lambda signal, which are coming from the response of the analyzer (noted with asymptotic shape at about 90s) and the calibration of UEGO, that is possibly out of range (fluctuations at the same moment).

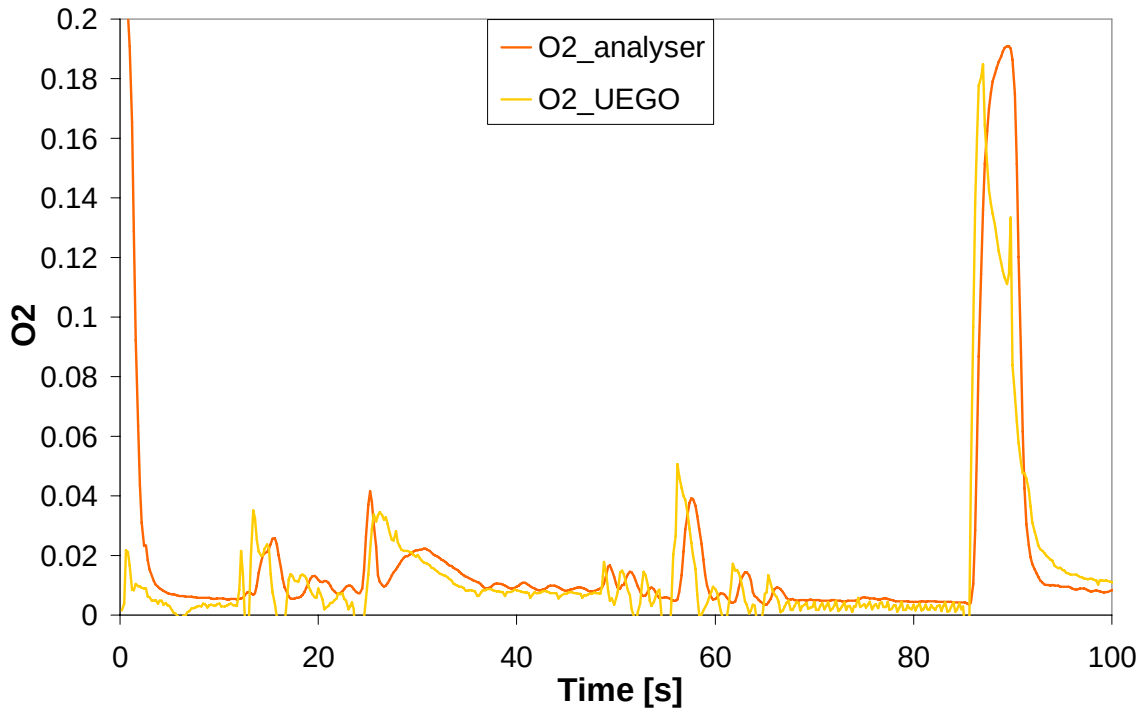

Figure 31 Comparison of oxygen fraction in exhaust gas computed from UEGO signal and from O_2 analyser signal in 5Hz acquisition. Lambda signal is much faster than the analyzer signal. Differences in mean values may originate from lambda sensing system calibration or analysers errors

In general, it is preferable to use signals of the same quality or similar characteristics. This means that when all other exhaust gases are measured by analyzer it seems more convenient to employ the analyzer signal for the oxygen, instead of UEGO signal, which has similar response in exhaust gas changes.

3.3 Overview of the Steps of Quality Assurance

The complexity of the exhaust aftertreatment design problem and the time pressure has forced automotive industry and respective laboratories working in this area to establish cooperation through data and models exchange. The researcher may deal with experimental data coming in different formats and unknown quality level, while details of the measurement instrumentation and experimental layouts are not always available.

The need for a quality assurance tool that ensures the validity of the experimental data is obvious. Such a tool may use qualitative observations and mathematical-statistical background to identify patterns, errors and deficiencies in data that is hard to find in high dimensions datasets.

The quality assurance methodology presented in this work is accomplished through a user-friendly environment coded in commercial software packages (MS-EXCEL, MATLAB/Simulink and LabView). In the following sections, each one of the following steps of the proposed methodology is separately discussed.

- transformation of the raw experimental data in a standardized format
- preprocessing of the data according to the methodology of Heywood
- phasing of the data to correct piping delay and analysers response
- missing data calculations and cross-checking
- qualitative observations and modal analysis
- mass balances calculations
- comparative statistical analysis

3.4 SELECTION, TRANSFORMATION, PREPROCESSING

Experimental data comes in several formats, according to the specific laboratory that carried out the experiments. In many cases, raw experimental data includes oversupply of measurements and information, like engine operation variables that are not directly useful to exhaust aftertreatment devices study while there exists also several cases with lack of data. Quality assurance of experimental data must be able to recognize at a glance the datasets and treat them accordingly to a standardized flowchart that ensures

- Exclusion of deficient experiments
- Categorization of the datasets
- Recording and storing over supplied info for possible future use
- Extraction of useful data
- Recovering missing data through calculations

Figure 32 shows such a flowchart for experimental datasets treatment in LTTE-UTh

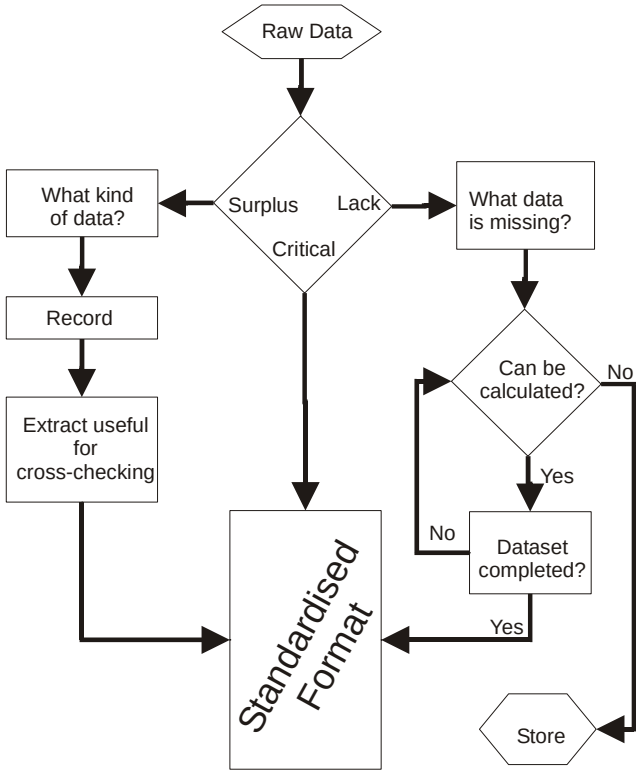

Figure 32 Flowchart for treatment new raw data and decision taking for use or not. A dataset with defective measurements is possible to be used if these measurements can be recovered.

The raw experimental data are time series of gas species concentrations, temperatures, lambda signal, mass flow rate and vehicle speed. LTTE, like other laboratories of this kind, has developed its own standard format shown in Table 8 for writing down minimum set of data from routine engine tests. A standardized format enables automated further processing through spreadsheet operations.

Table 8 LTTE standard format

Time (sec)	CO meas. inlet	HC1 meas. inlet	NOx meas. inlet	CO meas. exit	HC1 meas. exit	NOx meas. exit	CO2 meas. inlet	CO2 meas. exit	O2 meas. inlet	O2 meas. Exit	T inlet cat	T exit cat	lambda	mfr	Veh speed

In the past several researchers have established methodologies for calculating the real exhaust gas fraction at the catalyst inlet (see for example [160] and references). Heywood [13] proposed a methodology for transforming the raw data into wet molar fractions, which corresponds in the real exhaust gas fractions entering the catalytic converter, accordingly to the following set of calculations. The overall combustion reaction of the fuel can be written as

$$C_n H_m O_r + \frac{n_{o_2}}{\phi}\left(O_2 + 3.773 N_2\right) \rightarrow n_p \begin{pmatrix} \tilde{x}_{C_a H_b} C_a H_b + \tilde{x}_{CO} CO + \tilde{x}_{CO_2} CO_2 \\ + \tilde{x}_{O_2} O_2 + \tilde{x}_{N_2} N_2 + \tilde{x}_{NO} NO \\ + \tilde{x}_{NO_2} NO_2 + \tilde{x}_{H_2O} H_2O + \tilde{x}_{H_2} H_2 \end{pmatrix} \tag{0.14}$$

where ϕ is the measured equivalence ratio, n_{O_2} is the number of O_2 molecules required for complete combustion $\left(n + m/4 - r/2\right)$, n_p is the total number of moles of exhaust products and $\tilde{x}_i$ is the wet mole fraction of the ith component.

Using an atomic balance for each element and the definition of mole fraction, we obtain a system of five equations

$$n = n_P \left(a\tilde{x}_{CH_{b/a}} + \tilde{x}_{CO} + \tilde{x}_{CO_2} \right) \tag{0.15}$$

$$m = n_P \left(b\tilde{x}_{CH_{b/a}} + 2\tilde{x}_{H_2O} + 2\tilde{x}_{H_2} \right) \tag{0.16}$$

$$r + 2n_{O_2}\lambda = n_P \left(\tilde{x}_{CO} + 2\tilde{x}_{CO_2} + \tilde{x}_{NO} + 2\tilde{x}_{O_2} + \tilde{x}_{H_2O} \right) \tag{0.17}$$

$$7.546 n_{O_2}\lambda = n_P \left(2\tilde{x}_{N_2} + \tilde{x}_{NO} \right) \tag{0.18}$$

$$\tilde{x}_{CH_{b/a}} + \tilde{x}_{CO} + \tilde{x}_{H_2} + \tilde{x}_{H_2O} + \tilde{x}_{N_2} + \tilde{x}_{NO} + \tilde{x}_{CO_2} + \tilde{x}_{O_2} = 1 \tag{0.19}$$

The additional assumption is made, based on the available exhaust gas composition data, that CO_2, CO, H_2O, H_2 molar fractions are correlated by

$$\frac{\tilde{x}_{CO}\tilde{x}_{H_2O}}{\tilde{x}_{CO_2}\tilde{x}_{H_2}} = K \qquad (0.20)$$

where K is a constant with commonly used values of 3.8 and 3.5.

Engine exhaust gas composition is often determined by analyzing a fully dried sample stream for CO_2, CO, O_2 and NO_x, and a fully wet (uncondensed) stream for unburned hydrocarbons. In this case the fuel/air equivalence ratio is given by

$$\phi = \frac{2n_{O_2}}{n_p\tilde{x}_{H_2O} + n_p\left(1-\tilde{x}_{H_2O}\right)\left(\tilde{x}^*_{CO} + 2\tilde{x}^*_{CO_2} + 2\tilde{x}^*_{O_2} + \tilde{x}^*_{NO} + 2\tilde{x}^*_{NO_2}\right) - r} \qquad (0.21)$$

where $\tilde{x}_i^*$ denotes the dry mole fraction and $\tilde{x}_i$ denotes the wet mole fraction.

Dry and wet mole fraction are related by

$$\tilde{x}_i = \left(1-\tilde{x}_{H_2O}\right)\tilde{x}_i^* \qquad (0.22)$$

$$n_p = \frac{n}{\tilde{x}_{CH_{a/b}} + \left(1-\tilde{x}_{H_2O}\right)\left(\tilde{x}^*_{CO} + \tilde{x}^*_{CO_2}\right)} \qquad (0.23)$$

$$\tilde{x}_{H_2O} = \frac{m}{2n}\frac{\tilde{x}^*_{CO} + \tilde{x}^*_{CO_2}}{\left[1 + \tilde{x}^*_{CO}\Big/\left(K\tilde{x}^*_{CO_2}\right) + \left(m/2n\right)\left(\tilde{x}^*_{CO} + \tilde{x}^*_{CO_2}\right)\right]} \qquad (0.24)$$

$$\tilde{x}_{H_2} = \frac{\tilde{x}_{H_2O}\tilde{x}^*_{CO}}{K\tilde{x}^*_{CO_2}} \qquad (0.25)$$

$$\tilde{x}_{N_2} = 1 - \sum_{i=1}^{n}\tilde{x}_i = \frac{3.773n_{O_2}}{\phi n_P} - \frac{\tilde{x}_{NOx}}{2} \qquad (0.26)$$

To derive this set of equations it was assumed that fuel contains no Oxygen, Carbon to Hydrogen ratio of exhaust gas hydrocarbons is equal to that of fuel and that exhaust gas hydrocarbons concentration was measured by the analyzer as a mole fraction of C_1.

3.5 PHASING OF THE RAW EXPERIMENTAL DATA

Carbon monoxide emissions from internal combustion engines are controlled primarily by lambda and they are correlated by a single curve [161]. NOx and HC

emissions are depended of a great number of factors. In general HC are minimum at λ~1.1 and are increased at rich mixtures (lack of oxygen) and extremely lean ones (because of partial burning, ultimate misfires, combustion chamber deposits scavenging). NOx emissions are strongly affected by the combustion temperature thus they are increased for λ~1.1 and lowered in rich and lean regimes.

Accordingly, the signal time correlation may be accomplished based on the following main steps:

- Vehicle speed in combination with engine out temperature is used as baseline. The response of the routinely employed today thermocouples with less than 0.5mm external sheath diameter, is quite fast (time constant less than 100ms) and exhaust temperature near exhaust valve responds quickly to the changes of engine operation.
- Lambda phase is checked if it is coming from an UEGO sensor or is phased if it is computed from an analyzer signal.
- Mass flow rate, which is correlated with lambda signal (A+F), is phased
- CO signal is correlated and phased with lambda signal
- NOx signal correlated and phased with temperature
- HC signal can be correlated with mfr and lambda signal. During accelerations there is efficient combustion (HC decreasing-mfr increasing) and during decelerations there is increased HC emissions due to the removing of combustion chamber HC deposits.

In general, if there is not knowledge for the experimental layout first order constant θ of equation 1.1 is assumed to be zero. Nevertheless, common values of θ are 0.3 to 2 and they can be incorporated in time lag τ with small effect in accuracy of data phasing Figure 33 shows O_2 signal measured by a paramagnetic analyzer, phased with θ estimation and with θ incorporated in time lag using as correlation baseline the lambda sensor signal for a 5Hz acquisition. Obviously, there is not significant loss in accuracy of the signals.

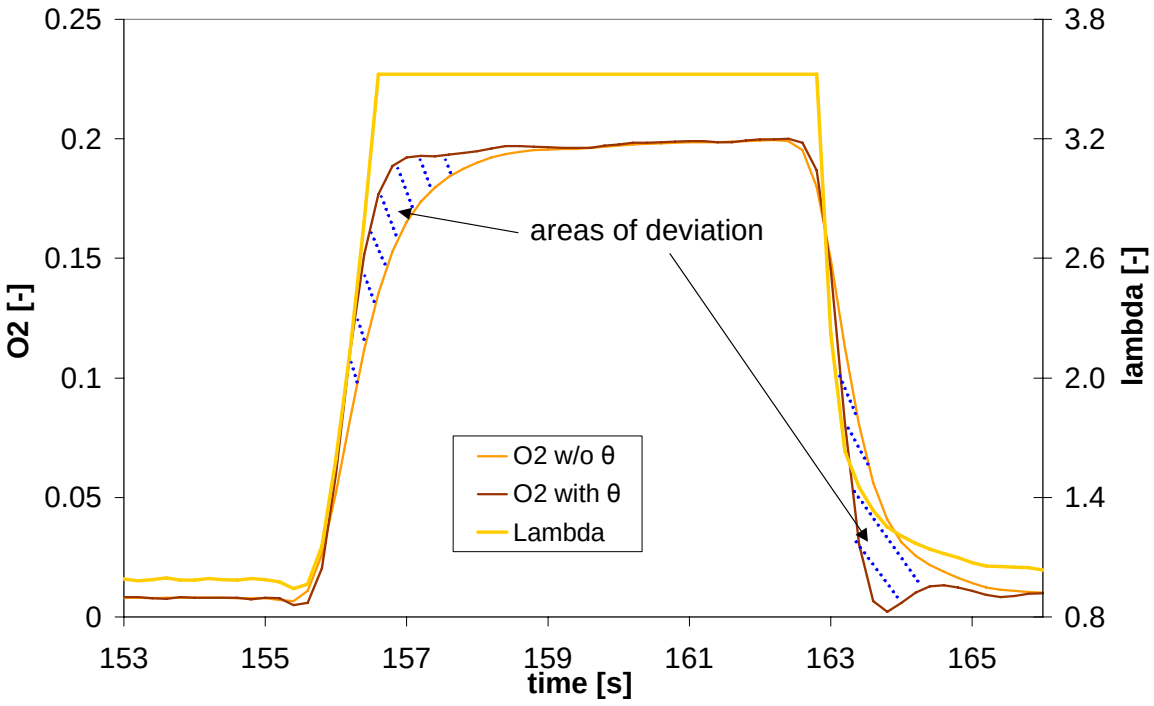

Figure 33 Differences in signal response when the first order constant of equation 1.1 is known and when there is no knowledge of it.

The correlation of the signals is time independent for the inlet and for the outlet of the converter, as all the measurements are acquired at the same point in each case. Once a part of signal is synchronized the complete time-series is synchronized. Of course, due to changes in exhaust gas velocity, the input and the output signal cannot be synchronized everywhere. Synchronization of traces of these signals at the beginning of the driving cycle is eliminating significant phase differences coming from different acquisition pipe lengths. Further phasing of inlet and outlet signals is possible with knowledge of exhaust line geometrical characteristics through calculation of the exhaust gas velocity and the instant time needed for a unit mass to travel from one measuring point (inlet) to the other (outlet).

Figure 34 shows the better phasing between signals upstream and downstream the catalytic converter that was achieved with the calculation of the traveling time between the two measurement points. This time could be calculated from gas velocity into the exhaust pipe, u_{gas}, and the distance between the two measurement points, l.

$$\tau_1 = \frac{u_{gas}}{l}$$

The traveling time calculated here can be incorporated in the phasing differential equation in order to correct the variable phase between two sampling points. The equation (1.1) would become for the outlet signals

$$\theta \frac{dy(t)}{dt} + y(t) = x(t - \tau - \tau_1) \qquad (0.27)$$

This correction has limted value if it is considered that the outlet signal is used for modeling comparison reasons, the existing instrumentation limitations in accuracy and because of eddies and mixing existence in the converter diffuser as noted by [162]. Indeed, it improves the results when tuning the model with a computerized optimization algorithm, as it provides more accurate calculations of F'[a].

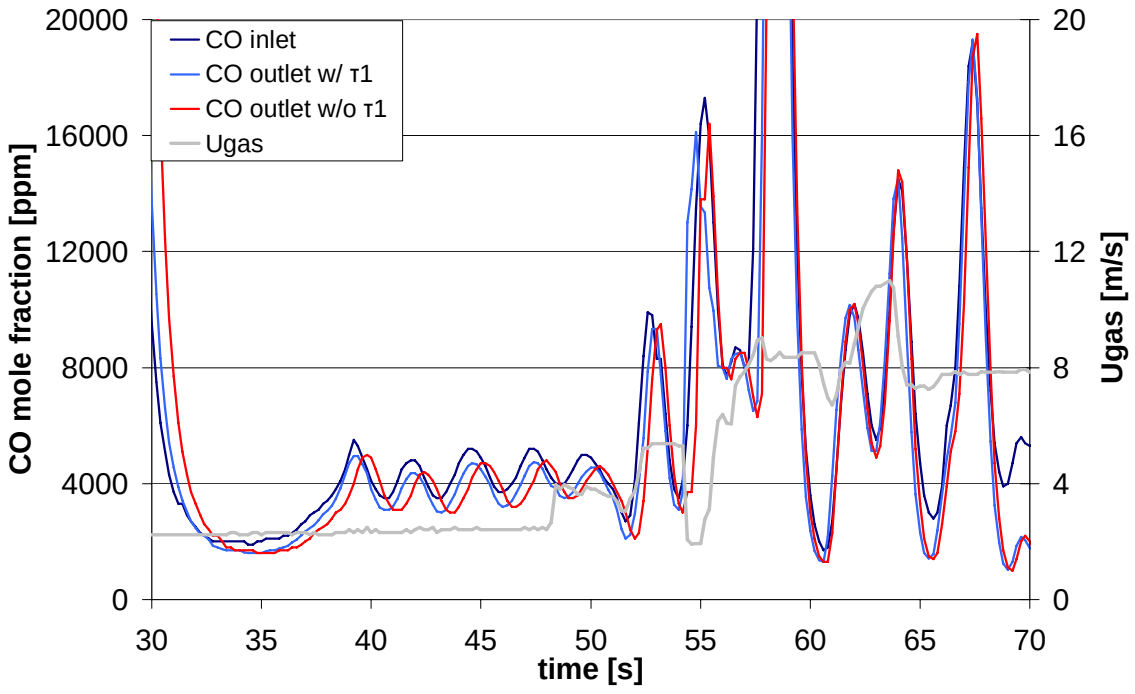

Figure 34 Phasing of the signals downstream the catalytic converter by taking into account the time needed for a unit mass to travel between the measuring points upstream and downstream the converter. If τ_1 variable of equation 1.15 is not calculated the inlet and the outlet signals are not well phased during low mass flow rates.

[a] F' is the objective function that is minimised in optimization algorithm calculations. In catalytic converter applications for this thesis, it is depended on measured inlet data and experimental and computed outlet data by definition. In house experience has shown that insufficient phasing between measured inlet and outlet data introduces significant errors to the F' that could lead optimization algorithm to non-global solutions.

Figure 35 shows the phased data of the inlet signals for the unphased case shown in Figure 28. Considering the lack of experimental layout knowledge the signals where phased assuming that θ is successfully incorporated in time lag τ.

These steps are dependent on the engine management. In the case shown, fuel cut is applied during deceleration (thus no combustion) and while lambda increases, NOx emissions are decreasing. This is an example of a minor step that is coming from qualitative observations.

Although optical observation of the signal phasing quality is a reliable method, quantification must be implemented. In general correlation factors of the signals present a good measure of synchronization but it must be adapted in each case of engine through qualitative observations. It is better to extract correlation factors during transient phenomena where the signals' variation is high. The basic idea of application of these factors comes from the knowledge of qualitative correlations between the signal as these referred in this chapter.

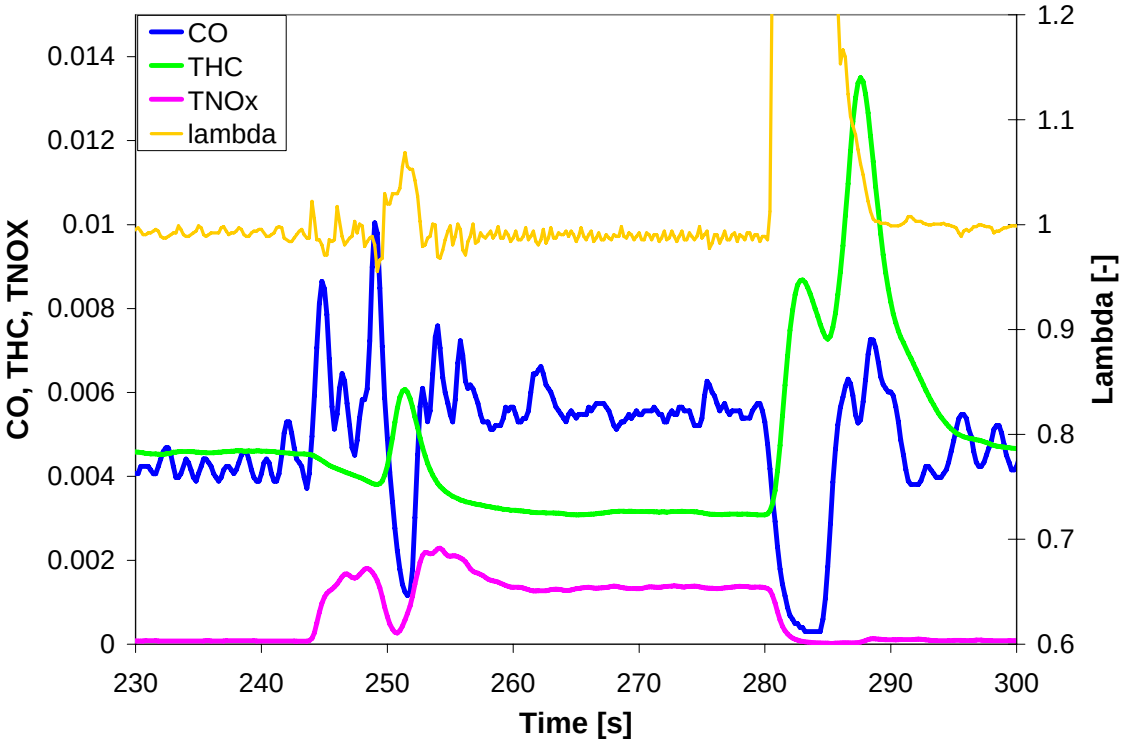

Figure 35 Correctly phased data of the inlet measurements of the figure 6. Lambda peak values are correctly associated with CO lows, HC temporarily increase due to combustion chamber scavenging and NOx decrease is mainly correlated with the mass flow rate decrease because of fuel cut during deceleration.

An additional measure is the N_2/O_2 atom ratio. N_2 and O_2 mass balance through engine control volume borders denotes that the ratio of their total atomic masses should be constant and equal to the respective of ambient air.

$$\frac{N_2\ atoms}{O_2\ atoms} = \left(\frac{2\tilde{x}_{N_2} + \tilde{x}_{NO}}{2\tilde{x}_{O_2} + \tilde{x}_{CO} + 2\tilde{x}_{CO_2} + \tilde{x}_{H_2O} + \tilde{x}_{NO}} \right)_{exh.gas} = 3.773 \quad (0.28)$$

A secondary calculation for checking inlet and outlet phasing and differences between analysers, which has a great impact on the exhaust aftertreatment devices study, is the subtraction of inlet and outlet measurements while catalyst is inactive (e.g the first 10-15s)

$$rel.error = \frac{\left| \sum_{t=0}^{t_1} \left(\tilde{x}_{i,inlet} - \tilde{x}_{i,outlet} \right) \right|}{\sum_{t=0}^{t_1} \tilde{x}_{i,inlet}} \quad (0.29)$$

Ideally this quantity must be zero. Differences from zero value indicate either wrong phasing of inlet and outlet data or random errors, as different inlet and outlet analysers response or acquisition sampling problems.

Figure 36 presents a summary of analyzers data phasing processes made through spreadsheet operations. The summary includes time delays and responses of analyzers, some statistical data for N_2/O_2 atom ratio and air to fuel ratio, the signal correlation factors matrix for two periods (0-300s – variable engine operation and 155-165s – transient engine deceleration) and the relative errors of analyzers signal for the period 5-20s when the catalytic converter is inactive. All the data of this report is incorporated into a quality measure for the datasets that is prposed in section 3.5 of this thesis.

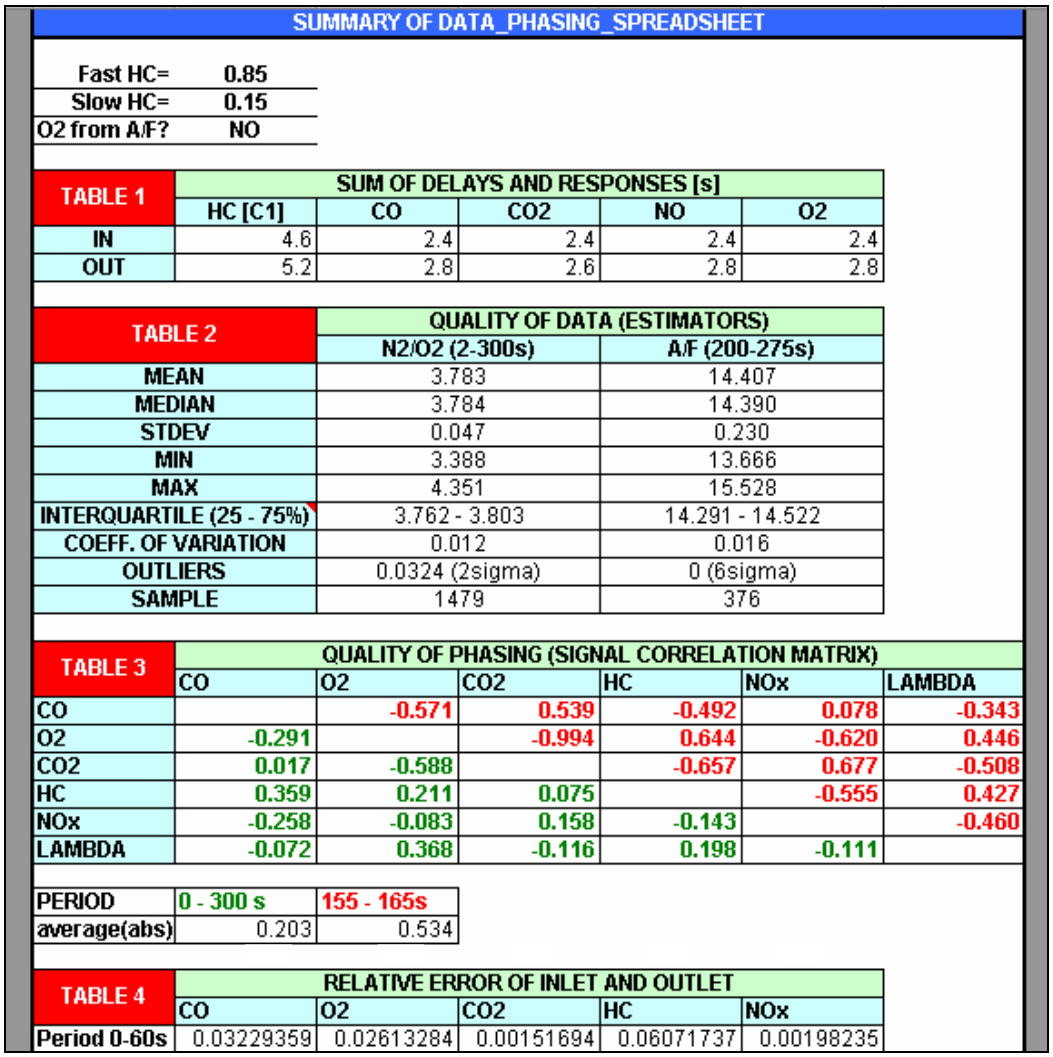

SUMMARY OF DATA_PHASING_SPREADSHEET

Fast HC=	0.85
Slow HC=	0.15
O2 from A/F?	NO

TABLE 1	SUM OF DELAYS AND RESPONSES [s]				
	HC [C1]	CO	CO2	NO	O2
IN	4.6	2.4	2.4	2.4	2.4
OUT	5.2	2.8	2.6	2.8	2.8

TABLE 2	QUALITY OF DATA (ESTIMATORS)	
	N2/O2 (2-300s)	A/F (200-275s)
MEAN	3.783	14.407
MEDIAN	3.784	14.390
STDEV	0.047	0.230
MIN	3.388	13.666
MAX	4.351	15.528
INTERQUARTILE (25 - 75%)	3.762 - 3.803	14.291 - 14.522
COEFF. OF VARIATION	0.012	0.016
OUTLIERS	0.0324 (2sigma)	0 (6sigma)
SAMPLE	1479	376

TABLE 3	QUALITY OF PHASING (SIGNAL CORRELATION MATRIX)					
	CO	O2	CO2	HC	NOx	LAMBDA
CO		-0.571	0.539	-0.492	0.078	-0.343
O2	-0.291		-0.994	0.644	-0.620	0.446
CO2	0.017	-0.588		-0.657	0.677	-0.508
HC	0.359	0.211	0.075		-0.555	0.427
NOx	-0.258	-0.083	0.158	-0.143		-0.460
LAMBDA	-0.072	0.368	-0.116	0.198	-0.111	

PERIOD	0 - 300 s	155 - 165s
average(abs)	0.203	0.534

TABLE 4	RELATIVE ERROR OF INLET AND OUTLET				
	CO	O2	CO2	HC	NOx
Period 0-60s	0.03229359	0.02613284	0.00151694	0.06071737	0.00198235

Figure 36 Summary of preprocessing. The report includes the phasing times, some estimatiors for the quality of the data, the correlation factors that give a good picture of the phasing and the relative error between inlet and outlet of the catalyst, during the first seconds when it is inactive.

3.6 MISSING DATA CALCULATIONS AND CROSSCHECKING

Section 2.3.1 defined the minimum number of experimental data required for the accurate study of catalytic converter operation and a simple methodology to match the real mole fractions of exhaust gas. This prerequisite is not always fulfilled, as in several cases there is lack of data in respect to the minimized experimental data format or there are defective measurements in an experimental dataset. Additionally, field tests (e.g. measurements of converters operation installed on vehicles under real driving conditions) have constraints on the sensors or analysers that can be installed. The rest of the data acquired remains valuable and can be used to extract further information of real catalyst operation. On the other hand alternative calculations of exhaust data can be used for cross-checking of acquired signals.

Common cases that there is lack of data are the following examples

- Lack of oxygen and/or lambda measurement at the outlet.
- Measuring only the legislated emissions and lambda
- Defective measurements that cannot be used

Of course, there is a limited number of data that can be replaced or calculated depended on the rest of measured data. In this section we present a set of calculations that can be used to crosscheck data or recover missing data, within a reduced accuracy compared to the direct measurement.

LAMBDA AND OXYGEN SIGNAL

Starting from equation 1.14 we can define lambda in an alternative way.

$$\frac{3.773 n_{O_2}}{\phi n_P} - \frac{\tilde{x}_{NOx}}{2} = 1 - \tilde{x}_{CO} - \tilde{x}_{CO_2} - \tilde{x}_{H_2O} - \tilde{x}_{H_2} - \tilde{x}_{NOx} - \tilde{x}_{HC} - \tilde{x}_{O_2} \Rightarrow$$

$$\lambda = \frac{n_P \left(1 - \tilde{x}_{CO} - \tilde{x}_{CO_2} - \tilde{x}_{H_2O} - \tilde{x}_{H_2} - \frac{\tilde{x}_{NOx}}{2} - \tilde{x}_{HC} - \tilde{x}_{O_2} \right)}{3.773 n_{O_2}} \Rightarrow$$

$$\lambda = \frac{\left(1 - \tilde{x}_{CO} - \tilde{x}_{CO_2} - \tilde{x}_{H_2O} - \tilde{x}_{H_2} - \frac{\tilde{x}_{NOx}}{2} - \tilde{x}_{HC} - \tilde{x}_{O_2} \right)}{3.773 \left(1 + \frac{m}{4n} \right) \left(\tilde{x}_{CO} + \tilde{x}_{CO_2} + \tilde{x}_{HC} \right)} \tag{0.30}$$

where $\tilde{x}_{H_2O}$ and $\tilde{x}_{H_2}$ are functions of $\tilde{x}^*_{CO_2}$ and $\tilde{x}^*_{CO}$. Figure 37 shows a comparison between the two different ways of calculating lambda. In literature (e.g. [163] and references therein) several ways forhave been reported for calculating lambda. The majority of them is based upon several assumptions, like the knowledge of the fuel composition, while the calculations are very accurate, over the accuracy of the instrumentation, time-consuming and complicated so that there is no sense to use them in common cases.

Equations (1.4) and (1.13) can be used to recover data as follows:

1) When there is lack of lambda and O_2 measurement using equations (1.9) and (1.18) results:

$$\left.\begin{aligned}\lambda &= \frac{n_p\left(\tilde{x}_{H_2O}+\tilde{x}_{CO}+2\tilde{x}_{CO_2}+2\tilde{x}_{O_2}+\tilde{x}_{NO}\right)}{2n_{O_2}}\\ \lambda &= \frac{n_p\left(1-\tilde{x}_{CO}-\tilde{x}_{CO_2}-\tilde{x}_{H_2O}-\tilde{x}_{H_2}-\frac{\tilde{x}_{NO}}{2}-\tilde{x}_{HC}-\tilde{x}_{O_2}\right)}{3.773n_{O_2}}\end{aligned}\right\}\Rightarrow$$

$$1=\frac{3.773\left(\tilde{x}_{H_2O}+\tilde{x}_{CO}+2\tilde{x}_{CO_2}+2\tilde{x}_{O_2}+\tilde{x}_{NO}\right)}{2\left(1-\tilde{x}_{CO}-\tilde{x}_{CO_2}-\tilde{x}_{H_2O}-\tilde{x}_{H_2}-\frac{\tilde{x}_{NO}}{2}-\tilde{x}_{HC}-\tilde{x}_{O_2}\right)}\Rightarrow$$

$$\begin{aligned}\tilde{x}_{O_2} &= \frac{2-9.546\tilde{x}_{CO_2}-5.773\tilde{x}_{CO}-5.773\tilde{x}_{H_2O}-2\tilde{x}_{NO}-2\tilde{x}_{H_2}-2\tilde{x}_{HC}}{9.546}\ or\\ \tilde{x}_{NO} &= \frac{2-9.546\tilde{x}_{CO_2}-5.773\tilde{x}_{CO}-5.773\tilde{x}_{H_2O}-2\tilde{x}_{H_2}-2\tilde{x}_{HC}-9.546\tilde{x}_{O_2}}{2}\ or\\ \tilde{x}_{HC} &= \frac{2-9.546\tilde{x}_{CO_2}-5.773\tilde{x}_{CO}-5.773\tilde{x}_{H_2O}-2\tilde{x}_{NO}-2\tilde{x}_{H_2}-9.546\tilde{x}_{O_2}}{2}\end{aligned} \qquad (0.31)$$

HC and NO measurements calculation cannot be safely used because the dependence on the rest of the signals with different analysers responses results in great relative errors in respect to their low molar fractions in exhaust gas. On the other hand, the lambda signal independent O_2 calculation is reliable, as shown in Figure 38.

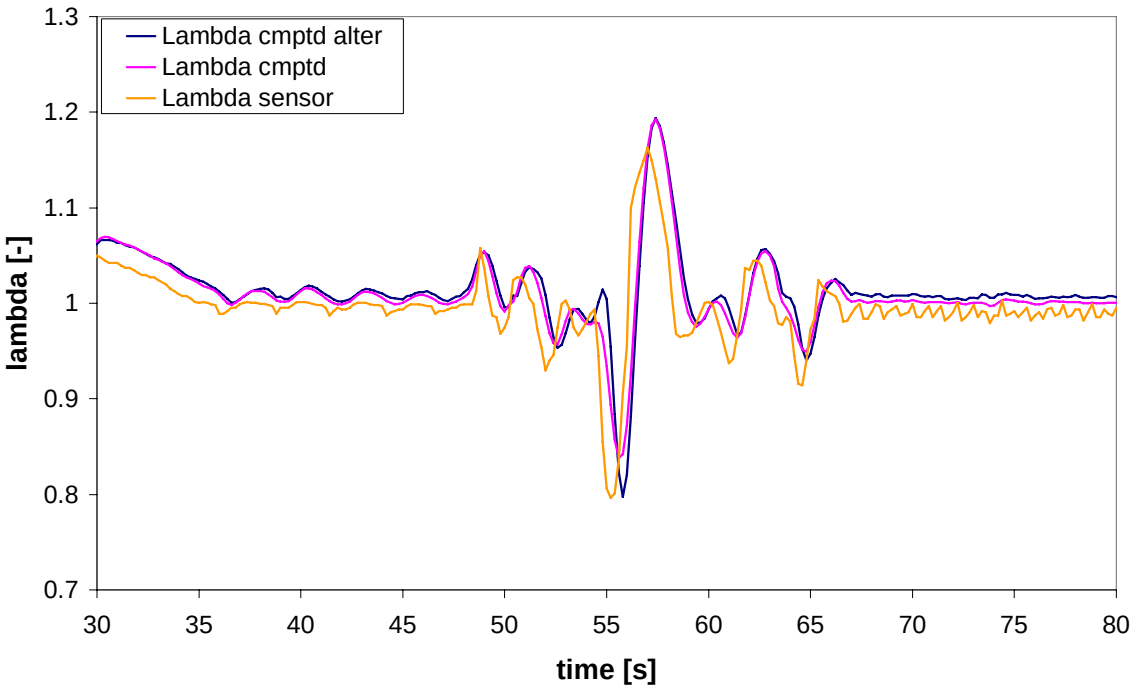

Figure 37 Lambda is calculated in different ways and compared with the lambda measured by the UEGO sensor.

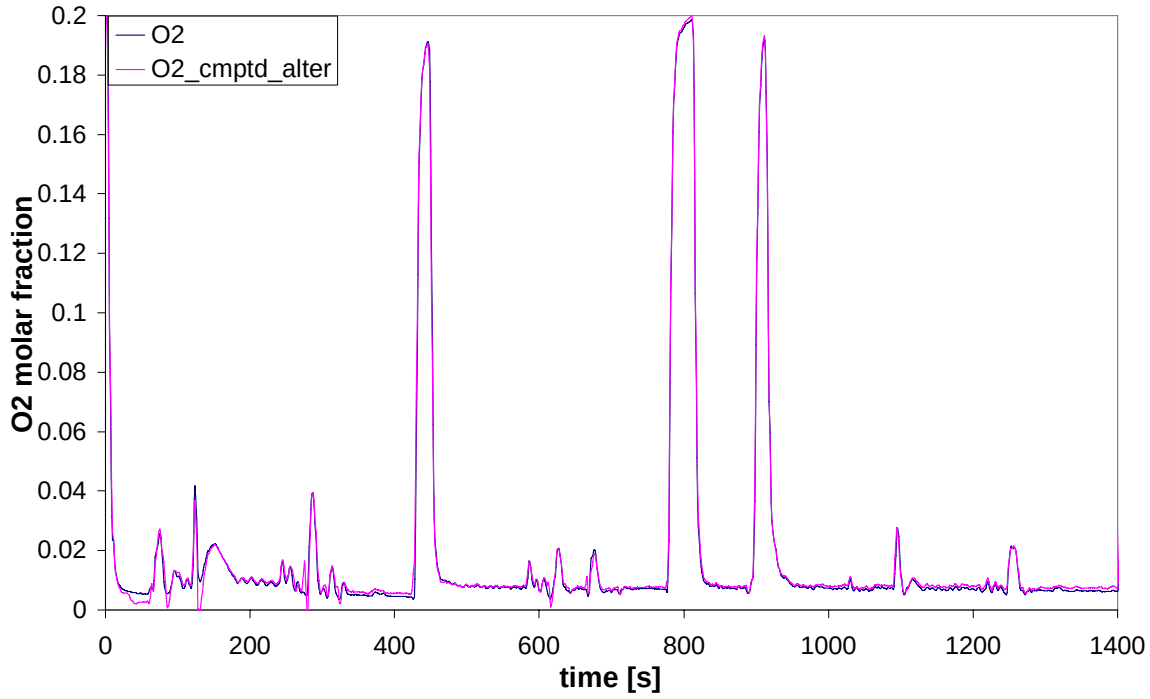

Figure 38 O_2 calculation comparison from equation 1.19 with the measured signal from analyser.

CO_2 SIGNAL

When there is lack of CO_2 measurement the signal can be calculated using a computational iterative method giving as convergence criterion the minimization of the sum of absolute error between the two definitions of lambda given by equations (1.9) and (1.18). An analytical solution of this system of equations results in a fourth order polynomial. Figure 39 shows the comparison between measured CO_2 and computed CO_2.

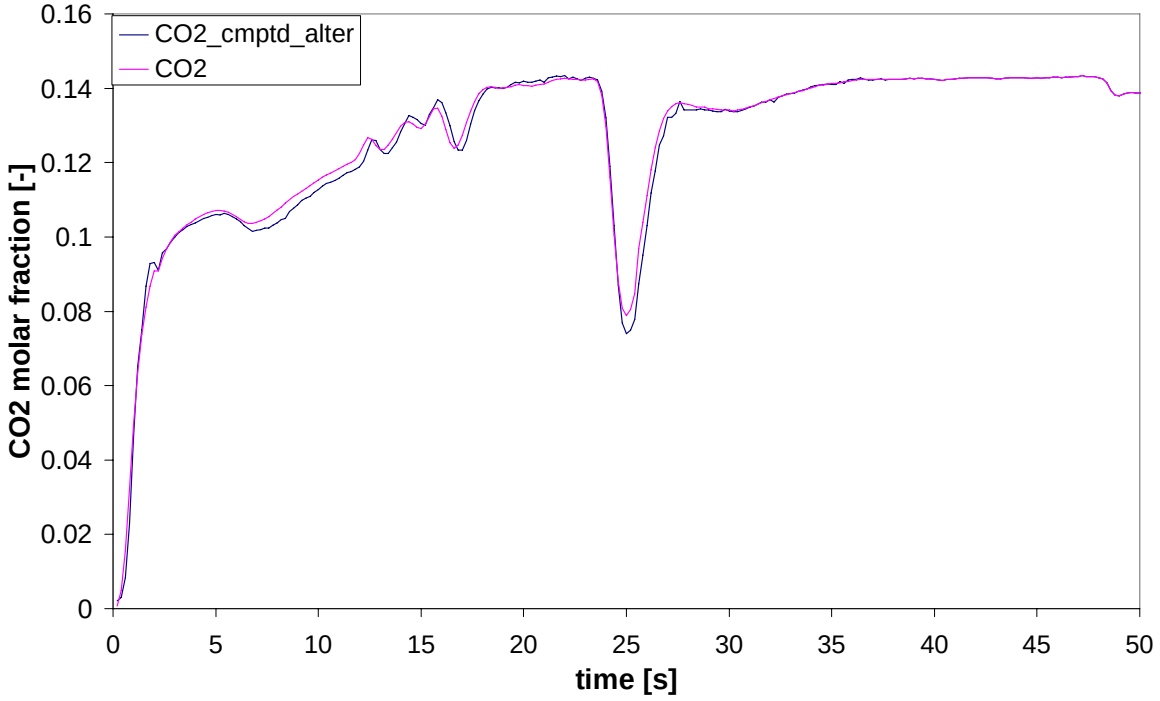

Figure 39 CO_2 signal calculation with an iterative way and comparison with the respective one measured with analyser

EXHAUST GAS MASS FLOW RATE

The calculation of exhaust gas mass flow rate can be done by the traditional calculations depending on the experimental procedure

In the case of intake air flow rate and lambda measurement, exhaust gas flow rate is calculated by the following equation. Special attention must be given to the signal phasing of intake air flow sensor and the lambda sensor

$$\dot{m}_e = \dot{m}_a \frac{\lambda \cdot \left(A/F\right)_s + 1}{\lambda \cdot \left(A/F\right)_s}$$

For constant volume sampling as indicated by the legislation exhaust gas mass flow rate is calculated by the equation

$$\dot{m}_e = \rho_e \frac{dV}{dt} \cdot \frac{CO_{2,diluted}}{CO_2}$$

3.7 QUALITATIVE OBSERVATIONS

A qualitative approach is also essential. Useful information on the engine management can be extracted by observing the experimental datasets. A fine example is the comparison of two gasoline-fueled engines of 2.0lt and 1.0lt that is shown in Figure 40 and in Figure 41. The 2.0lt engine is operated in slightly rich regime in order to reduce engine out NOx emissions, while the 1.0 lt one is operated at slightly lean fuel mixture. In the case of 1.0lt engine lambda is calculated from the exhaust gas concentrations, as there is a lack of lambda sensor measurement. Lambda management strategy in both cases enriches mixture during accelerations and cuts fuel during decelerations. Despite these, there is a main difference in the engine management during deceleration. In the case of 2.0lt engine the intake throttle is closed while 1.0lt engine shows an instant peak of exhaust gas mass flow rate. Once the specific engine management strategy is identified for a given engine, a visual control over all the respective modes present in the driving cycle could reveal possible measurement errors.

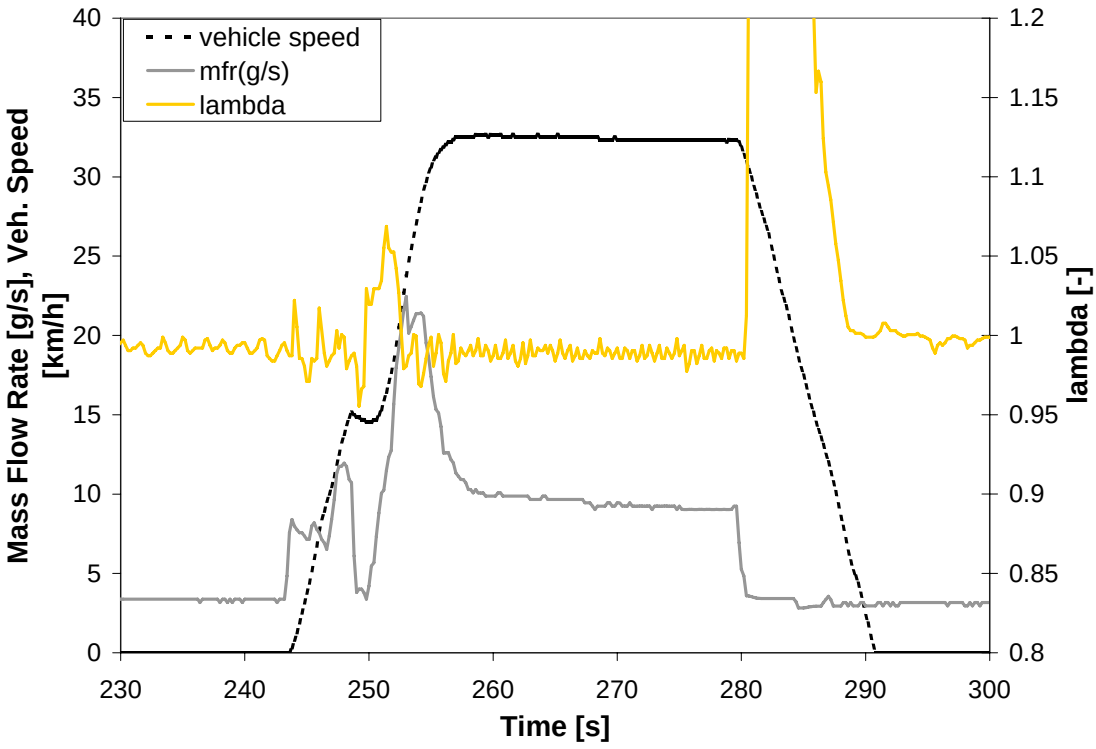

Figure 40 Low speed acceleration and deceleration events of UDC for the case of a 2.0 l engine. Engine is operating slightly in rich regime (λ~0.99). Fast data acquisition system (5Hz) enables the observation of instantaneous phenomena taking place during gear shifting and deceleration.

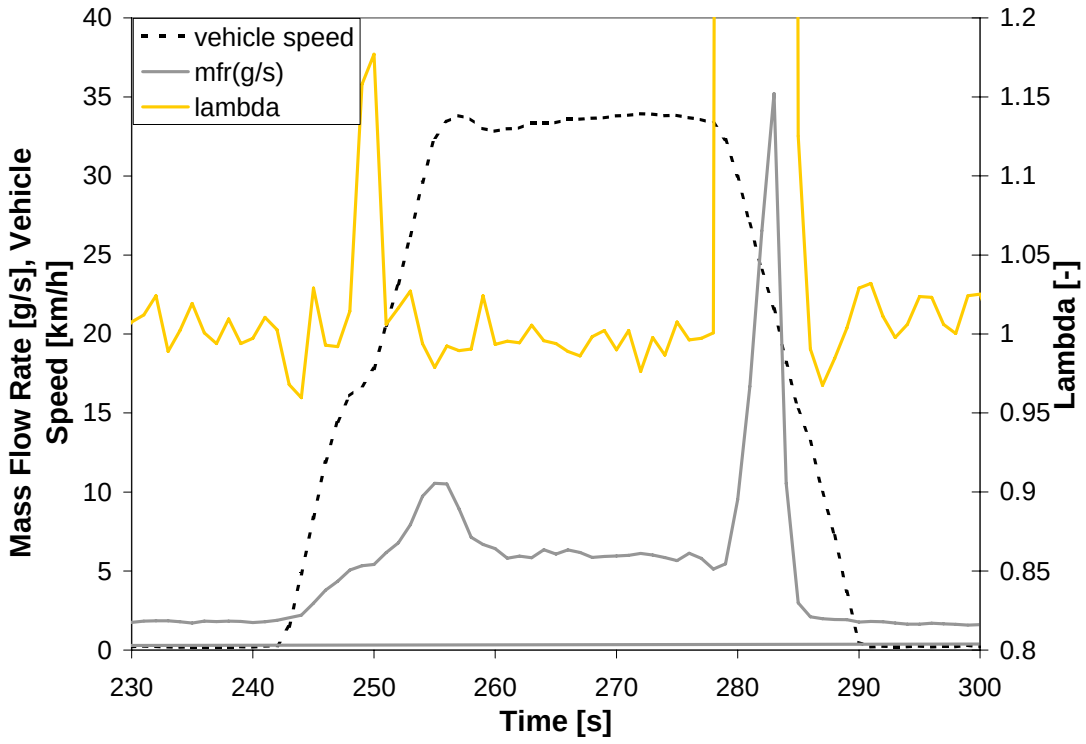

Figure 41 Low speed acceleration and deceleration of UDC for the case of 1.0 l engine. Engine is operating slightly in lean regime. (λ~1.01). A slow acquisition rate (1Hz) is producing aliased signals that constrain the information extraction from an experiment, as shown in mass flow rate pattern. These cases are analysed better with cumulative graphs.

Additional, qualitative observations on the signals can be made. Figure 41 shows an 1Hz acquisition where is obvious that there is aliased signal and smoother acceleration in comparison with the one in Figure 40 that is acquired in 5Hz. This type of qualitative checks could be possibly computerized by means of power spectral density graphs produced by FFT.

Further visual checks are possible regarding the response of the mass flow rate signal. In certain cases this signal is taken from the ECU input and is adequately fast, as that in Figure 40, compared to the more sluggish signal of Figure 41.

N_2/O_2 atoms ratio and air to fuel ratio shown in Figure 36 can be used as preliminary data quality estimators. Combined to optical qualitative observations evaluation of statistical variations in these quantities can reveal a possible bad dataset.

3.8 MODAL ANALYSIS

The driving cycle of typical legislated driving cycles for U.S. and the Europe can be separated into the following modes.

- Acceleration mode
- Deceleration mode
- Cruising mode
- Idle mode
- Cold start (Period that aftertreatment devices are inactive ($T_{exhaust}<T_{light-off}$))

The engine and exhaust treatment devices are operating differently in each one of the above modes, according to the specific engine management system and philosophy applied by the engine manufacturer. Mixture enrichment is common during accelerations, while decelerations in modern engines are characterized by fuel cut for example. During steady state operation (idle and cruise) the A/F ratio can be rich, lean or close to stoichiometry depending on the manufacturer settings [69,164,165]. The initial period needed for the exhaust aftertreatment devices to reach their light-off temperature is essential, because it produces about 50% - 80% of the total cumulative tailpipe emissions of the legislated cycle.

Other researchers have already proposed a quantitative measure that can be employed to characterize these modes. It is named "positive acceleration kinetic energy per unit distance" (PKE)[166]. It is defined as follows:

$$PKE = \frac{\sum_{i=1}^{n}(V_{i+1}^2 - V_i^2)}{\frac{\sum_{i=1}^{n} V_i}{n} \cdot \Delta t} = \frac{\sum_{i=1}^{n}(V_{i+1}^2 - V_i^2)}{\overline{V} \cdot \Delta t} \quad (0.32)$$

where V_{i+1} is the final speed and V_i is the initial speed in a positive acceleration ($a>0$) manoeuvre which forms part of a trip or microtrip. PKE has the units of acceleration and can be regarded as the representative acceleration for a micro-trip (a stop-to-next-stop driving segment), or for the complete trip. In this work, PKE is extended and used as a definition of the instantaneous driving condition. In this extended definition, each microtrip is considered to be the distance traveled by the vehicle during a short time period, typically shorter than 1 second, consisting of three time segments (i=1,2,3). This distance is calculated as the average speed over the three time segments (n=3 typically selected for smoothing), multiplied by this

period time. Using the experimental vehicle speed and PKE, the driving cycle can be distinguished into acceleration, deceleration, cruise and idle modes. The experimental data is linked to each mode for further treatment, allowing by this way a better view of the engine and catalyst operation.

Figure 42 shows the PKE and vehicle speed versus time. The assumption made is that for PKE>0.2 m/s² the vehicle accelerates and for PKE<-0.2 m/s² the vehicle decelerates. The graph shows the distinction of each mode in the driving cycle, and it can be used as a criterion for the quality of the experiment. This is obvious in the gear changes during acceleration where PKE fluctuates.

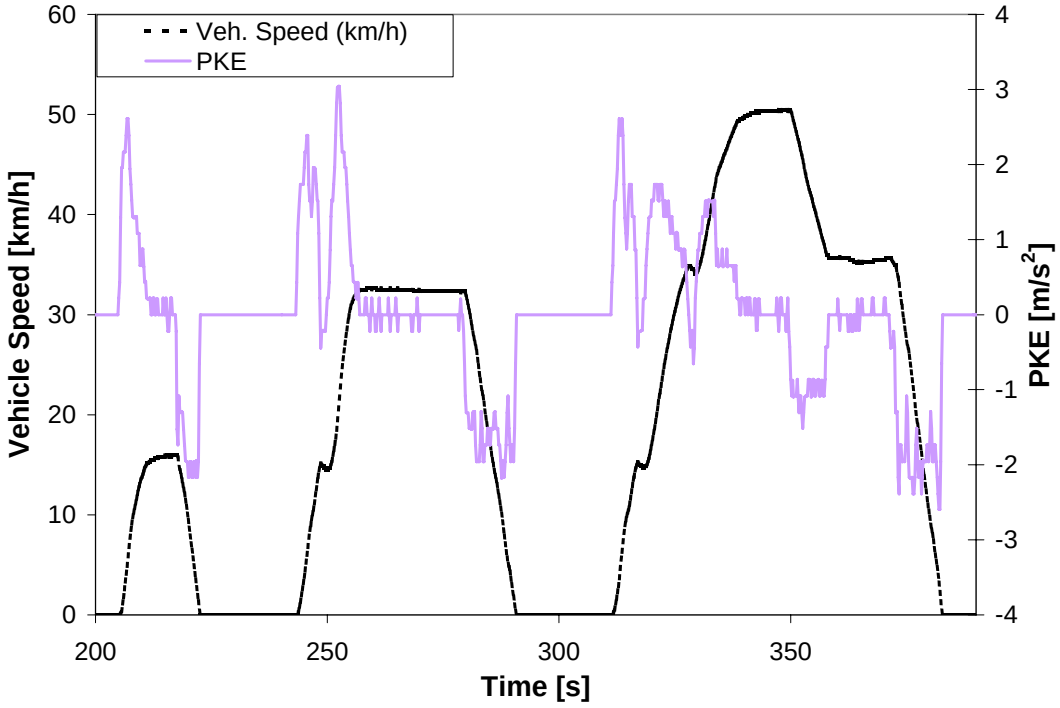

Figure 42 Positive Kinetic Energy criterion and vehicle speed versus time during a part of the NEDC. In this way, the driving cycle is discretized into four modes: idle, cruise, acceleration and deceleration, depending on the values of PKE.

Engine out emissions are strongly correlated with the driving modes. The knowledge of the emissions impact in each mode is essential for the exhaust aftertreatment devices design. A great advantage of the implementation of PKE is that it allows the comparison between different driving cycles, where different engines can be compared by means of their respective modal analysis data, like the one shown in Figure 43 and Figure 44. These figures are produced by processing of engine-out, cumulative CO, HC, NOx and O_2 (molar) emissions during the individual modes of the driving cycle.

Figures of this kind can also be used for emissions downstream the exhaust gas aftertreatment device to show the periods of the converter 's operation failures and the possible reasons for this.

.

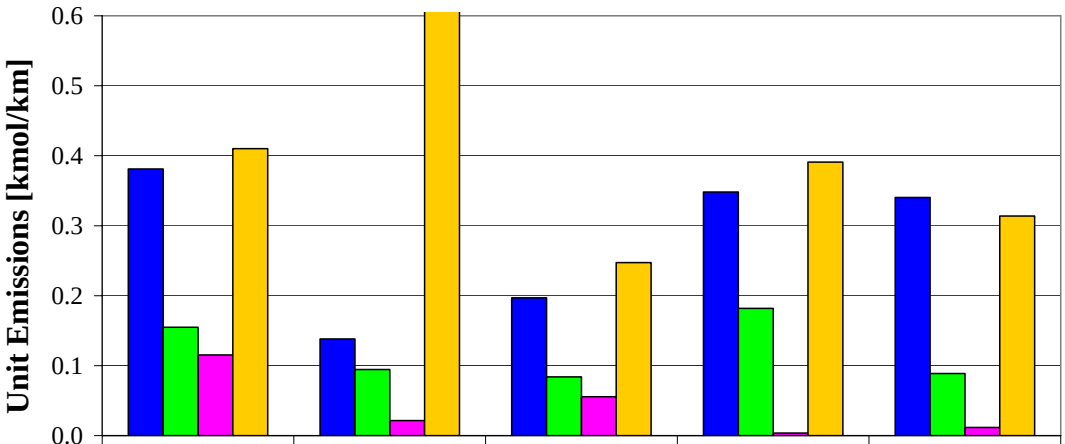

	kmol/km out during accelerations	kmol/km out during decelerations	kmol/km out during cruise	kmol during idle	kmol out during T<300 oC
CO	0.381	0.138	0.197	0.348	0.340
HC	0.155	0.095	0.084	0.182	0.089
NOx	0.115	0.022	0.056	0.004	0.012
O2	0.410	0.895	0.247	0.391	0.314

Figure 43 Cumulative emissions per km of a 2.0 l engine during NEDC. The engine management is tuned for slightly rich operation, a rich cold start and fuel cut during accelerations that assist oxygen storage filling. Increased NOx emissions result from a relatively high compression ratio.

Of course engine management has a principal role in the results of the modal analysis. Increased mass flow rate and mixture enrichment during acceleration produces higher emissions of NOx, while an overall excess of O_2, can be attributed to possible fuel cuts during decelerations. An engine with very "tight" and close to stoichiometry lambda management, presents a totally different behavior as it will be shown in chapter 3

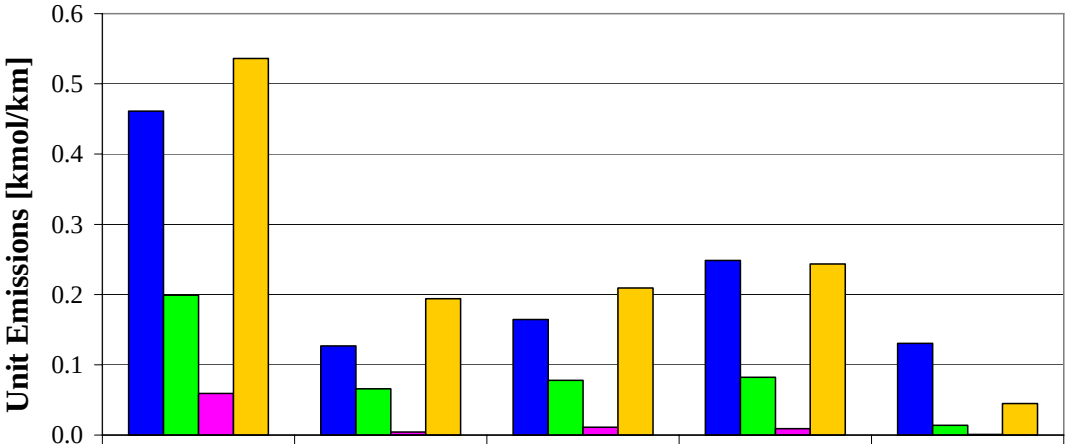

	kmol/km out during accelerations	kmol/km out during decelerations	kmol/km out during cruise	kmol during idle	kmol out during T<300 oC
CO	0.461	0.127	0.165	0.249	0.130
HC	0.199	0.066	0.078	0.082	0.014
NOx	0.059	0.004	0.011	0.009	0.001
O2	0.536	0.194	0.209	0.243	0.045

Figure 44 Cumulative emissions per km of a 4.6 l engine during FTP-75. The engine is operating always close to stoichiometry, except during cold start where it shifts to the rich regime. This type of engine needs a catalytic converter focused mainly on oxidation processes

Concerning the quality assurance, the datasets that are coming from a single experiment (e.g. the same engine tested several times) must present similar behavior in each mode, concerning that they follow the same control strategy.

3.9 MASS BALANCES CALCULATIONS

All the procedures mentioned above concerned engine-out experimental data, which is what is coming into the converter. It is of major importance to ensure that this data is error free, in order to assist modeling and design optimization of exhaust treatment devices. This section focuses on the exploitation of information that can be acquired by the application of species and element molecular balances across the catalytic converter. As explained in the previous sections, the composition of exhaust gas entering the converter is adequately described, for our purpose, by eight chemical species, that is: N_2, CO_2, H_2O, H_2, O_2, CO, HC, NO_x[167].

The transient catalysts' performance regarding the consumption of reactants and the production of inert products over the legislated cycle, can be visualized by means of chemical species production-consumption graphs of the type of Figure 45 (part of extra urban driving cycle for two experiments on the same vehicle). A close inspection of this figure reveals a number of differences in the transient emissions characteristics. For example, the initial consecutive accelerations of the EUDC produce intense emissions fluctuations. On the contrary, the acceleration from 70-100km/h (region around time=1050s with no gear shift) has not such intense emissions fluctuations, that can be partially explained by the the fact that there is not a gear shift. During a gear shift the engine is known to instantaneously increase speed because of the decoupling of the clutch, having an analogous effect in exhaust gas composition, because of cylinder scavenging and several other phenomena. As already mentioned instrumentation responses and the nature of the experimental layout is not capable of measuring these phenomena, which introduce perturbations in the datasets. This type of observations may be employed to produce further consistency checks between the signals of reactants and products.

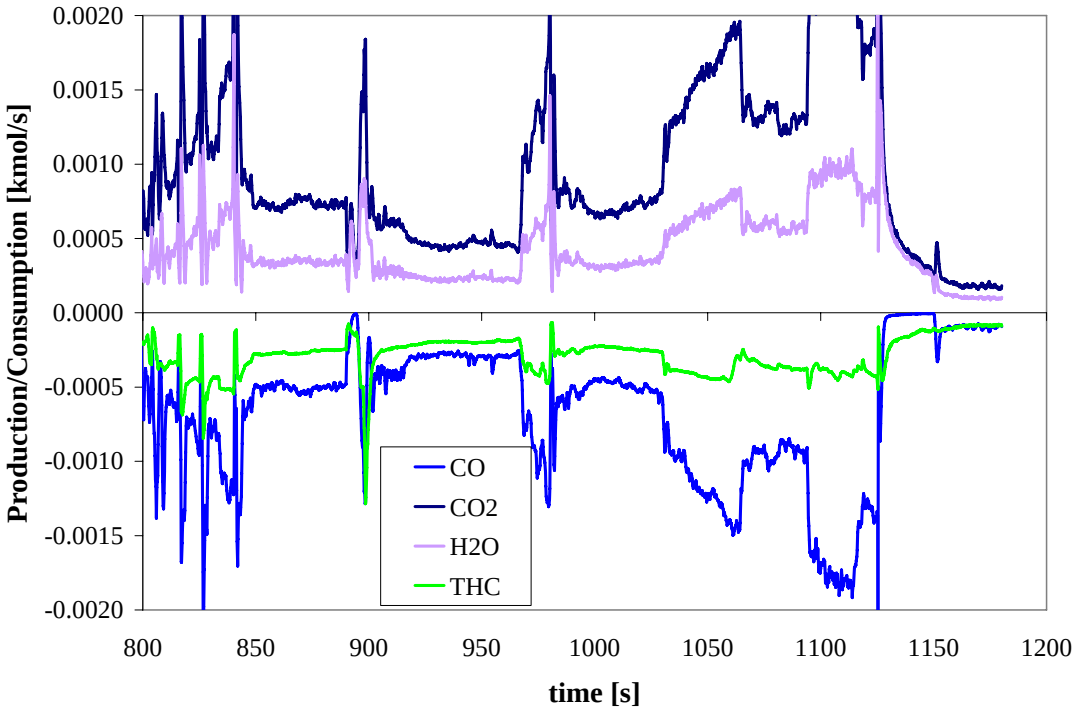

Figure 45 Species balances of CO, HC consumption and CO_2, H_2O production in a catalytic converter installed on the exhaust line of a 2.0 l engine during EUDC. These types of graphs reveal additional information on the quality of experimental data and they are used for cross-checking between experiments of the same vehicle. In this case fluctuations during acceleration at about 1050 s seem to come from problematic data in the specific regime.

A check of this kind can be based on elemental molecular balances. As an example, carbon and oxygen balances are presented in Figure 46 for two NEDC tests of the same engine with different catalysts installed.

Ideally, the elemental carbon balance should be a zero line. This type of behavior is approximately (within a certain tolerance) demonstrated during the cruise and idle modes of the driving cycle of Figure 40. On the other hand, there exist observable deviations from the zero line during acceleration and deceleration periods. Generally, the deviations in the carbon balance hint to experimental errors. In the case of transients, a fast response of the order of 0.1s (0 to 90% of full scale) would be required for all analysers employed in the acquisition. This could support a valid, say, 5 Hz acquisition, provided that accurate phasing is also obtained. Obviously this is not the case in Figure 46 where the observable deviation could be probably attributed to the usual, more sluggish, analyzers response that cannot successfully match the 5 Hz acquisition.

The situation is more complex as regards the origin of the more pronounced deviations in the oxygen balances. Starting with the observable oxygen deficit during deceleration at about 280 s, this can be mainly attributed to the filling of the oxygen storage. The less pronounced fluctuating deviation during the acceleration at about 250 s is more difficult to attribute, because of the combined effect of a slight acceleration enrichment with the associated instability of the control, also affected by the requirements of the gear shift.

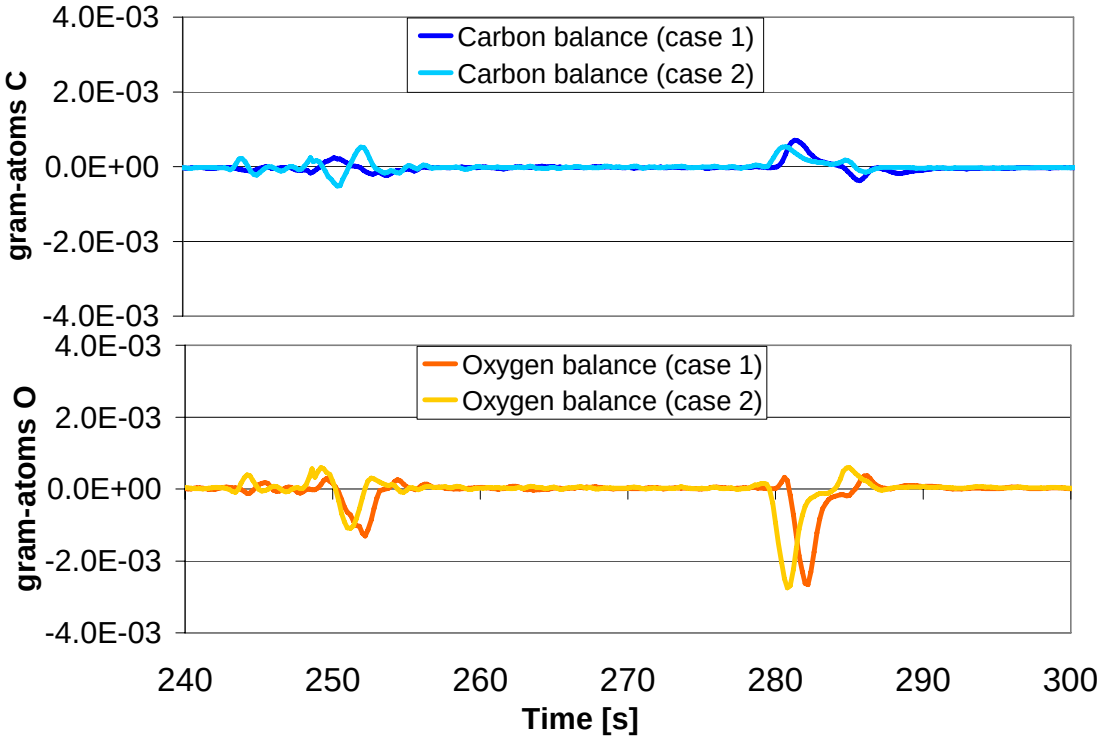

Figure 46 Elemental balances for C and O_2 across a catalytic converter installed on the 2.0 l engine on NEDC. Ideally elemental carbon balance should be a zero line, while oxygen balance may deviate from zero due to storage processes. Fluctuations of carbon balance at about 250 and 280 s (transient periods) are attributed to the response of the analysers. Negative oxygen values are attributed to storage filling during lean operation of the engine

Obviously, a certain level of experimental errors is always justified, and the usefulness of this type of diagrams lies in the comparison between different tests of the same vehicle and similar exhaust treatment system. Returning to the example of Figure 46 and up to a certain level of experimental error tolerance, the two cases are of equivalence level of experimental quality. In both cases there are similar levels of oxygen deficit that show similar behavior in oxygen storage filling.

3.10 Formulation of a Quality Measure

In the previous sections, a methodology was developed to check the quality of datasets and make possible corrections or recover any missing data. The main goal of this chapter is to assess the quality of the datasets through a standardized method. This can be done with the use of a customized measure for this process that is neither definite nor exhaustive but is open to several modifications and additions.

In order to formulate a criterion for the assessment of the quality of the datasets we have first to define its features.

- The criterion should be normalized, that is to range between zero and unity, in order to allow direct comparison between the datasets.
- It must be independent from engine and catalytic converter design characteristics or experimental procedure.
- It must be depended on characteristics of the datasets, the achieved phasing and other features discussed in the previous sections of this chapter.

The quantities that will be used in the definition of the quality measure are based on the standardized format employed in LTTE and sum up to the following:

Number of measurements: the maximum number of these measurements is 15; there should be five species measurements upstream the converter (CO, HC, NOx, CO_2, O_2) and the respective ones downstream, one measurement for lambda or A/F, two measurements for temperatures (upstream and downstream) and one for exhaust flow rate. They are separated into three categories:

- independent, which refer to the measurements coming directly from analysers or sensors (emissions, temperatures, etc.)
- dependent, which are any measurements calculated by the combination of two or more dependent signals (exhaust flow rate)
- missing, which are measurements that can be either recovered or have a small effect in the proper use of the raw dataset (e.g. O_2 outlet)

Percentage of outliers: outliers of the signals both for lambda ($> 6\sigma$) and N_2/O_2 atom ratio ($> 2\sigma$). While N_2/O_2 atom ratio should be constantly around value of 3.773, lambda can deviate further depended primarily on the engine control system (e.g. fuel cut during decelerations).

Acquisition frequency: higher acquisition frequency results in better representation of transient character of the experiment. The frequency of 2Hz is typical for the periodic oscillations of the transport phenomena inside the converter, which define the converter's operation practically. The current analyser technology, used in typical automotive tests, achieves a maximum acquisition frequency of 10Hz.

Average of correlation factors: The correlation factors refer to the ones that are resulting from phasing between the related signals as described at the beginning of the chapter. This measure determines the achieved quality of phasing and indirectly describes the decrease in the quality of the dataset coming from different analysers and sensors responses.

Average relative error between inlet and outlet during the period that the catalyst is inactive: it shows the relative quality of the input and the output signals due to different measuring scales, thus different resolution, and different measuring devices possibly used.

But how all these factors can be weighted? An arbitrary selection of weighting factors has to be taken into account based on previous experience and empirical observations concerning the effect of each quality "measure" to the total quality of the datasets. Of course, the use of normalized values results in linear dependencies of the factors measuring the datasets' quality. This can lead in several cases to a wrong estimation of the dataset quality as each factor should be considered to contribute unequally to the overall quality. A characteristic example is the case of missing or dependent measurements. One of them, in a total of 15, hardly affects the use of the dataset. On the other hand, the case of three dependent measurements dramatically decreases the overall quality of the dataset, considering the summation of the experimental error. In conclusion, the first two factors discussed here, should have a power law dependency, as a result of their higher importance to the total quality of the dataset.

DEFINITION OF THE FACTORS

In order to conform to the LTTE format, the required number of measurements to complete a dataset is 15. The relationship between dependent, independent and missing measures is

$$No.\_dependent + No.independent + No.mis\sin g = total\_measures \Rightarrow \\ NDM + NIM + NMM = TM \tag{0.33}$$

Each of these has to be combined into a single factor that will be weighted to describe the effect of measurements consistency in the quality of dataset. This factor has to be equal to unity when all measurements are independent and equal to zero when all measurements are dependent or missing. As already has been noted, this factor should not have a linear dependency on the dependent or missing values. A product of these factors, raised to the third power gives the behavior shown in Figure 47 that is close to the desired one

$$\left(\frac{NDM\left(TM-NIM\right)\left(TM-NMM\right)}{TM^3}\right)^3 = \\ \left(\frac{\left(TM-NIM-NMM\right)\left(TM-NIM\right)\left(TM-NMM\right)}{TM^3}\right)^3 \tag{0.34}$$

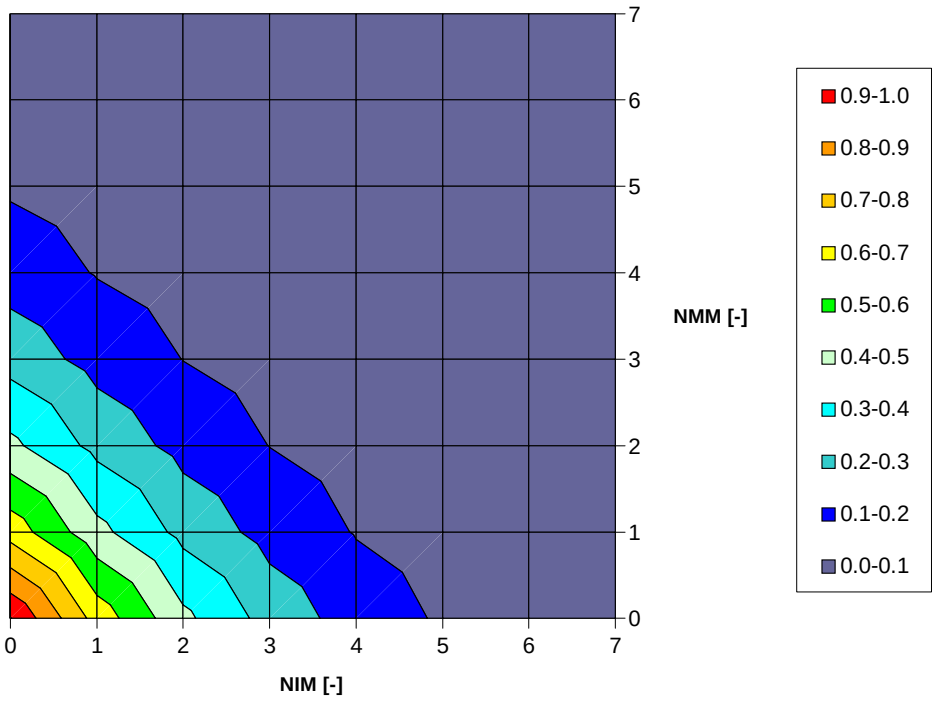

Figure 47 graph of equation 1.22 as a function of NIM and NMM

Concerning lambda and N_2/O_2 atom ratio outliers, a percentage of 30% in each case have a strong effect in the quality of the dataset. As regards lambda, outliers are considered values that exceed the limit of 6 standard deviations over a period, concerning that lambda control of the engine may allow great fluctuations of this

signal (e.g. during a deceleration). N_2/O_2 atom ratio should be constant at the value of 3.773 according to theory [13] but slightly offset mean values and oscillations around the mean are acceptable since it is a combination of several other signals with different responses. In convenience, it is assumed that acceptable values should lie in the range of ±2 standard deviations around the mean value over a period. Both of these values are raised to the third power in order to have non-linear dependency. The factor describing the effect of the outliers is an average of the third powers of lambda and N_2/O_2 atom ratio outliers and is represented in Figure 48 as function of lambda and N_2/O_2 atom ratio outliers

$$\frac{\left(\frac{N_2}{O_2}_{-outliers}\right)^3 + \left(\lambda_{-outliers}\right)^3}{2} \qquad (0.35)$$

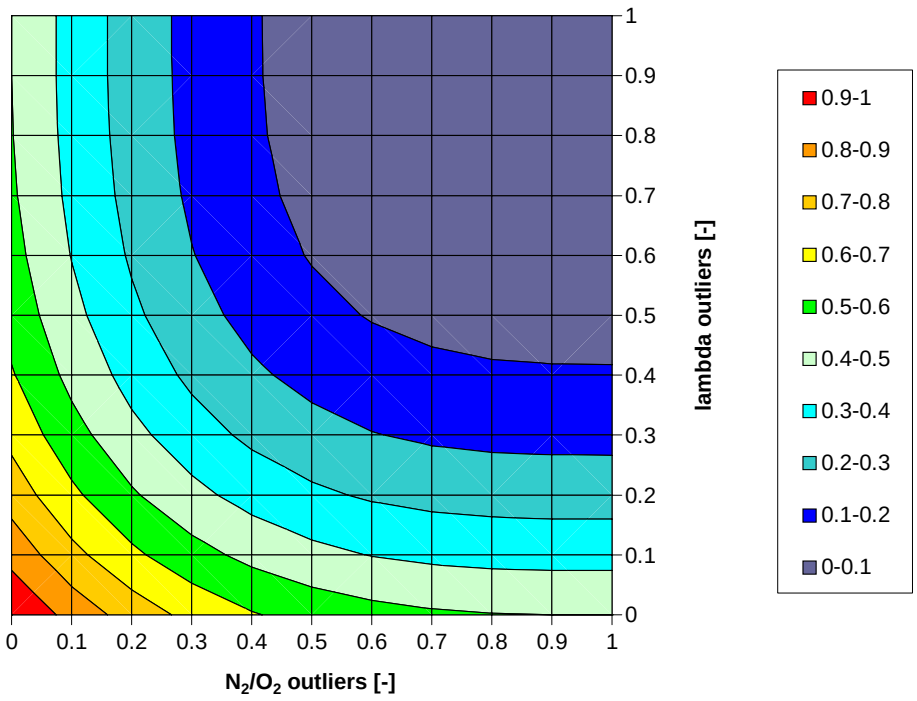

Figure 48 Graph of equation 1.23 as a function of lambda and N_2/O_2 atom ratio outliers

The rest of the quantities (3,4,5) are already normalized and they will be multiplied by a weight factor. The final formulation for the quality criterion of datasets is given in equation

$$
\begin{aligned}
&Quality\,Criterion = \\
&0.40\left(\frac{(TM - NIM - NMM)(TM - NIM)(TM - NMM)}{TM^3}\right)^3 \\
&+0.25\frac{\left(\frac{N_2}{O_2}_{-outliers}\right)^3 + (\lambda_{-outliers})^3}{2} \\
&+0.05\frac{Acquisition\ frequency}{10} \\
&+0.25\mu_{Correlation\,Factors} \\
&+0.05\mu_{Relative\,Error_{in\_out}}
\end{aligned}
\tag{0.36}
$$

Application of this criterion in 15 cases of the database of LTTE results the following (these cases will be discussed in extent later)

Table 9 Results of the quality measure assessment for the cases of the LTTE database

	Case I	Case II	Case III
1	0.7122	0.5169	0.7161
2	0.6996	0.5873	0.7082
3	0.6994	0.5568	0.6613
4	0.7012	0.5245	0.6955
5	0.7049	0.5463	

These values are in general in accordance with qualitative observations and the efforts for modeling the complete experiments, as shown in chapters 5, 6 and 7. The Case II is very difficult to be fitted by modelling calculations, the Case I is producing generally good results, while Case III is an intermediate state. It should be mentioned that the first case in each dataset was giving better modeling results than the rest in the same datasets, which matches the prediction of this primitive quality measure.

3.11 SYNOPSIS OF THE QUALITY ASSURANCE PROCEDURE

The above building blocks may be integrated in a preliminary test data quality assurance procedure which includes computer-aided along with manual steps, according to the tentative flowchart of Figure 49, which is briefly explained below:

Raw data acquired must be first transformed into a standard format adopted by the specific Lab. A standard format enables further processing of the data in spreadsheets or with software simply and error free. At this point, the acquired dataset is checked for completeness, as mentioned in section 2.3.1. Previous experience has shown that this type of tests, usually lack completeness of data. In some cases, data deficiency can be overcome by calculations. If the dataset is complete, the procedure described in section 2.3.2 for signal synchronization follows.

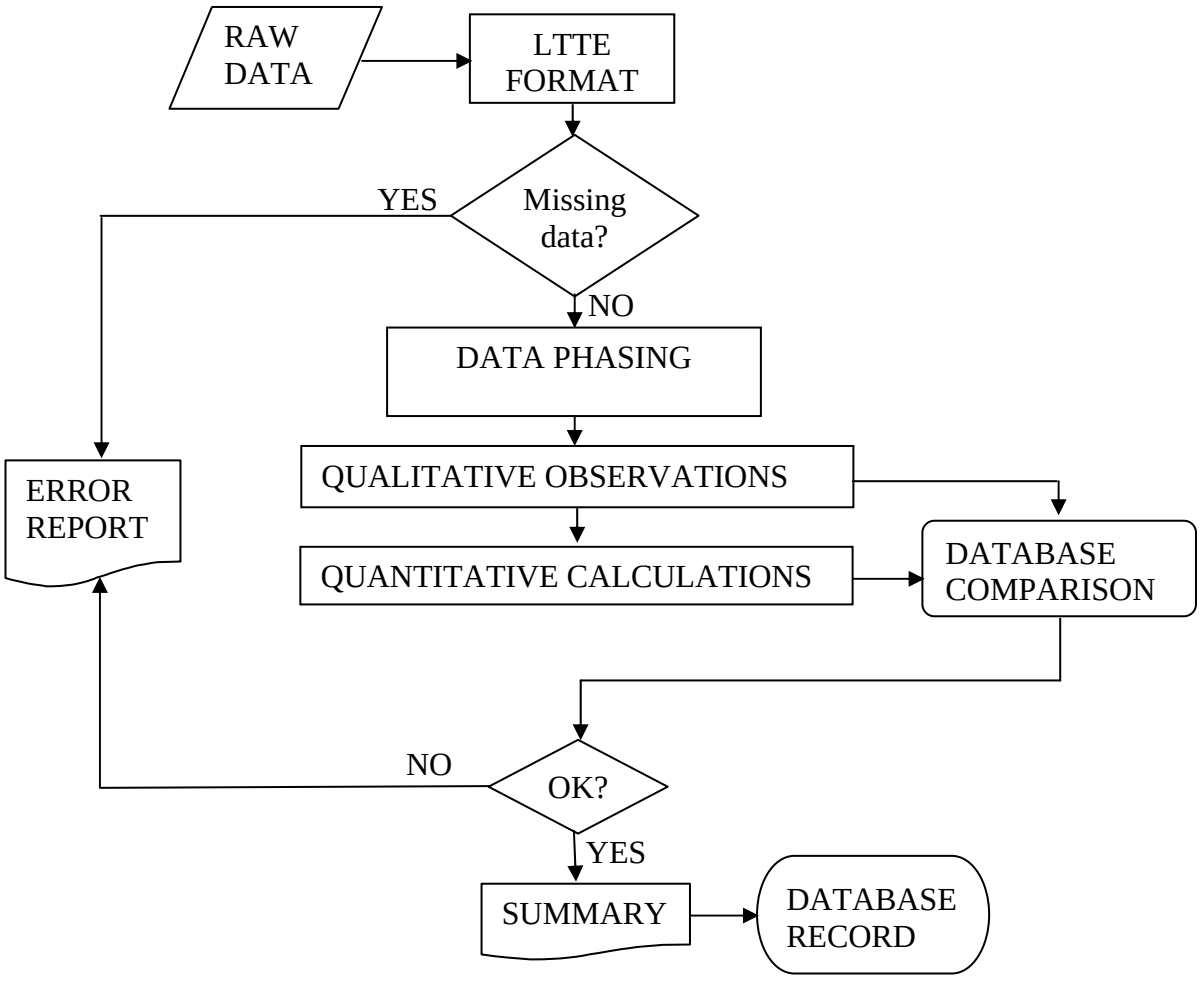

Figure 49 Flowchart of a preliminary quality assurance methodology. It includes data phasing and cross-checking through qualitative observations and quantitative calculations.

The next step is to perform qualitative observations on the operation of the engine in the various modes, the signals quality and other aspects. The summary is recorded and compared with the respective ones existing in the database. Implications of the type of engine, its displacement, management system and the exhaust treatment system installed are employed in the cross checking of the data. Afterwards, quantitative observations are performed with the assistance of several calculations and graphs produced by the software. Such graphs include molecular balances and cumulative unit emissions of exhaust gas species, as well as a number of cross checking calculations.

When a case study is successfully completed, it is recorded in the database with a complete report, for future use.

CHAPTER 4

COMPARATIVE STUDY OF DIFFERENT ENGINE MANAGEMENT CHOICES

A cooperative effort made in automotive industry in the recent years targets to the practical elimination of tailpipe emissions, through engine design improvements, sophisticated on-board control use, advanced catalytic technology application and intensive study of the overall system. These aspects have already been discussed in the previous chapters. The discussion in this chapter aims at the study of different engine management strategies that are selected to serve the special requirements of four commercialized systems. Here, the management strategy in each case is identified and correlated with both the engine design status and the exhaust aftertreatment system used. The results of this discussion assist the in depth understanding of the special characteristics of each case and several modeling concepts that will be discussed in the following chapters.

4 COMPARATIVE STUDY OF DIFFERENT ENGINE MANAGEMENT CHOICES

4.1 INTRODUCTION

Over the past several years, manufactures have made significant steps to improve engine design and engine management in order to produce engines with the lowest possible emissions. On the other hand, exhaust aftertreatment technology has moved from a general purpose catalyst to an exhaust aftertreatment system tailored for each engine. The intensive cooperation between the vehicle manufacturer and the emission system supplier became ever more crucial. The link between engine and aftertreatment device is a sophisticated engine management that utilizes advanced control strategies to reduce increased engine- out emissions during cold start and transient operation points (acceleration, deceleration) and to assist the optimal behavior of the exhaust aftertreatment system.

Modern engine control design should follow these directives without significant loss in power and comfort, and the use of advanced catalytic technology should practically eliminate the tailpipe emissions in order to conform to the future legislation. A good understanding of engine behavior and optimum selection of engine management strategy for each application case are essential prerequisites for system's success.

A widely used design methodology of such systems in the past was based on semi-empirical rules [83]. For a given engine, with known engine-out data, the type of the exhaust aftertreatment system is selected over a large database of catalytic devices. The catalytic devices may have already demonstrated a typical behavior in a similar application and/or have demonstrated specific properties and behavior over laboratory data if they are newly developed. The best converter is selected using a "trial and error" approach. The fine tuning of the system is accomplished via small modifications to the engine management.

The analysis of typical experimental data can reveal valuable information regarding the engine management strategy. The techniques employed to support fast catalyst heating up or increased stored oxygen in the catalyst are typical examples. The extraction of confident results is an important prerequisite to support the optimization of the overall system "powertrain - engine management -

aftertreatment device". Of course, the validation of such results over a stastistically significant sample is essential, considering the intrinsic statistical variation of the engine operation.

Because of the transient nature of the experiments, it is very difficult to extract quantitative results from instantaneous observations. A second- by- second investigation of experiments could reveal some isolated events that are possibly contributing to catalyst deficiencies, but this is not an adequate way to quantify them. Though, the detailed analysis of the datasets over the different operation modes becomes essential as it enables direct quantified conclusions. Modal analysis issues have already been discussed in chapter 3. In this chapter, we will show how they are implemented over a range of cases of different engines during US and EU legislated driving cycles.

4.2 Overview of the Cases

Three different engines will be investigated here, which are tested over different legislated driving cycles (FTP and NEDC) and are equipped with different exhaust treatment systems. The respective data for these cases is presented in Table 10. Obviously, these cases include a large variety of engines and catalytic devices. The object here is the study of the engine management strategy that is selected for each case and not the performance of the entire system. This aims to reveal the choices made in each case to link the engine behavior with the better catalytic converter performance.

Table 10 Data of cases under engine management study

Name	Vehicle Engine displacement	Test	Aftertreatment			
			Type	Volume	Position	
CaseI	Peugeot 406 2.0 l	NEDC (EURO III)	3WCC, Pt:Rh	2.4l	Underfloor	
CaseII	Mercedes Benz E-Klasse, 2.4l		3WCC, Pd:Rh	1.0 l	Close Coupled	Two in parallel
CaseIII	Mercury Grand Marquis, 4.6l	FTP-75 (ULEV)	3WCC, Pt:Pd:Rh	0.8 l	Close Coupled	Two in parallel
CaseIV	Peugeot 406, 2.0l HPi	NEDC (EURO IV)	3WCC, Pt:Rh	0.8 l	Close Coupled	In serial
			NOx Trap	3.0 l	Underfloor	

The study will be separated into the following three parts, suggested by the structure of the legislated test cycles:

- Operation during cold start
- Operation at urban driving
- Operation at extra-urban driving

During these periods, the operation modes are analyzed with respect to the engine out temperatures, the mass flow rates, lambda and molar species emissions. The modes of operation are acceleration, deceleration, cruise, idle and cold start. All these modes are related to the engine or vehicle speed, as shown in chapter 3, except the cold start that is a visually defined period specific for each case. The cold start

mode of operation is defined as the period when the exhaust aftertreatment device is inactive (usually below the light-off point). During this period, the engine management typically follows a completely different strategy compared to the rest of operation in the majority of the vehicles.

The intrinsic variations of the data due to the different experimental layouts, have a key role to the evaluation of these systems. The direct comparison of data should be careful, considering that the sensors are located at different points of the exhaust line in each case and have different responses. This stands for the temperature measurements mainly, as the gas temperature changes along the exhaust line, while the responses of the sensors and the analysers are the principal sources for differentiations in comparison studies.

4.3 Overview of the Engine Behavior

The visual inspection of the engine behavior, regarding temperature, mass flow rate and lambda variation, during the test is essential to identify the principles of the engine management strategy which are selected in each case (Figure 50 to

Figure 53). The visual inspection is facilitated by the repeated patterns of legislated driving cycles (see Figure 2 and Figure 3). For example, during the NEDC the vehicle repeats the pattern of urban driving four times that enables the direct visual comparison of the engine management strategy versus time.

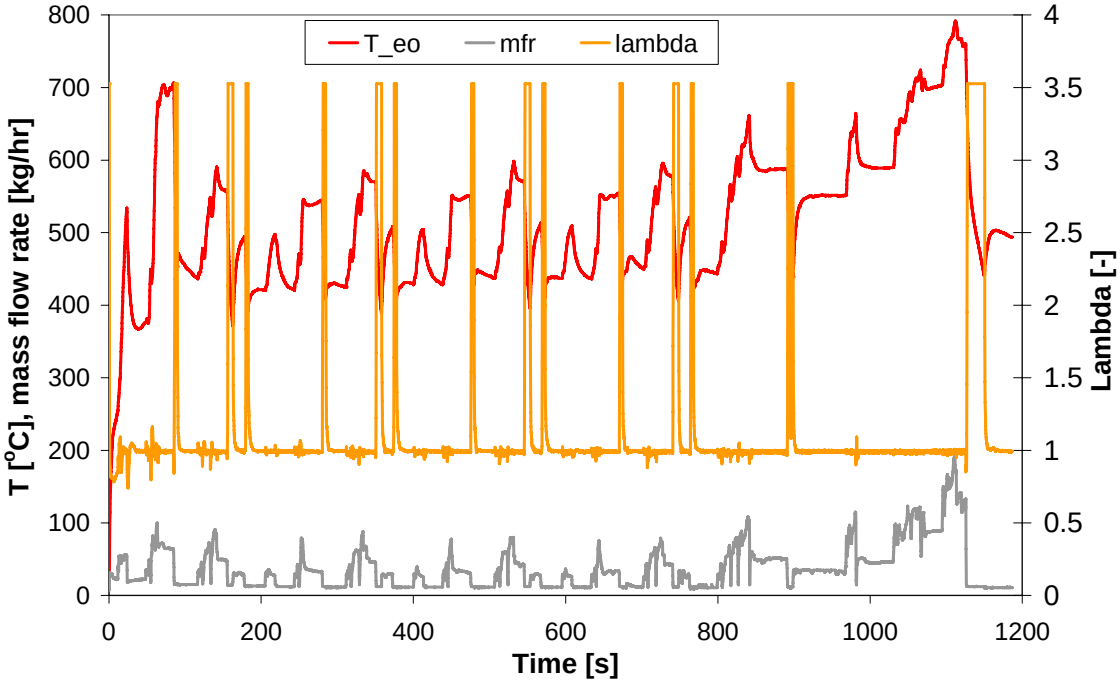

Figure 50 Lambda, exhaust gas mass flow rate and engine out temperature variation for the CaseI engine tested in NEDC.

Figure 50 presents the behavior of Case I engine during NEDC legislated test. During cold start period, which is visually estimated as the first 80 seconds period, the engine operates on an "open loop" lambda control that shifts operation to the rich side. At the same period the engine out gas temperature and mass flow rate increase, in order to provide adequate heat to the catalytic converter to reduce the heat up time and initiate its operation. This strategy is used in several vehicles and is the result of spark advance modifications and intake throttle manipulations.

The interesting part of this management strategy is found during the transient part of the driving cycle. During accelerations, lambda is slightly shifted to the rich

side in order to provide adequate power (see Figure 12). This rich environment tends to empty the oxygen storage capacity of the three-way catalytic converter. During sharp decelerations, when no engine power is needed the management cuts-off fuel delivery and the oxygen storage is filled up.

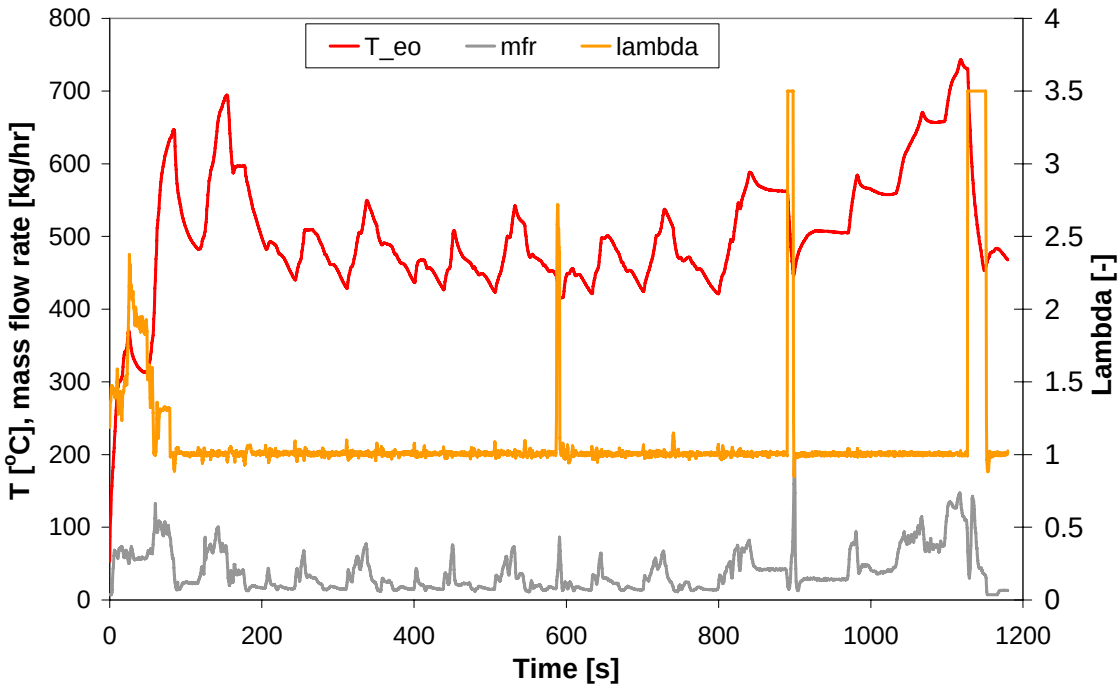

Figure 51 Lambda, exhaust gas mass flow rate and engine out temperature variation for the CaseII engine tested in NEDC.

Figure 51 shows an overview of the management for the Case II engine. In this case, the cold start operation is differentiated from the rest of operation also. Here, the lambda is clearly shifted to the lean side, accompanied by advance modification and extra mass flow in order to improve catalyst heat up [168]. Shifting to the lean side is a choice to ensure oxygen storage filling and catalyst surface pre-oxidation that improves low temperature operation. Taking into account that the operation of the engine is shifted slightly to the lean (as will be shown later in this chapter) there is no need to assist oxygen storage filling. This is done in three cases, which are indicated in Figure 51 with the lambda breakthroughs. These three spikes of lambda, aim at the filling of the oxygen storage capacity after prolonged acceleration or cruise operation and are defined probably by the post catalyst oxygen sensor signal [1].

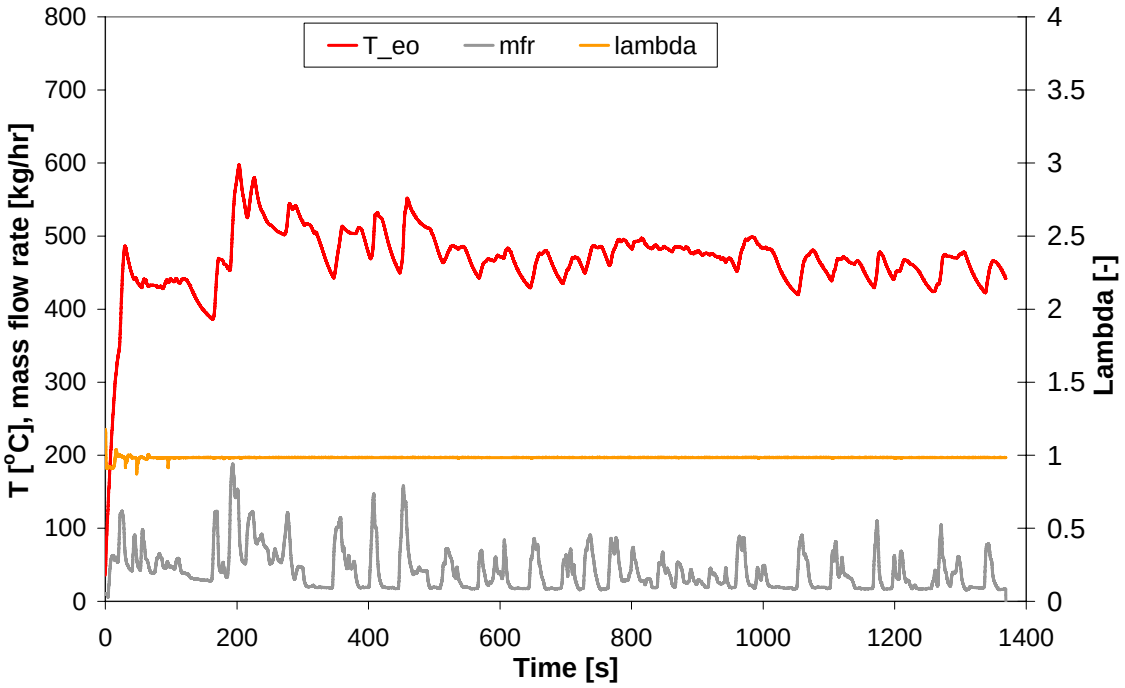

Figure 52 Lambda, exhaust gas mass flow rate and engine out temperature variation for the CaseIII engine tested in FTP-75.

Figure 52 presents the behavior of the engine of Case III that is tested in FTP-75 legislated driving cycle. As in the case of the Case I engine during cold start period the lambda control is open looped and shifted to the rich. No other special modification can be seen for this period. The main characteristic of this management strategy is the tight lambda control, slightly shifted to the rich side. This aims at the use of a tailor made catalyst for the specific exhaust gas conditions determined by the associated engine management [168]. This is a typical example of an older engine that is equipped with an advanced catalytic converter and an engine management tailored for the optimum performance of the overall system, in order to conform to later stringent legislation.

Figure 53 presents the engine management of an advanced aftertreatment system. The system comprises a close-coupled catalytic converter and an underfloor NOx trap in series. The engine management has to be tailored to assist the operation of both devices which operate within different lambda and temperature windows. A three-way catalytic converter needs increased temperatures in order to achieve monolith temperatures higher than its light-off point, while the NOx trap needs lower than 350^{o}C temperatures to maintain high NOx storage efficiency. The

unavoidable temperature increase due to exothermic reactions in the three-way catalytic converter is treated with special exhaust line design. In addition to these, the regeneration of NOx trap begins at higher than 450°C, which can be achieved with engine management modifications, but special care must be given in order to avoid thermal ageing of catalyst during long term use.

The lambda management is an advanced optimization problem also. The specific exhaust system operates as a three-way catalyst during stoichiometric or rich engine operation and as an oxidation catalyst and a NOx trap during lean conditions. As already discussed in chapter 1, the regeneration of the NOx trap can be established with rich pulses. In this case, the width and the duration of the pulses must be optimised in order to maintain good fuel economy, override possible catalytic reactions at the front catalyst and deliver adequate rich environment at the front of the NOx trap to assist complete regeneration. The decision for the initiation of the NOx trap regeneration is taken by on-board control by taking into account the storage status of the NOx trap and the mode of driving [169].

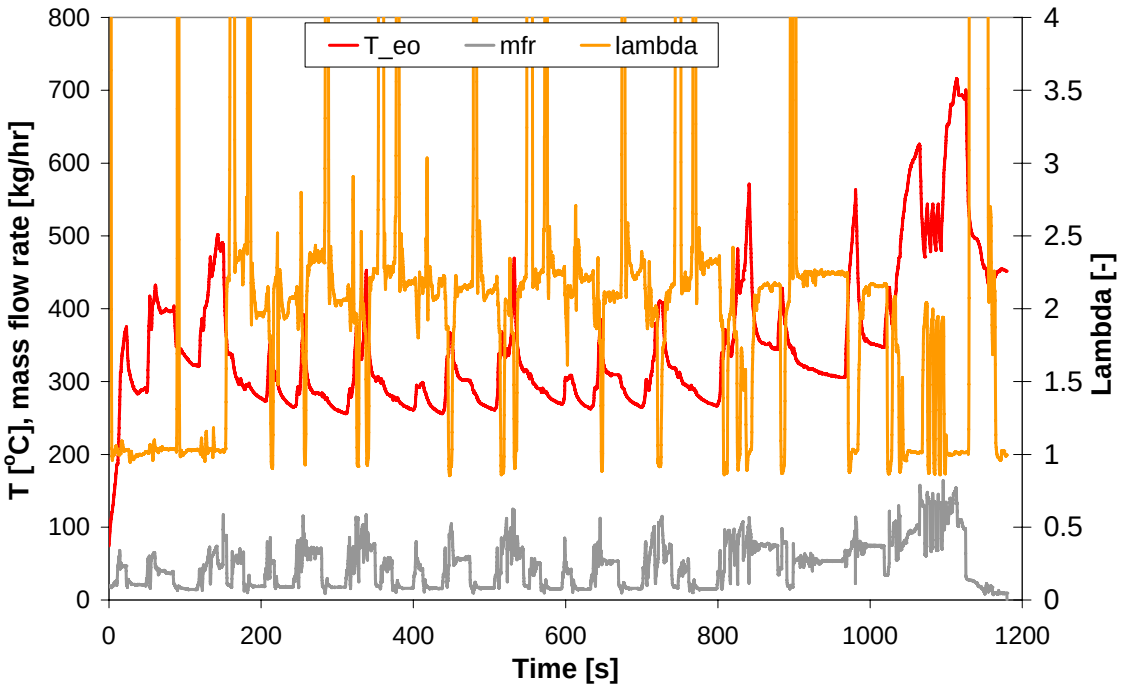

Figure 53 Lambda, exhaust gas mass flow rate and engine out temperature variation for the CaseIV engine tested in NEDC.

A modal analysis is able to describe the engine management strategy during the different driving conditions and to further assist the optimum design of the exhaust system.

4.4 Modal Analysis of Engine Management

In this section, the operation of the system engine-engine management-aftertreatment device(s) is analyzed at different modes of driving. The data that is analyzed is addressed at the exhaust line considering that the primary target is the understanding of the basics of the engine management in each case. The latter is considered as the link for the optimum operation of the system. The analysis at the different modes of operation will be made for the four cases described in Table 10 for the exhaust gas molar fractions of CO, THC, NOx andO_2, the engine out temeperatures and the lambda values.

Figure 54 to Figure 56 represent at a glance the operation of the engines at the different modes of driving. The respective discussion has been made in the previous section for the entire driving cycle. In these figures the bars represent the average value per mode of driving and the red lines the deviation of this value expressed as the interquartile range[a].

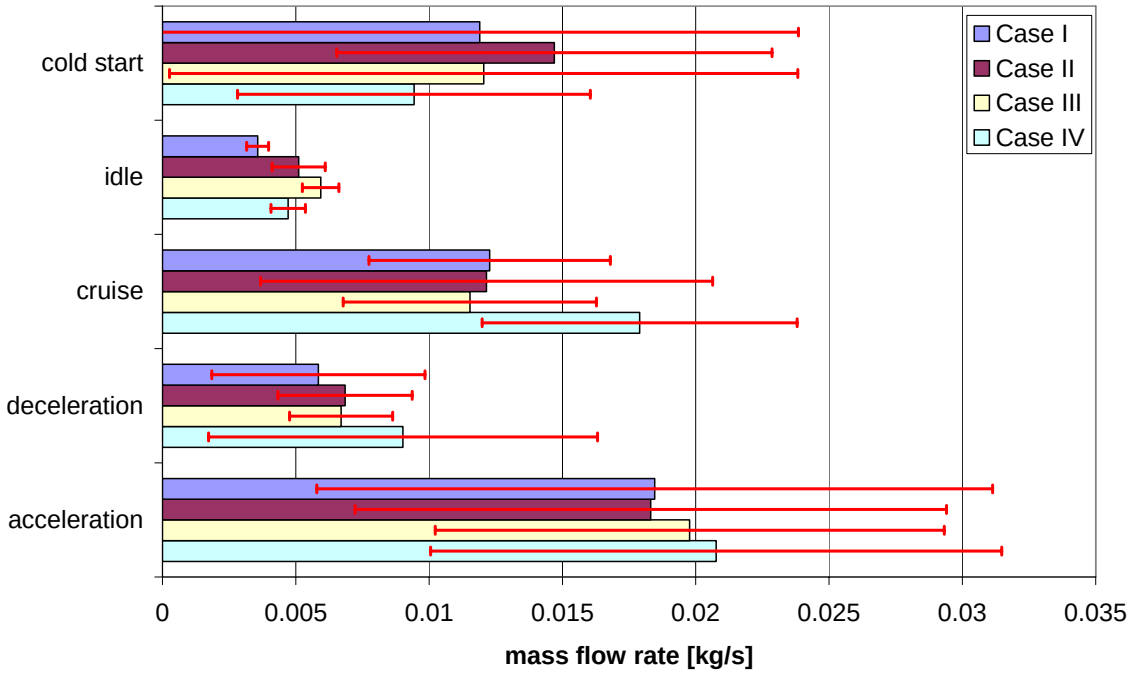

Figure 54 Mass flow rate of modal analysis for all cases

[a] Interquartile range is defined as the central range where the 50% of the values lies. The 25% of lower and the 25% of higher values has been excluded. This is used as a more confident and descriptive measure than the standard deviation especially in the cases of transient engine operation.

As shown in Figure 54 in all cases the mass flow rate differentiates during the several modes of operation according to the selected engine management strategy. Cases II and IV use a more advanced mass flow rate control shown by the large ranges of variation. Case II has a higher fluctuation of mass flow rate during "steady state" modes (idle and cruise) than the other cases as a result o secondary air assisted into exhaust to aid catalytic performance. Case IV shows increased variations during decelerations that are attributed to the NOx trap thermal regeneration assistance.

Lambda control varies significantly from case to case as has already been noted. The tightness of the control around a rich value is clearly shown for Case III, while the cold start and the deceleration strategies can be identified at a glance.

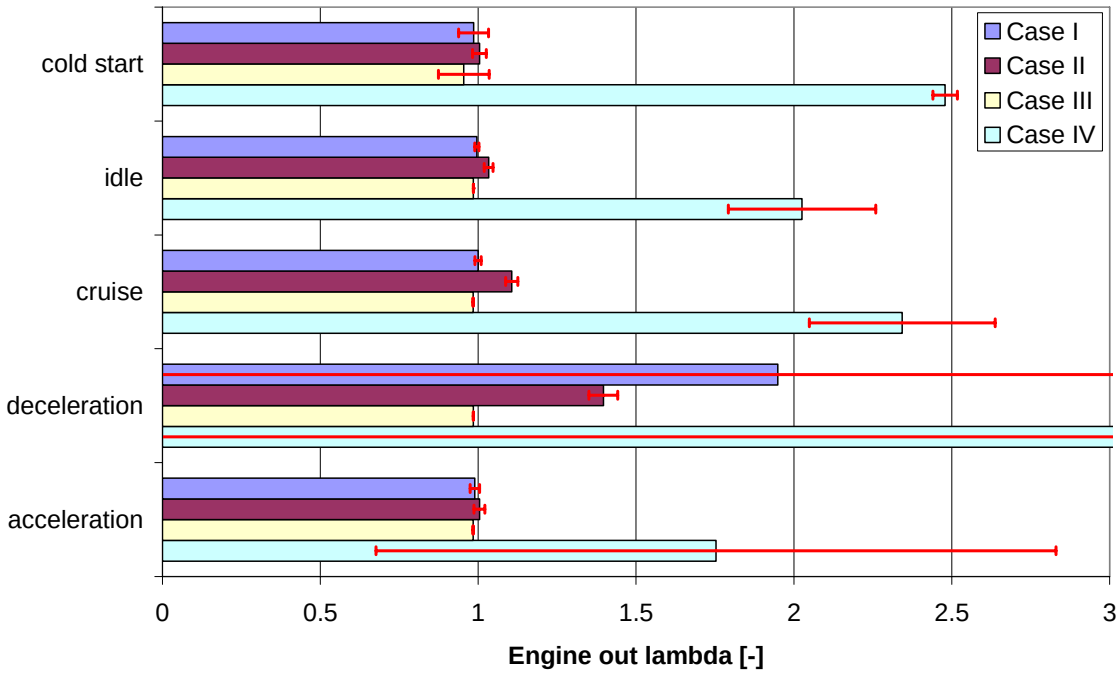

Figure 55 Engine out lambda of modal analysis for all cases

Temperature windows of operation are essential to achieve increased efficiencies during all modes of operation. The values shown in Figure 56 are sampled at different locations of the exhaust line and cannot be directly compared. As expected, the lean burn SI engine produces significant lower engine out temperatures, which may decrease the precatalyst efficiency. Of course this temperature range is required to maintain high NOx storage efficiency in the NOx

trap. The stoichiometric[a] Case III engine produces lower temperatures than stoichiometric engines of cases I and II although it operates at slightly rich region and is tested in FTP-75 driving cycle. This is attributed to the lower power delivery of this engine that is about 2/3 of the other two engines.

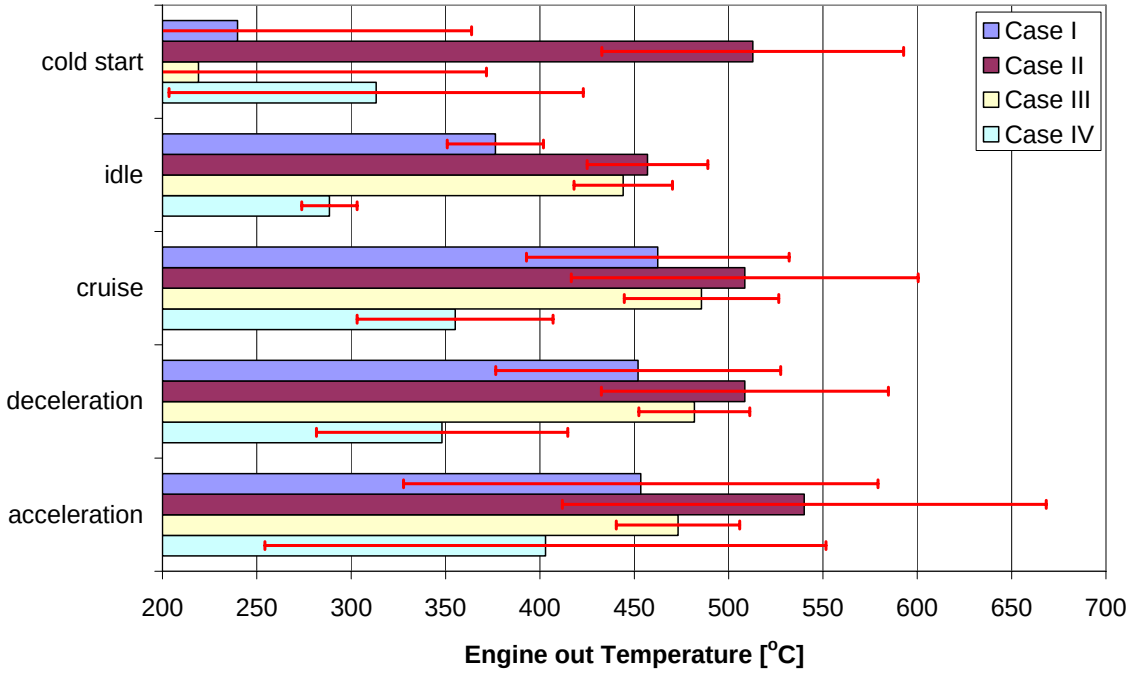

Figure 56 Engine out temperatures of modal analysis for all cases

[a] The term stoichiometric is used to declare engine operation close to λ=1±0.05

4.5 ENGINE OUT EMISSIONS ASSESSMENT

Figure 57 presents the modal analysis for the engine-out exhaust gas molar emissions. Obviously, advanced engine design is able to combine reduced engine out emissions with high output power delivery. This is better understood if we take a look at the cases I and IV. The engines in these cases are fitted on the same car and share the same design principles. Of course the Case IV engine is newer than the Case I one. The cold start emissions are lower in the case of the newer engine evidently. The NOx trap regeneration requirements for rich pulses worse the CO and THC emissions during acceleration while improve the NOx engine out emissions. During all the other modes the Case IV engine out emissions are generally better than the respective of the Case I engine, except that of THC. Increased THC emissions are necessary to maintain high temperature at the pre-catalyst, but they should be treated effectively by this device.

The Case II engine that is shifted slightly to the lean side is expected to perform at lower engine out emissions especially during transient driving. Despite its higher cylinder displacement than the Case I engine, the advanced engine management enables lower overall emissions for the majority of the driving modes. Higher CO emissions are expected to be treated effectively in the close coupled catalyst considering the excess of engine out O_2. The lower THC engine out emissions reveal advanced engine design and manufacture as these emissions originate mainly from oil in crevice volumes of the combustion chamber.

The data of Case III engine refers to the one bank of the exhaust only. Despite this fact, the engine-out emissions are lower, in general, compared to the rest of the engines, although it operates at rich combustion mixture. This is attributed to the significantly lower specific power. A peculiar characteristic here is that the O_2 emissions are significantly lower than the rest of the cases. A reasonable question is if the selected aftertreatment system is adequate during all modes of operation for this system and of course for the rest of the cases.

Figure 58 presents the modal analysis for the tailpipe exhaust gas molar emissions. In all cases the exhaust treatment systems perform at least a tenfold reduction. Despite this fact, it is clear that each choice of the exhaust treatment system demonstrates significant differences to the rest choices. Obviously, the

system of the Case II performs best for CO and THC emissions, while the Case IV system achieves comparable emission output to the rest of the systems.

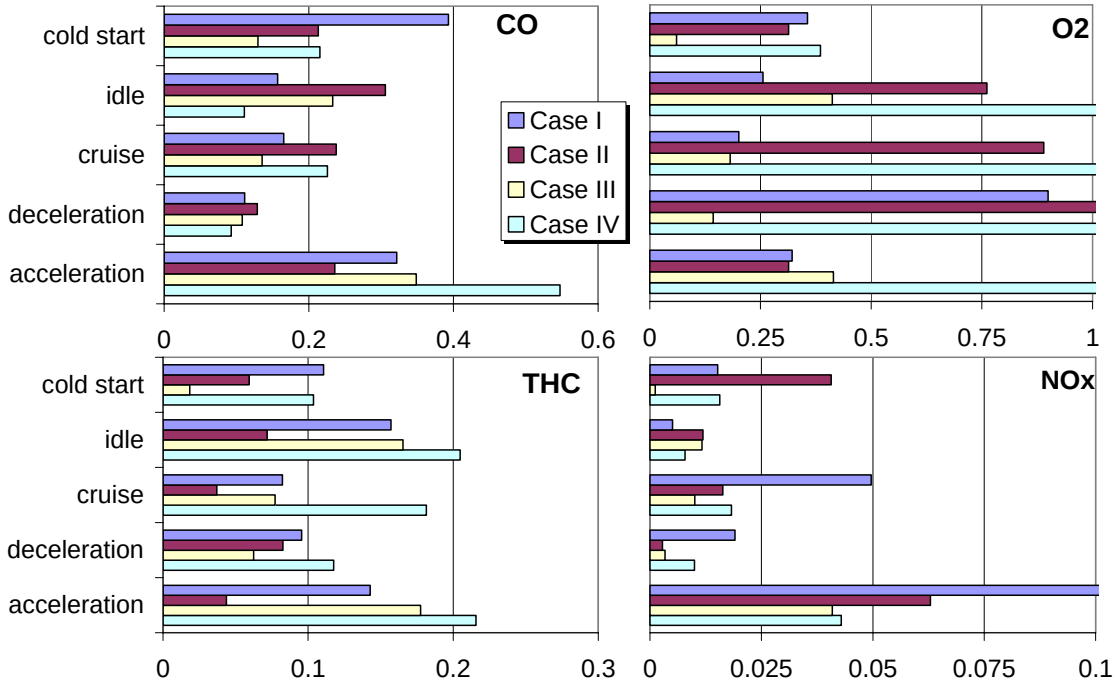

Figure 57 Summary of modal analysis of engine out gas molar emissions for all cases. Units are in mol per km of driving except idle mode that is mol.

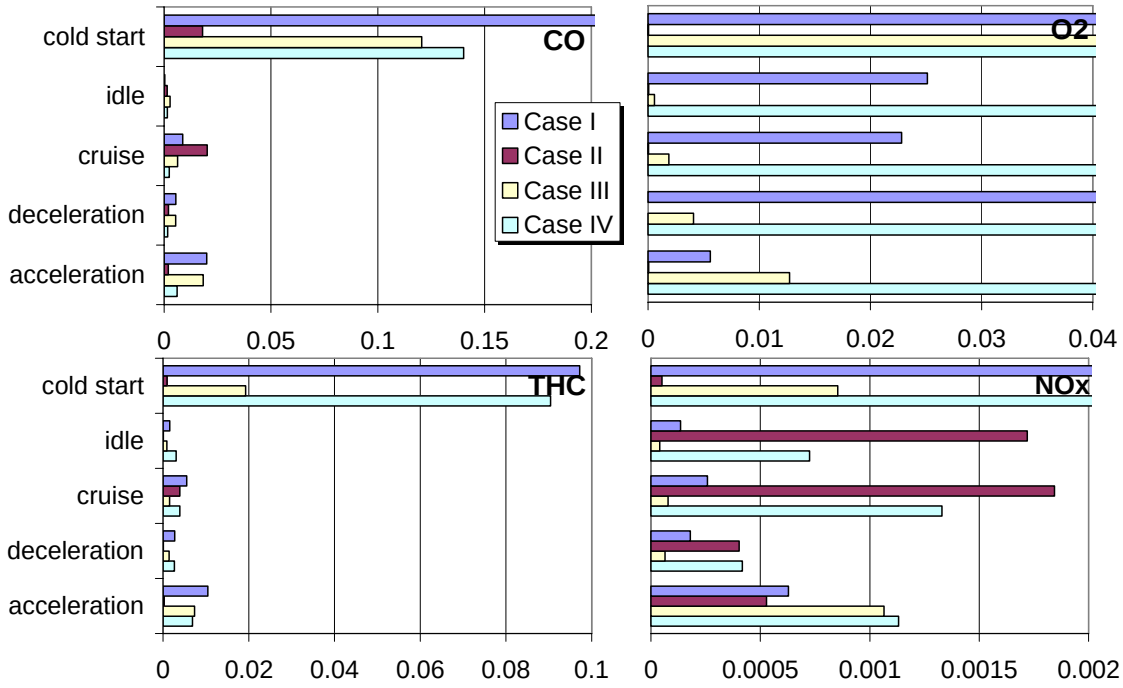

Figure 58 Summary of modal analysis of tailpipe gas molar emissions for all cases. Units are in mol per km of driving except idle mode that is mol.

During cold start, when the catalysts are inactive the vehicles show increased emissions. Especially for the Case II that has a very fast light-off, the direct comparison should be careful, as the rest of the engines operate for a longer period in this mode. In addition, acceleration and cruise modes are responsible for a large portion of emissions in all cases, a fact that is explained by the increased mass flow rate and the power demands.

The four systems under study use various afretreatment technologies that are tailored to specific targets each. Case I, which is a typical underfloor 3WCC, compared to the Case II (close coupled location) is inferior only to the light-off emissions. The light-off point is achieved at about 80s of NEDC in the first case, while only at 15s at the latter case. On the other hand shifting lambda control to the lean side improves CO and THC tailpipe emissions and fuel consumption but inhibits optimum NOx performance of the three-way operation. This can be seen from the increased NOx emissions in all modes of driving for the Case II.

The exhaust treatment system of the Case III, tested in FTP-75 driving cycle, seems to have a good overall performance, but this may be attributed to intrinsic differences between US and EU driving cycles such as higher temperatures. Nevertheless this system shows an enhanced performance for NOx emissions considering that its lambda control is shifted to the rich side. The CO and THC emissions are lower than in the other cases probably due to lower specific power output as already noted.

The most recent system of Case IV, that is comprised of a small close coupled three way catalytic converter and a NOx trap, does not show significantly higher overall efficiency than the rest of the cases. Especially when compared to the Case I, which share similar engine, is assessed as inferior to NOx emissions that is the primary target of the system. Of course it must be considered that the engine of Case IV operates at lean mixture which inhibits three-way NOx performance. The rich pulses to assist NOx trap regeneration produce increased CO and THC, which are evident in engine out emissions and are treated effectively in the precatalyst and the NOx trap.

4.6 Aiming at the Exhaust Line Design Assistance

An extended application of the modal analysis is to identify and assign the effect of changes in the exhaust line design. Modal analysis should be able to predict, within certain accuracy, how efficient will be the application of a given exhaust treatment device or a hypothetical change of position of an existing device. This should be considered mostly as a decision- taking tool and not an analytical design tool. The latter is covered by engineering modeling that aims to study more precisely the effect of the characteristics of a given catalytic converter.

An important aspect in this kind of application is the assessment of the behavior of a catalytic converter under certain conditions that match characteristic data of the modal operation of the engine. Of course, the catalytic converter should belong to a family of converters that share the same washcoat technology with respect to thermal characteristics, PGM deposition techniques and oxygen storage behavior. This would reduce time, effort and repeated work done by the exhaust treatment system developers [170] and will establish a common data exchange format.

This type of identification for each engine and catalytic converter should be based on the three principal characteristics affecting the behavior of every exhaust aftertreatment device; lambda, mass flow rate and temperature. The behavior of each catalyst should be recorded in each mode of driving in order to produce efficiency maps like the one shown in Figure 59. In this figure

The question that has to be answered by this kind of analysis is which modifications should be made in an existing system in order to conform to future legislation. For example the system of Case II should further reduce NOx emissions. To accomplish this, a NOx reduction device should be fitted. If we use a NOx trap the benefit will not be large probably as from the results of the case IV. On the other hand the system of the Case III that is the most promising needs modifications of the engine management to operate the engine at the rich side while the one of the Case I needs close-to-stoichiometry operation.

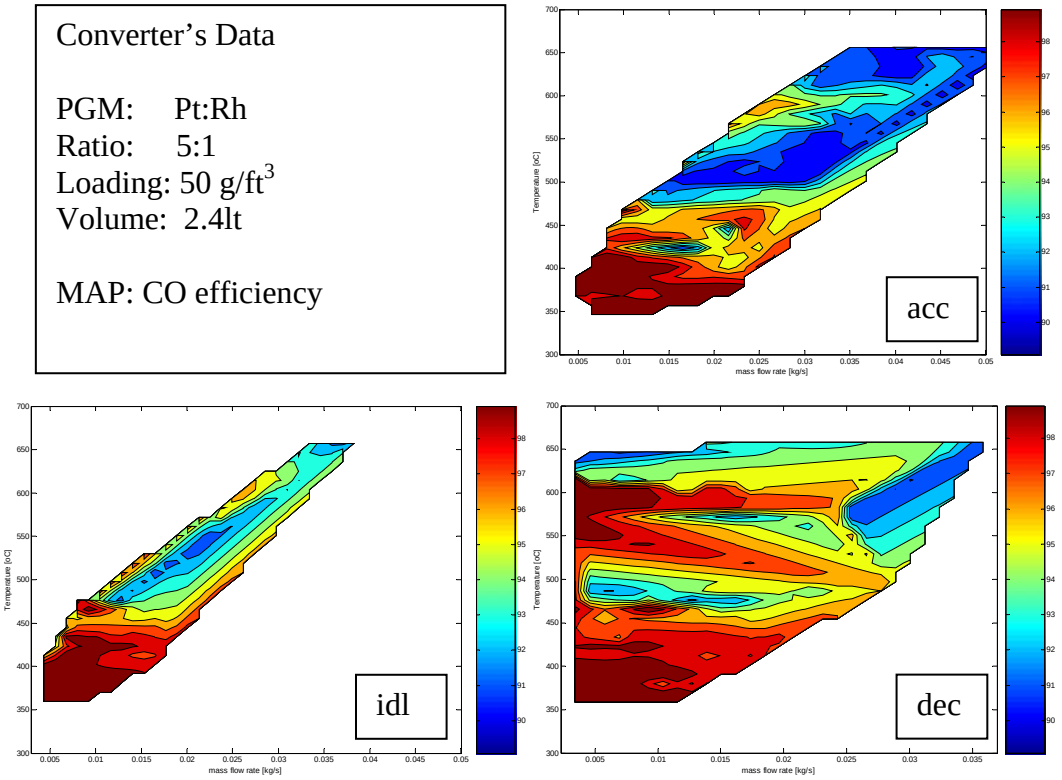

Figure 59 CO efficiency maps during modes of driving for the catalyst of Case I

A possible solution would be the use of low volume close coupled system to treat mainly the low engine out NOx emission. The device already used should be placed afterwards and should be air assisted to ensure similar operation to the current status. Of course validation of this solution should be assisted primarily by engineering modeling in order to study the performance under real conditions.

4.7 Conclusions

Identification of engine management characteristics is a crucial step in the procedure of optimum design of exhaust gas treatment systems. Once this valuable data is known to the engineer, he becomes able to recognize the aspects that the application of an exhaust treatment system should cover. In order to support fast and in time commercialization of the systems the engine behavior must be identified at a glance. The most important data is engine-out temperature, lambda and exhaust gas mass flow rate. Further extension of this approach to aftertreatment systems should provide data regarding inlet and exit emissions for the aftertreatment device.

Modal analysis aims to provide such important information which can assist the initial design of the entire exhaust line. If the information of the engine-out exhaust gas is available, the engineer could decide over a database of aftertreatment devices or combinations of them which one to use for the initial design. Modal analysis can be transformed into a decision taking engineering tool that moves exhaust line design far from traditional trial and error approach.

APPLICATION TO REAL WORLD CASE STUDIES

This section is an intermediate part that introduces the reader to some technical aspects and hints commonly found in real world applications. The target is to show that the engineering design of commercial catalytic converters includes large amounts of uncertainties primarily related to the interaction of the components of the specific system under study, comprising powertrain, engine management and catalytic converter.

A Short Reference to the Scope and the Aims of the Applications

The optimum design of the catalytic converter is the result of a systematic effort at various design levels, already discussed in the previous chapters. The final product has to be

- Highly effective as regards as the removal of pollutant gases
- Durable, that is to maintain its good performance during its lifetime
- Delivered at low cost

The discussion of the previous chapters has shown that the engineering design of the catalytic converter binds together experimental findings, modeling and electronic control. In a short, several fields and design parameters that strongly affect the performance of the converter can be distinguished. These fields include macroscopic design parameters, physical and geometrical characteristics, and of course exhaust gas flow characteristics at the converters. Some examples of these parameters are shown in Table 11, which is neither definite nor exhaustive.

Table 11 catalytic converter's design parameters

	Design Field	**Design Parameters**
1	Catalyst impregnation	Precious metal type, loading and ratio
2	Exchange Area	Frontal area, length, channel density
3	Thermal inertia	Substrate and washcoat mass
4	Heat transfer	Monolith conductivity, insulation
5	Mass transfer	Porosity, porous size, precious metal dispersion
6	Flow field	Converter shape, channel shape
7	Input data	Engine type and management, exhaust line design

The first three fields shown in Table 11 are key parameters to the design of a high efficient catalytic converter. The parameters of the catalyst impregnation field determine the efficient use of noble metals in the converter, the exchange area by definition enhances the performance and the thermal mass practically defines the time period for the warm up of the converter. Of course, the impact to the cost, the manufacturing process and engine performance must also be considered.

The most complex and most studied field is the field of catalyst impregnation. Catalysts impregnated into advanced washcoat formulations are known to have a synergistic effect [111] with the support also known as SMSI. The deposition techniques of PGM especially in relevance to the ceria particles position are well known to enhance catalytic performance [171]. Depending on the precious metal and the precious metal content, different amounts and/or compositions of washcoat are necessary to keep the chemical balance between active sites and surface area in the desired range[88]. The precious metal loaded is not fully exposed and is not equally distributed at the radial and axial position [172]. It has to be noted that for different precious metal loading levels, the density of precious metals in the oxide mixture is different, having an unknown effect (depending on the boundary conditions) on the system performance [88].

Some remarkable questions is how the findings of fundamental research are implemented into the final full scale products and how can an engineering model be used to assist the macroscopic design of the catalytic converters?

An important aspect that has to be accounted when trying to reply to these questions is the existing differences in catalyst input data when the engines are tested under real driving conditions and the significant differences in the performance of catalytic converter manufactured in the same way when fitted even to the same engine [156].

Examples of these are shown in Figure 60 and Figure 61. The CO engine-out emissions of Figure 60 vary significantly although they come from the same engine tested in FTP-75 procedure. This is probably the result of the different behavior of the engine control as different catalytic converters are fitted in each case. Figure 61 shows the CO emissions at the converter's outlet for two pairs of identical catalysts fitted on the same engine and tested according to the FTP-75 protocol. Although it is expected to have similar performance between the same catalysts, they show significant differences in the light-off (Cat.A) and during the warmed phase (both pairs). These differences in performance can be attributed either to the state and the history of each catalytic converter or to the different inlet data due to variations similar to those of Figure 60. When attempting to model such applications what matters is not the exact definition of kinetic parameters or the accurate fit between experimental data and computation but the prediction (within certain accuracy) of the major catalyst performance characteristics at the lower computation cost.

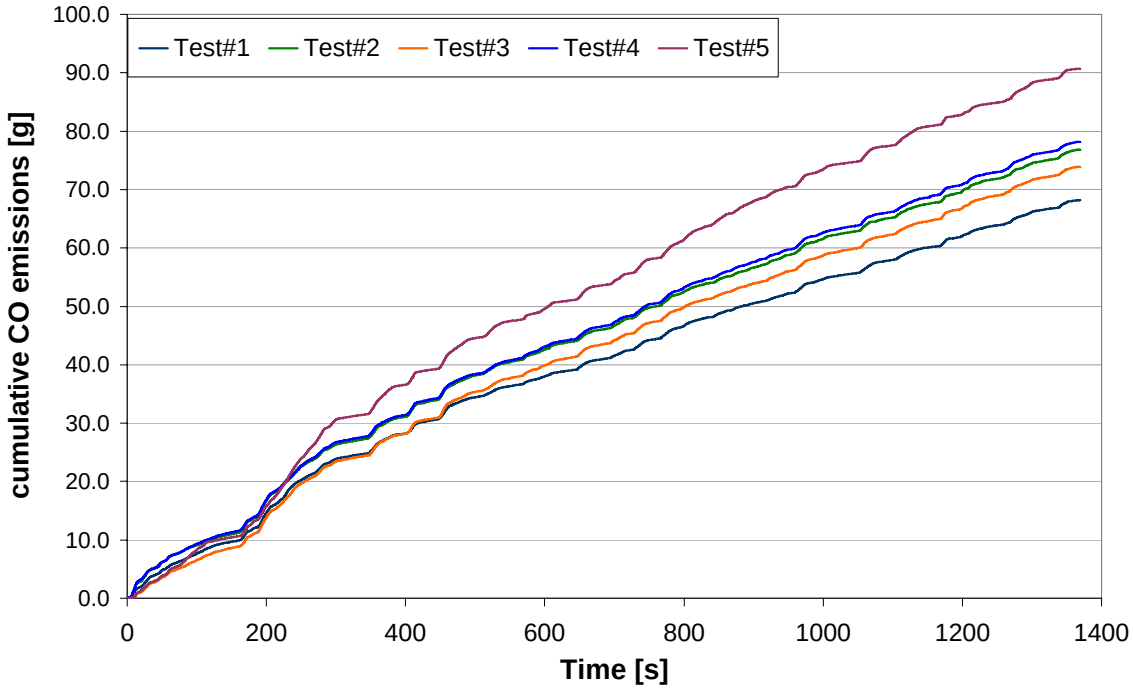

Figure 60 CO engine –out cumulative emissions of the same engine tested in FTP-75 for five

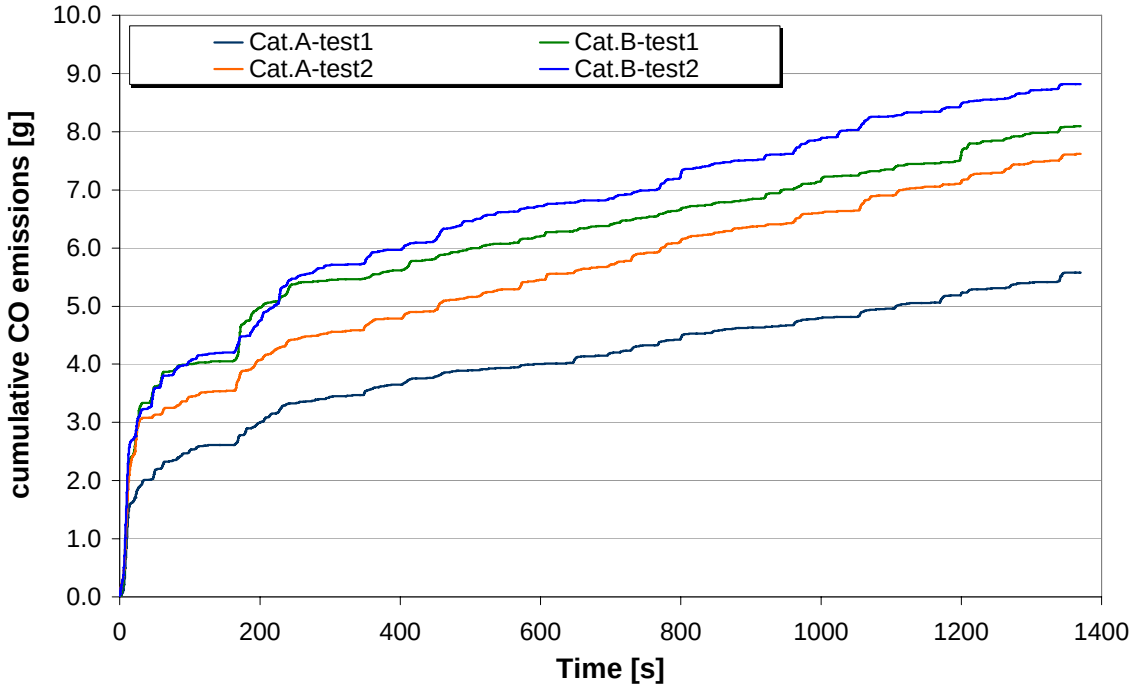

Figure 61 Converter outlet cumulative CO emissions for two pairs of catalysts fitted at the same engine

The model must be tuned to fit each application and enable the extension of the results to other cases while keeping the same level of accuracy.

On the other hand, modern catalytic converters have an efficient operation at higher than 95% conversion efficiency for all the species. Even catalytic converters with low precious metal loading or reduced exchange area are able to maintain increased conversion efficiency during warm operation. The differences between the converters are attributed to the efficient or not treatment of the transient operation when emissions special inlet conditions are present. Transient parts (e.g. acceleration) are characterized by increased mass flow rates and temperatures (both have a negative impact in external mass transfer) and increased CO, THC and NOx emissions with decrease in exhaust gas O_2 content. Engineering modeling is destined to identify the major reasons for the insufficient operation of the converters and possibly propose solutions oriented to macroscopic design.

The following sections present an application (and validation) of the model developed in this thesis to several real world optimization case studies. Although these datasets are not exhaustive, they provide a wide range for model validation and spread over several important design aspects of catalytic converters. These case studies can be summarized up to the following (see Table 12 for details)

- Optimization of the precious metal loading of three-way $Pt/Rh/CeO_2$ (5:1, 400cpsi, 2.4l) catalysts supported on commercial γ-alumina support. The catalytic converters are positioned at an underfloor position. The system conforms to the EUROIII legislation
- Optimization of the channel density of three-way Pd/Rh (14:1, 1.0 l) catalysts supported on commercial γ-alumina support. The catalytic converters are positioned in a two bank exhaust line in parallel, close-coupled to the engine. The system conforms to the EUROIII legislation
- Parametric study the channel density and the precious metal loading and ratio of three-way $Pt/Pd/Rh/CeO_2$ catalysts supported on commercial γ-alumina support. The catalytic converters are positioned in a two bank exhaust line in parallel, close-coupled to the engine. The system conforms to the ULEV legislation
- Study of the regeneration strategy of engine management for an exhaust system of a close-coupled three-way catalytic converter (Pd/Rh, 600cpsi, 0.8 l) and a NOx-trap (400cpsi, 3.0 l) in serial. The system conforms to Euro IV legislation.

The following applications aim at the investigation of the effects of these macroscopic design parameters considering the catalyst efficiency in the exhaust line

as the principal performance measure of the study. The experimental data is modeled using the simplifications discussed in chapter 2, in order to avoid superfluous complexity and decouple the effects of each modeling level in a certain extent.

Table 12 Summary of data for the cases under study

Vehicle	Position	Purpose	PML (g/ft3)	cpsi	thickness nominal [mil]	Volume [l]	Pt	Pd	Rh
Grand Marquis, 4.6 l	CC	Start up 3WCC	150	900	2.5	0.8	1	13	1
			170		2.0			15	
			125					10.5	2
Peugeot 406, 2.0 l	UF	Main 3WCC	50	400	6.5	0.6	7	0	1
			10			2.4			
			100						
			30						
Mercedes-Benz E-Klasse, 2.4l	CC	Start up 3WCC	100	400	6.5	1.0	0	14	1
				600	3.5				
				900	2.5				
				1200					
			70	900					
Peugeot 406, 2.0 l HPi	CC	Start up 3WCC	150	600	4.0	0.8	9	5	1
	UF	NOx Trap	100	400	6.5	3.0	1	10	2

CC = Close Coupled, UF = UnderFloor

The management of such large datasets and multi-objective study of these applications, indicate the extended presentation of the results. For space economy, it is selected to present the extended field of study with the current model only for the first case. In this thesis the model output was also enriched with several crosschecks to assess the tuning results, which also support an in-depth knowledge either to the behavior of the model or the behavior of the catalytic converter if we assume that the tuning is successful. This thorough examination tends to identify special issues that affect the dynamic operation of the catalytic converter and provide valuable information to assist designing.

The main objective of the study of these cases is to locate trends regarding specific design parameters, assign rules for the engineering design of the catalytic converter as regards the macrosopic design variables and also prove the validity and the applicability of the methodology developed in the frame of this dissertation.

CHAPTER 5

CASE STUDY: VARIABLE PRECIOUS METAL LOADING (Pt/Rh CATALYSTS)

The effect of precious metal loading is studied in this chapter. The experimental data come from a 2.0 l spark ignition engine, designed for EURO 3 emissions standards and fitted with an underfloor ceramic monolithic catalytic converter of 2.4 l volume. The exact washcoat formulation is not disclosed, but catalyst performance reveals adequate oxygen storage. The data was preprocessed and quality assured as described already in chapter 3 and the engine management characteristics were identified and discussed in chapter 4. In the latter case, it was shown that management is tailored to assist oxygen storage capacity filling. In what follows in this chapter the cases of variable PML catalytic converters are modeled using a proper reaction scheme selected according to the chapter 1 discussion. The tunable variables of the model are estimated according to the methodology developed in chapter 2. The results are extended to a case of a smaller catalytic converter.

5 CASE STUDY: VARIABLE PRECIOUS METAL LOADING

5.1 OVERVIEW OF THE CASE

In this section, the model's kinetic parameters are tuned to fit the behavior of four reference catalysts of equal size, (2.4 l), loaded with 10, 30, 50, 100 g/ft^3 precious metal respectively, 7:1 Pt to Rh ratio, installed on a 2 liter displacement, stoichiometric spark ignition engine. The catalytic converters share the same washcoat formulation and their performance is tested on the chassis dynamometer, according to the NEDC legislated cycle. The main objective is to check the model's accuracy and predictive ability, and possibly draw a correlation of the kinetic performance of each converter with its respective Precious Metal Loading level. The results will be extended to the case of a smaller catalyst with the same washcoat formulation, a precious metal loading of 50 g/ft^3 and 0.6 l volume.

The system under study in this chapter is comprised by:

1. A straight-four 2.0 l stoichiometric spark-ignition engine
2. An advanced engine management with fuel cut-offs during deceleration
3. An underfloor main three-way catalytic converter of 400cpsi, with typical single layer washcoat formulation and Pt:Rh loading.

The catalytic converters are placed underfloor, about 1.5m away from the engine. This results to an average inlet temperature in the converter of about 380^{o}C for the majority of the driving cycle. The data of the catalytic converters is shown in Table 13.

The experimental data is processed through the in-house quality assurance system described in Chapter 3. The engine operates in the slightly rich regime, presumably for the sake of reducing engine-out NOx emissions and increasing power output. The fuel management strategy enriches the mixture during accelerations and cuts fuel during decelerations. The engine management follows the common strategy of exhaust temperature increasing during cold-start by spark advance modifications.

The modal analysis of the emissions and the mass balances at the catalytic converter inlet are presented in Chapter 4. As expected, the engine- out emissions of the specific engine, are subject to a reasonable statistical variation [156]. The

differences in the performance of the catalytic converters can be attributed to different engine out emissions, but essentially to the activity of their washcoats.

Table 13 Data for the case of variable precious metal catalytic converters

CASE	I				
Test Name	Cat.#1	Cat.#2	Cat.#3	Cat.#4	Cat.#5
Vehicle Engine	2.0 l, SI, EU-III				
Position	Underfloor				
large axis [m]	0.12				
small axis [m]	0.12				
length [m]	0.05	0.20			
Volume [l]	0.60	2.40			
cpsi	400				
thickness nominal [mil]	6.5				
PML (g/ft^3)	50		10	30	100
Pt	7				
Pd	0				
Rh	1				
OSC	unknown (estimated 600 mol/m^{3}WC)				
Stabilisers / Promoters	Unknown				
Comments					

5.2 Study of the Experimental Data

Figure 62 to Figure 64 present the cumulative emissions for CO, THC and NOx from experimental data. As expected, the engine out emissions of the specific engine, are subject to a reasonable statistical variation [156], as shown in the first column of he activity of their washcoats.

Table 14, also compared to oncoming EU and US standards. The differences in the performance of the catalytic converters can be attributed to different engine out emissions, but essentially to the activity of their washcoats.

Table 14 Engine-out emissions for the specific engine and legislated emission standards

	Engine out	***Euro 4***	***ULEV***
CO (g/km)	7.0 – 7.6	1.0	1.0
HC (g/km) (C1)	1.7 - 2	0.1	0.028
NOx (g/km)	2.8 - 3	0.08	0.117

Obviously, these variations of the engine- out emissions make the direct comparison of these results difficult if we consider that the 50g/ft^3 catalyst seems far more active than the Cat.#5 that has its double precious metal loading. Despite this fact, a number of useful observations can be made.

The light-off of occurs at about time=80s from start of the NEDC for all the converters. This is reasonable considering the underfloor position of the converter and its increased volume. Additionally all the converters except Cat.#1 (the shorter one) perform fairly good during the urban driving part of the NEDC, while they lose their high efficiency at the extra urban part.

Figure 62 presents the cumulative emissions for CO. Obviously, the Cat.#2 shows a high efficiency immediately after the light-off that results to lower cumulative emissions at the end of the cycle. If we account that all the converters, except Cat.#1, have the same thermal mass the faster light-off of the Cat.#2 is assigned to the inlet data and it has nothing to do with the intrinsic performance of the converter. Cat.#1, which is the smaller converter, has the fastest light-off that is evident in Figure 63 also.

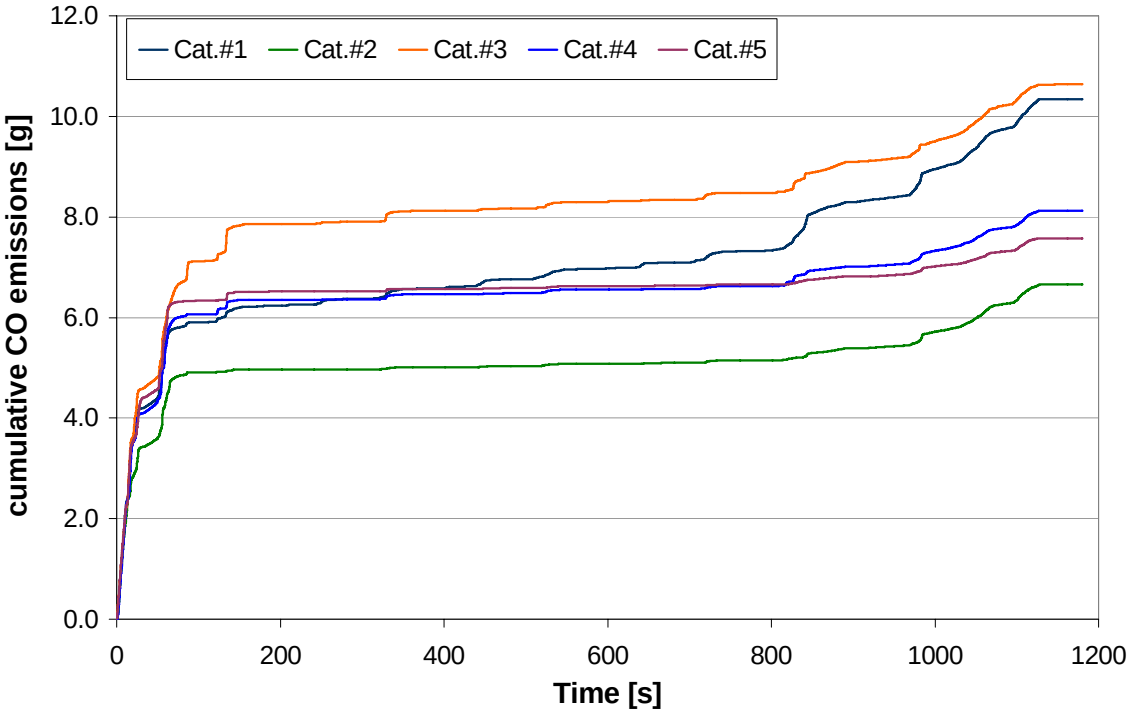

Figure 62 Comparison of experimental cumulative CO emissions for the Case I catalytic converters

The performance of the converters can be assessed by their behavior during the warm operation after the light-off instant. Between the four catalysts of equal size there is a clear trend with respect to the precious metal loading level; the higher the loading the more efficient the converter. In similar to the CO emissions, the THC performance shown in Figure 63 reveals a trend proportional to precious metal loading during the warm operation. Especially for Cat.#2 and Cat.#4 which have similar levels of precious metal loading (50 and 30 g/ft^3 respectively) it seems to have very similar performance (their curves are almost parallel). The advantage of the higher PML is clear during the extra-urban driving where increased mass flow rates and temperatures exist. At this part the Cat. #5 with the highest PML is clearly superior for all three pollutant species, as it is able to treat effectively the higher flow rates.

The 2.4 l catalysts treat NOx emissions effectively during the warm operation except some breakthroughs at about 150s, as shown in Figure 64. This is reasonable if we account for the shifted- to- rich operation of the engine that has been already shown in Chapter 4. The smaller catalyst of 0.6 l shows a faster light-off than the rest of the catalysts but is unable to maintain a highly efficient operation during the rest

of the driving cycle as it has not adequate length, and consequently exchange area, to assist this kind of operation.

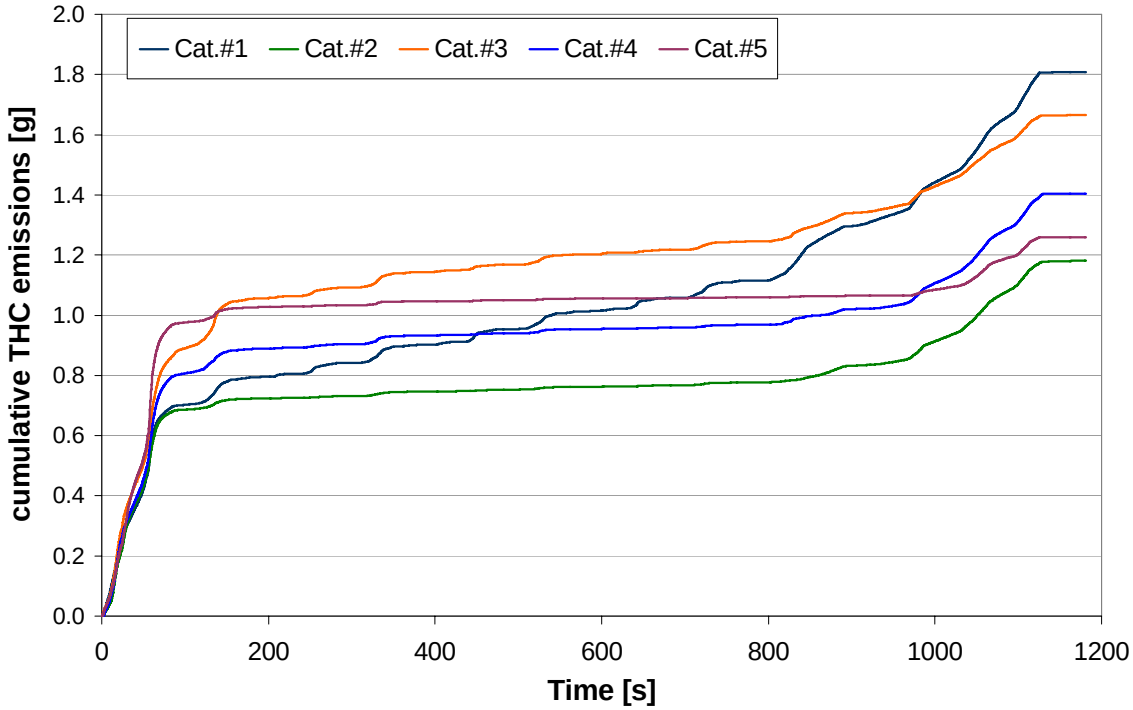

Figure 63 Comparison of experimental cumulative THC emissions for the Case I catalytic converters

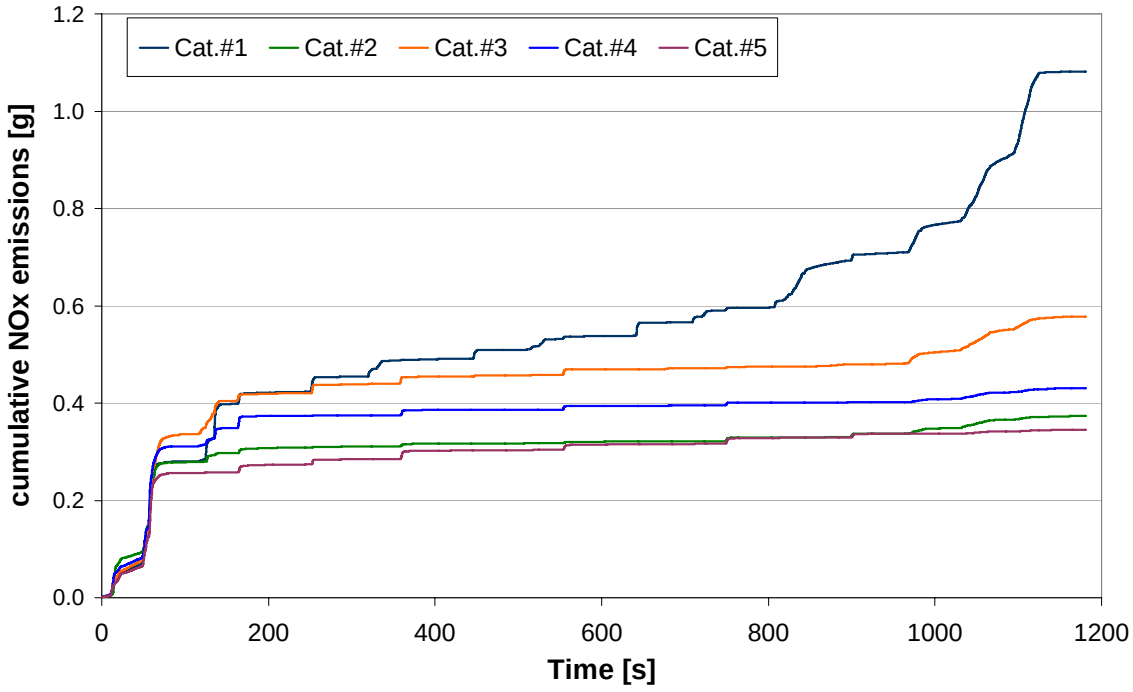

Figure 64 Comparison of experimental cumulative NOx emissions for the Case I catalytic converters

5.3 TUNING THE MODEL TO FIT ALL THE CASES

In this section, we will use the model presented in Chapter 2 to fit the behavior of the converters. If we account for the Pt:Rh basis of the washcoat, and the lambda and temperature range of operation for the converters, we select a simple reaction scheme consisted of eight reactions; four for the description of the Redox chemical reactions with exhaust gas species and four for the oxygen storage processes. We assume that these reactions are the dominant and although several other catalytic reactions may still exist, it is assumed to have negligible effects or be too slow to compete with the dominant ones. It is also assumed an adequate oxygen storage capacity of 600 mol/m^3 washcoat, a value consistent with the literature (for example [34]). This relatively increased oxygen storage is regularly filled-up by the engine management strategy (fuel cuts during braking).

Table 15 Reaction scheme

	Reaction	logA	E
1	$CO+\frac{1}{2}O_2 \rightarrow CO_2$	A_Ox	90000
2	$H_2+\frac{1}{2}O_2 \rightarrow H_2O$		
3	$C_aH_b+\left(a+\frac{b}{4}\right)O_2 \rightarrow aCO_2+\frac{b}{2}H_2O$		
4	$CO+NO \longrightarrow CO_2+\frac{1}{2}N_2$	A_Red	95000
5	$2CeO_2+CO \rightarrow Ce_2O_3+CO_2$	A_Ce	120000
6	$\left(4a+b\right)CeO_2+C_aH_b \rightarrow \left(2a+\frac{b}{2}\right)Ce_2O_3+aCO_2+\frac{b}{2}H_2O$		
7	$Ce_2O_3+\frac{1}{2}O_2 \rightarrow 2CeO_2$		
8	$Ce_2O_3+NO \rightarrow 2CeO_2+\frac{1}{2}N_2$		

The model is tuned with GenOpt for the cases of Cat.#2, Cat.#3, Cat.#4 and Cat.#5. The results of the tuning are shown in Table 16 along with the resulted performance measure values.

Table 16 Overview of the results of the case study

		CASE				
		I.1	I.2	I.3	I.4	I.5
Tuned parameters						
1	A_Ox	13.00		11.60	12.60	13.50
2	A_Red	13.30		11.90	12.80	13.60
3	A_Ce	7.60		6.90	7.40	7.60
Performance measure						
F' (current work)		0.7896	0.8136	0.8946	0.9005	0.8173
F' (Pontikakis [3])		0.9236	0.9518	0.9421	0.9501	0.9477

5.4 DISCUSSION ON THE MODELLING RESULTS

Considering that all catalysts share the same washcoat formulation with different PML, we expect that the tuned variables shall follow a trend versus the PML level. For space economy we present only the results of the 10g/ft³ catalyst loading extensively (Cat.#3), considering that the quality of the computed data is similar for all the cases. For the rest of the cases we present only the cumulative emissions. We choose this case as the most representative, considering that it is the weakest catalyst and the diffusion or reaction limitations are more intense.

The comparison of computed and measured cumulative as well as instantaneous emissions curves are presented in Figure 65, Figure 66, Figure 67 and Figure 68 and show a good fit between the model and the real behavior of the 3WCC.

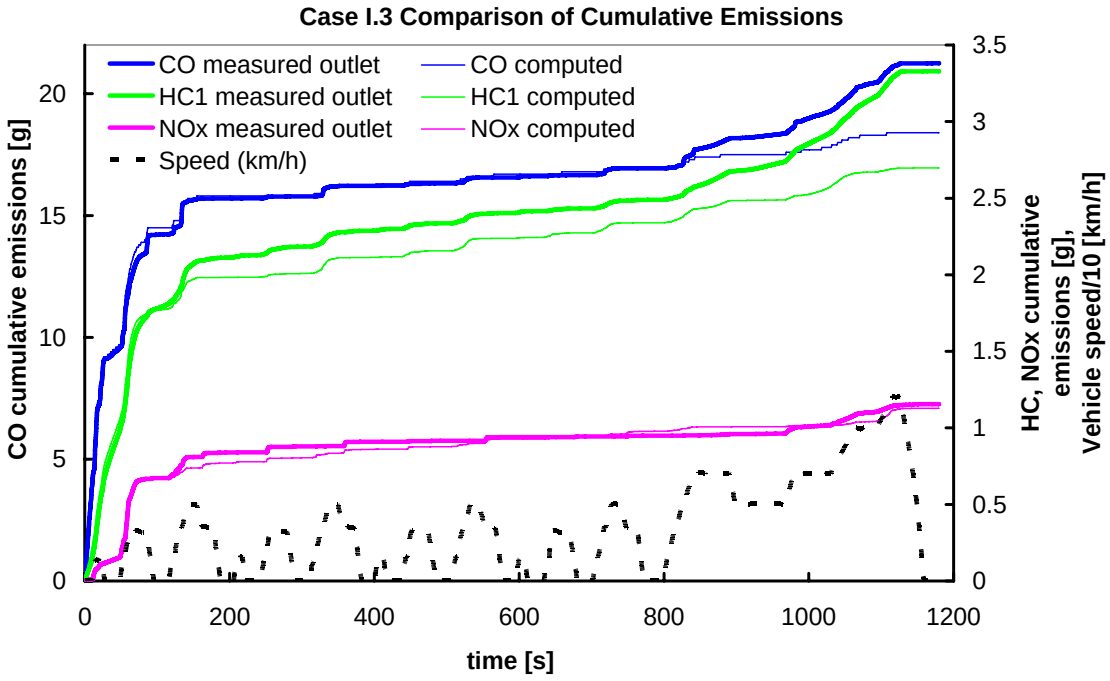

Figure 65 Computed and measured cumulative emissions of the 10g/ft³ Pt:Rh catalyst.

Apparently, the model successfully matches the light-off behaviour of the catalyst, as well as subsequent breakthroughs during acceleration. The role of oxygen storage and release reactions in matching the CO breakthrough behaviour is better assessed by including in the graph the computed level of filling of the total washcoat's oxygen storage capacity. As shown in Figure 66, the model shows that CO breakthroughs are

ascribed to empty oxygen storage capacity. During the first 780s, cold start and urban driving period, these breakthroughs are successfully predicted while during extra-urban driving period (780-1180s) are outlined. It must be mentioned that the maximum values of the CO breakthroughs (e.g. at 250, 515 and 600s) are not predicted by the model, presumably due to an oxygen storage submodel weakness.

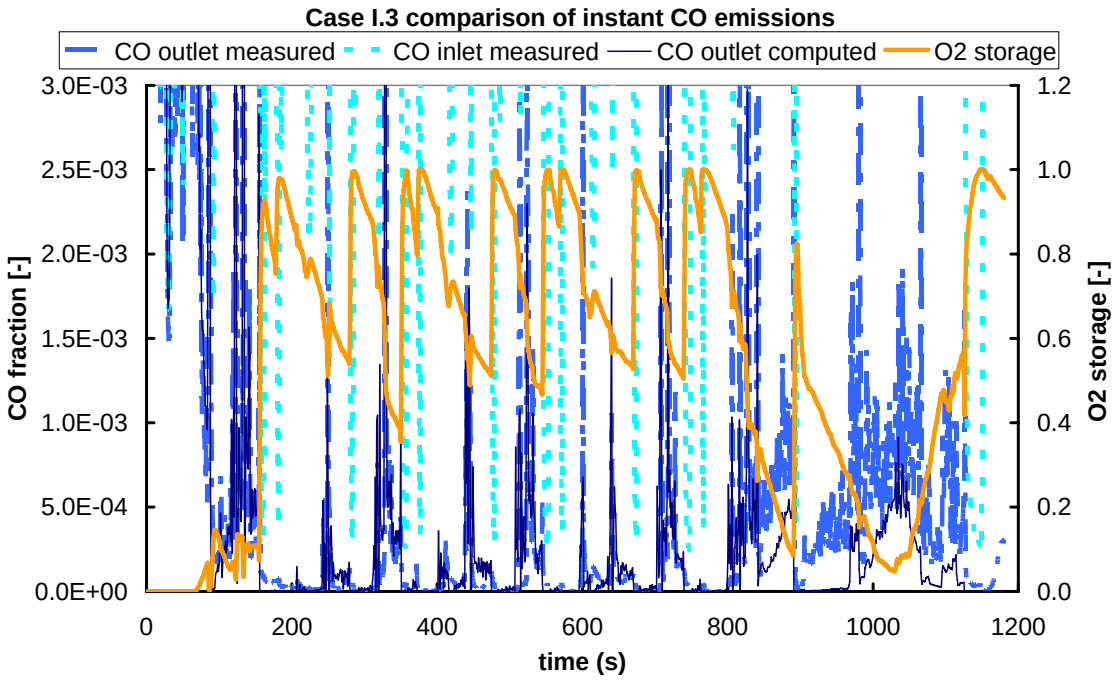

Figure 66 Computed and measured instantaneous CO emissions of the 10g/ft^3 Pt:Rh catalyst.

The same situation appears in Figure 67, where the computed and measured instantaneous THC emissions at converter inlet and exit during the NEDC are given. The connection between HC breakthroughs and oxygen storage phenomena in the washcoat is apparent also here. The model results are of the same quality as in the previous figures, since the model predicts the events (HC breakthroughs) of the urban part of the cycle, not only qualitatively, but also quantitatively, in a certain extent. HC light-off behaviour is also matched with a good accuracy. In HC comparison graphs must be taken into that in real exhaust gas there are thousands of HC species and current modelling approach assumes only one of them. This could be a reason for the failure of the model during the period from 90 to 210s. The shape of the computed curves, generally fits the experimental data and outlines the overall behavior of the specific catalytic converter concerning the hydrocarbons. As with the

case of CO instantaneous emissions, the model underestimates THC tailpipe emissions during the extra-urban part of the cycle.

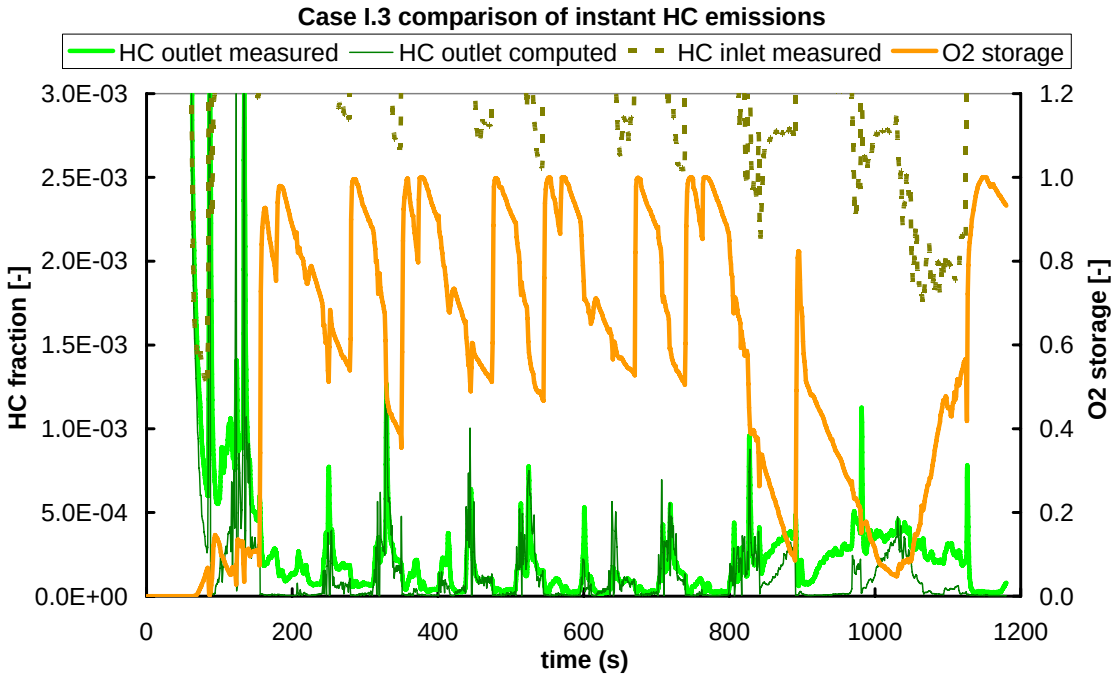

Figure 67 Computed and measured instantaneous THC emissions of the 10g/ft^3 Pt:Rh catalyst. The model assumes a single HC specie in the exhaust gas.

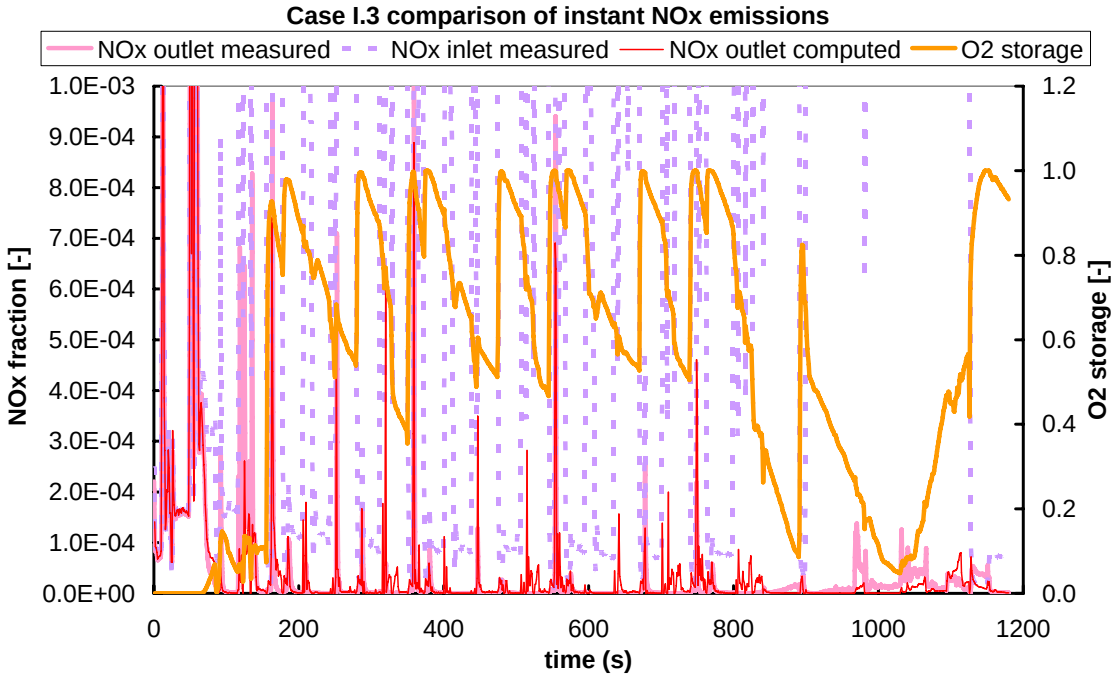

Figure 68 Computed and measured instantaneous NOx emissions of the 10g/ft^3 Pt:Rh catalyst.

For the case of the NOx instantaneous emissions the model captures successfully the light-off transition and outlines every NOx breakthrough as shown in Figure 68. In certain periods, for example the periods 100-150s and extra urban part, the model overestimates catalyst efficiency, while in others (like the period 300-500s) it predicts instantaneous emissions successfully.

It is evident from the comparison of the instantaneous emissions that the Ceria storage function has a minor role during the light-off. The light-off temperature is determined by the activity of the Redox chemical scheme and only after the catalytic converter reaches a proper temperature the reactions in ceria are practically active, which is shown also in Figure 71. It has been claimed that the Ceria reduces the light-off temperature by enhancing Redox reactions, but this property is by definition compensated into the pre-exponential factors of these reactions. In addition to that the initial status of the oxygen storage is unknown which is probably the main reason for the improper fit at a short period right after the light-off (about 80 – 100s).

The model decouples in a certain extent the double role of Ceria as a RedOx enhancer and an oxygen storage component and enables a better view of the principle phenomena occurring inside the catalytic converter. Figure 69 presents a comparison between computed and measured temperatures. The model fits quite well the outlet temperature response during the cycle. And this, despite the fact that this is a 1-D model and the outlet temperature is measured behind the cone while the respective computed one is at the last node of the catalyst. The deviation during the first seconds, when the catalyst is cold is attributed to flow maldistribution effects that are discussed elsewhere [162]. After the light-off, it is well known that any 2-D or 3-D temperature effects can be neglected, as the converter behaviour is close to an adiabatic reactor.

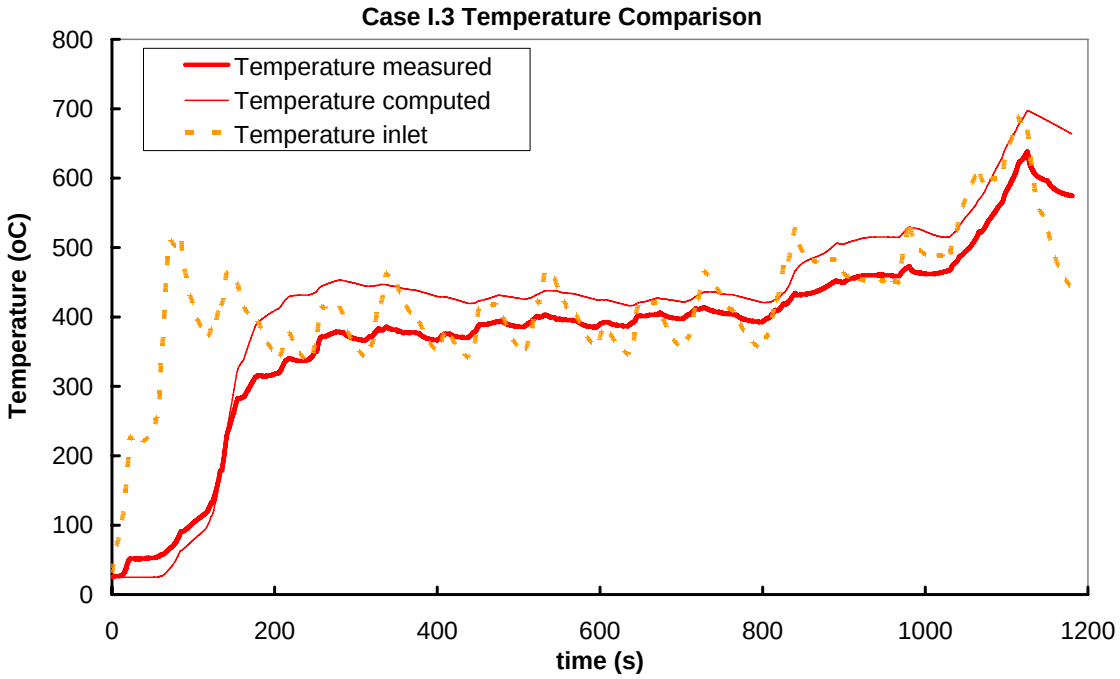

Figure 69 Measured converter inlet and exit temperatures and computed exit temperature of the 10g/ft^3 Pt:Rh catalyst.

Figure 70 and Figure 71 are used for cross-checking of the computed results. In Figure 70 computed fraction of oxygen stored/released in/from washcoat is compared to the respective fraction that is calculated from experimental measurements according to the formula derived by Theis [173].

$$O_2(stored\ or\ released) = \frac{(A/F_{eo} - A/F_{tp})\left[12(x_{CO} + x_{CO_2}) + 44x_{THC} + 2(x_{H2} + x_{H2O})\right]}{4.32MW_{air}}$$

Obviously the model captures the dynamic behaviour of the oxygen storage qualitatively and in several cases quantitatively. In extra urban period it seems that our oxygen storage model is insufficient, a fact that is attributed to the main assumption of the ceria submodel that all of the processes are taking place in the surface ceria and the contribution of the bulk layers is unconsiderable. During the extra urban driving period, where the temperatures are elevated, the oxygen diffusion in the ceria lattice becomes significant and is described by an exponential law versus temperature [134]. Additionally, ceria model is not capable to match the maximum values of the oxygen storage process that can be also ascribed to the same

reason. Of course the quality and the differences in the responses of the measured signals must also be considered to introduce minor errors.

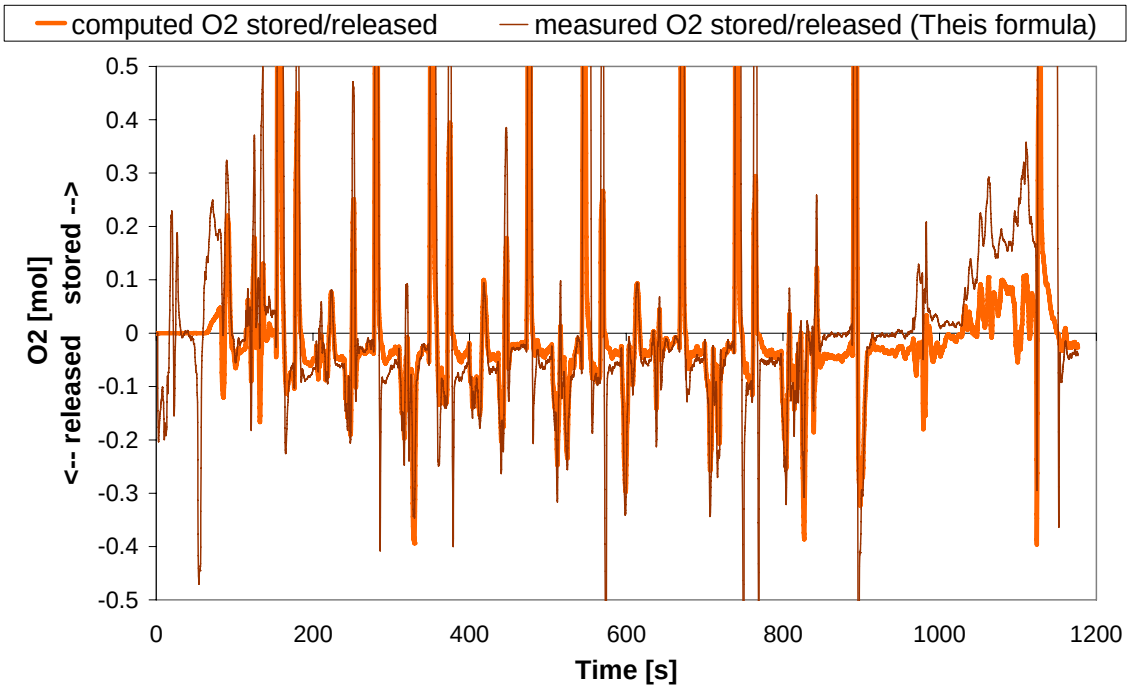

Figure 70 Comparison of the computed and experimentally calculated O_2 that is stored in the washcoat or released from the washcoat of the 10g/ft^3 Pt:Rh catalyst. The calculation from experimental data was made according to the formula of Theis [173]

Figure 71 is a snapshot of the chemical processes inside the catalytic converter. The simplified approach of the reduced reaction scheme enables the investigation of the relative reaction contribution in the consumption of each chemical species. It can be seen that the results of the tuned model are consistent with the physical sense that we have for the chemical processes. The majority of the reactants (CO, THC and NOx) are consumed by the RedOx reactions that are taking place over the PGM. Ceria has a secondary regulative role as it contributes about 15% on average for CO and THC and less than 5% for NOx. Especially in the case of NOx, it can be seen that the reaction of ceria oxides with NO becomes important only at the transient phase of deceleration and possible neglection in the reaction scheme wouldn't have a significant effect.

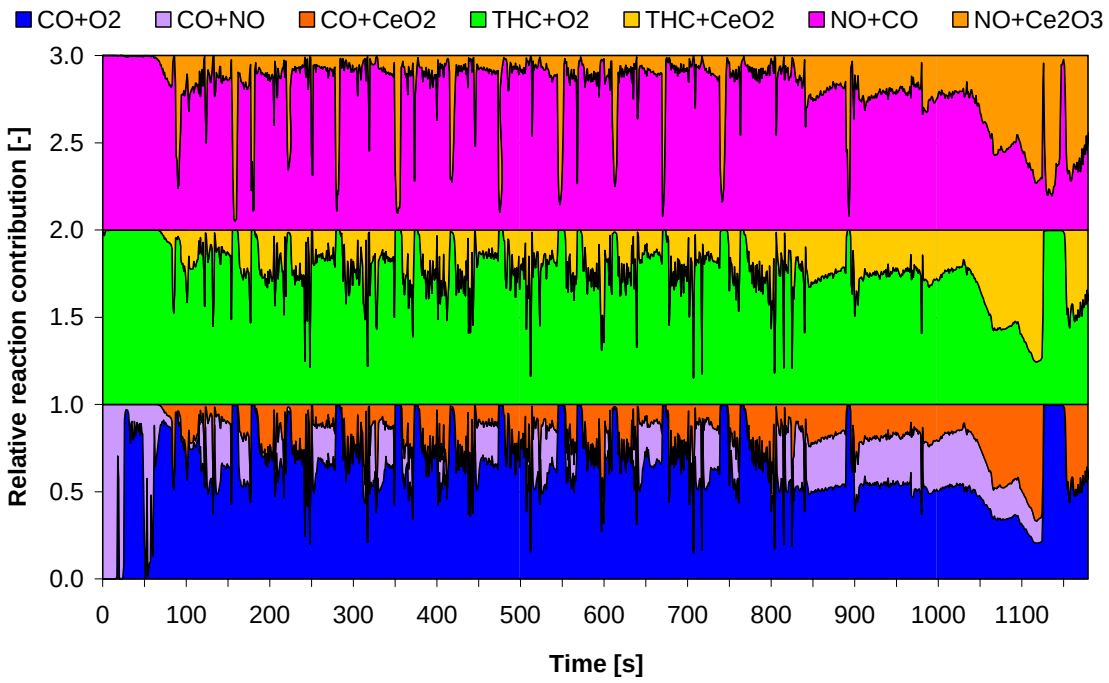

Figure 71 Relative reaction contribution in the consumption of the pollutants CO, THC and NOx inside the 10g/ft^3 Pt:Rh catalyst.

The results of Figure 65 to Figure 71 show that the model is able to predict the operation of a catalytic converter tested in a legislated driving cycle within a certain accuracy. Additionally, the crosschecks of the Figures Figure 70 and Figure 71 reveal the robustness of the current modelling status. The minimum tunable parameters approach enables easy application to other cases. In what follows, we will present the tuning results of the rest of the cases.

Figure 72 to Figure 74, show the comparison of the cumulative computed and measured emissions for the cases of the 50g/ft^3, 100g/ft^3 and 30g/ft^3 respectively. Similarly to the case of 10g/ft^3, the model captures the cold start and the light-off transition (period 60 to 80s) for CO, THC and NOx in all cases. The deviations at the period from 80 to 120s can be attributed to the initial status of the oxygen storage capacity in these cases also. The model's accuracy suffers again during extra-urban driving. This is acceptable for the specific use of the model, where a good estimation of the overall converter performance in respect to a reference case is needed.

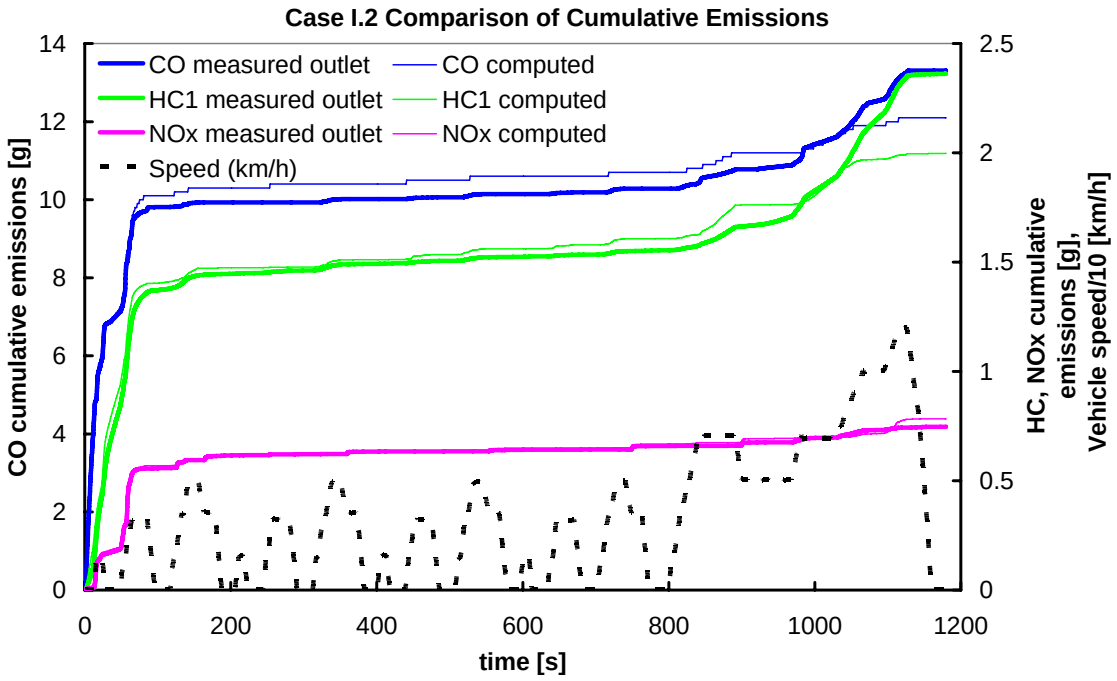

Figure 72 Computed and measured cumulative emissions of the 50g/ft^3 Pt:Rh catalyst

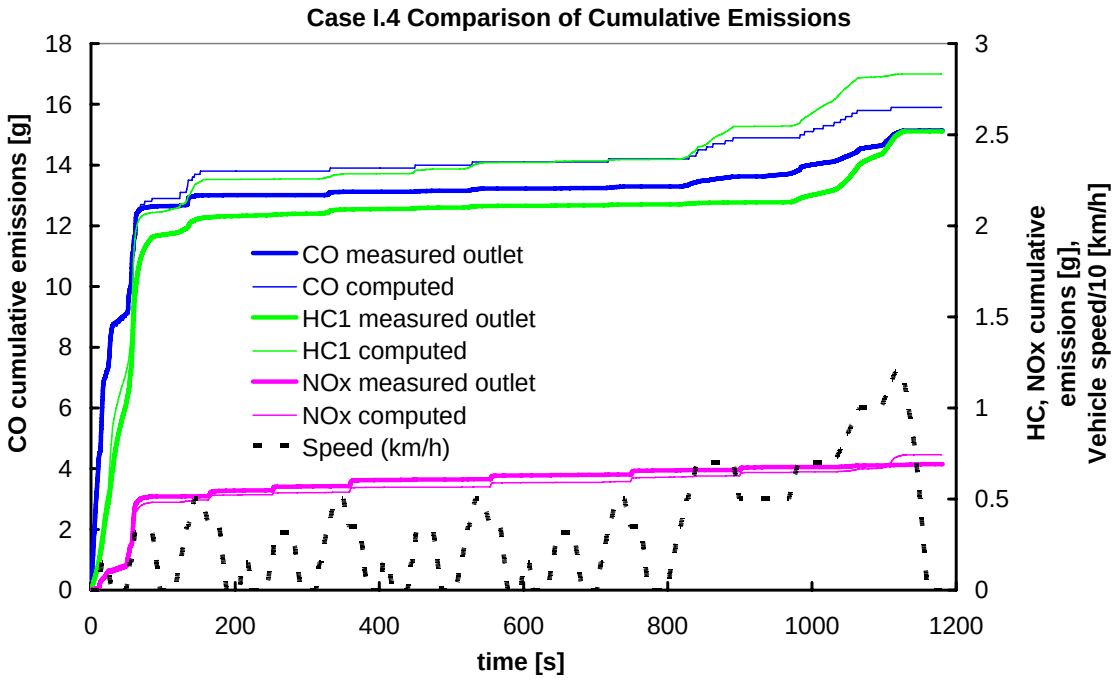

Figure 73 Computed and measured cumulative emissions of the 100g/ft^3 Pt:Rh catalyst

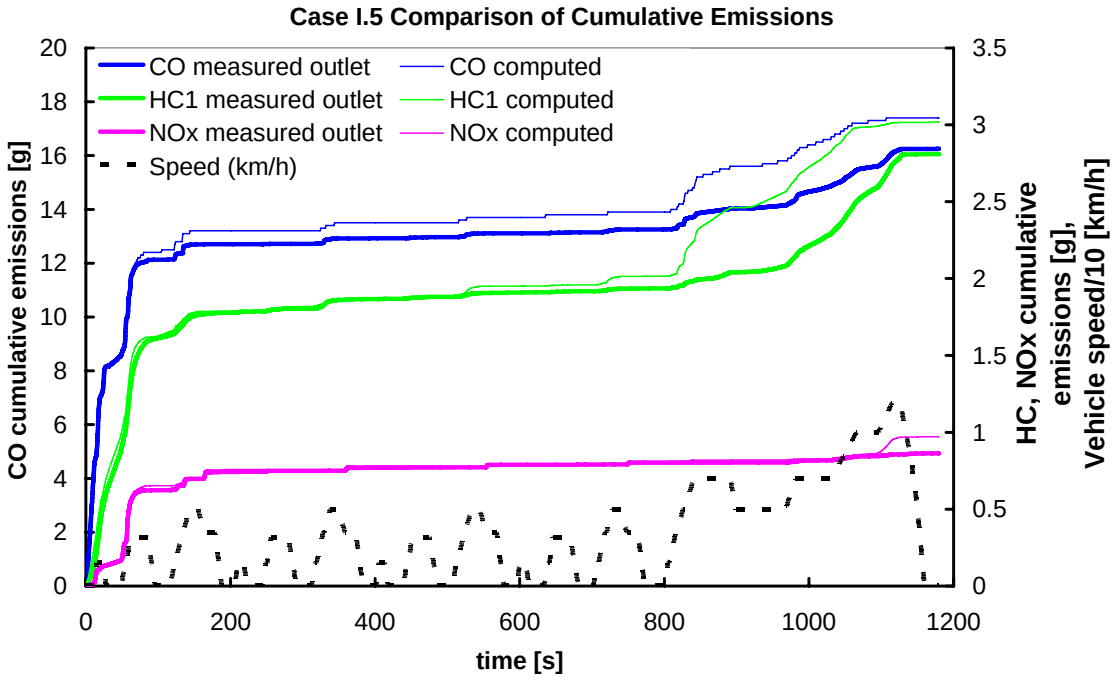

Figure 74 Computed and measured cumulative emissions of the 100g/ft^3 Pt:Rh catalyst

The tuned data of the 2.4 l, 50g/ft^3 converter (Case I.2) is tested in the 0.6l catalytic converter of the same washcoat and the same level of precious metal loading (Case I.1) and the results are shown in Figure 75. The model has a similar behaviour in this case and the tuned variables of Case I.2 fit well the operation of this catalyst.

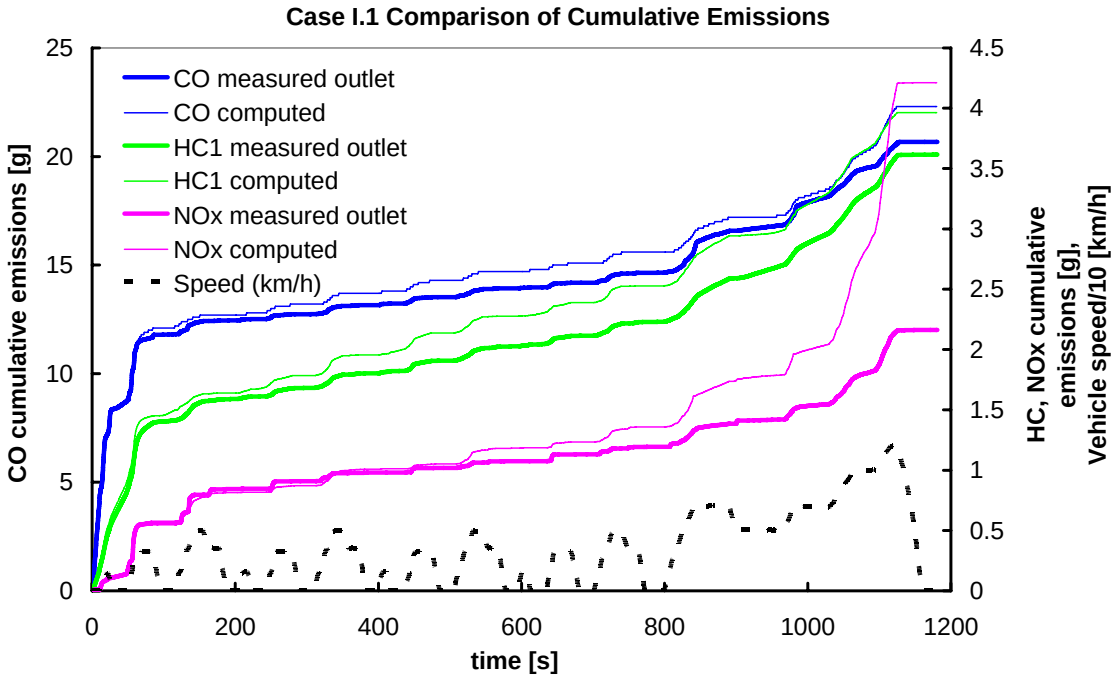

Figure 75 Computed and measured cumulative emissions of the smaller catalytic converter (0.6l) with 50g/ft3 Pt:Rh catalyst loading.

An important aspect in optimum catalytic converter design is the determination of the limiting step of catalysis between reaction rate and bulk diffusion. Although the calculation for steady state applications is trivial, in time-varying applications it is more difficult to conclude to secure results. Common dimensionless numbers that give a sense of these phenomena (e.g. Thiele modulus) do not have direct application if we take into account the variations of exhaust gas composition, temperature and mass flow rate, not only versus time but in the axial position also. If we consider two efficiencies, one for diffusion from bulk gas to the solid and one for reaction in the solid phase, both ranging from 0 to 1, a catalyst utilization factor, ranging from -1 to 1, can be defined as

$$\eta_{diff,i} = \frac{moles\ of\ specie\ i\ diffused\ in\ the\ washcoat}{moles\ of\ specie\ i\ in\ the\ bulk\ flow}$$

$$\eta_{reaction,i} = \frac{moles\ of\ specie\ i\ in\ the\ washcoat\ reacted}{moles\ of\ specie\ i\ diffused\ in\ the\ washcoat}$$

$$\eta_{cat,i} = \eta_{diff,i} - \eta_{reaction,i}$$

Figure 76 shows the catalyst utilisation factor in correlation with the vehicle speed for CO and NOx for three representative cases. We must mention that the THC response follows CO response and O_2 response follows the respective one of the NOx. These curves are not shown for simplicity. It can be seen that all catalytic converters are oscillating in the two limiting regions. As we move upward from reaction limiting region ($\eta_{cat,i} < 0$) to the diffusion limiting region ($\eta_{cat,i} > 0$) we meet the weakest catalyst (Case I.3 – 10g/ft^3) firstly, the strongest catalyst (Case I.4 – 100g/ft^3) secondarily and at last the medium loaded short catalyst (Case I.1 – 50g/ft^3, 0.6l). Obviously, there is an optimum point for the PML where any further increase will not result significant changes in the catalytic converter efficiency considering it will be diffusion limited [33]. An additional observation is that the NOx utilisation factor in the cases I.1 and I.4 where the reaction rate is adequate is shifted towards the diffusion limiting area, a fact that makes it sensitive to the increased mass flow rates and decreased geometrical surface areas. This is consistent with [88].

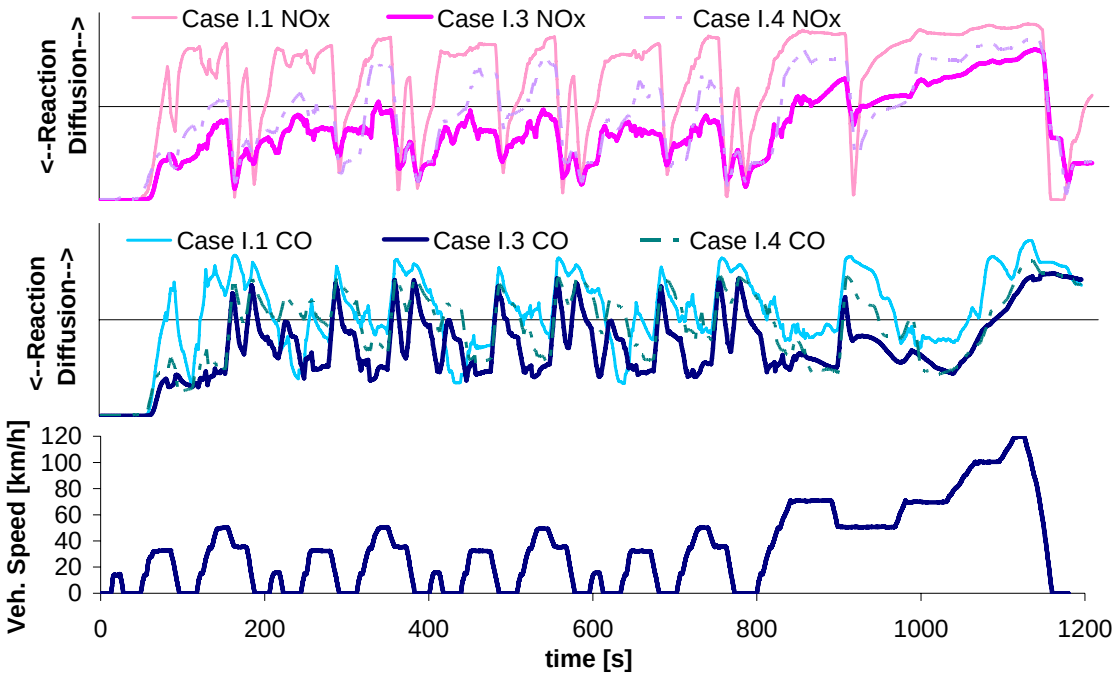

Figure 76 Model's prediction of catalytic converters' operation in the reaction or diffusion limited region. Figure shows three representative cases of 2.4 l catalyst with 10g/ft^3 PML (case I.3), 2.4 l catalyst with 100g/ft^3 PML (case I.4) and 0.6 l catalyst with 50g/ft^3 PML (case L1) versus driving pattern.

Figure 77 shows the tuned values of the three pre-exponential factors for the oxidation, reduction and ceria reactions respectively. The pre-exponential factors of the RedOx reactions are following a power law versus precious metal loading level, while for ceria reactions there is an asymptotic trend towards a maximum value. The latter maybe dependent on the ceria model used that accounts only for a surface ceria layer. Of course, the sample is not statistically significant to extract a definite law, but the trend that comes up is helpful for the design process.

It has to be noted here that any trend is dependent primarily on the special manufacturing techniques of each washcoat formulation. A general law should have no validity by its own, but should be dependent to a reference washcoat with specific characteristics. To accomplish this, the model must be tuned to a reference catalytic converter and consequently to a specific washcoat formulation, and fit the rest of the catalysts. The resulting kinetics for the noble metals reactions of this case study, are fitted with the following equation

$$\frac{\log A}{\log A_{ref}} = \left(\frac{PML}{PML_{ref}} \right)^{0.07}$$

This equation is successfully used to the other case studies of this dissertation, always by tuning a reference catalyst firstly. Of course, the validity of this finding should be tested over a large variety of cases.

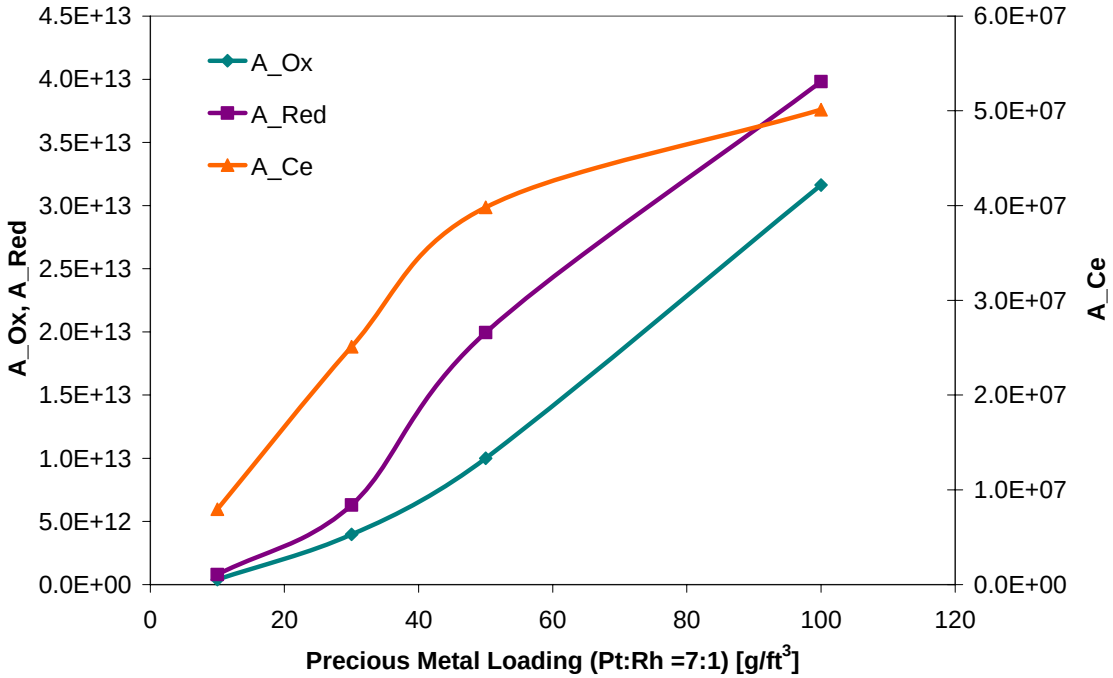

Figure 77 Tuned values of the three tunable variables of the model. A_Ox for the oxidation reactions, A_Red for the reduction reactions, A_Ce for the Ce reactions

5.5 CONCLUDING REMARKS

An improved mathematical model of three-way catalytic converter operation was employed in a case study with five commercial Pt:Rh catalytic converters of varying precious metal loading and size. The process comprised the following steps:

The raw experimental data were pre-processed and checked through an integrated quality assurance system

The catalytic converter 's characteristics were identified, with reference to the washcoat chemical environment and a number of valid assumptions were made concerning its undisclosed properties.

The three tunable variables of the model were optimised with the aid of an optimisation algorithm and the modelling results were postprocessed, validated with experimental data and crosschecked with literature references.

The operation of all catalysts was modelled with only three tunable parameters that correspond to eight dominant chemical reactions. It is evident from the results, that the real world catalytic converter's performance can be successfully modelled by an 1-D model with apparent global reactions.

It was found that catalytic converter operation during urban driving can be matched within certain accuracy with the assumption that Ceria reacts only at the surface layer without any contribution of the bulk layers. On the other hand, more precise and complex modeling would reduce the speed and versatility of the model that is essential in engineering applications. This conclusion is being studied extensively in recent works [57,90] and remains an open issue for further investigation.

The extended case study with the five catalytic converters confirmed the following:

The OSC is essential for the increased efficiency of the catalytic converters and is correlated with the precious metal implementation in the washcoat.

Increase in precious metal loading enhances catalyst activity, which is limited by the diffusion of gas species from the bulk flow to the washcoat. There is an optimum between PML and catalyst design data (length, volume, cpsi).

NOx reduction is very sensitive to space velocity and/or geometric area effects.

CHAPTER 6

CASE STUDY: VARIABLE CHANNEL DENSITY (Pd/Rh CATALYSTS)

The effect of monolith channel density is studied in this chapter. The experimental data comes from a 2.4 l V6 spark ignition engine, designed for EURO 3 emissions limits. The exhaust line comprises two banks, one for each engine bank, fitted with two close coupled ceramic monolithic catalytic converter of 1.0 l each. In this case also, the exact washcoat formulation is not supplied and the washcoat level is modeled as a black-box with three-way function and oxygen storage. The data was preprocessed and quality assured as described in chapter 3 and the engine management of the engine was identified and discussed in chapter 4. In the latter case it was shown that management is tailored to assist oxygen storage filling when it is determined by the engine management. In what follows in this chapter the cases of variable channel density catalytic converters are modeled using a proper reaction scheme selected according to the discussion of chapter 1. The tunable parameters of the model are estimated according to the methodology developed in chapter 2. The results are extended to a case of a catalytic converter with different precious metal loading levels.

6 CASE STUDY: VARIABLE CHANNEL DENSITY

6.1 OVERVIEW OF THE CASE

An important parameter of the catalytic converter design is the monolith channel density. Increased channel density is increasing the exchange area between gas flow and solid catalytic surface and thus enhances the catalytic performance. On the other hand, an increase of the channel density has negative effects, as for example increased backpressure and increase in thermal inertia of the catalytic converter [88]. A common technique to reduce the negative impact of such design modifications is the use of thin walled catalytic converters. The thin walled substrates are impregnated with a thinner washcoat layer that affects other properties related to the catalytic efficiency. The detailed discussion of these properties and the respective mechanisms is a subject of fundamental research that is beyond the scope of this chapter. The engineering design of such catalytic converters includes simultaneous optimization of interacting design parameters like washcoat loading, washcoat thickness, substrate thermal properties and monolith dimensions.

The system studied in this chapter comprises the following components:

- A V6 2.4 l stoichiometric spark-ignition engine with two banks of exhaust line (one for each side of cylinders)
- An advanced engine management with fuel cut-offs during deceleration and possibility of secondary air injection to the converter
- Two close coupled start-up three-way catalytic converters in parallel, with advanced two-layer washcoat formulation and 100g/ft^3 Pd:Rh loading.

The data of the cases, performed in NEDC, is presented in Table 17. In what follows the model, which is presented in chapter 2, is tuned to fit the behavior of the catalytic converter of one bank only. It is assumed that the exhaust gas characteristics are identical for both of the two exhaust banks.

We set the tuning of the Cat.#2 converter (600cpsi) as the reference and the starting point for this study. This choice is made because this case achieved the higher value of quality measure among the cases studied in this chapter as shown in Table 9. For this reason, it is assumed that the results of the tuning should be more confident with this specific case. The results of this case will be extended to the rest

of the cases of this chapter, considering that channel density is a geometrical characteristic that is not affected by tuned kinetic parameters. Of course, intrinsic differences due to a number of parameters discussed in Chapter 1 (e.g ageing procedure, or manufacturing uncertainties) should exist between the washcoat formulation of these catalysts, which may affect the modelling success. Separate tuning of the model to match the behaviour of each catalytic converter would not be sensible, since we look into the model's capacity as an engineering tool.

This case study aims at the macroscopic investigation of the variation of channel density considering the catalyst efficiency in the exhaust line as the major performance measure of the study. The objective is to find any trends regarding the channel density and assign rules for the engineering design of the converter.

Table 17 Data for the case of variable channel density catalytic converters

CASE	II				
Test Name	Cat. #1	Cat. #2	Cat. #3	Cat. #4	Cat. #5
Vehicle Engine	2.4 l, SI, EU-III				
Position	Close Coupled				
large axis [m]	0.11				
small axis [m]	0.11				
length [m]	0.12				
Volume [l]	1.00				
cpsi	400	600	900	1200	900
thickness nominal [mil]	6.5	3.5	2.5		
PML (g/ft^3)	100				70
Pt	0				
Pd	14				
Rh	1				
OSC	unknown (estimated 600 mol/m^3WC)				
Stabilisers / Promoters	Unknown				
Comments					

6.2 STUDY OF THE EXPERIMENTAL DATA

Figure 79 to Figure 81 present a comparison of the measured cumulative emissions of CO, THC and NOx for the five catalytic converters listed in Table 17. Considering that all other design parameters are kept constant, it would be expected that the catalyst efficiency be proportional to the channel density, that is, "the denser - the more efficient", considering the relative increase in the apparent catalytic surface area of the converters.

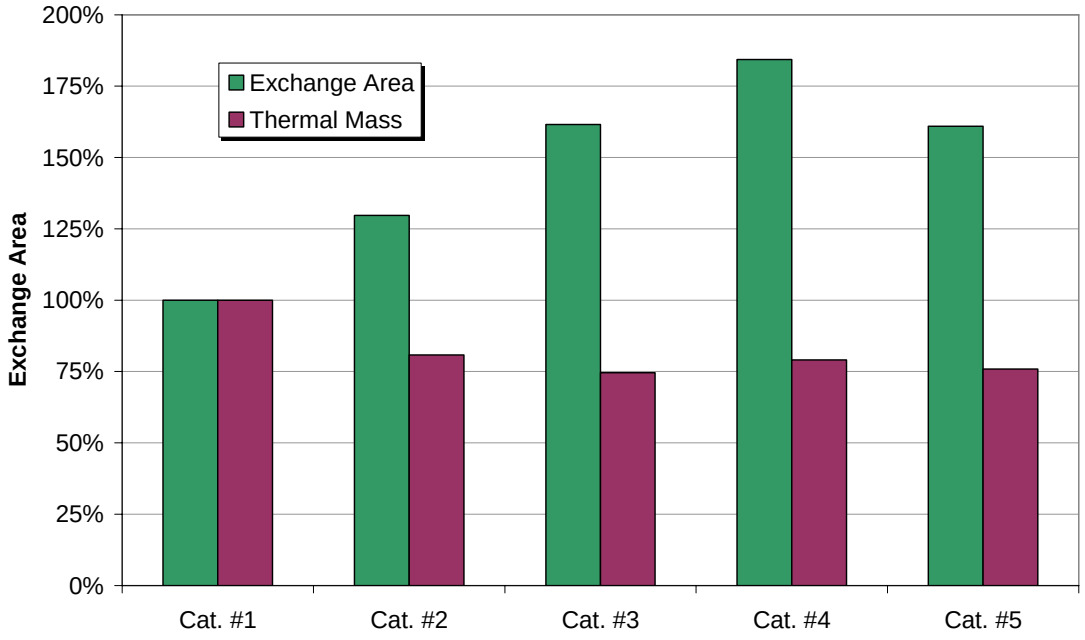

Figure 78 Comparison of apparent exchange surface area and thermal inertia for the catalytic converters of the case study. Reference catalytic converter Cat.#1 (400 cpsi)

Experimental results in Figure 79 to Figure 81 do not follow that rule. For the case of CO emissions the Cat.#3 (900 cpsi) seems to be the most efficient while for THC and NOx emissions shows similar performance to the Cat.#4 (1200 cpsi). This fact is attributed to the faster light-off of the Cat#3 system due to its lower thermal inertia (heat capacity) as it is shown in Figure 78.

The operation of oxygen storage is prominent regarding CO and THC performance. As shown in Figure 79 the CO breakthroughs at about 150, 280, 350 and 1000 s of the NEDC can be attributed to the oxygen storage filling level, but this will be discussed in the later sections of this chapter. The same stands for THC emissions, as shown in Figure 80 also, but HC conversion efficiency seems to be less sensitive to the dynamics of oxygen storage.

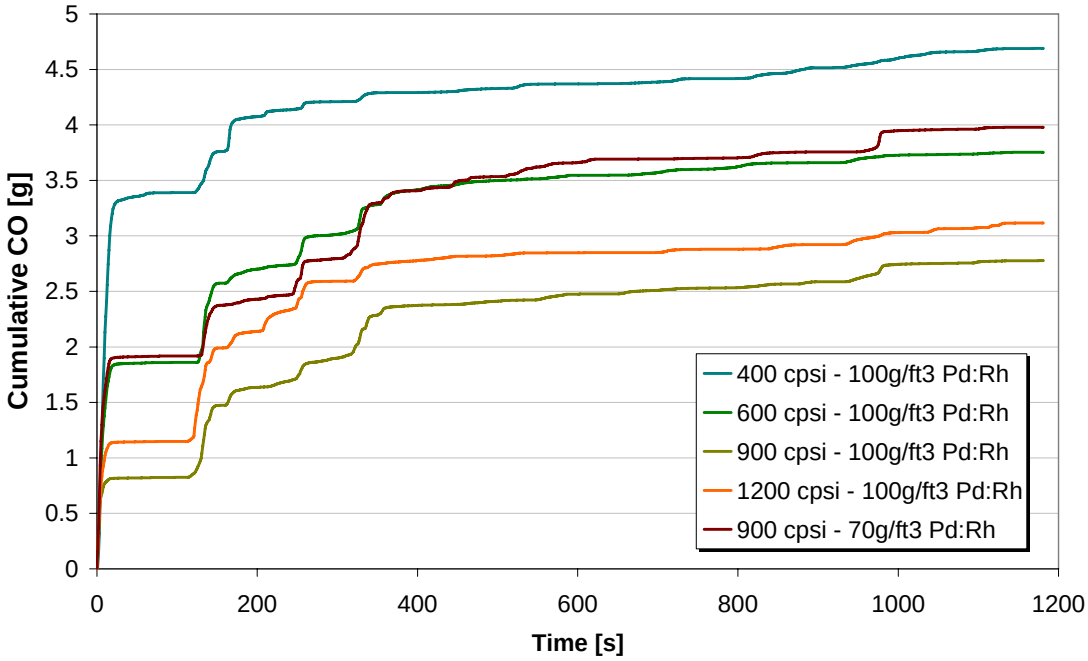

Figure 79 Comparison of measured cumulative CO emissions for the Case II catalytic converters

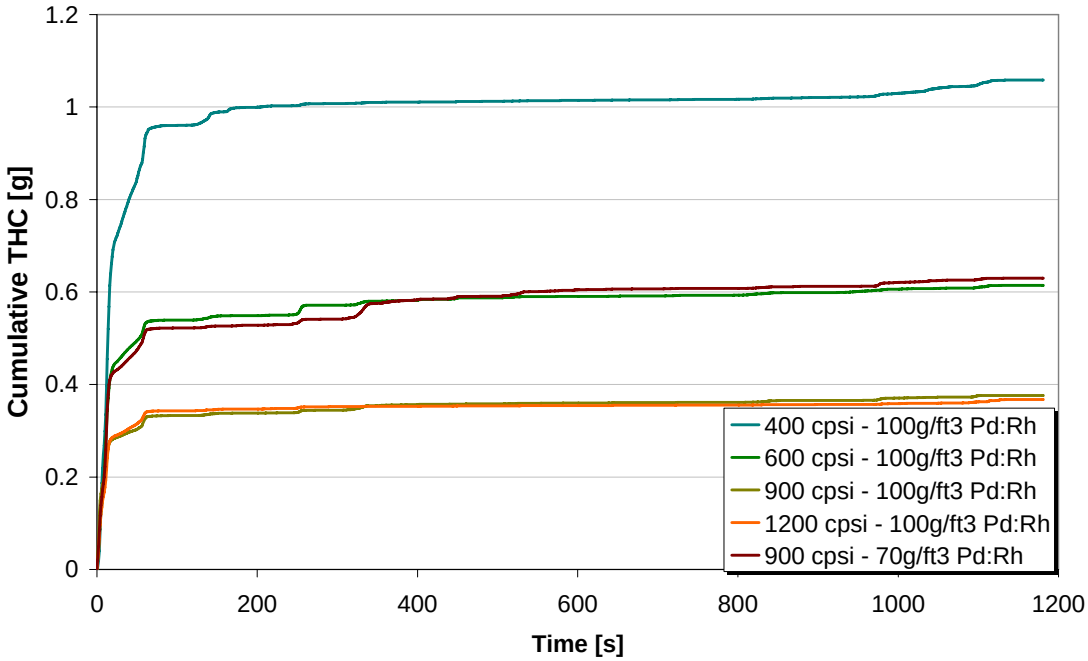

Figure 80 Comparison of measured cumulative THC emissions for the Case II catalytic converters

An important issue is the behavior of NOx emissions, which is shown in Figure 81. Practically, they seem to be unaffected by the change in the channel density. This stands especially for the first seconds when all catalysts show the same light-off behavior for NOx. This behavior can be explained by the advanced

washcoating technology applied to these converters. The catalytically active phases are deposited in two separate layers of washcoat, resulting to a special variation of catalytic activity according to the layers order from surface to the wall [174]. In several cases the thermal contact between these layers is disturbed in order to fully promote specific behavior. For the specific case, where a two layer washcoat technology was applied, the first layer promotes the oxidation of CO and THC and the second layer has a common three- way behavior.

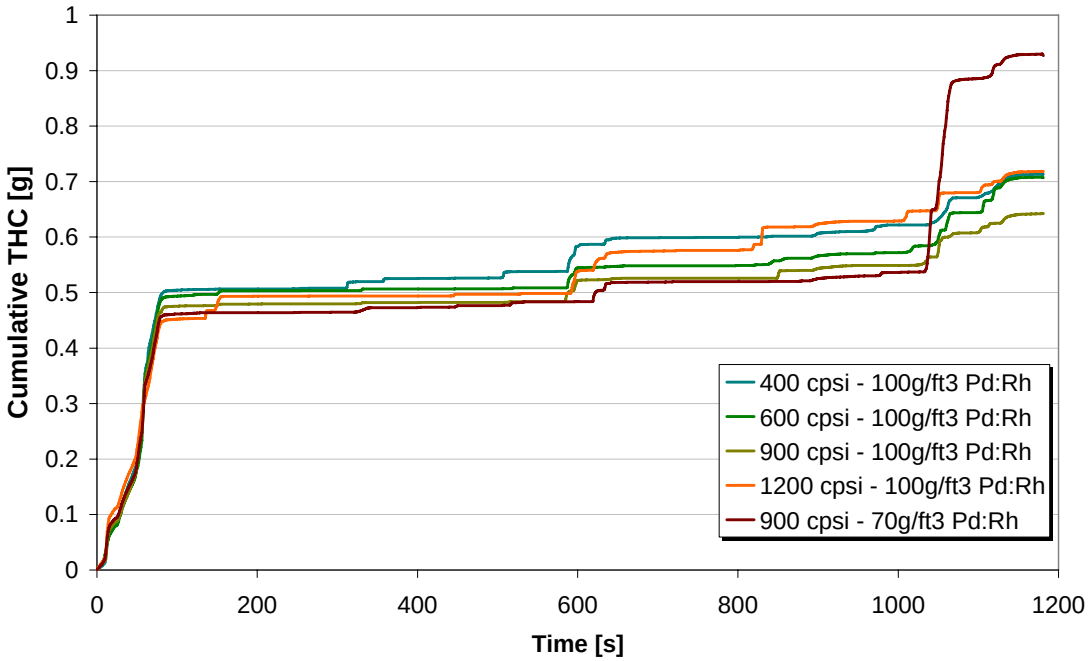

Figure 81 Comparison of measured cumulative NOx emissions for the Case II catalytic converters

During the first seconds (about 95-100s) when an air assisted cold start takes place (lean operation for the catalytic converter), the majority of CO and THC are consumed into the first layer, resulting into a fast first layer light-off (at about 8s). At this moment the second layer has not been adequately heated up, and the CO that reaches the second layer is not sufficient to promote NOx reduction. Of course, the heat of the first layer is transferred to the second layer and the ceramic substrate assisting the warm up of the converter. The NOx breakthroughs of Figure 81, evident at later moments at about 600, 800 and 1050 s, are accompanied by 100% CO efficiency (indicated with straight lines in Figure 79). This is strong evidence that the first layer promotes catalytic oxidation and the second layer RedOx function to promote also NOx reduction. If there is adequate exhaust gas oxygen to eliminate

CO at the first layer, the NOx efficiency decreases dramatically as insufficient exhaust gas CO content reaches the bottom layer.

It can be easily shown that two light-off moments can be addressed to this type of layered washcoat formulation. The light-off point for the first layer is reached much faster than the light-off point for the second layer. The thermal mass (heat capacity) of the converter is responsible to maintain the efficient operation after the second light-off point against the inlet temperature fluctuations. The two light-off points are evident in Figure 79 to Figure 81 at about time= 8 seconds (!) for CO and HC and at about the time= 60 seconds for NOx.

An important issue that is shown from the specific experimental data is that the operation of the catalytic systems is almost equivalent during warm operation and the differences are found to isolated events primarily affected by the behavior of the entire system. For example, CO and NOx emissions show a breakthrough at about 1000s for the Cat.#3 and Cat.#5 cases. This is probably attributed to the value of equivalence ration ($\lambda>1$) of engine out exhaust gas, which inhibits the reducing function of catalytic converter. Obviously, the comparison of almost equivalent systems must be thoughtful considering the intrinsic uncertainties of such applications.

In what follows, the behavior of the catalytic converters will be assessed with the aid of the model. Special attention will be given to the match of the light-off behavior, as this is responsible for the major part of the overall cycle emissions.

6.3 TUNING TO THE REFERENCE CATALYST

The model employed in this work accounts for a single layer washcoat only. A basic assumption that was used in the past to model such applications was that the different catalytic activity of the two layers was lumped into the kinetic parameters. This approach was proven able to predict either the rapid light-off or the warm operation of the converter, but not both of them simultaneously. The discussion on experimental results revealed significant differences in the catalytic activity and the thermal response between the top and the bottom washcoat layer for all the catalytic converters under study. The model was not capable of predicting the rapid light-off at about 10th second for CO and THC but only the behavior after the 60th second. On the other hand, efforts to fit the high CO and THC efficiency during the first seconds resulted to extravagant kinetic parameter values or unreasonably low values of thermal properties for the monolith.

Kirby in his patent [175], declares that rapid light-off times in dual layer washcoats catalytic converters are achieved when the mass ratio of the two layers (outer to inner) is less than unity. In order to fit both the light-off and the warmed-up operation of the catalytic converter it is assumed that the double layer washcoat is equivalent to a two bed monolith with different characteristics. The first bed, which is equivalent to the Pd-only top layer, is considered as a short oxidation catalyst with no oxygen storage and the second bed, which corresponds to the Pd:Rh bottom layer, as a longer catalyst with a full three-way reaction scheme (see Table 18 for details).

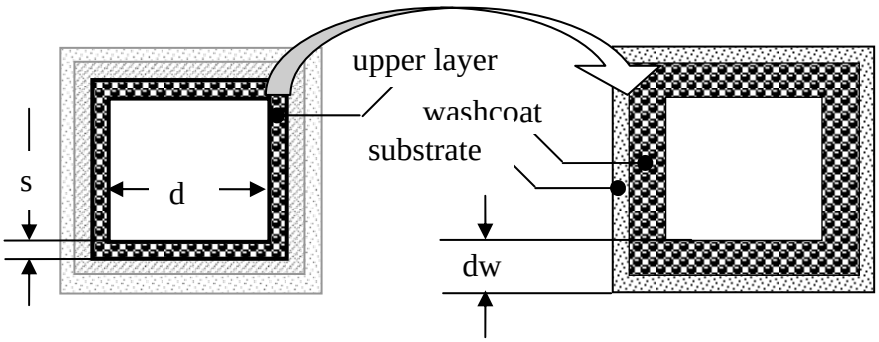

Figure 82 Schematic representation of thermal masses equivalence.

The thermal mass of the first bed has to be equal with the thermal mass of the upper layer in order to have similar thermal response. We could assume that the two beds have equal frontal area and thermal properties and different length and density of washcoat and substrate. We could further assume that the washcoat and substrate density of the first bed is the same and can be calculated by the known thermal mass of the top layer of the original catalytic converter. Let us assign the indicator 1 to the original top layer and the indicators 2 and 3 to the substrate and the washcoat respectively of the equivalent first bed of the current approach as shown in Figure 82

$$1 = top \quad layer, \quad 2 = substrate, \quad 3 = washcoat$$

$$L_1 \cdot \rho_1 \cdot s_1 \cdot d_1 = L_2 \cdot \rho_2 \cdot s_2 \cdot d_2 + L_3 \cdot \rho_3 \cdot s_3 \cdot d_3 \Rightarrow$$

$$L_1 \cdot \rho_1 \cdot s_1 = L_2 \cdot \rho_2 \cdot (s_2 + s_3) \quad \underset{s_2+s_3=d_w}{\overset{s_1=r\cdot d_w}{\Rightarrow}}$$

$$\rho_2 = \frac{L_1 \cdot r}{L_2} \cdot \rho_1 \Rightarrow$$

$$\rho_2 = \frac{0.115m \cdot 0.1}{0.015m} \cdot 1600\, {}^{kg}\!/_{m^3} = 1227\, {}^{kg}\!/_{m^3}$$

The above described approach results to the following converter operation characteristics:

- The first bed reaches the light-off temperature rapidly due to its low thermal inertia and CO and HC exothermic oxidation reactions are initiated in the first bed resulting to a further temperature increase of the solid phase
- The exhaust gas outlet temperature from the first bed is also increased through convective heat transfer with the solid phase of the first bed. This heat is used to heat up the second bed that is the bulk thermal mass of the catalytic converter (bottom washcoat layer plus ceramic substrate)
- The second bed is heated up to the light-off temperature for the second set of reactions (full 3-way scheme) and the catalytic converter operates in warm phase.

GenOpt was used to tune the kinetic parameters. It was selected to use different parameters for the oxidation reactions of the two beds, as different

technology is applied to the two layers. The results of the optimization are shown in Table 18.

Table 18 Set of kinetics to match the Case II Cat.#2

		Reaction	logA	E
1st bed	1	$CO+\frac{1}{2}O_2 \rightarrow CO_2$	13.8	90000
	2	$H_2+\frac{1}{2}O_2 \rightarrow H_2O$		
	3	$C_aH_b+\left(a+\frac{b}{4}\right)O_2 \rightarrow aCO_2+\frac{b}{2}H_2O$		
2nd bed	1	$CO+\frac{1}{2}O_2 \rightarrow CO_2$	10.5	90000
	2	$H_2+\frac{1}{2}O_2 \rightarrow H_2O$		
	3	$C_aH_b+\left(a+\frac{b}{4}\right)O_2 \rightarrow aCO_2+\frac{b}{2}H_2O$		
	4	$CO+NO \longrightarrow CO_2+\frac{1}{2}N_2$	12.2	95000
	5	$2CeO_2+CO \rightarrow Ce_2O_3+CO_2$	6.8	120000
	6	$(4a+b)CeO_2+C_aH_b \rightarrow \left(2a+\frac{b}{2}\right)Ce_2O_3+aCO_2+\frac{b}{2}H_2O$		
	7	$Ce_2O_3+\frac{1}{2}O_2 \rightarrow 2CeO_2$		
	8	$Ce_2O_3+NO \rightarrow 2CeO_2+\frac{1}{2}N_2$		

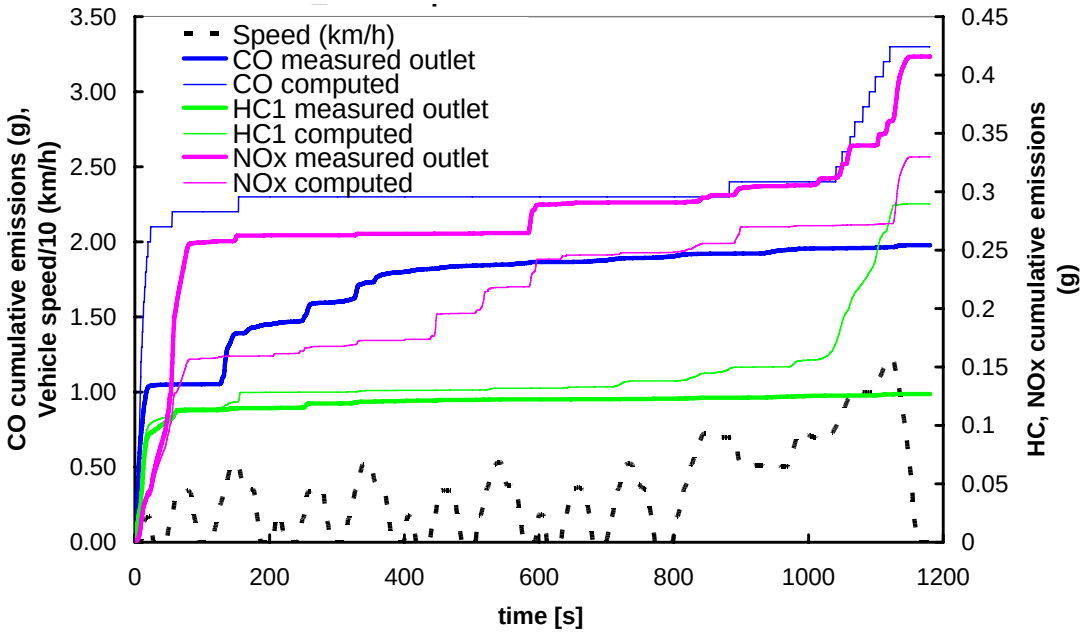

Figure 83 Computed and measured cumulative emissions of the 600cpsi Pd:Rh catalyst.

The comparison of the cumulative emissions is shown in Figure 83. The model captures the behavior of the catalyst for THC up to a certain extent. The same stands for NOx if we exclude the two breakthroughs at about 450 and 550 s. During extra-urban driving, the model loses its accuracy. This is a known weakness of the model as the oxygen storage submodel accounts only for a surface storage layer that has been already discussed in the Chapter 5. The model match for the CO cumulative emissions is not so good but this can possibly attributed to ceria model as will be shown in instantaneous emissions.

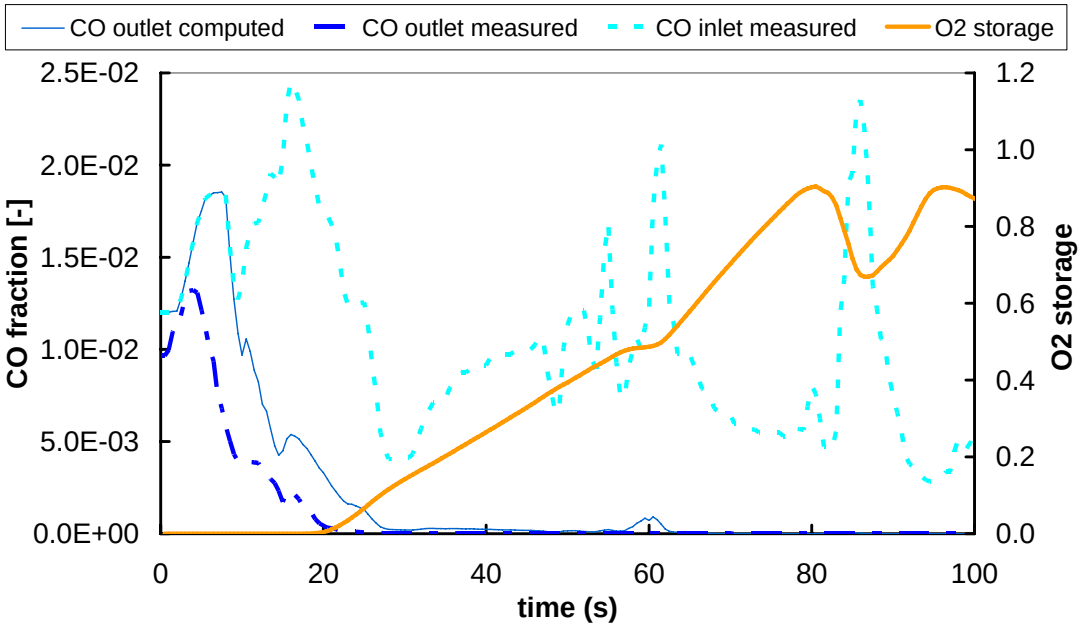

Figure 84 Computed and measured instantaneous CO emissions of the 600cpsi Pd:Rh catalyst during light-off.

In general, the model shows good agreement with the experimental instantaneous emissions for all species. The rapid light-off is matched quite well both for CO and THC as shown in Figure 84 and Figure 85. Especially for THC the model shows a great fit up to 60s that is considered as the light-off point of the bottom layer. At this moment, the conversion efficiency for THC is close to 100%.

Figure 86 to Figure 88 present the instantaneous efficiencies during the complete driving cycle. It can be seen that the behavior of the THCs is matched quite well as the model is able to predict converter- out emissions even during operation at higher than 99% efficiency. The same stands in several cases for NOx where the model predicts accurate NOx emissions (for example about 600 and 1100 s). CO

behavior is not matched as well although the model is able to predict CO breakthroughs because of oxygen storage deficiency

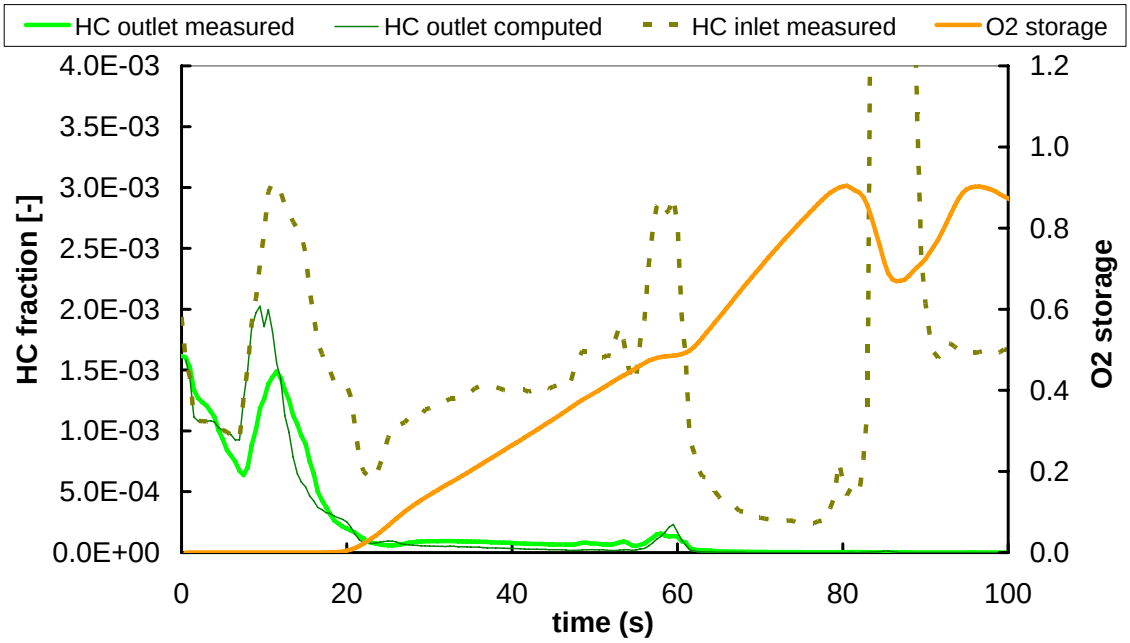

Figure 85 Computed and measured instantaneous THC emissions of the 600cpsi Pd:Rh catalyst during light-off.

As shown in Figure 86, the model predicts that several oxygen storage depletions are accompanied by outlet CO breakthroughs that are confirmed by the measurements. The incapability of the model to fully match the CO outlet behavior could be attributed either to possible bad inlet oxygen signal or to the oxygen storage model. As regards oxygen storage model one possible reason would be a complex behavior of the oxygen storage or several kinds of unknown interactions between the two layers. The model loses completely its accuracy during extra-urban for CO and the same stands for THC and NOx as shown in Figure 87 and Figure 88. It has to be noted here that the converter operates higher than 99% efficiency and the computed output results shown at these figures refer to the same level of computed efficiency.

The model shows a long period after 600s when the oxygen storage is continuously depleting. At this period, the computed output shows decreased efficiency for CO and THC eventually. The measured data on the other hand, shows that catalytic converter maintains its high efficiency (close to 100%). This can be

attributed to bulk ceria storage property that can support oxygen feeding to the catalytic surface even under these circumstances.

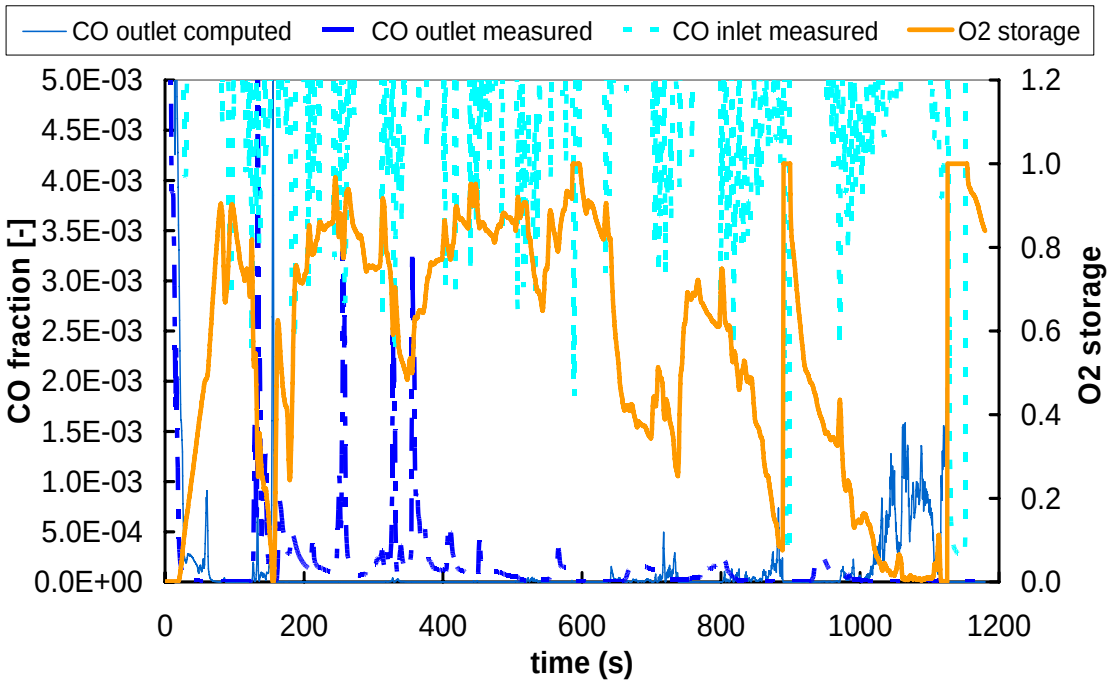

Figure 86 Computed and measured instantaneous CO emissions of the 600cpsi Pd:Rh catalyst

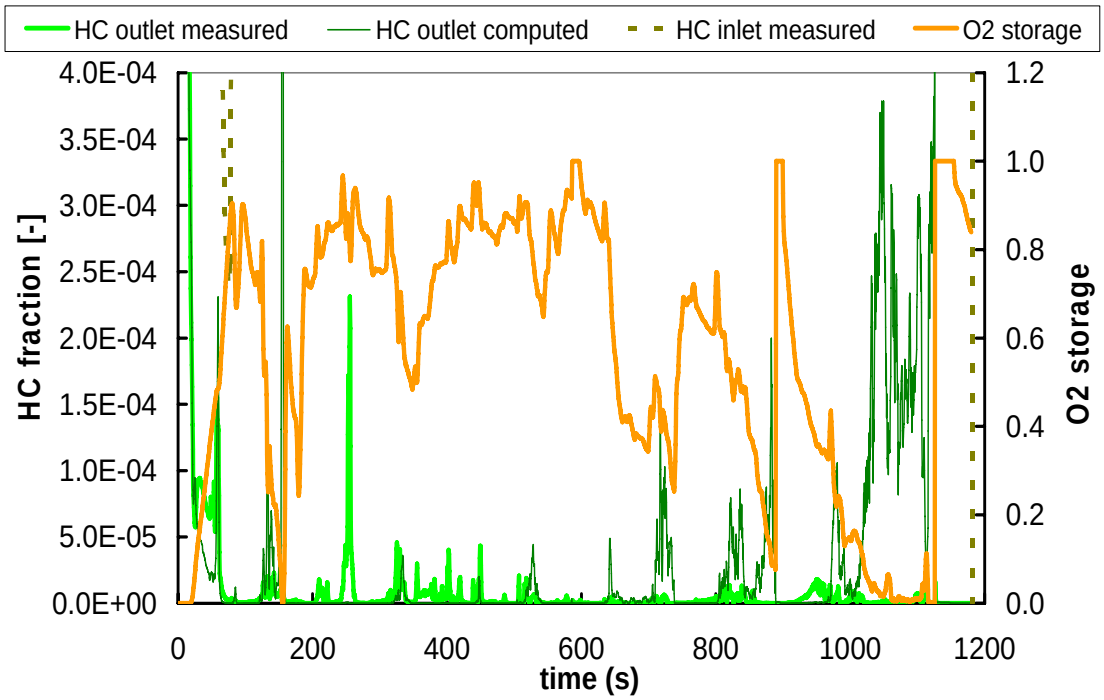

Figure 87 Computed and measured instantaneous THC emissions of the 600cpsi Pd:Rh catalyst

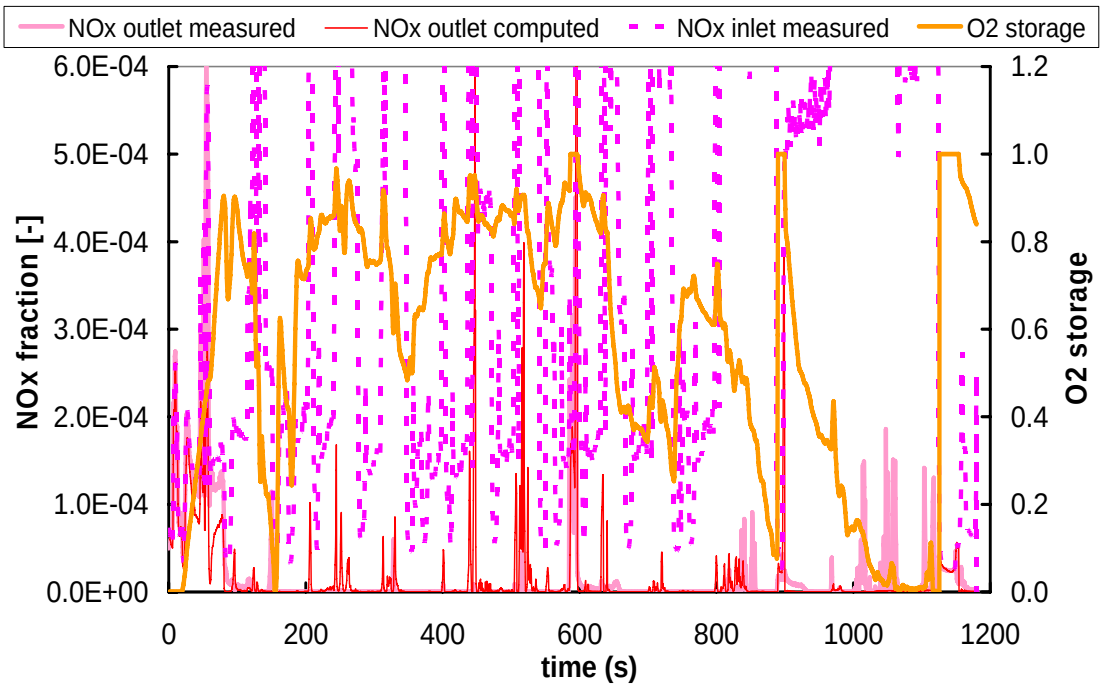

Figure 88 Computed and measured instantaneous NOx emissions of the 600cpsi Pd:Rh catalyst

Of course, the current approach of two beds catalytic converter is not as accurate as a double layer washcoat approach. It seems that in many cases the first bed is very active so it consumes the entire CO inhibiting by this way the NOx reduction (for example at 250s). The same case was used by Pontikakis [3] (pp. 166-171). Compared with the previous status the current approach is closer to reality. As regards THC emissions Pontikakis fail to predict the instantaneous behavior while for NOx the tuning had resulted 100% efficiency for the most of the time. Any NOx breakthroughs there are attributed to the total consumption of CO. The behavior of CO is similar to both of the cases.

It is important to assess the tuning quality. As shown in Figure 89 the reactions on ceria play a key role to the performance of the converter, as they are responsible for the consumption of about a quarter of each species. Reactions on Palladium are the major mechanism to reduce catalyst out emissions while reactions on Rhodium seem to be less important. This can be explained by the ratio of the precious metals in the washcoat. Palladium is by far denser than Rhodium considering the 14:1 precious metal ratio used in this application. Qualitatively the model predicts this superiority of palladium loading.

In several cases we see that ceria reactions contribute the most to the conversion efficiency (e.g 150s). Possibly this is a weakness of the ceria model that

accounts for the total oxygen storage capacity at the surface layer and immediately available to the reactants. Possibly the ceria submodel needs to account for availability of only a portion of stored oxygen at each time as it is indicated by the mechanism of oxygen spillover and transfer into the bulk ceria lattice and vice versa.

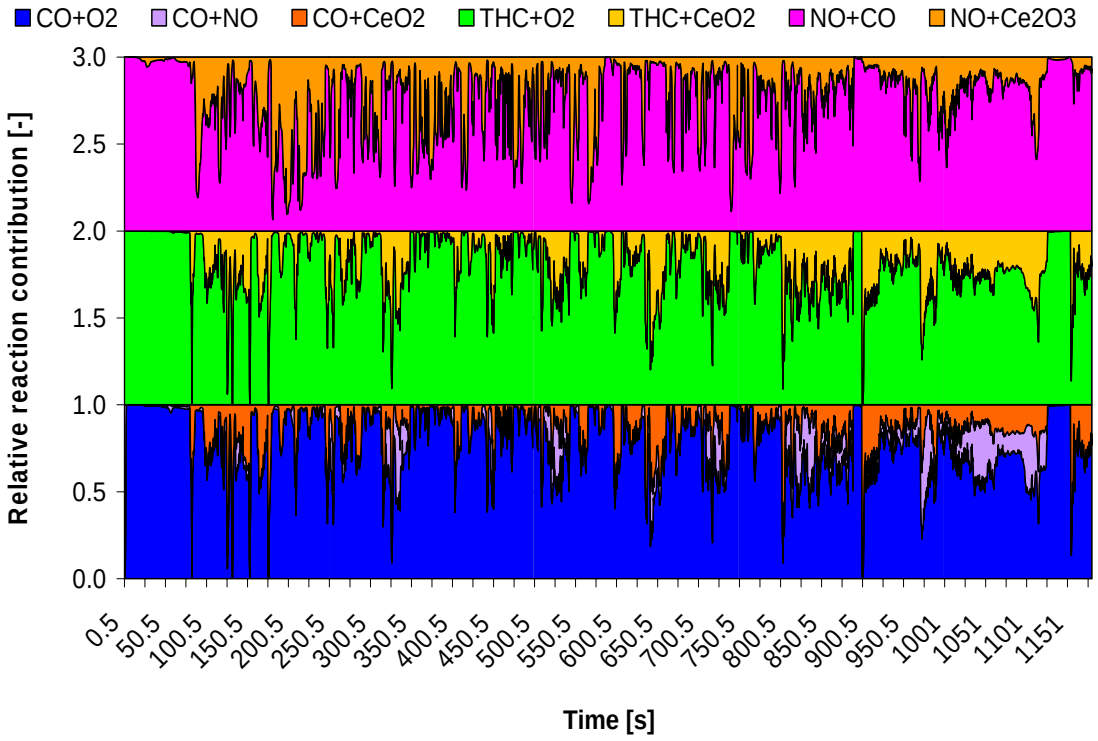

Figure 89 Relative reaction contribution in the consumption of the pollutants CO, THC and NOx inside the 600 cpsi Pd:Rh catalyst

6.4 Extension of the Tuning Results to the Rest of the Cases

In this section, the kinetic parameters found for the case of 600 cpsi catalytic converter are applied to the rest of the catalysts. The extension of the results is considered successful, as the model is able to predict the behavior of these cases in a similar way to the Cat #2 case. The most important part of these cases is the prediction of the rapid light-off that is responsible for more than 60% of the total emissions, considering that all catalytic converters operate at higher than 99% efficiency for the majority of the warmed operation. Another important aspect is the good prediction of the oxygen storage dynamics, as it is responsible for several breakthroughs observed in experimental data. It is selected to present here only some indicative instantaneous results for the economy of space and additionally present a comparison of the cumulative emissions for all cases. Unless otherwise noted, the situation depicted in each figure represents also the rest of the cases.

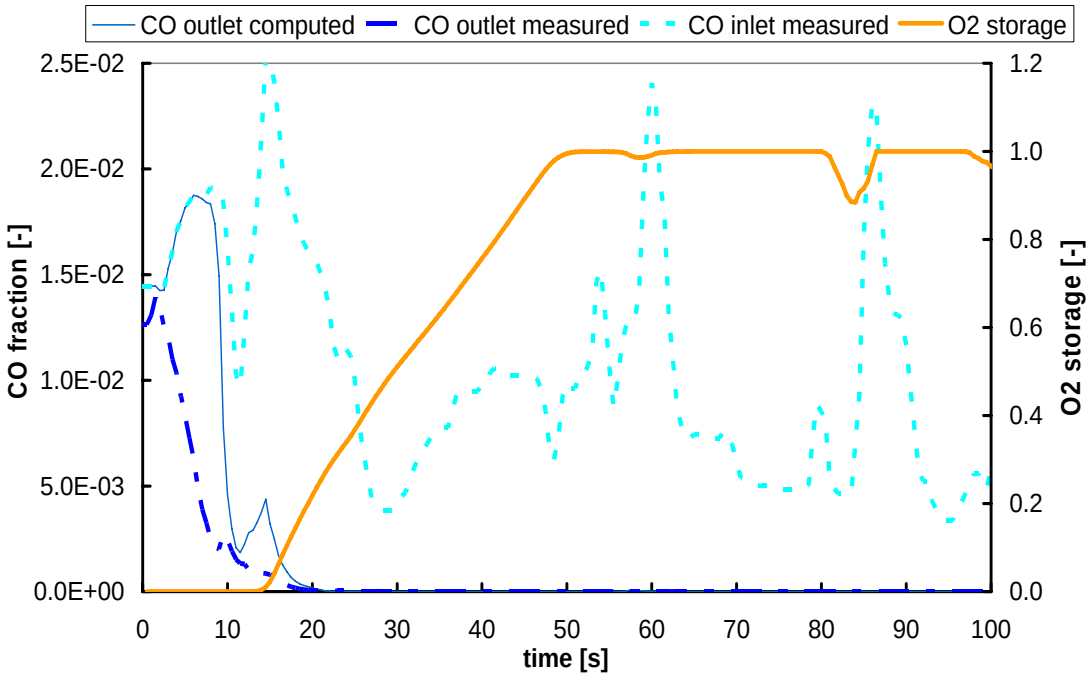

Figure 90 Computed and measured instantaneous CO emissions of the 1200cpsi Pd:Rh catalyst

Figure 90 presents the instantaneous CO emissions for the case of Cat#4 (1200cpsi) during light-off. The model fails again to predict accurately the instantaneous emissions during the rest of the cycle as it returns a similar behavior

to the Cat.#2 case. The light-off is matched quite well in this case and the same stands for the rest of the cases. This is a good validation for the approximation of the two beds modeling instead of a double layer model. As in the case discussed first, the oxygen storage dynamics are responsible for several CO breakthroughs.

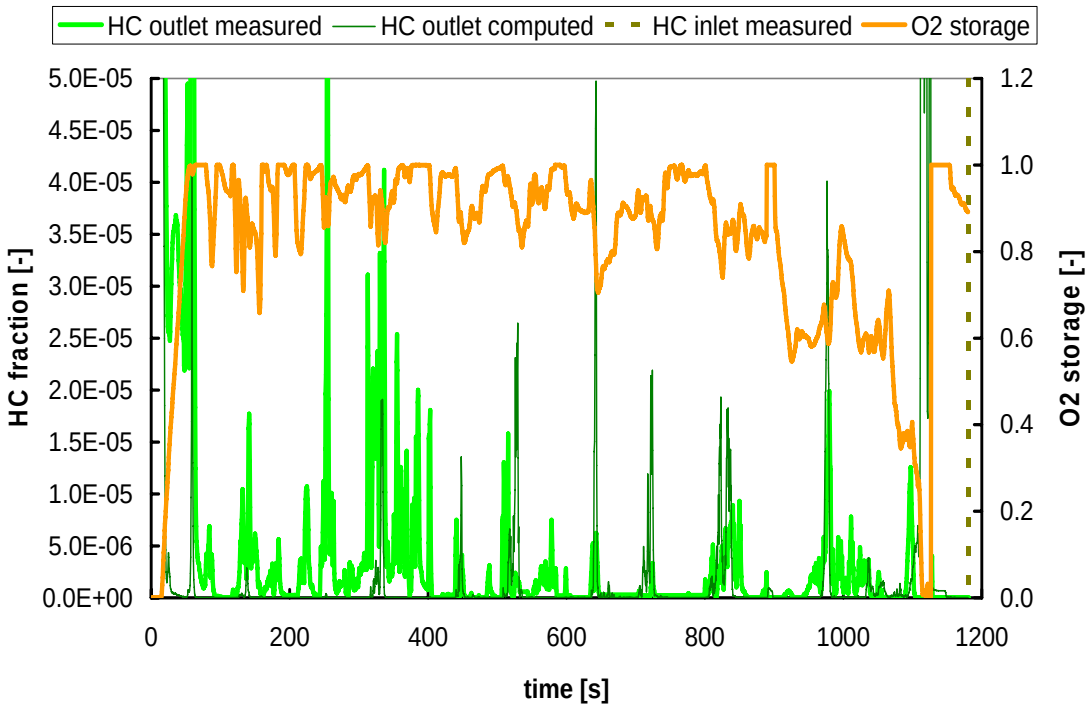

Figure 91 Computed and measured instantaneous THC emissions of the 900cpsi Pd:Rh catalyst

Figure 91 presents the emissions of THC for the case Cat#3. As in the case of Cat#2 the rapid light-off is predicted quite well and the instantaneous emissions of the THC are accurately predicted in the most of the instances. The quality of the results is similar for the rest of the cases. It must be emphasized that the results shown in this figure are referring to less than 10ppm, which is about 99.8% conversion efficiency. The model is capable to predict accurately the outlet in some cases (e.g. 450 and 800s) while in other returns 100% efficiency.

As regards NOx the model predicts well in several cases the instantaneous behavior. The results for case Cat#1 are presented in Figure 92. The success of the model is similar to the reference case and the same stands for the rest of the cases, which are not shown here for space economy. In general, the model matches the light-off at about 60s and the operation close to 100% while it successfully predicts the breakthroughs of the NOx outlet emissions.

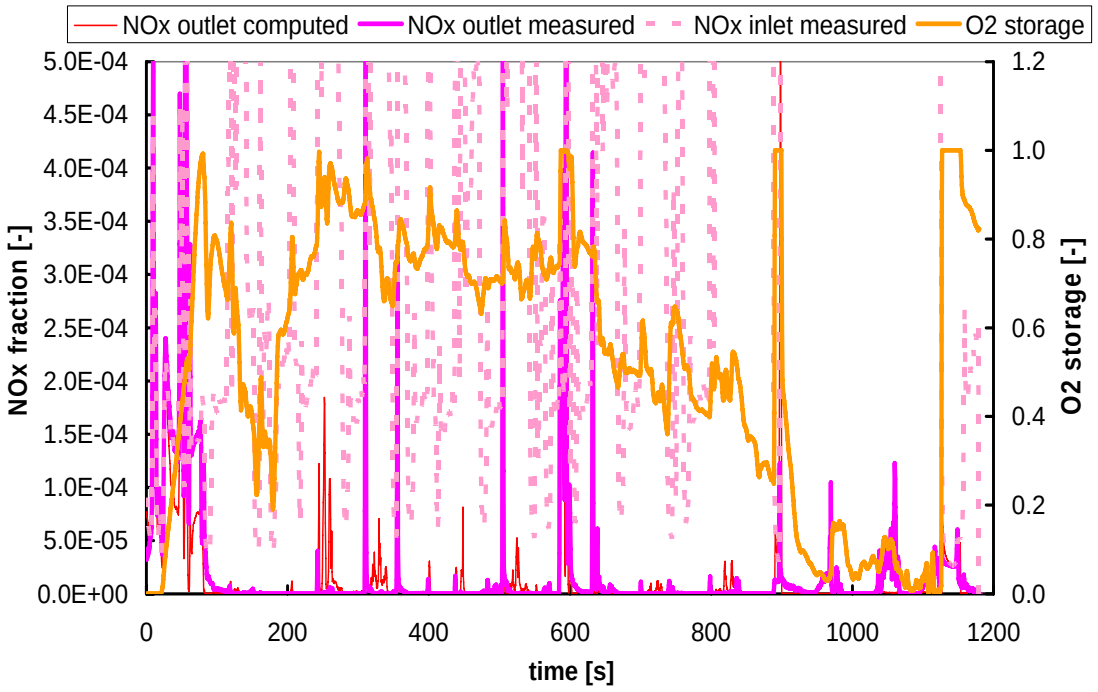

Figure 92 Computed and measured instantaneous NOx emissions of the 400cpsi Pd:Rh catalyst

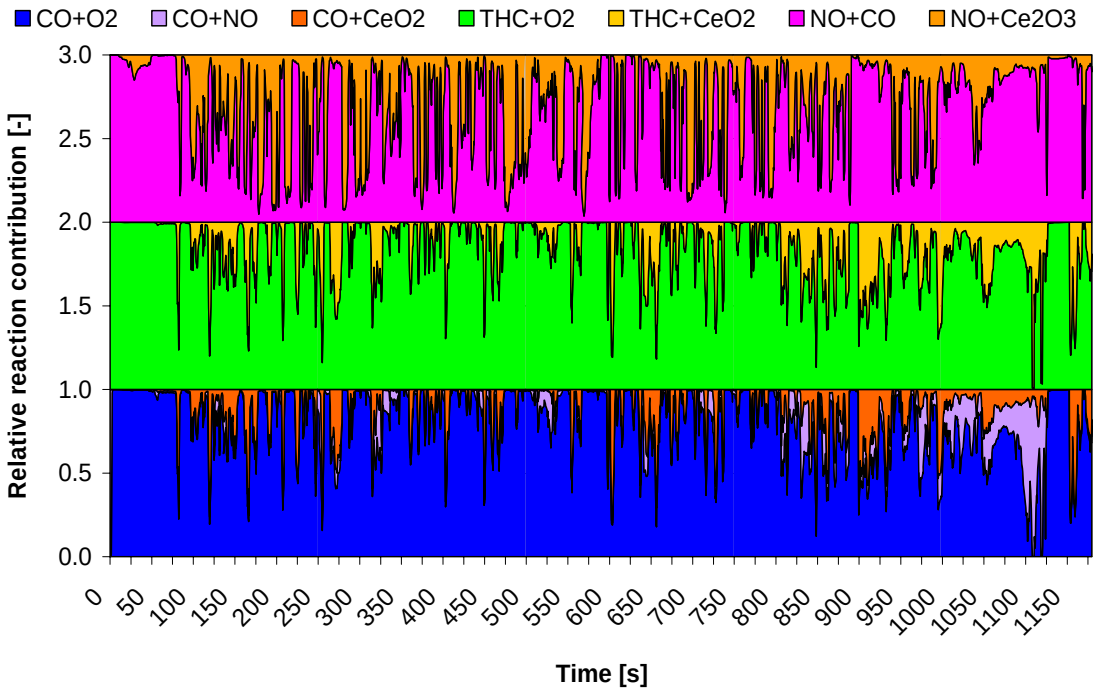

Figure 93 Computed reaction contribution diagram for case Cat#3

The computed contribution of the various reactions and consecutively of the precious metals is shown in Figure 93 for the case of the most active catalyst (Cat#3). The share of each precious metal is determined by the modeling results but this is also an indication of the activity of each catalyst. Similar to Figure 89, which refers to Cat#1 case, most of the species are shown to be consumed over Palladium and only a small portion over Rhodium. The same qualitative results are observed for the rest of the cases.

Even with the same engine, small variations in experimental procedure or slight differences in the washcoats (of the same formulation) are affecting the results. A reasonable question would be whether the optimization algorithm converges to a global solution for the kinetics considering that they are independent to the channel density. Figure 94 shows a comparison of the three tunable parameters of the model. Obviously, there are slight variations that are explained by possible variations in the final washcoat formulation, but they are not important. It seems that GenOpt converges to a global solution for the specific modeling approach and the washcoatcharacteristics.

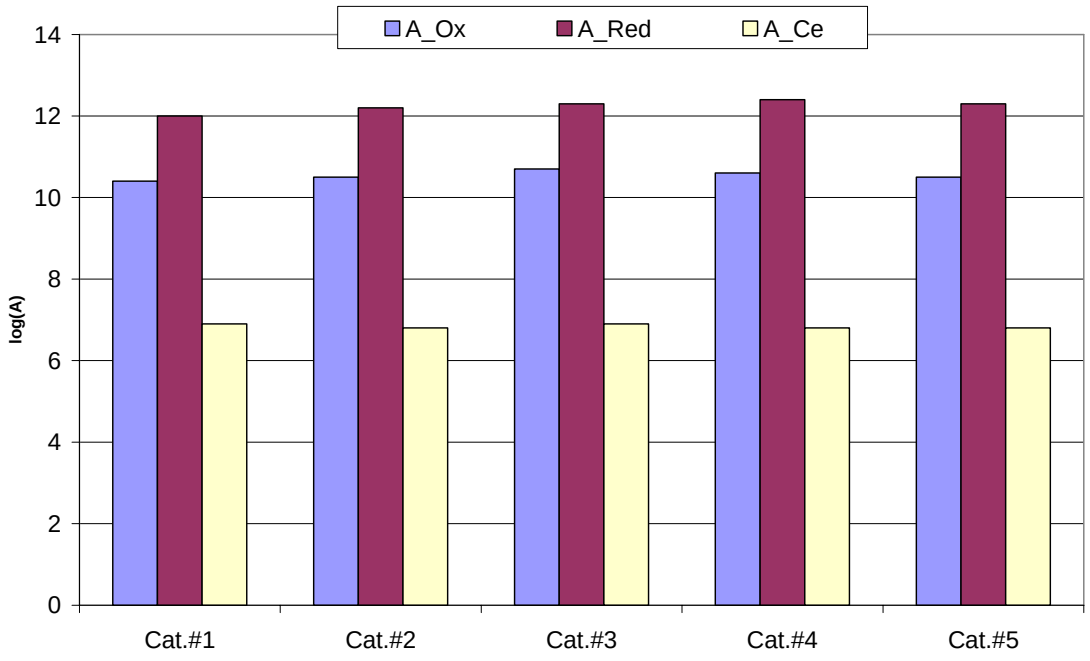

Figure 94 Comparison of kinetic parameters found by Genopt when the model tuned for each case separately.

6.5 Extension to the Lower Precious Metal Loading Catalyst

The tuned kinetic parameters are applied to the case Cat#5 that is a 900 cpsi catalytic converter with the same washcoat characteristics but lower precious metal loading. The kinetic parameters are reduced according to a power law for reactions over precious metal and to a log-linear law for the reactions on Ceria, as found in chapter 5.

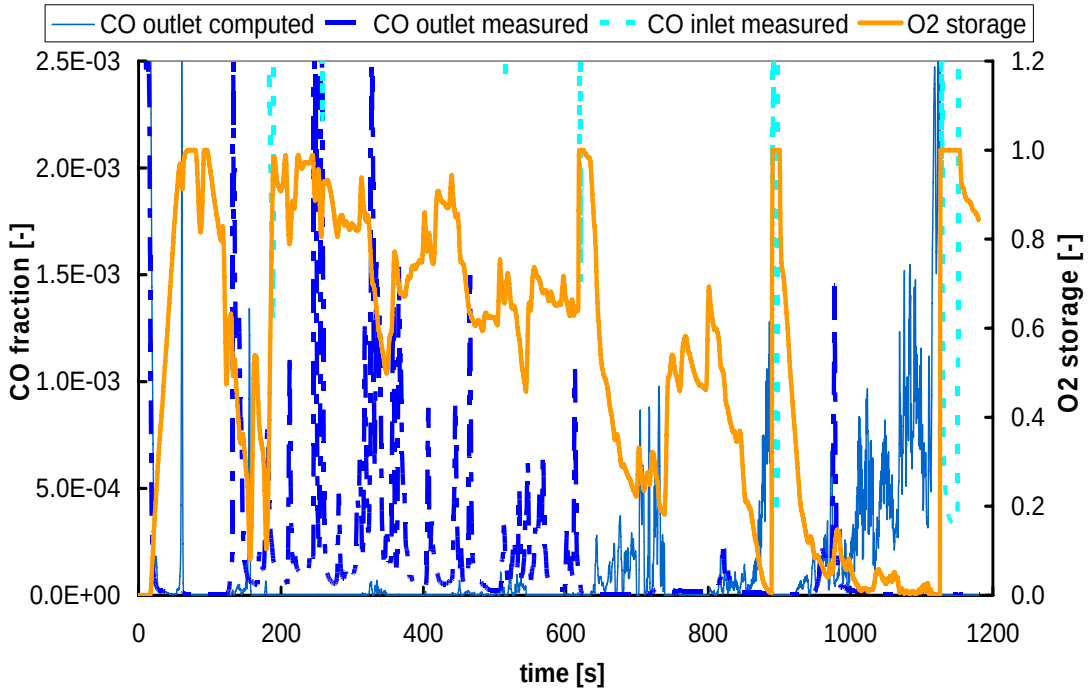

Figure 95 Computed and measured instantaneous CO emissions of the 900cpsi - 70g/ft^3 Pd:Rh catalyst

The extension of the results according to the findings from chapter 5 can be considered successful. The model shows the same behavior as shown in Figure 95, Figure 96 and Figure 97. The CO and THC rapid light-off are matched in a certain accuracy, while the matching of the model during the warm operation follows the discussions made for the rest of the cases. It has no further meaning to discuss in detail the results of this case. The main finding to underline is the successful use of the trend for the precious metal loading found in the previous chapter.

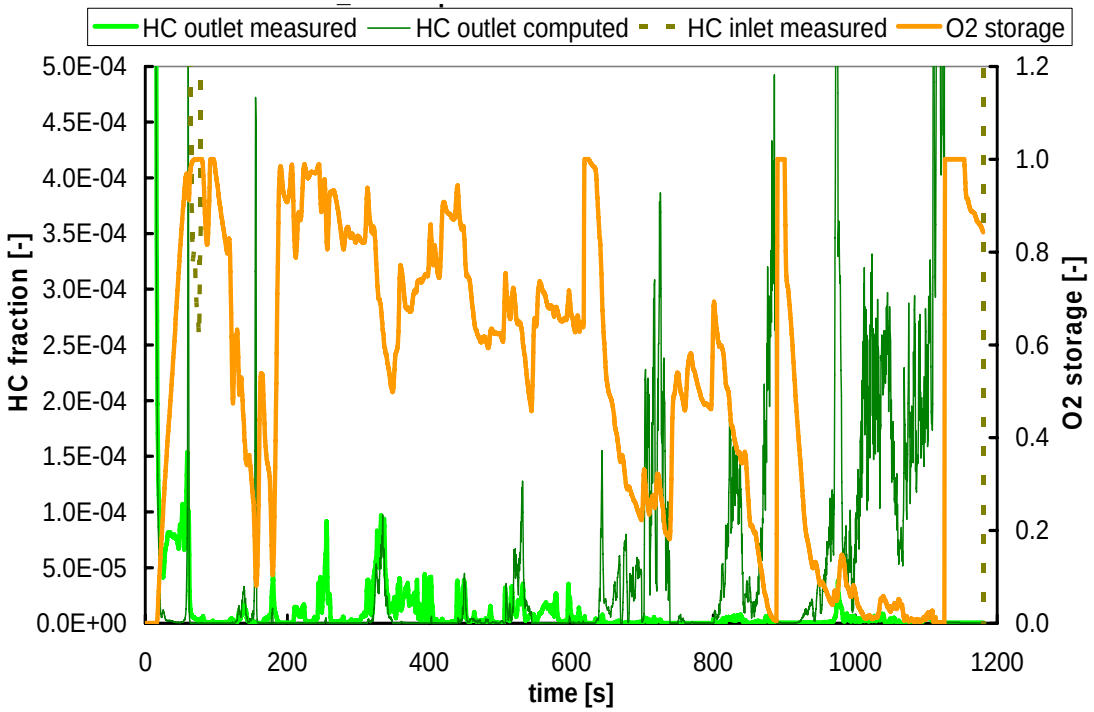

Figure 96 Computed and measured instantaneous THC emissions of the 900cpsi - 70g/ft^3 Pd:Rh catalyst

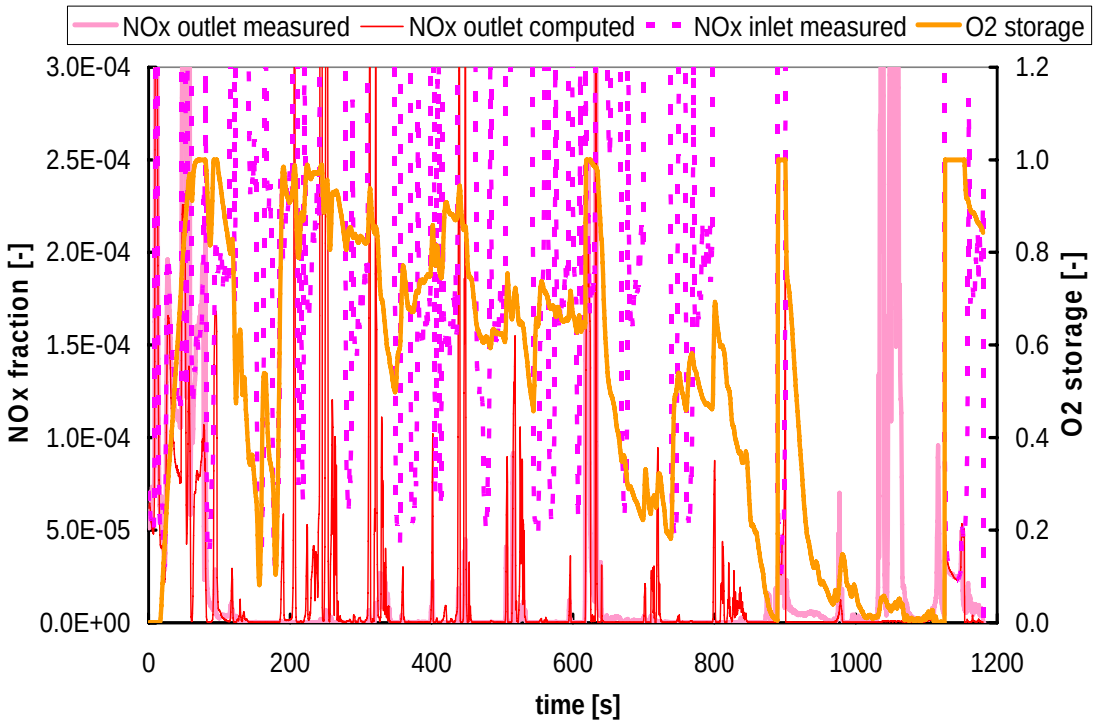

Figure 97 Computed and measured instantaneous NOx emissions of the 900cpsi - 70g/ft^3 Pd:Rh catalyst

6.6 Concluding Remarks

The model was tuned to fit the behavior of five, layered Pd:Rh catalytic converters with variable channel density. A simplified reaction scheme was employed, consisting of eight reactions with three tunable parameters.

Although the results are not as accurate as those of the previous case, the model produces the experimentally observed trend regarding the variable channel density. As found in experimental results, the performance of 900 and 1200 cpsi is quite similar, although 1200cpsi has higher manufacturing cost and significant negative impact at exhaust backpressure.

The light-off period has a major role to the overall performance. The light-off moment is depended primarily by the thermal inertia of the washcoated monolith.

The inability of the model to fit accurately the total cycle operation is attributed partially to the low quality of the experimental data. The low quality of the experimental data is addressed to the calculation of lambda and oxygen content in exhaust gas by the signals of the rest of analysers and the low acquisition rate

In order to fit the rapid light-off the double layered technology of the washcoat was modeled as a two bed catalytic converter. CO and THC oxidation function only and low thermal mass feature the first bed. This assumption greatly improved the overall results but was not able to accurately predict the light-off. The failure is attributed to flow distribution phenomena and 3-D effects that cannot be predicted by the 1-D model used.

It has to be noted here that the quality of the experimental data is significantly lower to the other cases of this study. A major problem of these datasets is the 1Hz acquisition rate that hinders good phasing of the datasets especially during the transient phases, considering the different analysers' responses. This is believed to affect the quality of modeling results compared to the respective ones from Chapter 5.

CHAPTER 7

CASE STUDY: VARIABLE PRECIOUS METAL RATIO (Pt/Pd/Rh CATALYSTS)

This chapter presents a parametric study of precious metal loading versus channel density. It is well known that both these design parameters enhance catalytic activity as has been already presented in chapters 1, 5 and 6. The object here is to model the cases according to the rules extracted from chapters 3, 5 and 6 and extract some trends for the additional effect of the type and ratio of the catalysts used. The experimental data come from a 4.6 l spark ignition engine, designed for EURO 3 emissions limits and fitted with a close coupled ceramic monolithic catalytic converter of 0.8 l. Again, the exact washcoat formulation of the three-way catalytic converter is not disclosed. The data was preprocessed and quality assured as described already in chapter 3 and the engine management was identified and discussed in chapter 4. In the latter case it was shown that management is tailored to assist engine operation at slightly rich regime, using very tight lambda control. This reduces the role of oxygen storage in the washcoat. The catalytic converters are modeled using a proper reaction scheme selected according to the discussion of chapter 1 and the tunable parameters of the model are estimated according to the methodology developed in chapter 2.

7 CASE STUDY: VARIABLE PRECIOUS METAL RATIO

7.1 OVERVIEW OF THE CASE

This chapter deals with advanced trimetallic washcoat formulations. Traditionally, the trimetallic formulations are applied to double layer washcoats, in order to take advantage of the catalytic activity and the special characteristics of each one formulation and avoid unwanted precious metal interactions. A common application is to use a layer with Pd-only formulation and a layer with Pt:Rh formulation. This is done in order to isolate palladium particles from rhodium ones, as they tend to create alloys with palladium covering the external surface [174]. Their relative position (top or bottom) is selected according to the desired attributes of the catalytic converter and the special characteristics of the associated engine management [168].

The catalysts studied in this chapter feature a double- layered, trimetallic three-way catalytic converter, fitted at a close coupled position on a 4.6l V8 engine that is tested according to the FTP-75 driving cycle. The exhaust line consists of two identical pieces (one per engine bank) and the engine management is tailored to assist the special operation characteristics of these converters. Specifically, the lambda control is shifted to the rich side of operation and the temperatures at the face of the converters lie in the range from 600 – 700^{o}C during hot operation, as already discussed in Chapter 4.

The layered washcoat formulation of the catalytic converters features a top layer of Pt:Rh basis and a bottom layer of Pd-only catalyst. The exact washcoat formulation, as well as the type of any promoters and stabilizers used, is unknown. For modeling purposes, it is assumed that the two layers are equivalent to a two-bed catalyst (in similar to chapter 6) that promotes different sets of reactions in each bed. In what follows, the model is tuned to fit the behavior of a reference catalytic converter (Cat#1). The resulting kinetic parameters are used, according to the findings of Chapter 5, to fit three more converters of different precious metal loading and and precious metal ratio. The data matrix of this case is shown in Table 19.

The engine management strategy plays a key role to the operation of the catalyst. The operation on the rich side with increased gas temperatures, promotes ceria to function mostly as a water-gas-shift and a steam reforming enhancer, rather

than as an oxygen storage component [52]. In this case, it is assumed that the ceria functions as a reforming enhancer rather than an oxygen storage component. This assumption was made in order to keep a simple reaction scheme. Nevertheless, runs of the model with both reforming and oxygen storage reactions has shown that the additional reactions further improve the overall conversion efficiency prediction.

Table 19 Data for the case of variable channel density catalytic converters

CASE	III			
Test Name	Cat.#1	Cat.#2	Cat.#3	Cat.#4
Vehicle	4.6l, SI, LEV			
Position	close coupled			
large axis [m]	0.12			
small axis [m]	0.08			
length [m]	0.11			
Volume [l]	0.83			
cpsi	900			
thickness nominal [mil]	2.5	2		
PML (g/ft^3)	150	170	125	
Pt	1			
Pd	13	15	10.5	
Rh	1			2
OSC	unknown (assumed 0 mol/m^{3}WC)			
Stabilisers / Promoters	Unknown			
Comments	RedOx + WGS + SR			

7.2 Study of the Experimental Data

Figure 98 to Figure 100 present cumulative emissions for CO, THC and NOx as were calculated from the test data. In this case also, the variations of the engine out data between the different tests hinder the direct assessment of experimental data. In general, the datasets are characterized by a rapid light-off for NOx emissions (almost immediately after the beginning of the test procedure) that is followed by a light-off for CO and THC at about 18s. This is a common characteristic of double layer washcoat formulations and has been discussed already in the cases of Chapter 6.

As shown in Figure 98 by the slope of the cumulative emissions after the 200th second, the CO performance during warm operation seems to be similar for all the catalysts, if we account for the existing variations of engine out data also. In general all converters seem to not have the adequate size to treat effectively the exhaust gas. Of course, they are designed as precatalysts in close coupled position and their major function is to treat cold start emissions by a rapid light-off.

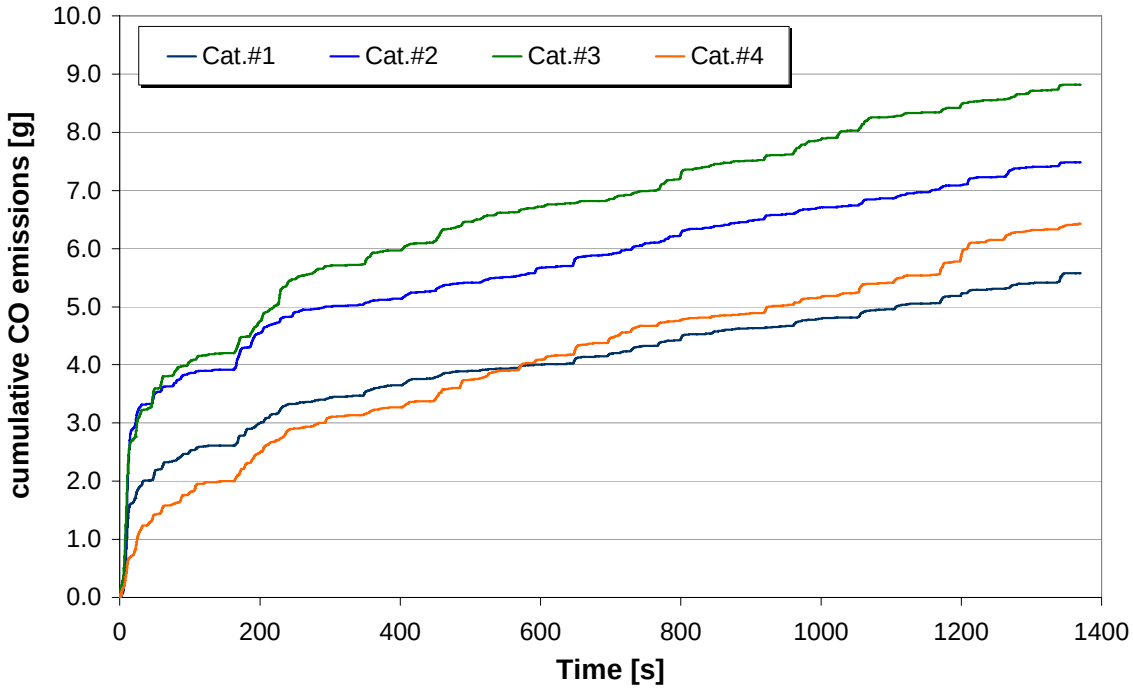

Figure 98 Comparison of measured cumulative CO emissions for the Case III catalytic converters

Figure 99 shows the cumulative emissions for THC, where there is a clear trend of conversion efficiency versus precious metal loading. Hydrocarbons are known to be oxidized over Palladium, that is the bottom layer. As shown in Figure

99 the Cat.#3 and Cat.#4 (125g/ft^3) are almost equivalent as regards as THC. In general, the behavior is very similar for all the catalysts as shown from the slope during warm operation. The differences in the THC cumulative emissions are attributed to the cold start emissions, which significantly differentiate. The unreasonably lower cold start efficiency of the catalyst with the highest precious metal loading could be attributed to the high variation found in the test data. The results indicate the existence of an optimum noble metal loading for THC conversion and any further increase has a negligible effect to the catalytic efficiency during hot operation. [34].

Between the Cat.#3 and Cat.#4 which have the same PML but different PM ratio, the Cat.#3 performs better for both THC and NOx. Of course, the differences consist of several isolated breakthroughs that could possibly be addressed to variation in test data. As shown in Figure 99 Cat.#4 is slightly worse than Cat.#3. This can be explained by the fact that a part of Pd of Cat.#3 was replaced by a part of Rh in Cat.#4. This slightly reduces THC performance but it seems to have a negligible impact to NOx performance as shown in Figure 100.

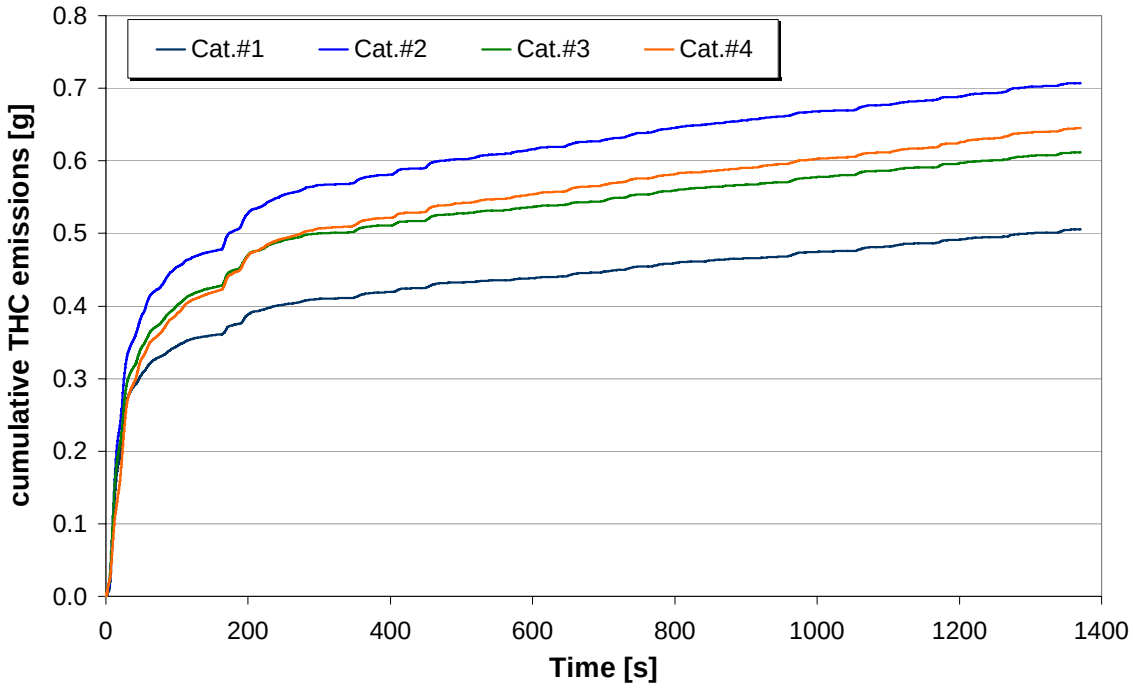

Figure 99 Comparison of measured cumulative THC emissions for the Case III catalytic converters

Figure 100 shows that the measured cumulative NOx emissions also follow a trend regarding the precious metal loading. Especially the Cat.#4 that has a higher Rh content than the rest of the catalytic converters does not show an improved conversion efficiency for the NOx as would be expected. Cat.#2 appears to have worse conversion efficiency than the Cat.#1 which has lower precious metal loading. This can be attributed either to the already discussed variation in test data, or to particle coagulation during aging due to low Rh content in the washcoat [88].

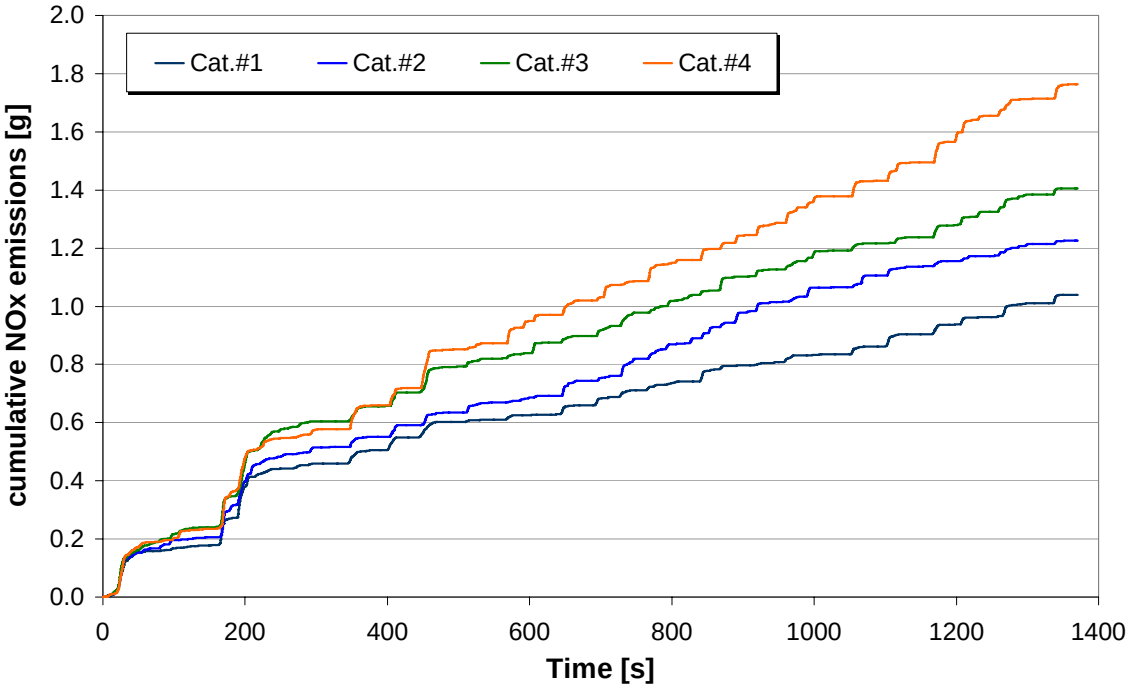

Figure 100 Comparison of measured cumulative NOx emissions for the Case III catalytic converters

7.3 TUNING OF THE REFERENCE CATALYST

All catalysts use a Pt:Rh formulation at 1:1 ratio for the washcoat top layer that is assumed to treat the NOx emissions. This stands, if we account that this ratio practically diminishes the oxidation function of this alloy when compared to its reduction function. The bottom layer of Pd-only formulation is used as a common three-way catalytic converter with enhanced light-off characteristics for CO and THC and reduced performance for NOx.

Several attempts to model the cases of this chapter with a typical three-way catalytic converter reaction scheme, similar to the one used in chapters 5 and 6, failed. It was decided to extend the reaction scheme with the reforming reactions in order to fit the behavior of the specific catalytic converters.

Table 20 Reaction scheme and kinetic parameters

Bed		Reaction	log A	E
1	1	$CO + NO \longrightarrow CO_2 + \frac{1}{2} N_2$	15	95000
2	1	$CO + \frac{1}{2} O_2 \rightarrow CO_2$	12.5	90000
	2	$H_2 + \frac{1}{2} O_2 \rightarrow H_2O$		
	3	$C_aH_b + \left(a + \frac{b}{4}\right) O_2 \rightarrow aCO_2 + \frac{b}{2} H_2O$		
	4	$CO + NO \longrightarrow CO_2 + \frac{1}{2} N_2$	11.3	95000
	5	$CO + H_2O \longrightarrow CO_2 + H_2$	9.35	105000
	6	$C_aH_b + aH_2O \rightarrow aCO + \left(a + \frac{b}{2}\right) H_2$		

Similar to the Chapter 6, the double layer is modeled by an equivalent system of two beds with different functions. The first bed is a short bed that accounts for the top layer with low thermal mass and NOx reduction function. A second, larger bed is used to model the bottom layer. The reaction scheme that is selected in this case features a single reaction for the first layer and five reactions for the bottom layer with three tunable parameters at a total. It is assumed that the values of activation energies for the water-gas-shift and steam-reforming reactions are 105000 J/kmol, a

value between Palladium and Ceria apparent activation energies selected in this thesis.

The CO/NO reaction of the first bed is manually tuned to fit the rapid light-off. The rest of the kinetic parameters are estimated by GenOpt. The reaction scheme along with the results of the tuning is shown in Table 20.

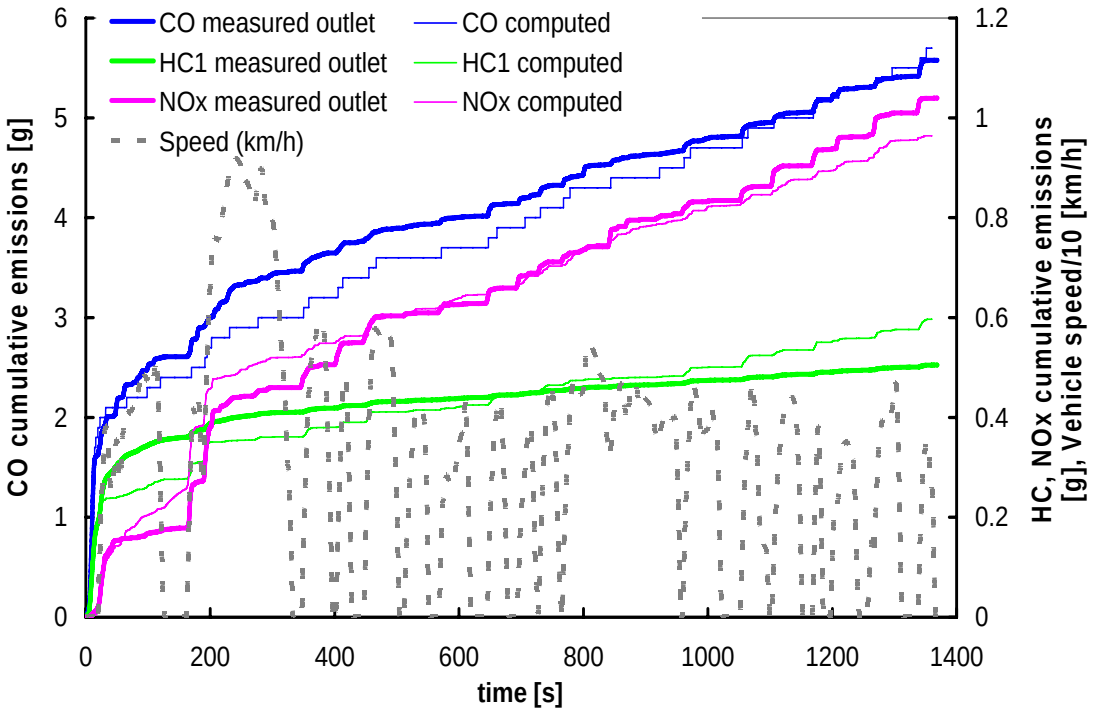

Figure 101 Computed and measured cumulative emissions of the 1:13:1 Pt:Pd:Rh catalyst

A comparison of computed and the measured cumulative emissions for the Cat.#1 is presented in Figure 101. The model shows a good fit both for CO, THC and NOx. The cold start period (up to 190s) is matched quite well for CO and THC, while for NOx only the overall behavior is predicted. The model predicts also the warm operation phase accurately, for CO and NOx while it is inferior regarding the THC. The most important is the prediction of the breakthrough for all pollutants at about 200 s and the change in the slope of the curves after that point (compared to almost 100% efficiency predicted for a short period just before 200s).

As shown in Figure 102 and in Figure 103, which present the instantaneous emissions for CO and THC, the fast light-off at about 18s from the beginning of the test is accurately predicted. The THC instantaneous emissions of the model output show a "sharp" behavior during warm operation but this is of minor importance

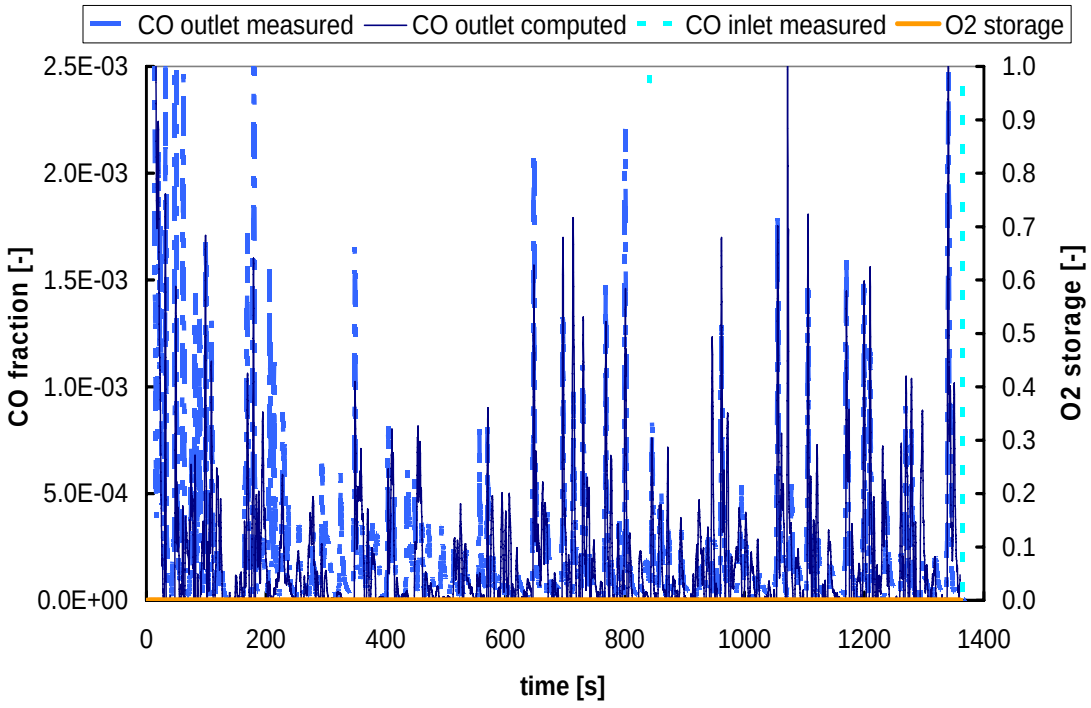

Figure 102 Computed and measured instantaneous CO emissions of the 1:13:1 Pt:Pd:Rh catalyst

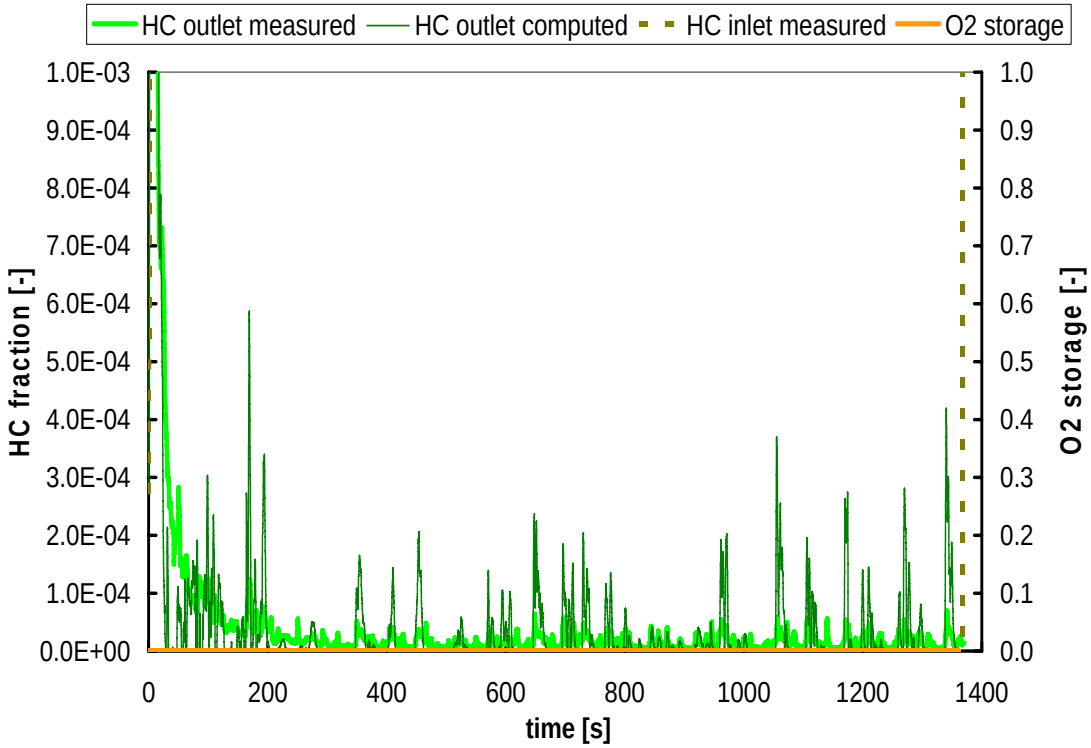

Figure 103 Computed and measured instantaneous THC emissions of the 1:13:1 Pt:Pd:Rh catalyst

considering that the catalyst operates near 99% efficiency. An explanation to this can be given by the fact that we assume only one hydrocarbon specie instead of the

thousands that exist in exhaust gas. The results are not significantly improved even if we use two or even three hypothetical species of hydrocarbons. Nevertheless, the overall behavior of hydrocarbons is adequately matched for the specific catalytic converter.

Figure 104 presents the computed and measured instantaneous NOx emissions. An accurate prediction of the converter's NOx reduction function can be seen. The behavior of the instantaneous emissions is outlined, although in some cases, for example during 150-180s, the model fails to match the instantaneous emissions. In general, during the warm operation the NOx emissions are accurately predicted and the good estimation of NOx breakthroughs is remarkable.

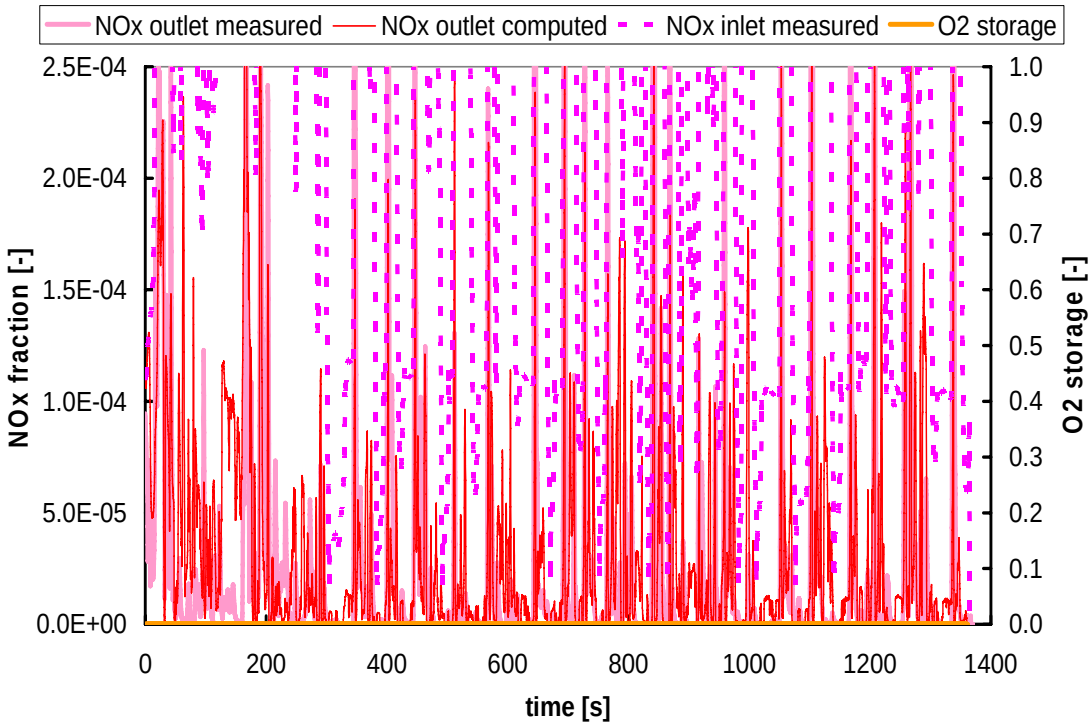

Figure 104 Computed and measured NOx instantaneous emissions of the 1:13:1 Pt:Pd:Rh catalyst

The assumption of the two beds to model the double layer technology successfully matches the rapid light-off in the beginning of the test, as shown in Figure 105. The model fails to predict the instantaneous conversion efficiency exactly at the beginning of the test but this is reasonable considering that the inlet temperature of the input data during the first 8s is lower than 200^{o}C (a typical threshold for the light-off of three way catalysis reactions). The measured conversion

efficiency in the period from 0-10s can be attributed either to experimental error or to an assisting device for fast light-off, for example front face heater. Such information is not provided so we selected to model this layout with typical model input data.

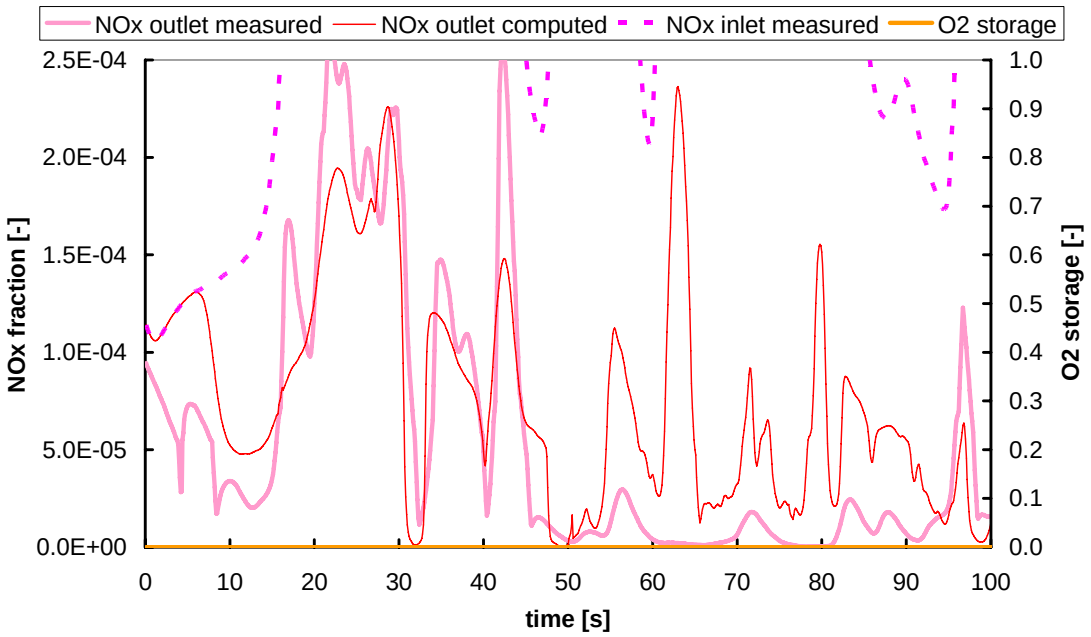

Figure 105 Computed and measured NOx instantaneous emissions of the 1:13:1 Pt:Pd:Rh catalyst during light-off

Obviously, the employment of the specific reaction scheme that uses the steam reforming and the water gas shift reaction is successful as it outlines within good accuracy the overall performance of the catalytic converter. GenOpt resulted in very low kinetic parameters at the attempts to model the catalyst behavior with oxygen storage function, even in the case that reforming reactions were excluded. The relative contribution of storage reactions was very low, a fact that strengthens the choice of the current reaction scheme.

7.4 EXTENSION TO THE OTHER CASES

The kinetic parameters that were estimated from GenOpt for the case Cat.#1 are extended to fit the cases Cat.#2, Cat.#3 and Cat.#4. The data is implemented according to the findings of Chapter 5. Specifically for each case, the loading of each precious metal is calculated and the kinetics are adjusted respectively. This is made in order to include the effect of the different precious metal ratio that was discussed in section 6.2.

For example, the Cat.#3 and the Cat.#4 that have a 125g/ft³ precious metal loading but different precious metal ratio should be considered as follows. In total, the catalytic converters have N parts of precious metal

$$N = Pt_{parts} + Pd_{parts} + Rh_{parts}$$

that is for each catalyst

$$N_{cat\#3} = 1 + 10.5 + 1 = 12.5$$
$$N_{cat\#4} = 1 + 10.5 + 2 = 13.5$$

or 10g/ft³ per part of precious metal for the Cat.#3 and 9.26g/ft³ per part of precious metal for the Cat.#4. As regards CO/NO reaction over Rh it is considered in the case of Cat.#3 a value of 10g/ft³ and a value of 18.5g/ft³ for the Cat.#4 to be used in the equation (see also chapter 5).

Table 21 Kinetic parameters used for the cases

	Cat.#1	Cat.#2	Cat.#3	Cat.#4
PML [g/ft³]	150	170	125	125
A_Ox	12.5	12.6	12.35	12.35
A_Red	11.3	11.4	11.15	11.35
A_SR_WGS	9.5	9.45	9.25	9.25

Figure 106, Figure 107 and Figure 108 show a comparison between measured and computed cumulative emissions for the cases of Cat.#2, Cat.#3 and Cat.#4 respectively. The model matches quite well the behavior of all the converters although it was not tuned separately for each case. Of course, the differences between the experiments and the washcoat characteristics after ageing introduce remarkable uncertainties. The kinetic data found for the first catalytic converter

seems to be robust enough to overcome these issues and fit the behavior of the rest of the catalytic converters within a certain good accuracy.

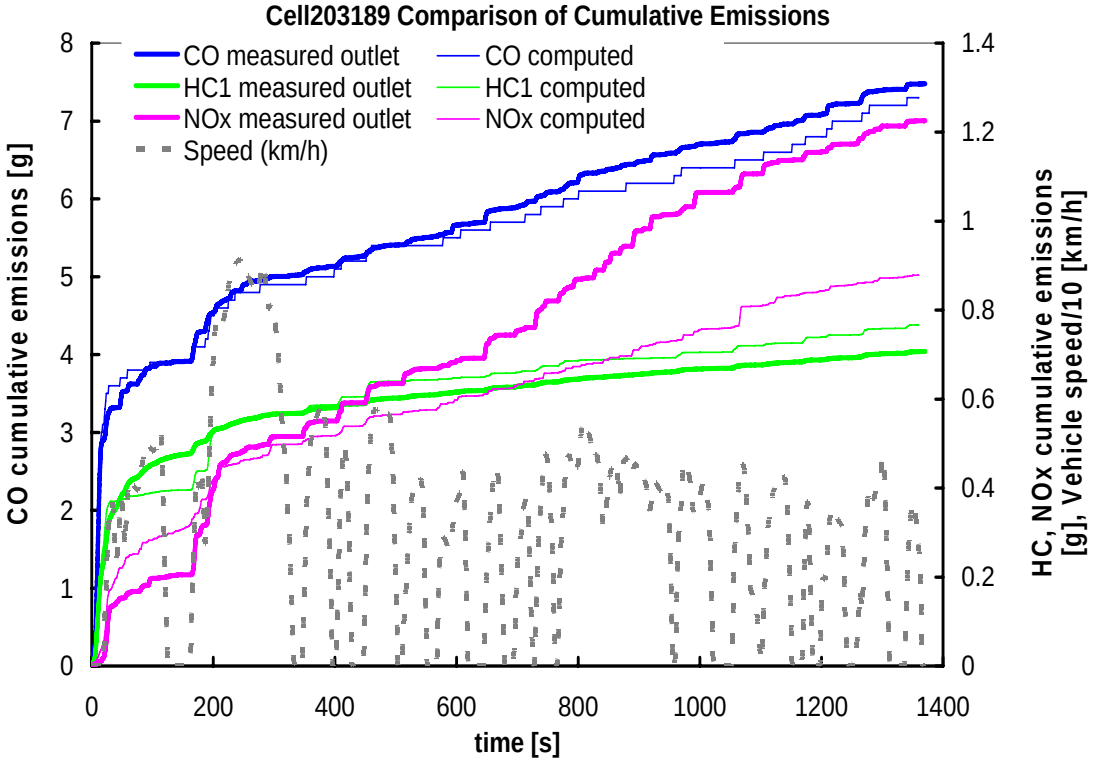

Figure 106 Computed and measured cumulative emissions of the 1:15:1 Pt:Pd:Rh catalyst.

Figure 106 shows the comparison of computed and measured results for the case of Cat.#2. The model predicts quite well the behavior of CO and THC emissions. Especially for THC the model shows an increased efficiency during the first 200s that is possibly attributed to the THC speciation, in similar to the Cat.#1 case. It is also underestimates the measured conversion efficiency of the single THC breakthrough at 200s but this of minor importance as it matches accurately the rest of the warm operation. The model fails to predict the NOx behavior quantitatively but is sensitive to the small NOx breakthrough and outlines the overall behavior. Despite this fact the model output is reasonable if we consider the significantly higher precious metal level. The experimental data show an irregular behavior during 700-950s that could be attributed to the specific experiment.

Figure 107 represents a very similar behavior for the Cat.#3. As regards THC, the model matches accurately the behavior up to 200s. The period after 200s is characterized for THC by several overestimated breakthroughs that can be attributed

to the oxygen storage. This behavior is observed in CO emissions also. Apparently, the ceria processes of this catalyst are more active, a fact than can be attributed to different ageing of the specific catalyst. The NOx emissions are outlined quite well but they are not predicted qualitatively because of some isolated breakthroughs.

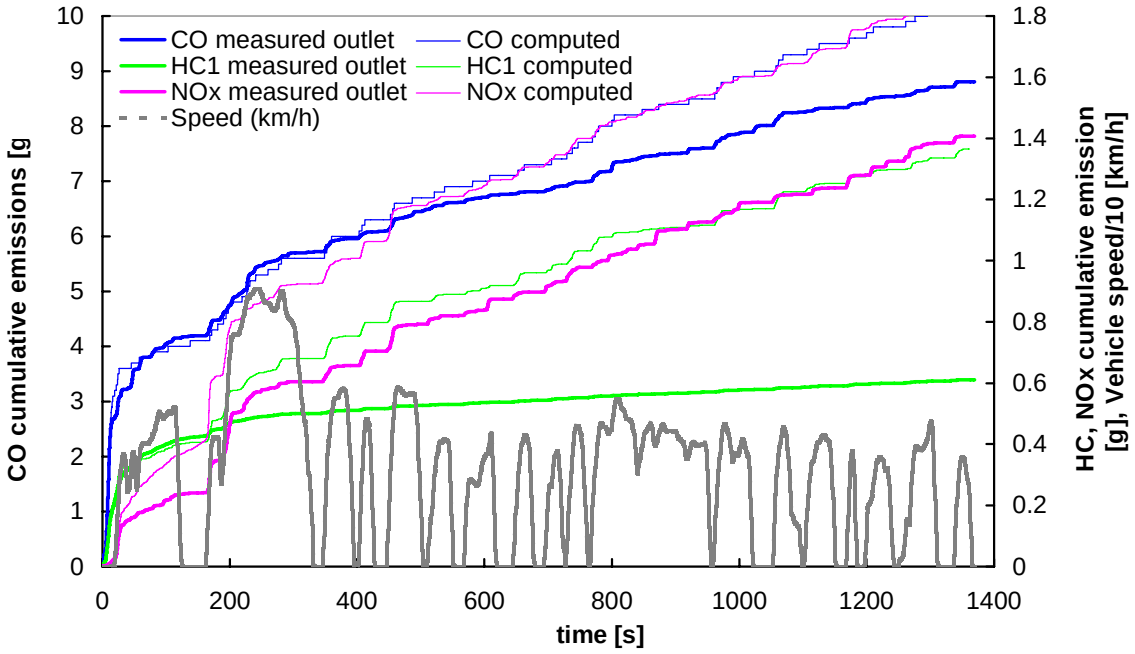

Figure 107 Computed and measured cumulative emissions of the 1:10.5:1 Pt:Pd:Rh catalyst.

Figure 108 represents a very similar behavior to the rest of the cases for CO and THC. The cumulative emissions of these species are outlined very well. NOx curve is not fitted so well by this specific set of kinetics. It seems that the extra loading of Rh has practically no effect. This fact can be attributed to reasons related to the washcoat aging procedure or manufacturing process that cannot be predicted by this model. Of course, in order to extract a secure conclusion about the effect of this change we need an extensive study over a statistically sufficient sample size.

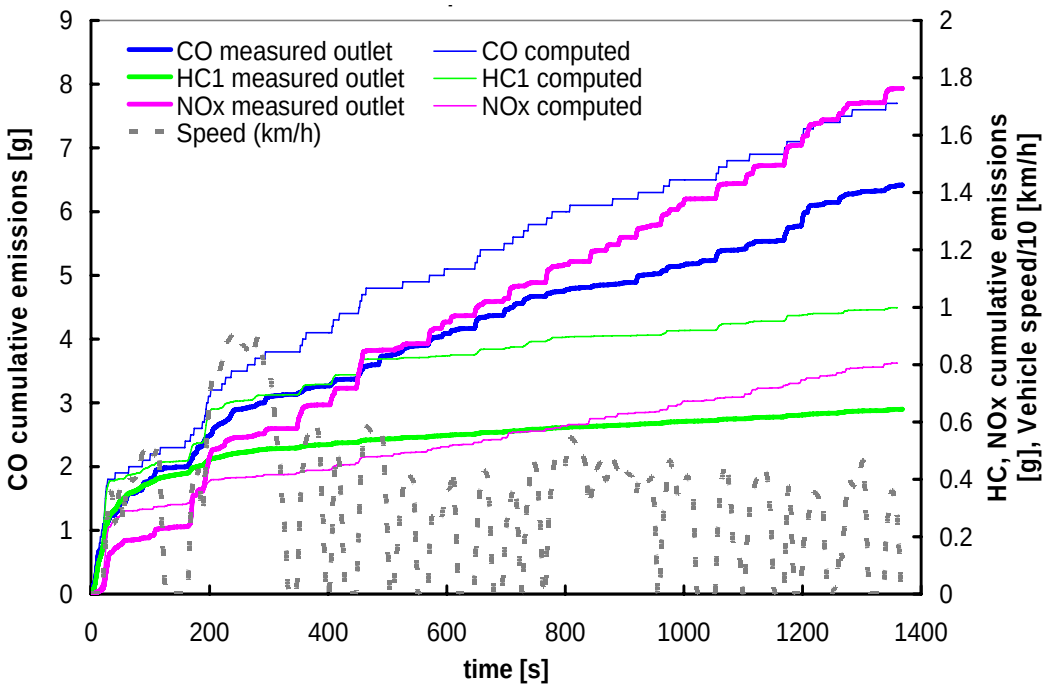

Figure 108 Computed and measured cumulative emissions of the 1:10.5:2 Pt:Pd:Rh catalyst.

The successful use of the tuned data to the rest of the cases implies that the selected approach for the modelling of the precious metal ratio is a valid one. Of course, we must always have in mind that the comparison between the measured and the computed results is subject to reasonable uncertainties that have to do either with the experimental procedure or the pre-treatment of the specific catalytic converter under study.

7.5 Concluding Remarks

The model fits well all the cases following the trend for relative PML extracted from chapter 5. It was demonstrated once more that the simplified approach adopted in the current thesis is flexible and applicable over a significant range of cases. Of course, the modeling results must be carefully considered in the design process and the need remains for further evaluation over a statistically sufficient sample size. This case study led to the following conclusions:

- The equivalent application of the two bed approach instead of a double layer washcoat was successfully used also in this case. Of course, we must keep in mind that this is just a simplification and that extension of the model to predict double layer washcoat is expected to improve the results.
- A different reaction scheme featuring water gas shift and steam reforming reactions was used in this case. This was indicated by the analysis of the engine management and was checked by runs of the model with a traditional reaction scheme. In order to not add more complexity the storage reactions on ceria were neglected.
- It was shown that the effect of the different precious metal ratio can be estimated, up to a certain extent, by proper calculations regarding the precious metal content of each catalyst.

CHAPTER 8

CASE STUDY: MODELLING AN ADVANCED EXHAUST SYSTEM FOR LEAN BURN APPLICATIONS

This chapter presents a study of an advanced aftertreatment system for a lean burn SI engine. A 0.8 litre pre-catalyst is located in a close coupled position, in orders to activate itself in a timely manner to treat the CO and HC and a 3 litre catalyst located under the floor of the car ensures an NOx storage and release function and a traditional three-way function. The three cases presented here vary according to the selected engine management strategy. The objective is to define the best engine management strategy for optimum performance of the entire system. The test data come from a 2.0 l spark ignition engine, designed for EURO 4 emissions limits and using an advanced management identified and discussed in chapter 4. The aftertreatment devices are modeled using a proper reaction scheme selected according to the discussion of chapter 1. The tunable parameters of the model are estimated according to the methodology developed in chapter 2.

8 MODELING OF A NOX TRAP SYSTEM

8.1 OVERVIEW

The exhaust aftertreatment system under study consists of a 0.8 l three-way pre-catalyst located in the vicinity of the exhaust manifold, whose purpose is to activate itself in a timely manner to treat the CO and HC. Another 3 l catalyst located under the floor of the car ensures an NOx storage and release function and a traditional three-way function. The storage function of the catalyst is supplied by a salt derived from the Barium alkali-earth metal that has a specific chemical affinity for nitrogen oxides.

The active coating of the catalyst contains platinum, palladium and rhodium, as well as barium salts. When the engine operates in lean mode, the nitrogen oxides, fully oxidized to nitrogen dioxide (NO_2) on the platinum, are stored in the form of nitrates on the barium-based materials.

Periodically, on the average for three seconds every minute, the NOx collected by the catalyst is released by briefly shifting the combustion mixture to rich. This operation increases the concentration of CO and HC that act as reducing agents. The nitrogen oxides are then released and chemically reduced into nitrogen (N_2) on the rhodium.

This storage – release sequence is controlled by the engine management system. It takes place in two stages, that are unnoticeable to the car driver :

- The engine management system evaluates the saturation state of the storage – release catalyst on a permanent basis. It activates the release of nitrogen oxides (by increasing the richness of the mixture) when the barium salt is saturated.
- When a variation of the oxygen content is detected, corresponding to the moment when all the nitrogen oxides were treated by the surplus CO and HC, the engine management system changes the engine operation, to return to stratified charge combustion with a lean mixture. The catalyst can then return to its normal NO_x storage mode.

The good knowledge of the filling level of the storage component is essential to the good operation of the system, because the NOx "conversion" rate is inversely proportional to the filling level. A number of patents has been issued that intend to contribute solutions to this important problem [176]

The treatment of the nitrogen oxides in lean mixture depends on the temperature of the exhaust gases. Beyond 500°C the efficiency of the nitrogen oxide storage – release catalyst is strongly reduced. Therefore, the catalyst was placed within the exhaust line at a position that ensures a temperature range from 300 °C to 450 °C, a window that corresponds to urban driving and during which the system treats more than 90% of the nitrogen oxides. Therefore, the control of urban pollution is especially well taken into account. On the road, when the temperature exceeds 500 °C, the engine management increases the richness of the mixture, which makes it possible to return to an exhaust gas composition that is treated by the traditional three-way catalyst.

Table 22 Data for the case of lean burn application

CASE	IV	
Test Name	Cat. #1 (3WCC)	Cat. #2 (NOx Trap)
Vehicle Engine	2.0 l, SI, EU-IV	
Position	Close Coupled	
large axis [m]	0.11	
small axis [m]	0.11	
length [m]	0.11	0.30
Volume [l]	1.00	3.00
cpsi	400	600
thickness nominal [mil]	6.5	3.5
PML (g/ft^3)	100	70
Pt	0	9
Pd	14	5
Rh	1	1
OSC / NOSC	unknown (estimated 600 mol/m^3WC)	unknown (estimated 200 mol/m^3WC)
Stabilisers / Promoters	Unknown	
Comments		

In this case, two different engine management strategies are followed. Both strategies start with a stoichiometric cold start to assist fast heating of the precatalyst and at about time=150s they switch to lean operation. The first strategy operates the engine at lean conditions up to time=1030s and then it switches back to stoichiometric operation while the second strategy continues lean operation up to the end of the NEDC. The objective here is to model the operation of the entire system in order to define the best engine management strategy that ensures fast heat-up, and subsequent keeping of high NOx storage efficiency. The model output will be used to look into the salient operation characteristics of the converter. The following steps are employed in the study:

- the tuning of the three-way converter
- the tuning of the NOx trap and
- the subsequent validation of the results for the entire system.

8.2 TUNING THE MODEL TO FIT THE PRECATALYST

The first step is to tune the model to fit the three-way pre-catalyst behavior. Although the target here is to match the behavior of the NOx trap the tuning of the pre-catalyst is useful for the application of the model to the complete exhaust system that will be presented in the following.

Table 23 Data provided for the three way pre-catalyst

Volume	0.8 l
Channel density	600 cpsi
Wall thickness	4 mil
Precious metal type	Pt:Pd:Rh (trimetallic)
Precious metal loading	100g/ft^3

The information that was provided for the pre-catalyst was limited to the data shown in Table 23. It was selected to use typical dimensions that result to the given volume. The washcoat and the substrate thickness were calculated to match the value of 4mil wall thickness.

Table 24 Set of kinetics to fit the three-way precatalyst

	Reaction	logA	E
1	$CO+\frac{1}{2}O_2 \rightarrow CO_2$	10.6	90000
2	$H_2+\frac{1}{2}O_2 \rightarrow H_2O$		
3	$C_aH_b+\left(a+\frac{b}{4}\right)O_2 \rightarrow aCO_2+\frac{b}{2}H_2O$		
4	$CO+NO \longrightarrow CO_2+\frac{1}{2}N_2$	11	95000
5	$2CeO_2+CO \rightarrow Ce_2O_3+CO_2$	7	120000
6	$\left(4a+b\right)CeO_2+C_aH_b \rightarrow \left(2a+\frac{b}{2}\right)Ce_2O_3+aCO_2+\frac{b}{2}H_2O$		
7	$Ce_2O_3+\frac{1}{2}O_2 \rightarrow 2CeO_2$		
8	$Ce_2O_3+NO \rightarrow 2CeO_2+\frac{1}{2}N_2$		

As shown in Figure 109 the model fits quite well the behavior of the precatalyst. Of course there are some regions where the model does not match accurately the measured data but this is reasonable considering the quality of the dataset. The same stands for the application of the model to describe the behavior of the precatalyst in the second case. The comparison of the cumulative and measured emissions for this catalytic converter is shown in Figure 110. The two precatalysts were fitted with the same kinetic data which is close to the ones tuned for the catalysts of the Pd/Rh precatalysts cases of chapter 6 that have similar precious metal loading level. The successful application of this data is a proof of the robustness and flexibility of the model and can be easily adapted to a variety of cases with only slight adjustment of its tuning parameters.

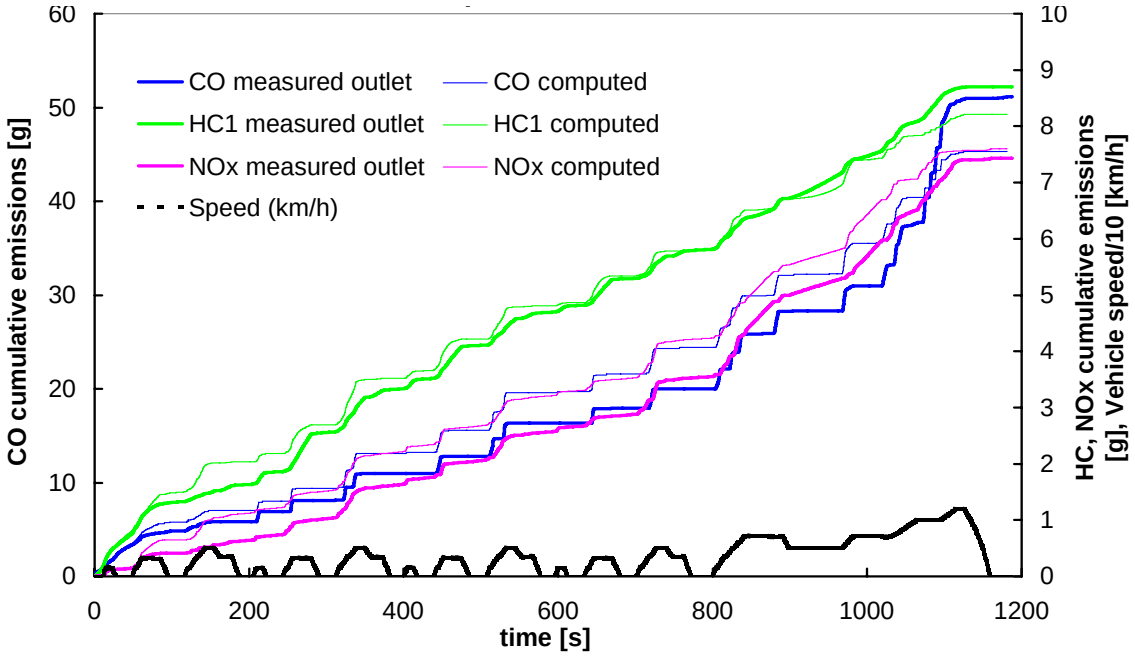

Figure 109 Computed and measured cumulative emissions of the precatalyst 1

The tuned kinetic data implies that the precatalyst has a low CO/NO reaction activity that maybe attributed to its low Rh content. Nevertheless there is no need to have a NOx reduction function considering the additional existence of the NOx trap downstream the precatalyst which is designated for this purpose.

The results of this tuning are very confident and can be easily employed to model the entire system's behavior by incorporating the model in the exhaust line both as an precatalyst and as a NOx trap as will be shown in the sequel.

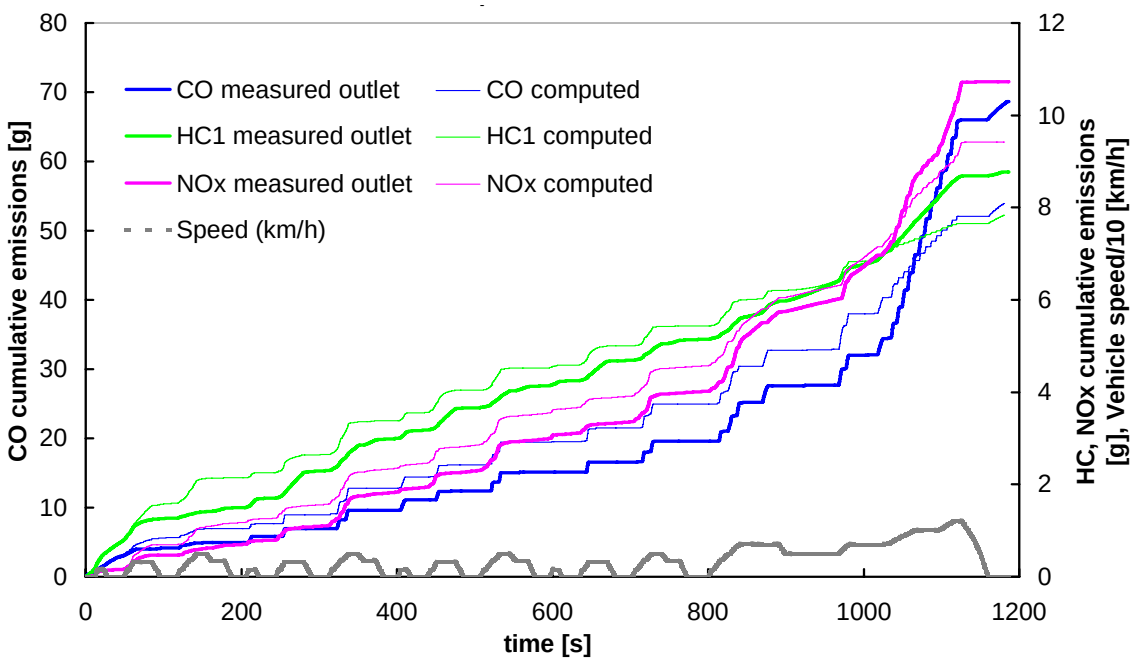

Figure 110 Computed and measured cumulative emissions of the precatalyst 2

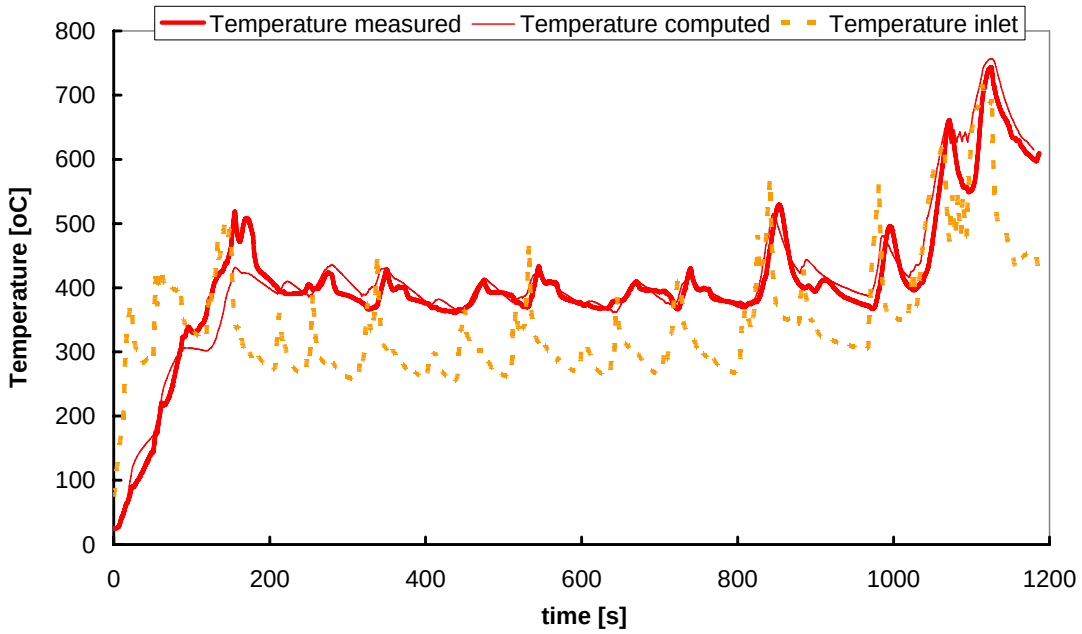

Figure 111 Computed and measured temperature comparison for the precatalyst 1

8.3 TUNING THE MODEL TO FIT THE NOX TRAP

It has already been noted in chapters 1 and 2 that the operation of a NOx trap is characterized by three regions. The first region is directly related to the catalytic activity of the Platinum particles that are used to oxidize NO to NO_2, a species that is easily adsorbed to Barium Oxides particles. The oxidation of NO to NO_2 is characterised by the thermodynamical instability of the NO_2 at temperatures higher than 300^{o}C.

The second region is related to the NOx storage processes that are modelled in a similar way to the oxygen storage processes as already discussed in Chapter 2. The NOx storage submodel comprised only three apparent reactions in order to avoid unnecessary complexity.

The third region refers to the thermal instability of the Barium nitrates that is occurring at elevated temperatures higher than 400^{o}C. At this temperature level the Barium Nitrates become thermally unstable and decompose to their components BaO and NO_2. This is modelled by a reversible storage reaction based on an apparent equilibrium between Barium oxides and Barium nitrates.

In this section we present a validation of the individual parts of the NO_x storage submodel, followed by the results of the tuning for the entire NOx storage device. Special emphasis is given to the behavior of the reversible NO oxidation over platinum and the reversible reaction of NO_2 storage and Barium Nitrates decomposition.

Figure 112 shows the computed conversion efficiency of NO oxidation to NO_2 over a very small oxidation catalyst (volume 0.1 l). The y-axis shows the ratio of NO_2 to NOx. The reaction rate becomes more susceptible to decreased levels of O_2 content in exhaust gas. The most important fact is that the model is able to predict the rate limitation due to thermal decomposition of the produced NO_2 at elevated temperatures. As shown in the figure, the decomposition becomes significant at temperatures higher than 300^{o}C.

Figure 113 presents a temperature ramp experiment to evaluate the thermal decomposition of the barium nitrates. As shown in this figure, the thermal decomposition of the barium nitrates begins at about 400^{o}C and rapidly proceeds, further increasing temperature. The NO oxidation and the thermal decomposition reactions are considered to have non-tunable kinetics, as they are primarily

dependent on temperature. The tuned values for these two reactions are shown in Table 25.

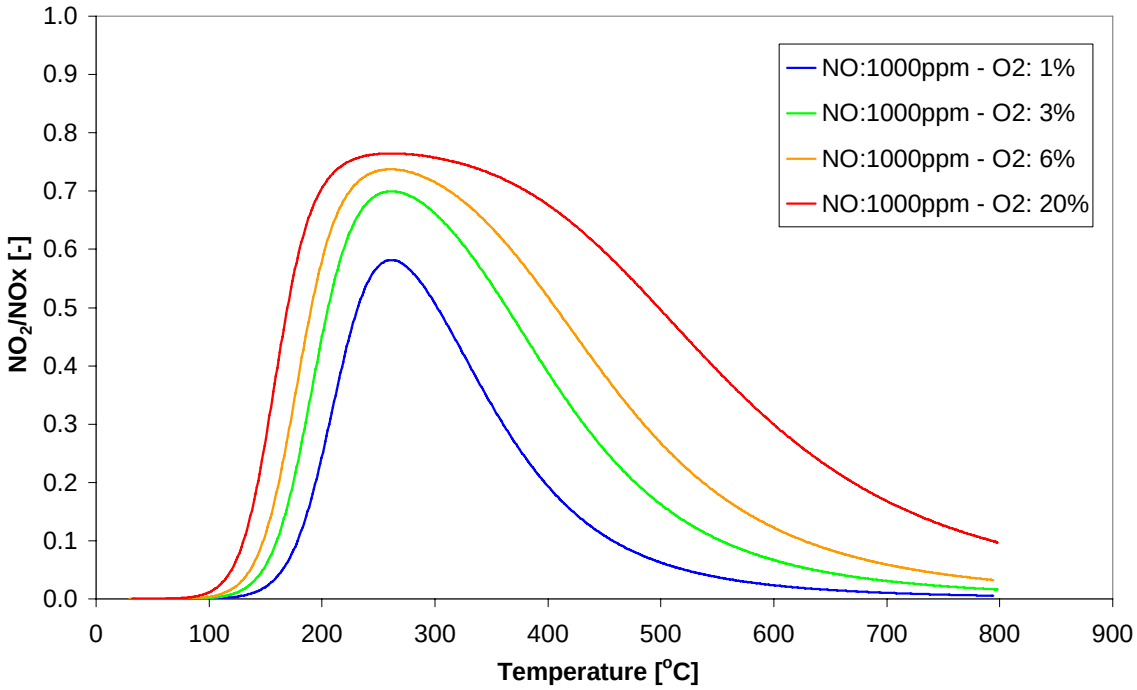

Figure 112 Temperature ramp run for the $NO+O_2 \leftrightarrow NO_2$ for different oxygen levels in exhaust gas

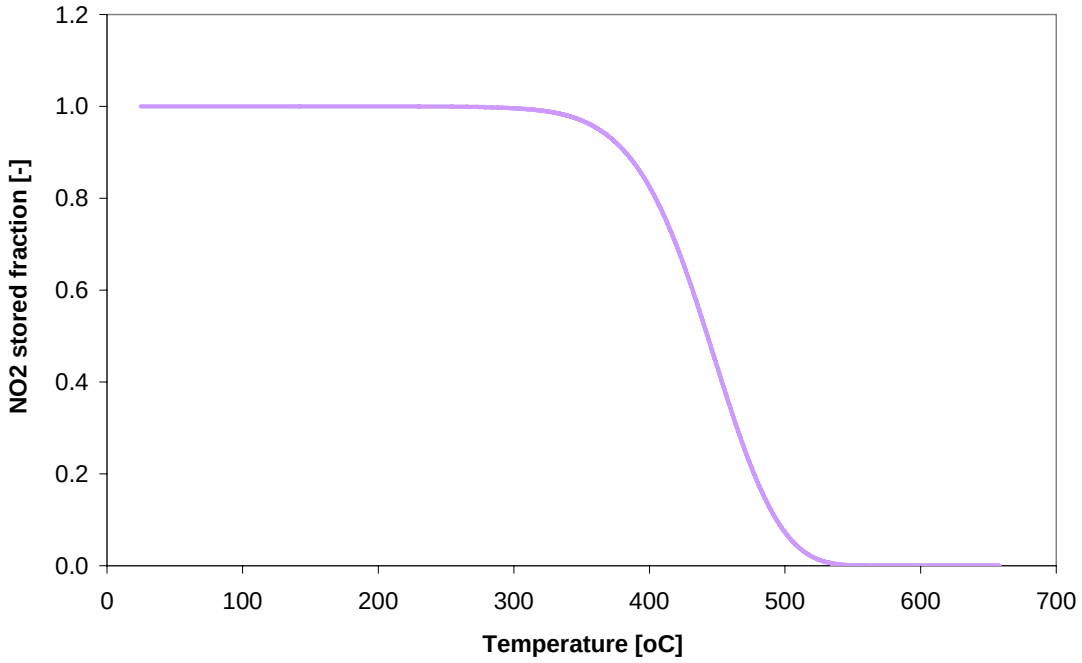

Figure 113 Temperature ramp for the thermal decomposition of barium nitrates

Table 25 Kinetic parameter for the NO←→NO_2 and the barium nitrate thermal decomposition

	logA	E
$NO + O_2 \leftrightarrow NO_2$	13.5	90000
$Ba(NO_3)_2 \rightarrow BaO + 2NO_2 + \frac{1}{2}O_2$	4	120000

The next step is the tuning of the model to fit the behavior of the NOx trap over the NEDC. The model is tuned to fit the two cases that correspond to the above-mentioned different engine management strategies. Figure 114 shows the measured and computed cumulative emissions for the first NOx trap that are observed following the switch-to-stoichiometry strategy at the end of the driving cycle. The model manages quite well CO and HC emissions except some breakthroughs during regeneration. As regards NOx emissions the model matches the cumulative data quite well except the part towards the end of the driving cycle.

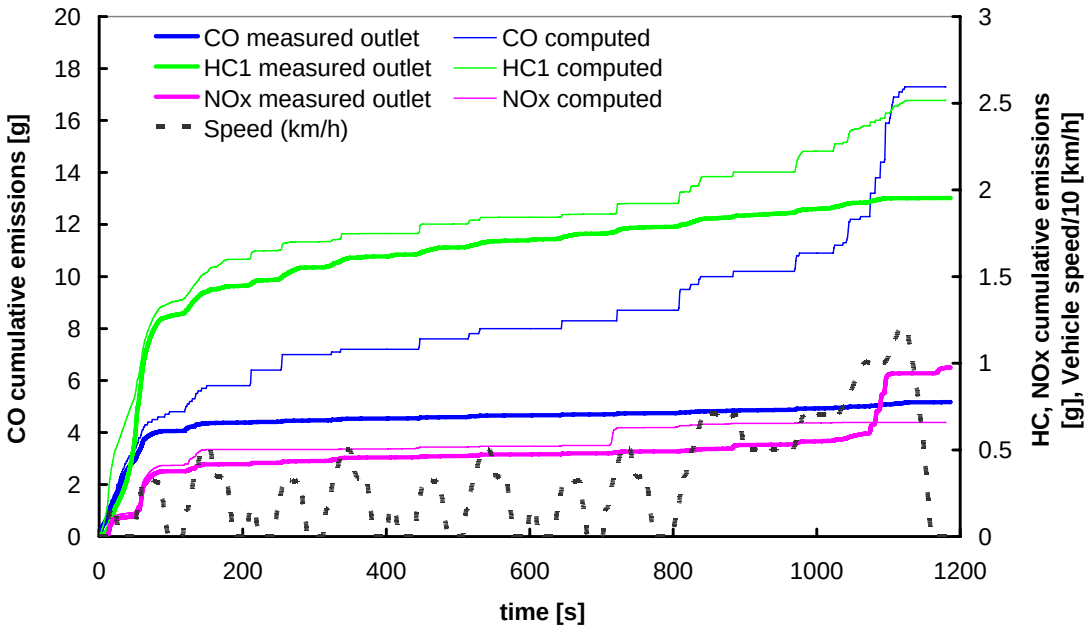

Figure 114 Computed and measured cumulative emissions of the NOx trap 1

Figure 115 presents the computed and measured instantaneous exit NOx emissios for NOx trap 1 for the period 0-600s and Figure 116 for the period 600-1200s. The model predicts accurately the cold operation of the trap during the first 150s, (where it stays practically inactive). During warm operation, the model is able

to predict the moments at which regeneration takes places but it cannot accurately determine the instantaneous emissions during regeneration. The same stands for the NOx trap 2 also. This is attributed to the instant depletion of the NOx storage under a rich pulse. The NOx that are released cannot be treated by the exhaust gas CO over Rh through the CO+NO reaction.

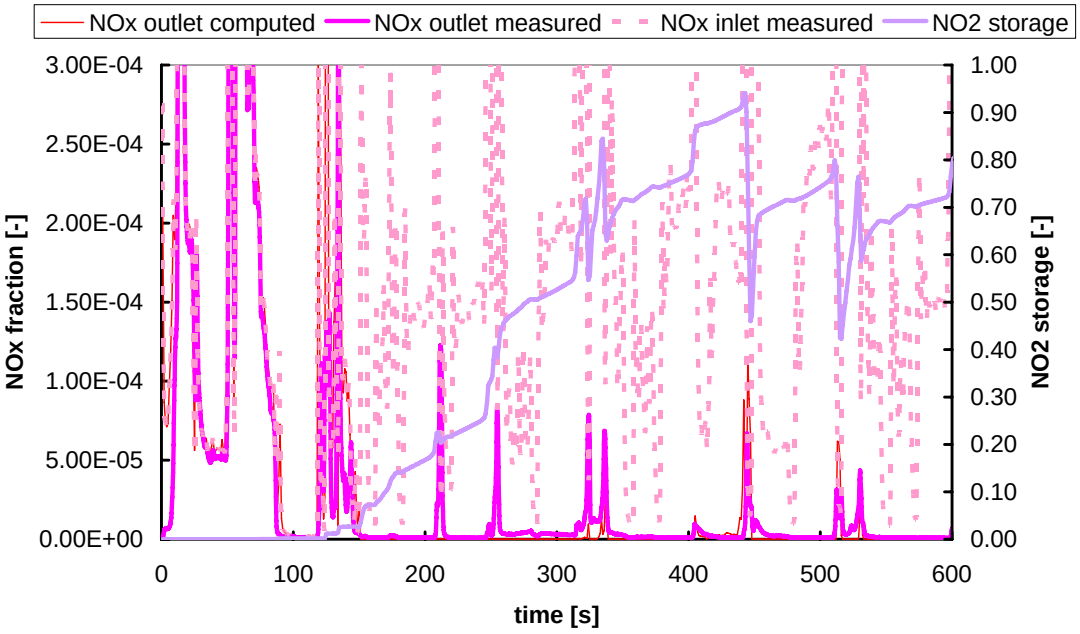

Figure 115 Computed and measured instantaneous NOx emissions (0-600s) for NOx trap 1

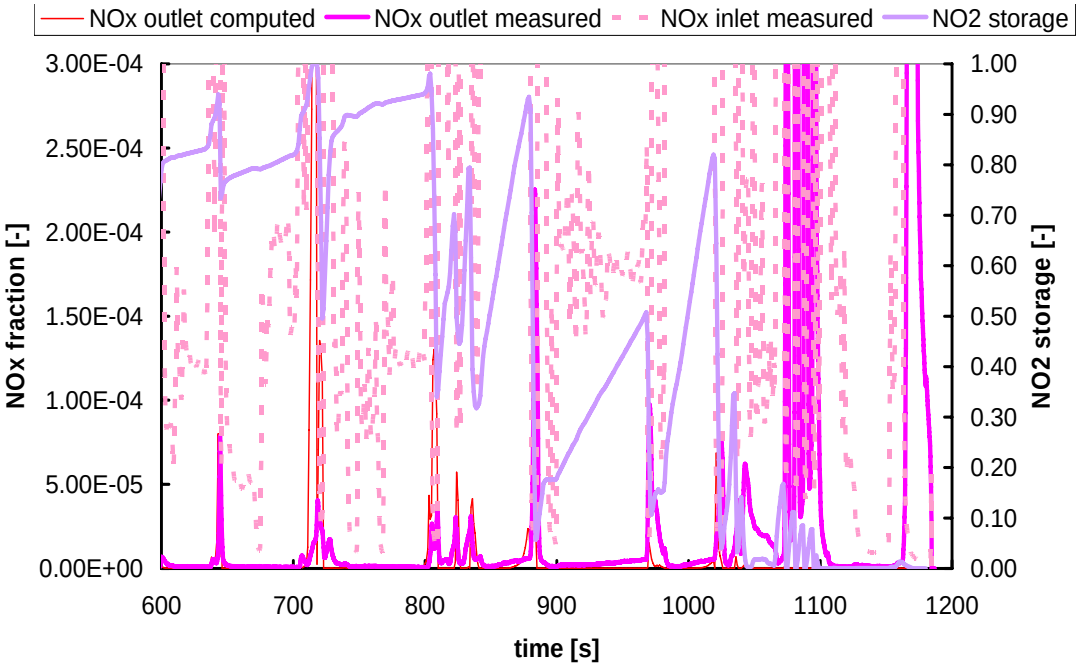

Figure 116 Computed and measured instantaneous NOx emissions (600-1200s) for NOx trap 1

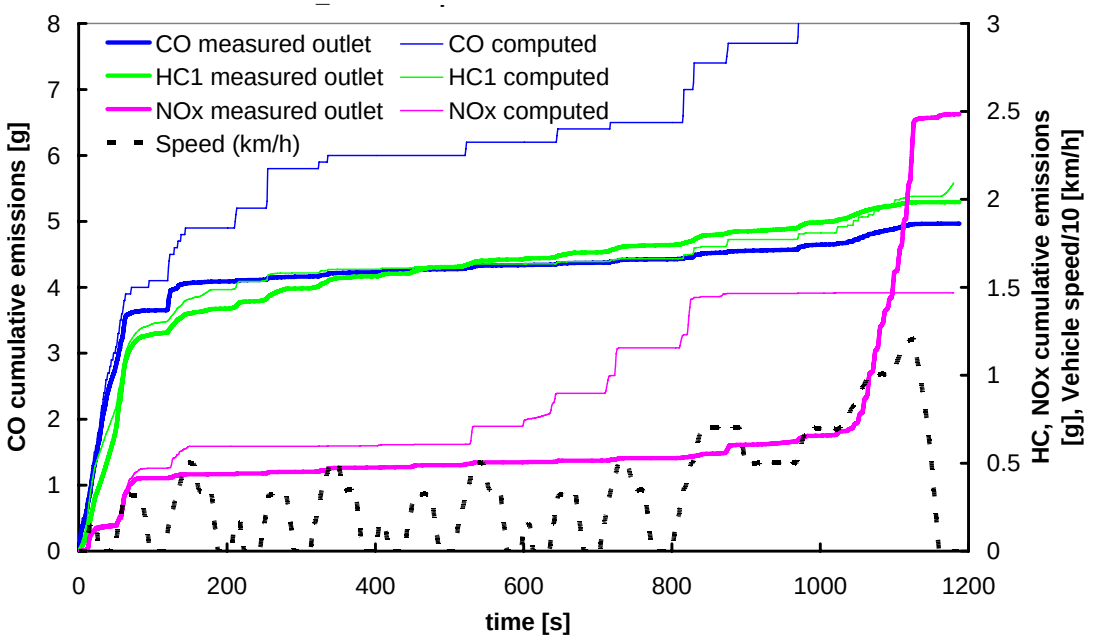

Figure 117 Computed and measured cumulative emissions of the NOx trap 2

Figure 117 shows a comparison of the measured and computed cumulative data for the NOx trap2. In respect to the first case Figure 118 and Figure 119 present the comparison of the instantaneous computed and measured NOx emissions for the second case. As regards model fit, the same observations apply as above. The model fails to predict quantitatively the NOx released during regenerations.

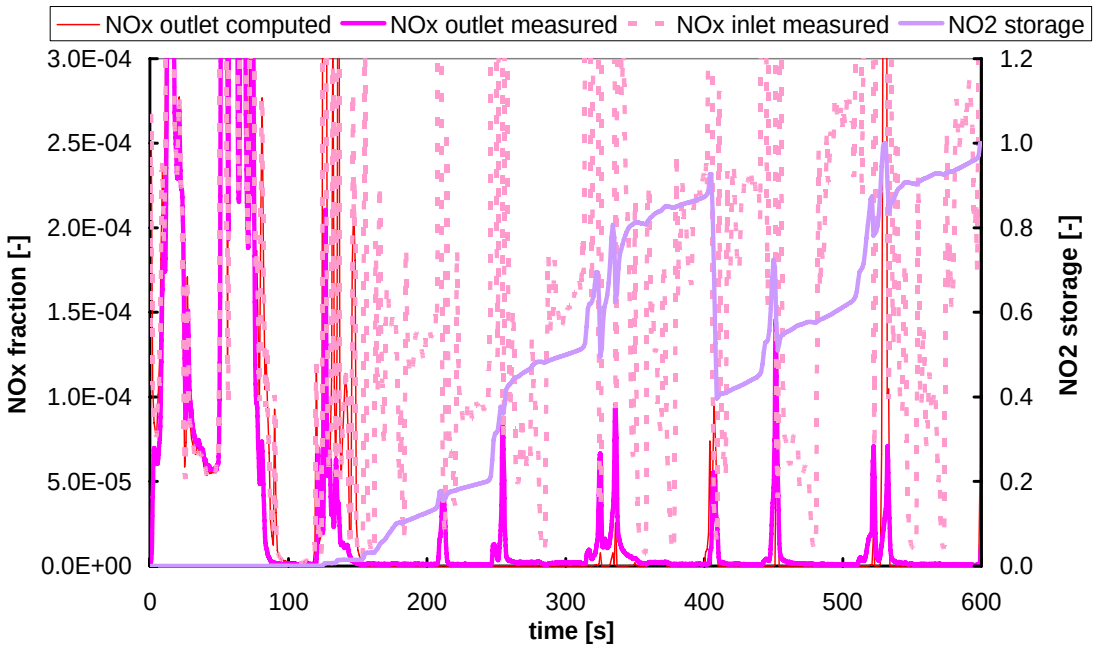

Figure 118 Computed and measured instantaneous NOx emissions (0-600s) for NOx trap 1

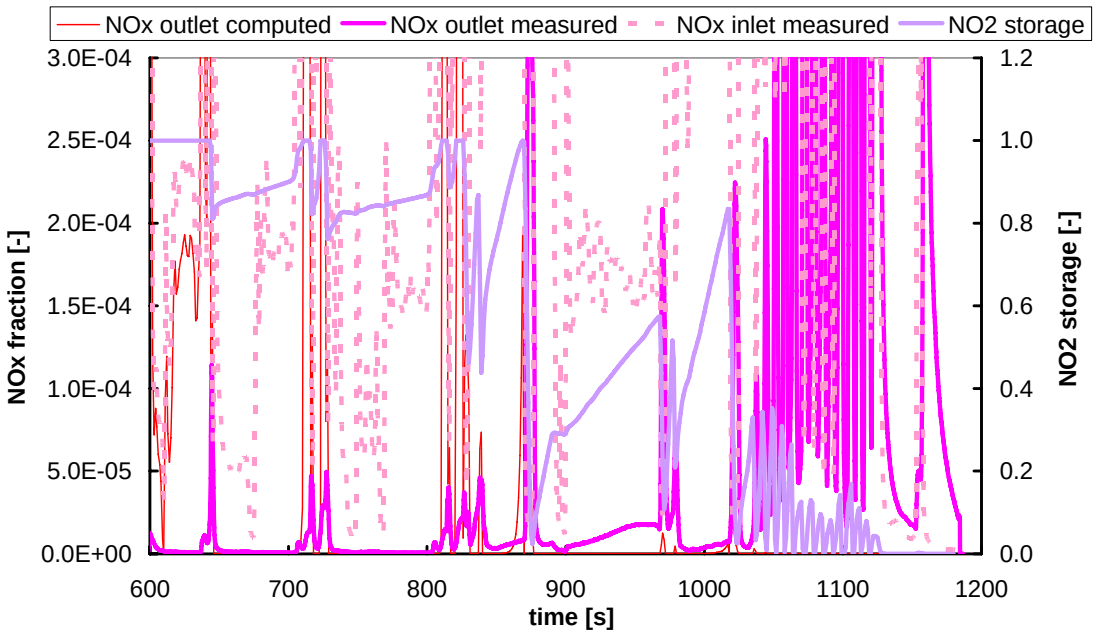

Figure 119 Computed and measured instantaneous NOx emissions (600-1200s) for NOx trap 1

Several literature models [151,177] have identified a hysteresis in the regeneration of the NOx trap and make use of an indirect mechanism to model it. The most common mechanism is that of shrinking core that assumes that the trapped NOx reacts at layers. This iis observed in our model also. The peaks during regenrartion can be vanished if the rate of the barium nitrates reduction with CO is slowed down. Figure 120 shows an example of it. On the left side are presented the results with a high regeneration rate and the respective value of NO_2 stored fraction for the front, the middle and the end of the trap. On the right hand side, the same data is presented for the case of a low regeneration rate. Obviously, the left case that has a rapid depletion of the stored NO_2 shows a sharp peak for computed NOx out emissions. The reverse situation stands for the right case where the NO_2 storage empties within a three second period.

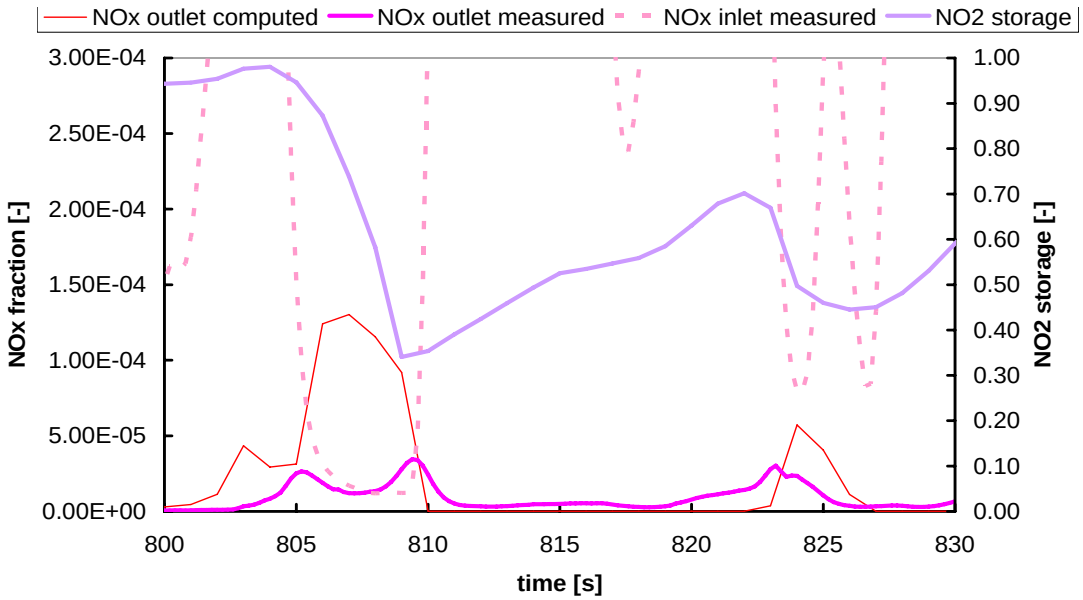

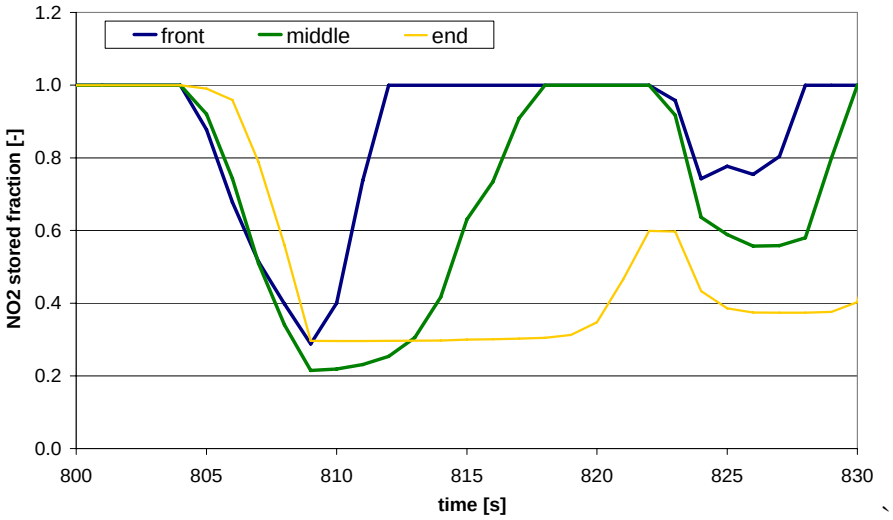

Figure 120 Comparison of a fast regeneration (right) and a slow one (left)

8.4 CONCLUDING REMARKS

- A newly developed NOx storage submodel was tested and evaluated
- The new storage submodel comprises three reactions for the trap storage and the regeneration mode and one for the NO oxidation to NO_2
- NO oxidation to NO_2 and barium nitrate thermal decomposition are validated separately and they are considered as non tunable reactions in the model
- The tuning efforts concluded that tuning of the NOx storage is sensitive to the given values of CO/NO reaction kinetics
- This is attributed to the nature of barium nitrates reduction. Barium nitrates react in layers with CO. This mechanism is modeled by several researchers as a shrinking core mechanism.
- Further development and more evaluation is needed for the model

CHAPTER 9

SUMMARY AND CONCLUSIONS

9 SUMMARY AND CONCLUSIONS

9.1 SUMMARY

This dissertation employed as a starting point, the results of the thesis of Pontikakis [3] published back in the 2003. An important contributions of Pontikakis to the three-way catalytic converter model, was the introduction of a new oxygen storage submodel that solves analytically the stored oxygen profiles in the washcoat. Further, he developed a genetic algorith and established a novel and more accurate tuning methodology for the model. The use of this automated tuning procedure significantly improved the results and revealed new, critical issues for further research. His proposals for future work, among others, underlined the need for the improvement of the model's usability and visualization of the modeling results.

A first step in the development of the present thesis was the development of a graphical user interface to improve the model applicability. The graphical user interface allowed the fast and error free preprocessing of the raw experimental data, the creation of the input files for the model and the use of the model through a graphical windows interface. For this purpose it was selected to use MS-EXCEL, a widely spread commercial software, in order to ensure the usability of the model even for beginners. A great effort was given to create a user-friendly application.

The postprocessing and the visualization of the results gave further capabilities to the graphical user interface. The results of the model are postprocessed and compared to the experimental data in an automated way that is able to treat a great number of output files and large datasets quickly and accurately. The development of the postprocess procedure enabled the easy management of newly created output files that describe in detail the model results and enable an in depth crosschecking of the model with the experiment.

The successful application of the graphical user interface and its proved usability by several users in LTTE, encouraged the development of an automated quality assurance methodology for the experimental data. The target was to systematically reveal and assess common errors in the experimental procedure and the data acquisition and evaluate the quality of each dataset. As a starting point in this process, standardized graphs enabled the direct comparison between several experimental data by optical observations. Further, the development of software -

based phasing of the experimental data and the assessment of their quality with the use of a set of statistical estimators was the key to quantify in preliminary way the quality of the experimental datasets. The proposed quality measure that was discussed in this thesis needs to be extended and evaluated over more datasets.

The need for direct comparability among experimental datasets coming from different laboratories, test protocols and engine systems dictated the development of a standardized modal analysis. Although modal analysis was intended to be a part of the quality assurance methodology, its value as an engine management and exhaust aftertreatment assessment tool was soon demonstrated. Operation of the entire system of engine-engine management-aftertreatment device was evaluated over specific modes of driving with the use of a simple criterion developed in literature for the comparison of different driving patterns. Theoretically, this methodology can be used for the evaluation of the system even for "off-cycle" operation, which can assist systems design to match future legislation requirements.

So far, the tools that were developed in this thesis aim at the extension of the model usability, the treatment of the experimental data in a standardized way and of course the reduction of time, cost and human effort for the computer aided design optimization of exhaust treatment systems. As regards the computer aided design aspects, the model was viewed in a more rational and engineering way in order to simplify its use and decouple its complexity.

The most common approach in the literature was the in- depth search of the kinetic parameters and the proposal of complex, coupled reactions schemes with advanced reaction rate expressions. In the framework of his PhD thesis, Pontikakis developed DARWIN, an in-house optimization tool based on genetic algorithms for tuning the kinetic parameters of the model. Systematic kinetic parameter estimation with this tool revealed groups of solutions with very similar characteristics that did not belong to the unique global solution of the optimization. It was a curious fact that some of these solutions were returning a behavior closer to the physical sense. For example, they returned better distribution of the reactants among the reactions.

This observation was the motivation to review several issues related to the use of reaction schemes with global reactions and apparent rates. An extended literature review with respect to the catalytic properties of the several washcoat formulations and the materials used was crucial to this direction. The literature review that was discussed in chapter 1 familiarizes the reader to the engineering approach adopted

in this thesis towards simplification of the model use as it was discussed in the second chapter. The approach selected was to improve critical aspects of the model and give as minimum as possible effort to the kinetic parameters.

The reaction schemes that had been used in the past were reviewed and evaluated in order to classify their contribution. The result was to filter the extent of the phenomena and systematically conclude to

- The reduction from at least ten to a maximum of eight reactions for the description of the catalytic converter operation, with the assumption of a single hydrocarbons species.
- The reduction to a single tunable parameter per precious metal used instead of one or two tunable parameters per reaction used in the reaction scheme.
- This classification resulted to at least equal quality of results while reclaiming better control of the model and the tuning of the parameters

Further, it was selected to switch from the DARWIN that was tailored to the specific model, to a general-purpose optimization software featuring several optimization algorithms (GenOpt). Using GenOpt the tuning of the model was attempted with several optimization algorithms to conclude to the hybrid Particle swarm Optimisation – Generalised Pattern Search as the faster and the more robust algorithm for the specific application. This algorithm managed to give superior solutions to the parameter estimation problem. From this point on, the time-consuming manual tuning was completely abandoned. A significant contribution to the improvement of the tuned results was the redefinition of the objective function.

The last part of this study is dedicated to the extensive validation of the model and the entire methodology over an extended set of experimental test case studies. The case studies included catalytic converters of different geometrical characteristics and various precious metal type and loading, which are fitted to engines with different engine management characteristics.

The first case featured four catalytic converters of different precious metal loading. The model was tuned for each and matched the behavior within a very good accuracy. The results were successfully extended to a shorter catalytic converter. This case presented also the extended cross-checking and validation of the results that is made throughout this thesis. A first attempt to derive a trend of tuned

kinetic parameters and thus catalytic activity versus precious metal loading is presented. Of course, further validation will be necessary.

The second case featured catalytic converters of different channel density. The application of the model was not as successful as in the first case, but this was partially attributed to the quality of the dataset. On the other hand, the advanced double layer washcoat formulation of these catalysts may be beyond the capacity of the model. Model improvement to directly address a layered washcoat remains an open issue for the future.

The last three-way catalytic converter case featured various tri-metal washcoat formulations with varying precious metal ratio. This case had common characteristics to the variable channel density case. Both cases use an advanced double layer washcoat formulation and are positioned in close-coupled position. The model was successfully tuned for a reference case and the results were extended to the rest of the cases with satisfying accuracy.

Finally, a NOx storage submodel was developed and validated over two test datasets shown in the last chapter. The NOx storage submodel was formulated in a similar way to the oxygen storage submodel and featured only three additional reactions to the typical three- way reaction scheme. The model was able to predict the behavior of the NOx trap with sufficient accuracy, but it loses accuracy during the regeneration. It is believed that this is subject to the intrinsic solution procedure for the storage components of the washcoat.

9.2 CONCLUSIONS

At the beginning of this thesis, a number of questions had to be addressed. Firstly, it had to be answered why the model failed, in some cases, to match the experimental data. In this thesis, two cases examined in Pontikakis thesis [3] were also addressed, in greater detail, in order to enable direct comparison and assessment of the model improvements. The automated preprocessing and the quality assurance methodology developed help answer this question. It was proven that the preprocessing of the data is of great importance for the derivation of accurate modeling results. Previous in- house experience had shown that the processing of the raw data was made in a subjective matter, affecting the final quality of the computed results. It is not very clear if the current methodology can reach the quality of the corrected datasets that are produced by an experienced user in a time-consuming way, but it is definite that with the use of this procedure even a beginner can achieve very similar level of quality.

The quality assurance methodology that was developed in this thesis evaluates the quality of the datasets with the use of some statistical estimators and is able to identify experimental errors that could affect the modeling results. A demonstration of its application was the assessment of the low dataset quality of the channel density case. This also was the worst dataset regarding the modeling results. The extension of the quality assurance to the modal analysis of the measured catalytic converter operation assisted the systematic classification of principal directions regarding the reaction scheme over different washcoat formulations and operating conditions.

The most important contribution of this thesis to the field of catalytic converter modeling concerns the simplifications made to the overall approach of modeling. The model of this thesis originates from the milestone works of Voltz [93] and Oh and Cavendish [94] and belongs to a large group of models sharing similar principles. It was shown that the tuning of the kinetic parameters is of minor importance.

Specifically, this work demonstrated the existence of standard kinetic parameters sets for each washcoat formulation that can match the converter behavior with remarkable accuracy. It was shown that the approach of one tunable kinetic parameter per group of reactions over a specific catalyst (e.g. oxidation over

Platinum particles) is valid for the simplified approach of global reactions with apparent reaction rates used in this model. Of course, the validity of this approach is limited to engineering applications where what matters is not the detail description of the chemical phenomena inside the converter, but the prediction within certain accuracy of the overall performance of the converter. A further extension of this approach needs the in-depth study of each reaction at a fundamental research level in order to evaluate the macroscopic factors that affect its individual activity.

The use of several simplifications and assumptions, which have been discussed in this dissertation, and the use of computer-aided estimation of the tunable parameters concluded to a robust set of kinetic parameters. This was made possible only after decoupling in a certain extent the phenomena between mass transfer and complex chemistry. Two major weaknesses of the model were revealed; the modeling of storage processes in the washcoat and the modeling of advanced washcoat formulations like for example double layered washcoats. Although the latter was overridden in a certain extent by the use of a simple assumption, it was practically remained unsolved while the storage submodels were identified to be responsible for the major inaccuracies of the model.

9.3 FUTURE WORK

By the completion of this thesis, the author feels that the following issues (ranked in ascending order of importance) should be studied in the direction of improving modeling results, while retaining a compact modeling approach.

- Improved modeling of double layer washcoat applications. It was demonstrated here that each layer may feature different catalytic activity and thermal characteristics which affect crucial parts of catalyst operation - for example the light-off.
- The development of a submodel that accounts for bulk ceria storage. This is a different concept than that of porous solid diffusion as it refers to movements of oxygen atoms in the ceria lattice vacancies. This concept could be valuable also for the modeling of NOx storage over BaO.

APPENDIXES

APPENDIX A

A MODELING ESTIMATION OF THE RATE DETERMINING STEP BETWEEN CHEMICAL REACTION AND MASS TRANSFER

According to Figure 16 the steps 1, 2, 6 and 7 (diffusion from gas phase to catalytic active sites and vice versa) could be considered as possible diffusion limitation states, while the steps 3, 4 and 5 are compensated into catalytic reaction.

Consider a control volume for node i shown in Figure 121 that includes both gas and solid phase. Let us assume a mol of gas that is transported from bulk gas flow to catalytic active sites at time t-dt, reacts at a fraction over the catalyst at time t and the unreacted part diffuses back to the gas flow at time t+dt.

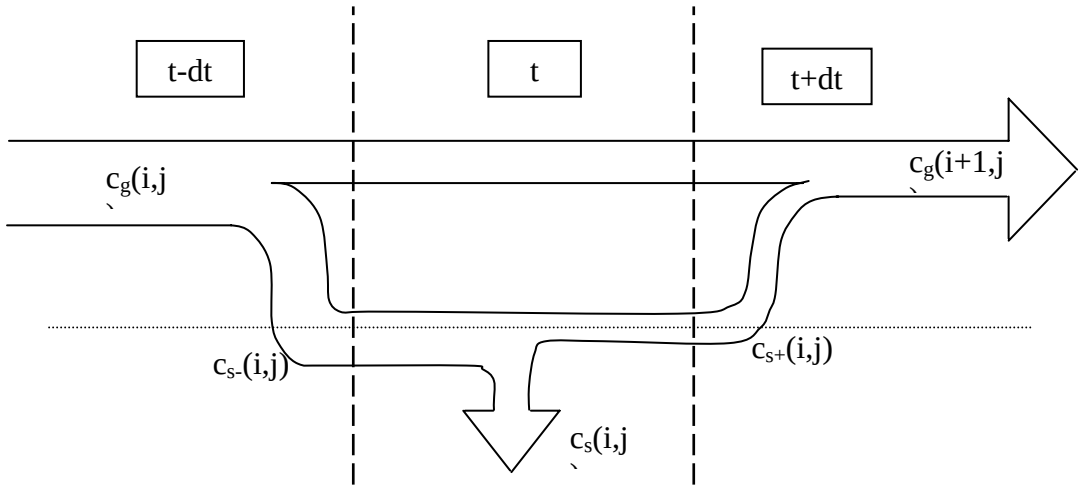

Figure 121 Exhaust gas diffuses to catalytic active sites, reacts and diffuses back to the bulk gas flow

For the portion of a specie j in the gas phase that adsorbs to the solid phase, we can write

$\eta_{ads} = \frac{c_{s-}(i,j)}{c_g(i,j)}$, where c_{s-} is the solid "concentration" at time just before reaction initiation

For the reacting portion of the solid concentration of specie j over node I we can write

$$\eta_{reaction} = \frac{c_s(i,j)}{c_{s-}(i,j)}$$

Let us consider a remaining solid "concentration" c_{s+} after the reaction completes. The reaction efficiency can also be written as

$$\eta_{reaction} = 1 - \frac{c_{s+}(i,j)}{c_{s-}(i,j)}$$

Further, we assume that all the reaction remainders are desorbed back in the gas phase, thus no specie is stored in the solid phase due to sorption (quasi static assumption).

$$\eta_{des} = 1$$

The total efficiency for each specie j per node i is

$$\eta_{tot} = \eta_{ads}\eta_{reac}\eta_{des} = 1 - \frac{c_g(i+1,j)}{c_g(i,j)} \Rightarrow$$

$$\frac{c_{s-}(i,j)}{c_g(i,j)}\left(1 - \frac{c_{s+}(i,j)}{c_{s-}(i,j)}\right) = 1 - \frac{c_g(i+1,j)}{c_g(i,j)}$$

The solver of the model calculates the final concentration on the solid phase, cs+. Solving for c_{s-} gives

$$c_{s-}(i,j) = c_{s+}(i,j) + c_g(i,j) - c_g(i+1,j)$$

Replacing this value in the previous equations results

$$\eta_{ads} = \frac{c_{s-}(i,j)}{c_g(i,j)} = \frac{c_{s+}(i,j) + c_g(i,j) - c_g(i+1,j)}{c_g(i,j)}$$

$$\eta_{reaction} = 1 - \frac{c_{s+}(i,j)}{c_{s+}(i,j) + c_g(i,j) - c_g(i+1,j)}$$

Finally, we can define the rate determining step for each specie mole consumption or production through the ratio of the two predefined efficiencies.

$$RDS = \eta_{ads} - \eta_{reac} = \begin{cases} > 0, & RDS \equiv mass\,transfer \\ = 0, & reaction \equiv mass\,tranfer \\ < 0, & RDS \equiv reaction\,rate \end{cases}$$

APPENDIX B

GRAPHICAL USER INTERFACES

An important aspect of engineering model is their usability and the interaction with the end-user. During the accomplishment of this thesis, a large set of macros in MS-EXCEL was created in order to establish a GUI that would be really helpful to the systems design engineer. The choice of MS-EXCEL use instead of the development of a stand-alone application was made to retain compatibility with widespread commercial software and to take advantage of the advanced spreadsheet operation of the parent software. These macros are used to:

- Check raw experimental data for common errors, preprocess and translate typical experimental raw data to real exhaust gas data in exhaust (will be discussed in the next chapter)
- Check the experimental data through a quality assurance methodology that is developed in this thesis (will be discussed in the next chapter)
- Create input files for CATRAN and operate CATRAN from MS-EXCEL user panel
- Postprocess and visualize the modelling results.

Previous experience in our laboratory had shown that the management of such large datasets (minimum size: 15 columns x 1200 rows) coming from typical automotive experiments had to be treated by an experienced user in order to deliver proper input files and experimentally study them. Even in the case of most experienced users, errors in the processed data were still present, while the time needed to process a single case was more than two hours.

Figure 122 The toolbar created to manage the sets of macros developed in this thesis

The necessity to automate this procedure and ensure the error free preprocess of the data has leaded to the development of a quality assurance procedure that will be discussed in the next chapter. Further development in this direction has resulted to a robust GUI built in MS-EXCEL that practically turned the model into an engineering

CAE tool. By taking into advantage the windows interface the user can use a set of macros to preprocess the data, run each case and visualize the results.

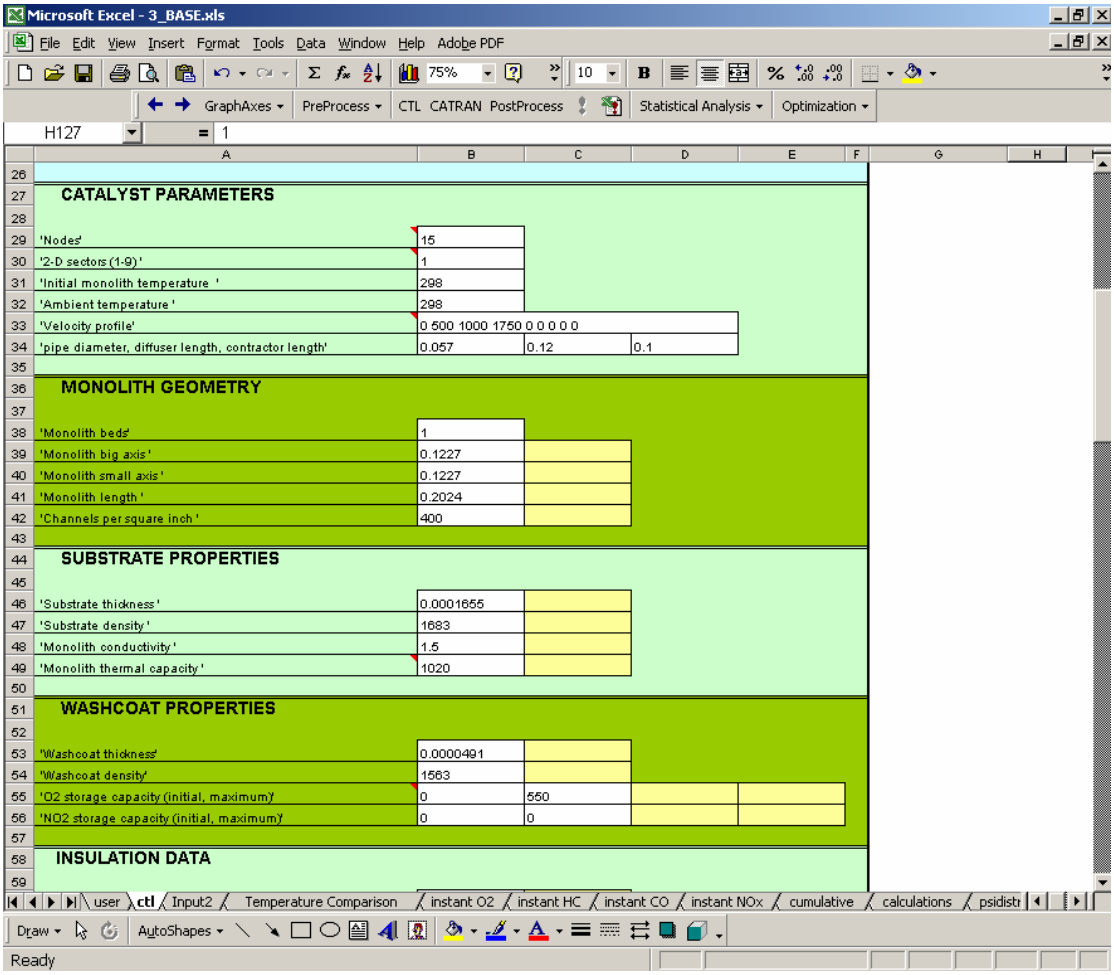

Figure 123 A snapshot of the worksheet used to define catalytic converter geometrical characteristics and auxiliary properties

Further, taking advantage of the powerful spreadsheets operations, several side calculations can be made either for catalytic converter characteristics or for model output. The latter reduces the model outputs to the absolutely necessary, thus increases the speed of each run and moves secondary calculations to the external postprocessing of the data.

Adaptation of the model in other environments, such as MATLAB/SIMULINK and LabView, as also established due to clients' needs or in-house priorities. Examples are briefly presented below

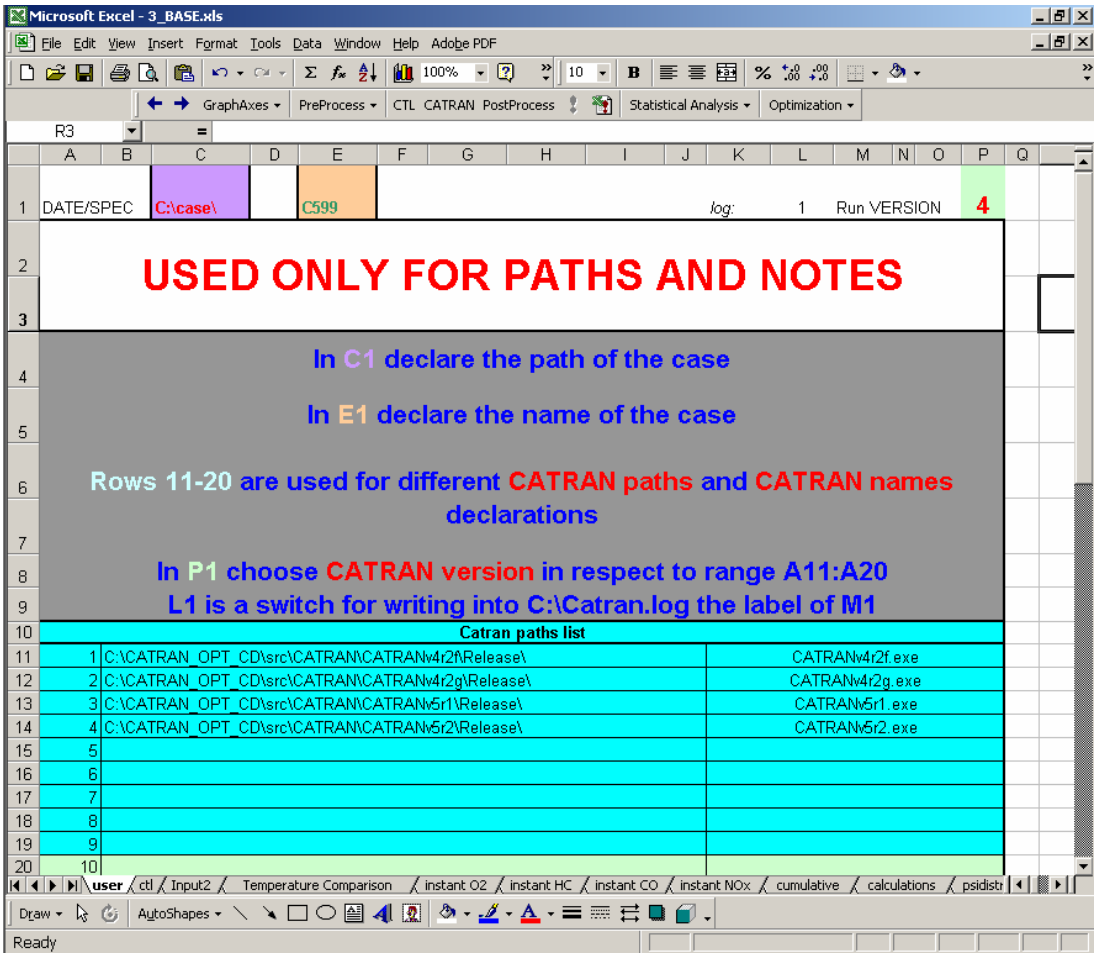

Figure 124 The user front panel to select case for run and model version

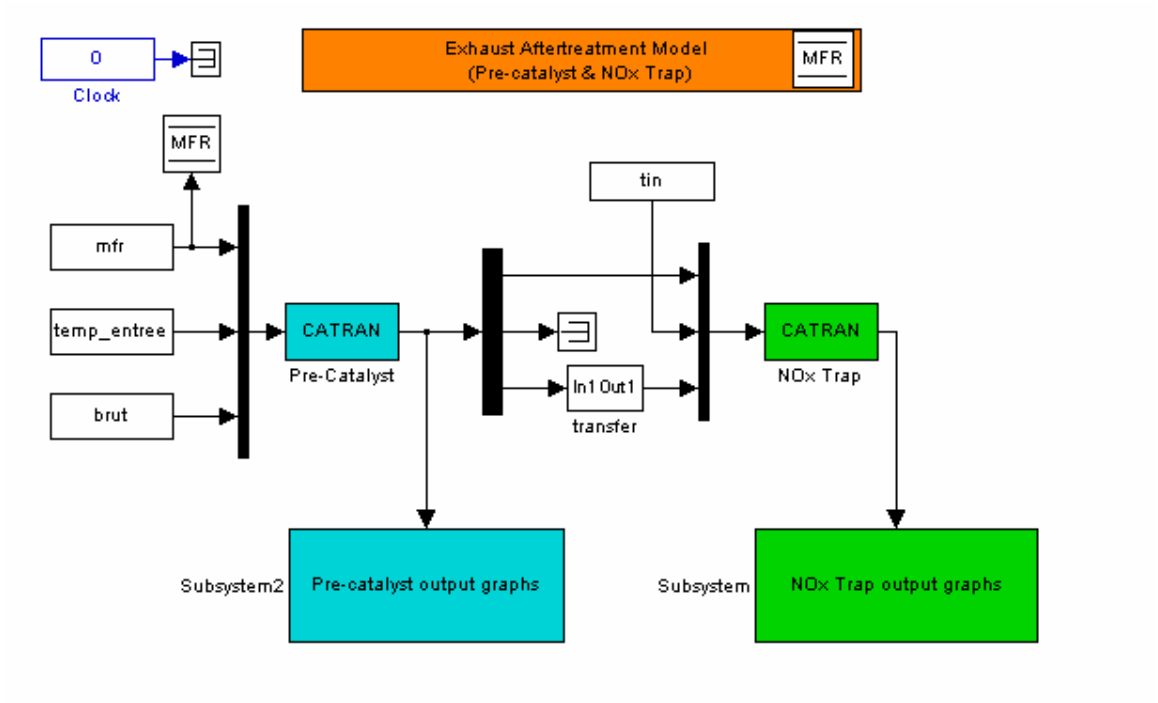

Figure 125 Simulink implementation of CATRAN for the case of a precatalyst in series with NOx adsorber

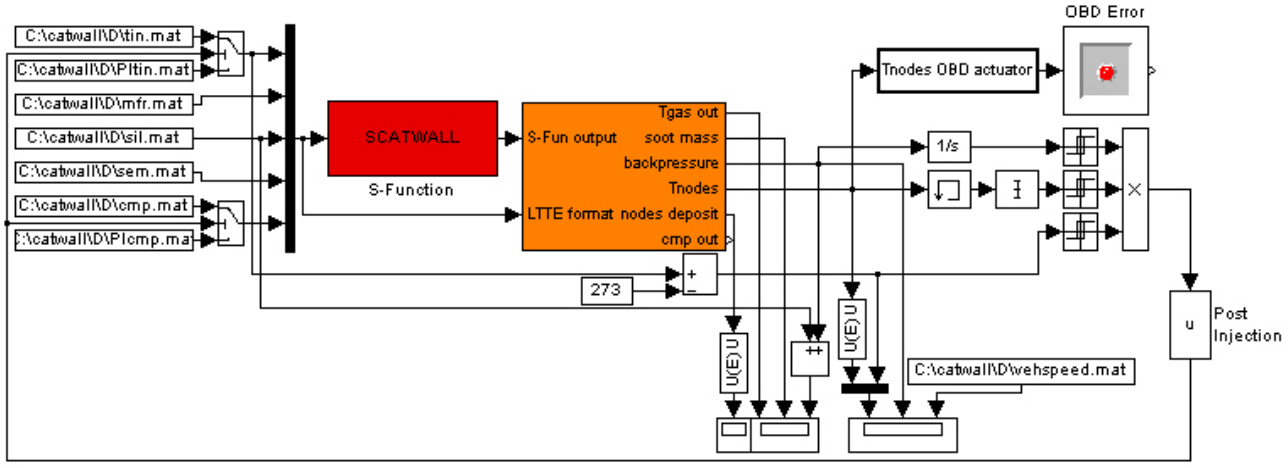

Figure 126 Simulink implementation of CATWALL 1D filter loading and regeneration model.

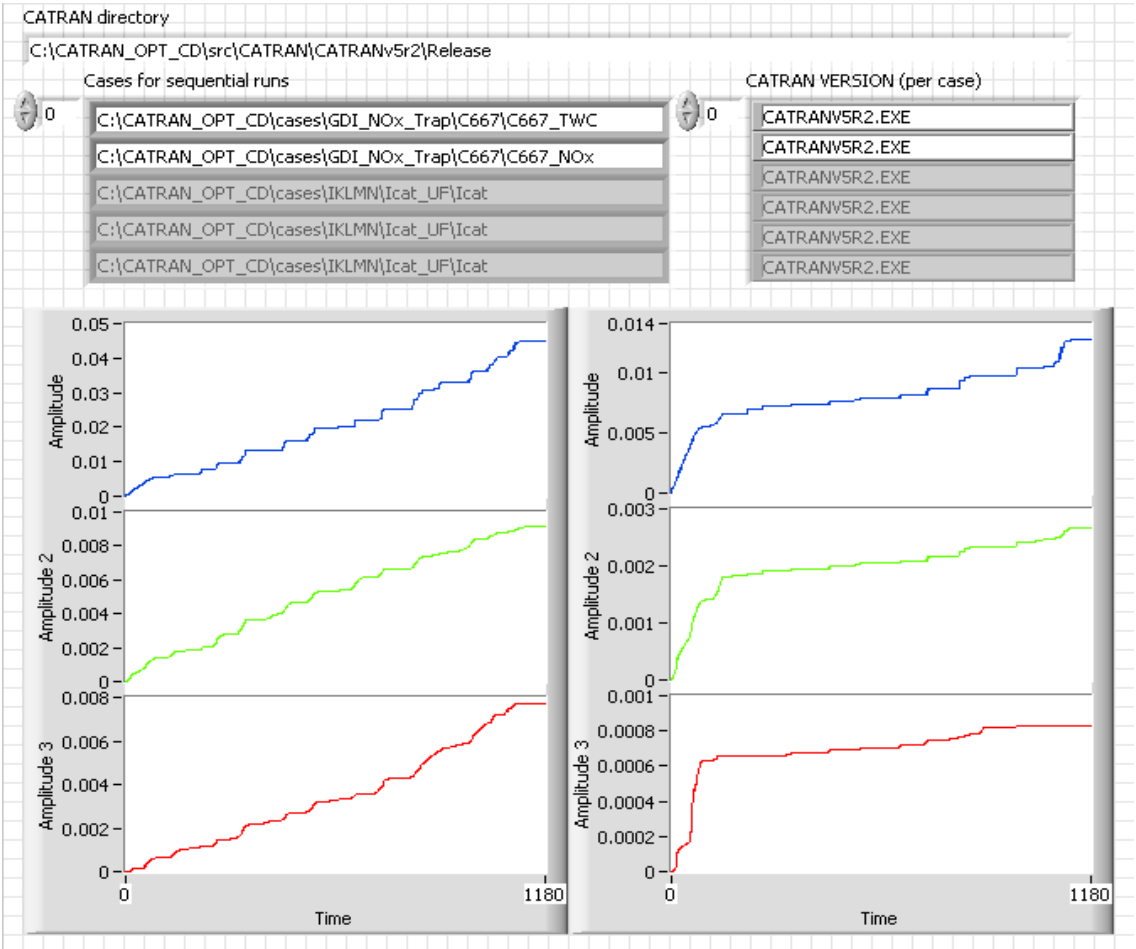

Figure 127 Labview implementation of CATRAN for the case of a precatalyst in series with NOx adsorber

REFERENCES

1 Votsmeier, M., Bog, T., Lindner, D., Gieshoff, J., Lox, E.S., Kreuzer, T., (2002): “A system(atic) Approach towards low precious metal Three-way Catalyst application”, SAE paper 2002-01-0345

2 Olsson, L. and Andersson, B. (2004): “Kinetic modelling in automotive catalysis”, Topics in Catalysis Vol. 28, Nos. 1–4, 89-98

3 Pontikakis, G. (2003): “Modeling, Reaction Schemes and Parameter Estimation in Catalytic Converters and DieselFilters”, PhD Thesis, Mechanical Engineering Dept., University of Thessaly, Volos 2003.

4 Wetter, M. (2004): “GenOpt® Generic Optimization Program – User Manual Version 2.0.0”, Technical Report LBNL-54199, Lawrence Berkeley National Laboratory

5 Konstantas, G. and Stamatelos, A. (2004): “Computer-Aided Design Optimization of Catalytic Exhaust Treatment Systems For Gasoline-Powered Cars”, ERCOFTAC Design Optimization International Conference, March 31- April 2 2004, Athens, Greece

6 Stratakis, G. (2004): “Experimental Investigation of Catalytic Soot Oxidation a and Pressure Drop Characteristics in Wall-Flow Diesel Particulate Filters”, PhD Thesis, Mechanical Engineering Dept., University of Thessaly, Volos

7 Konstantas, G. and Stamatelos, A. (2004): “Computer Aided Engineering Of Diesel Filter Systems”, Joint Meeting of the Italian and the Greek Section of the Combustion Institute, 17- 19 June 2004, Corfu Island, Greece

8 Bachman, W.H. (1997):“A GIS-Based Modal Model of Automobile Exhaust Emissions”, Environmental protection Agency (EPA/600/R-98/097); Air Pollution Prevention and Control Division

9 Maus, W., Brück, R., Holy, G. (1999): “Future Exhaust-Gas Aftertreatment Technologies for Spark-Ignition Engines; The Next Generation of Super Ultra Low Emission Vehicles”, Engine & Environment Pollutant Emissions Versus CO2, International Congress in Graz

10 Pischinger, S. (2004): “The future of vehicle propulsion – combustion engines and alternatives”, Topics in Catalysis, Vols. 30/31, pp.5-16

11 König, A., Herding, G., Hupfeld, B., Richter, Th. and Weidmann, K. (2001): “Current tasks and challenges for exhaust aftertreatment research. A viewpoint from the automotive industry”, Topics in Catalysis Vols. 16/17, Nos. 1–4, pp.23-31

12 Holgate, S.T. (Chairman) (1998): "Quantification of the Effects of Air Pollution on Health in the United Kingdom", U.K. Department of Health, The Stationery Office, London

13 Heywood, J. B.(1988): Internal Combustion Engine Fundamentals; McGraw-Hill Publishing Company; New York, NY.

14 Honda website: “The new 1.8lt VTEC Engine”, HDTV, available at http://worldwide.honda.com, 3 April 2006

15 European Federation for Transport and Environment (2004): “Waiting for Euro 5 and Euro 6 New Emission Standards for Passenger Cars, Vans and Lorries”, available in http://www.t-e.nu

16 Commission of the European Communities (2005): “Proposal for a regulation of the European parliament and of the council on type approval of motor vehicles with respect to emissions and on access to vehicle repair information, amending directive 72/306/EEC and directive xx/xx/EC”, Brussels, 21.12.2005

17 Smokers, R., Gense, R., Rijkeboer, R. and Dijkhuizen, A. (2004): “Expert judgement on the long term possibilities of conventional emission abatement technologies for passenger cars”, Topics in Catalysis Vols. 30/31, pp. 439-443

18 Brück, R., Hirth, P., and Maus, W. (1999): “The Necessity of Optimizing the Interactions of Advanced Post-Treatment Components in Order to Obtain Compliance with SULEV-Legislation”, SAE paper 990770

19 Schmidt, M. M., Brady, M. J., Summers, C., Reizig, M., Brück, R., Breuer, J. (2001): “New Catalyst Preparation Procedure for OBDII-Monitoring Requirements”, SAE paper 2001-01-0933

20 Samuel, S., Morrey, D. Fowkes, M., Taylor, D.H.C., Garner, C.P. and Austin, L., (2005): “Real-world performance of catalytic converters”, Proc. IMechE Vol. 219 Part D: J. Automobile Engineering

21 Burch, S. D., Biel, J. P. (1999): “SULEV and "Off-Cycle" Emissions Benefits of a Vacuum-Insulated Catalytic Converter”, SAE paper 1999-01-0461

22 Booth, M., Buglass, J.G. and Unsworth, J.F. (2001): “Tailoring fuels for the new millennium”, Topics in Catalysis Vols. 16/17, Nos. 1–4, 2001 39-46

23 Pfalzgraf, B., Fitzen, M., Siebler, J. and Erdmann, H.D. (2001) “First ULEV Turbo Gasoline Engine - The Audi 1.8 l 125 kW 5-Valve Turbo”, SAE paper 2001- 01-1350
24 Volkswagen website: “The new VW Golf TSI”, available at http://www.vw.com, 13 April 2006
25 Cernosek, R.W. (2000): “Review: National Laboratory Sensor Projects for CIDI/SIDI Engines”, DOE Workshop on Sensors for Fuel Cells and CIDI/SIDI Engines, Claremont Resort Berkeley, California January 25-26, 2000
26 Siemens AG website: (1999) “News release: For Siemens Engineers, the Way to Reducing Emissions is Along the Road of Hard NOx”, Available in Internet http://media.siemensauto.com , February 28 1999
27 Schmidt R., (2001): “Pressure Sensors for Automotive Applications”, AutoTecnology, December 2001
28 Sullivan, R., (2000): “Sensor Needs For Engine Management Of Spark Ignition (SI) Engines”, DOE Workshop for Sensors for Fuel Cells and CIDI/SIDI Engines, Claremont Resort Berkeley, California January 25-26, 2000
29 Shayler, P. J., Belton, C. and Scarisbrick, A. (1999): “Emissions and Fuel Utilisation After Cold Starting Spark Ignition Engines”, SAE paper 1999-01-0220
30 CATRAN, CATWALL, HEATRAN user manuals, University of Thessaly, 2005
31 Wipke, K., Cuddy, M., Bharathan, D., Burch, S., Johnson, V., Markel, T., and Sprik, S., (1998): “ADVISOR 2.0: A Second-Generation Advanced Vehicle Simulator for Systems Analysis”, Presented at the North American EV & Infrastructure Conference and Exposition (NAEVI 98), December 3-4, 1998, Phoenix, Arizona.
32 Farrauto, R.J. and Heck, R. M. (1999): “Catalytic converters: state of the art and perspectives”, Catalysis Today 51, 351-360
33 Shelef, M., McCabe, R.W., (2000): “Twenty-five years after introduction of automotive catalysts: what next?”, Catalysis Today 62 35–50
34 Gandhi, H.S., Graham, G.W., and McCabe, R.W., (2003): “Automotive exhaust catalysis”, Journal of Catalysis 216, 433–442
35 Nijhuis, T.A., Beers, A.E.W., Vergunst, T., Hoek, I., Kapteijn, F. and Moulijn, J.A. (2001): “Preparation Of Monolithic Catalysts”, CATALYSIS REVIEWS, 43(4), 345–380
36 Heibel, A. and Spaid, M.A.A (1999): “A New Converter Concept Providing Improved Flow Distribution and Space Utilization”, SAE paper 1999-01-0768
37 Will, N.S., Martin, A.P., Bordet, A., Cornet, P., Gondoin, C., Mouton, X., (1998): “Effect of Flow Distribution on Emissions Performance of Catalytic Converters”, SAE Paper 980936
38 Presti, M., Pace, L., Hodgson, J., Bella, G. and De Maio, A. (2002): “A Computational and Experimental Analysis for Optimization of Cell Shape in High Performance Catalytic Converters”, SAE paper 2002 – 01 – 0355
39 Schmidt, J., Waltner, A., Loose, G., Hirschmann, A., Wirth, A., Mueller, W., Van den Tillaart, J.A.A., Mussmann, L., Lindner, D., Gieshoff, J., Umehara, K., Makino, M. Biehn, K.P., Kunz, A. (1999). The Impact of High Cell Density Ceramic Substrates and Washcoat Properties on the Catalytic Activity of Three Way Catalysts. SAE paper 1999-01-0272
40 Andersen, P.J and Ballinger, T.H. (1999): “Improvements in Pd:Rh and Pt:Rh Three Way Catalysts”, SAE paper 1999-01-0308
41 Currier, N., Partridge, B., Lewis, S. and Parks, J. (2001): “Spatially Resolved Dynamic Measurement of Gas Phase Composition Inside Operating Catalysts - Support of Catalyst Model Development”, 2nd CLEERS Workshop, Dearborn, Michigan October 16-18
42 Ichikawa, S., Takemoto, T., Sumida, H., Koda, Y., Yamamoto, K., Shigetsu, M. and Komatsu, K. (1999): “Development of Low Light-off Three Way Catalyst”, SAE paper 1999-01-0307
43 Bernal, S., Calvino, J.J., Cauqui, M.A., Gatica, J.M., Larese, C., Perez Omil, J.A. and Pintado, J.M., (1999): “Some recent results on metal/support interaction effects in NM/CeO2 (NM: noble metal)”, Catalysis Today 50, 175-206
44 Golunski, S. E., Hatcher, H. A., Rajaram, R. R. and Truex, T.J. (1995): “Origins of low-temperature three-way activity in Pt/CeO2”, Applied Catalysis B: Environmental Volume 5, Issue 4, Pages 367-376
45 Roesch, S., Sermon, P.A., Wallum, A., Forrest, P.N. and Kaur, P. (2001): “Sol–gel Pd exhaust catalysts and hydrocarbon speciation”, Topics in Catalysis Vols. 16/17, Nos. 1–4, 115-118
46 Eriksson, S., Nylén, U., Rojas, S. and Boutonnet, M. (2004): “Review: Preparation of catalysts from microemulsions and their applications in heterogeneous catalysis”, Applied Catalysis A: General, vol. 265, 207–219

47 Piras, A., Trovarelli, A. and Dolcetti, G. (2000): “Remarkable stabilization of transition alumina operated by ceria under reducing and redox conditions”, Applied Catalysis B: Environmental Volume 28, Issue 2, Pages L77-L81
48 Horiuchi, T., Teshima, Y., Osaki, T., Sugiyama, T., Suzuki, K. and Mori, T. (1999): “Improvement of thermal stability of alumina by addition of zirconia”, Catalysis Letters 62, 107–111
49 Shinjoh, H., Tanabe, T., Sobukawa, H. and Sugiura, M. (2001): Effect of Ba addition on catalytic activity of Pt and Rh catalysts loaded on γ -alumina Topics in Catalysis Vols. 16/17, Nos. 1–4, 95-99
50 Williamson, W. B., Summers, J. C., Skowron, J. F. (1988): “Catalyst technologies for future automotive emission systems”, SAE paper 880103
51 Bedrane, S., Descorme, C., Duprez, D. (2002): “Investigation of the oxygen storage process on ceriaand ceria–zirconia-supported catalysts”, Catalysis Today 75, 401–405
52 Whittington, B.I., Jiang, C.J., Trimm, D.L. (1995): “Vehicle exhaust catalysis: I. The relative importance of catalytic oxidation, steam reforming and water-gas shift reactions”, Catalysis Today 26, pp. 41-45
53 Galdikas, A., Descorme, C., Duprez, D., Dong, F., Shinjoh, H. (2004): “Study of the oxygen diffusion on three-way catalysts: a kinetic model” Topics in Catalysis Vols. 30/31
54 Di Monte, R. and Kaspar, J. (2004): “On the role of oxygen storage in three-way catalysis”, Topics in Catalysis Vol. 28, Nos. 1–4, 47-57
55 Boaro, M., de Leitenburg, C., Dolcetti, G. and Trovarelli, A. (2000): “The Dynamics of Oxygen Storage in Ceria–Zirconia Model Catalysts Measured by CO Oxidation under Stationary and Cycling Feedstream Compositions”, Journal of Catalysis 193, 338–347
56 Lambrou, P.S., Costa, C.N., Christou, S.Y., Efstathiou, A.M., (2004) : “Dynamics of oxygen storage and release on commercial aged Pd-Rh three-way catalysts and their characterization by transient experiments”, Applied Catalysis B: Environmental 54, 229–242
57 Zhdanov, V.P., Kasemo, B. (1998): “Kinetic models of oxygen supply from CeO to active nanometer x particles of three-way catalysts”, Applied Surface Science 135, 297–306
58 Silveston, P.L.,(1995): “Automotive exhaust catalysis under periodic operation”, Catalysis Today 25, 175-195
59 Cho, B.K. (1988): “Performance of Platinum/Alumina Catalysts in Automobile Engine Exhaust with Oscillatory Air/Fuel Ratio”, Ind. Eng. Chem. Res. 27 (1), 30-36
60 Gandhi, H.S. and Shelef, M., (1988): “The Role of Research in the Development of New Generation Automotive Catalysts”, Catalysis and Automotive Pollution Control
61 Moulijn, J.A., Van Diepen A.E. and Kapteijn, F. (2001): “Catalyst deactivation: is it predictable? What to do?”, Applied Catalysis A: General 212, 3–16
62 Brandt, E. P.,Wang, Y. and Grizzle, J. W. (1999): “Dynamic Modeling of a Three-Way Catalyst for SI Engine Exhaust Emission Control”, IEEE TRANSACTIONS ON CONTROL SYSTEMS TECHNOLOGY, VOL. XX, NO. Y, MONTH
63 Jen, H.W., Graham, G.W., Chuna, W., McCabe, R.W., Cuif, J.P., Deutsch, S.E. and Touret, O. (1999): “Characterization of model automotive exhaust catalysts: Pd on ceria and ceria-zirconia supports”, Catalysis Today 50, 309-328
64 Nunan, J.G., Williamson, W.B.,Robota, H.J., Henk, M.G.(1995): “Impact of Pt-Rh and Pd-Rh Interactions on Performance of Bimetal Catalysts”, SAE Paper 950258
65 González-Velasco, J.R., Botas, J.A., Ferret, R., Pilar González-Marcos, M., Marc, J.L., Gutiérrez-Ortiz, M.A. (2000): “Thermal aging of Pd/Pt/Rh automotive catalysts under a cycled oxidizing–reducing environment”, Catalysis Today 59, 395–402
66 Granger, P., Lamonier, J.F., Sergent, N., Aboukais, A., Leclercq, L., and Leclercq, G. (2001): “Investigation of the intrinsic activity of ZrxCe1−xO2 mixed oxides in the CO + NO reactions: influence of Pd incorporation” Topics in Catalysis Vols. 16/17, Nos. 1–4, 89-94
67 Garin, F. (2004): “Review:Environmental catalysis” Catalysis Today 89 255–268
68 Lindner, D., Mussmann, L., Van den Tillaart, J.A.A., Lox, E.S., Roshan, A., Garr, G., Beason, R. (2000): “Comparison of Pd-only, Pd/Rh, and Pt/Rh Catalysts in TLEV, LEV Vehicle Applications – Real Vehicle Data versus Computer Modeling Results”, SAE paper 2000-01-0501
69 Kašpar, J., Fornasiero, P. and Hickey, N. (2003): “Automotive catalytic converters: current status and some perspectives”, Catalysis Today 77, 419–449
70 Haller, G.L. (2003): “New catalytic concepts from new materials: understanding catalysis from a fundamental perspective, past, present, and future”, Journal of Catalysis 216, 12–22
71 SAE website: “Catalytic Converters: Design and Durability e-Seminar” – DEMO Clips, available at http://www.sae.org, 19 September 2004

72 Griffin, J.R. (1999): “Closed Loop Catalyst Temperature Feedback for Controlled Catalyst Lightoff and Diagnostics for ULEV”, SAE paper 1999-01-0311
73 Holy, G., Brück, R. and Hirth P. (2000) “Improved Catalyst Systems for SULEV legislation: First Practical Experience”, SAE paper 2000-01-0500
74 Herz, R. K. and Shinouskis, E. J. (1985): “Dynamic Behavior of Automotive Catalysts. 4. Impact of Air/Fuel Ratio Excursions during Driving”. Ind. Eng. Chem. Prod. Res. Dev. (24), 385-390
[75] DE 100 36 453
76 Zhang, Hong, Pfleger, Corinna (Siemens AG, Muenchen) Verfahren zur Ueberpruefung des Wirkungsgrades eines NOx-Speicherkatalysatora. Deutsches Patent DE 198 23 921 A1, 2.12.99
77 Shamim, T., Shen, H., Sengupta, S., Son, S. and Adamczyk, A. A. (2002): “A Comprehensive Model to Predict Three-Way Catalytic Converter Performance”, Journal of Engineering for Gas Turbines and Power, Vol. 124, 421-428
78 Koltsakis, G.C., Konstantinidis, P.A. and Stamatelos, A.M. (1997): “Development and application range of mathematical models for 3-way catalytic converters”, Applied Catalysis B: Environmental, Vol.12, Iss.2-3, 161-191
79 Tsinoglou, D.N. and Koltsakis, G.C. (2003): “Effect of perturbations in the exhaust gas composition on three-way catalyst light off“, Chemical Engineering Science 58, 179 – 192
80 Mukadi, L.S. and Hayes, R.E., (2002): “Modelling the three-way catalytic converter with mechanistic kinetics using the Newton-Krylov method on a parallel computer“, Computers and Chemical Engineering 26, 439-455
81 Harmsen, J.M.A., Hoebink, J. H. B and Schouten, J. C. (2000): “Transient Kinetic Modeling of the Ethylene and Carbon Monoxide Oxidation over a Commercial Automotive Exhaust Gas Catalyst”, Ind. Eng. Chem. Res. 39, 599-609
82 Braun, J., Hauber, T., Tobben, H., Windmann, J., Zacke, P., Chatterjee, D., Correa, C., Deutschmann, O., Maier, L., Tischer, S. and Warnatz, J. (2002): “Three-Dimensional Simulation of the Transient Behavior of a Three-Way Catalytic Converter“, SAE paper 2002-01-0065
83 Lox, E.S. (2003): “State of the art methods for the development of automotive catalysts”, CAPOC6, Umicore Keynote
84 Silveston, P.L. (1996): “Automotive Exhaust Catalysis: Is Periodic Operation Beneficial?” Chemical Engineering Science, Vol, 51, No. 10, pp. 2419-2426
85 Maillet, T.,Barbier Jr., J. and Duprez, D. (1996): “Reactivity of steam in exhaust gas catalysis III. Steam and oxygen/steam conversions of propane on a Pd/Al,O, catalyst”, Applied Catalysis B: Environmental 9, 25l-266
86 Yamada, K., Tanaka, H. and Yamamoto, M. (1997): “Oxygen storage capacity on cerium oxide—Precious metal system”, SAE paper 970464
87 Zhang, G., Hirota, T., Hosokawa, Y. and Muraki, H. (1997): “Thermally stable Pt/Rh catalysts”, SAE paper 970929
88 Domesle, R., Lindner, D., Mueller,W., Mussmann, L.,Votsmeier,M., Lox, E.S., Kreuzer, T.,Makino, M.,Vogt,C.D. (2001): “Application of Advanced Three-way Catalyst Technologies on High Cell Density Ultra-Thin-wall Ceramic Substrates for Future Emission Legislations”, SAE paper 2001-01-0924
89 Muraki, H. and Zhang, G. (2000): “Design of advanced automotive exhaust catalysts”, Catalysis Today 63, 337–345
90 Descorme, C.; Taha, R.; Mouaddib-Moral, N. and Duprez, D. (2002). Oxygen storage capacity measurements of three-way catalysts under transient conditions, Applied Catalysis A: General 223, 287–299
91 Lafyatis, D.S., Bennett, C. J., Hales M. A., Morris, D., Cox, J. P. and Rajaram, R.R. (1999): “Comparison of Pd-only vs. Pd-Rh Catalysts: Effects of Sulfur, Temperature and Space Velocity”, SAE paper 1999-01-0309
92 Depcik, C.D. (2003): “Modelling Reacting Gases and Aftertreatment Devicesfor Internal Combustion Engines”, Mechanical Engineering Department, University of Michigan
93 Voltz S.E.; Morgan C.R.; Liederman D.; Jacob S.M. (1973). Kinetic study of carbon monoxide and propylene oxidation on platinum catalysts. Ind. Eng. Chem. Prod. Res. Dev. 12, 294-301.
94 Oh, S.H., Cavendish,J.C. (1985): “Mathematical Modeling of Catalytic Converter Lightoff – Part II: model Verification by Engine-Dynamometer Experiments”, AIChE Journal, Vol. 31, No. 6, (1985) 935-942
95 Mannila, P.; Salmi, T.; Haario, H.; Luoma, M.; Harkonen, M.; Sohlo, J. (1996). Stationary kinetics of essential reactions on automobile exhaust Pt-Rh/Al2O3 catalyst, Applied Catalysis B: Environmental 7, 179-198

96 Granger, P., Lecomte, J.J., Leclercq, L. and Leclercq G. (2001): “Kinetics of the CO + O2 reaction over three-way Pt-Rh catalysts”, Applied Catalysis A: General 218, 257–267
97 Bunluesin T.,. Gorte, R.J and Graham, G.W. (1998): “Studies of the water-gas-shift reaction on ceria-supported Pt, Pd, and Rh: implications for oxygen-storage properties”, Applied Catalysis B: Environmental 15, 107-l14
98 Hilaire, S., Wanga, X., Luoa, T., Gorte, R.J. and Wagner, J. (2004): “A comparative study of water-gas-shift reaction over ceria-supported metallic catalysts”, Applied Catalysis A: General 258, 271–276
99 Ciuparu, D., Lyubovsky, M.R., Altman,E., Pfefferle,L.D., and Datye, A. (2002): “Catalytic Combustion Of Methane Over Palladium-Based Catalysts”, Catalysis Reviews Vol. 44, No. 4, 593–649
100 Parvulescua, V.I., Grange, P., Delmon, B. (1998): “Catalytic removal of NO”, Catalysis Today 46, 233-316
101 Liu, Zhi-Pan and Hu, P. (2004): “CO oxidation and NO reduction on metal surfaces: density functional theory investigations”, Topics in Catalysis Vol. 28, Nos. 1–4
102 Cho, B. K. (1992): “Mechanistic importance of intermediate N2O + CO reaction in overall NO + CO reaction system I. Kinetic analysis”, Journal of Catalysis Volume 138, Issue 1, 255-266
103 Granger, P., Malfoy, P. and Leclercq, G. (2004): “Kinetics of the CO+ N2O reaction over noble metals II. Rh/Al2O3 and Pt–Rh/Al2O3”, Journal of Catalysis 223, 142–151
104 Amiridis, M. D., Mihuta, C., Maciejewskib, M. and Baiker, A. (2004): “The selective catalytic reduction of NO by hydrocarbons over Pt- and Ir-based catalysts”, Topics in Catalysis Vol. 28, Nos. 1–4, 141-150
105 Zygourakis, K. and Aris, R., (1983): “Multiple oxidation reactions and diffusion in the catalytic layer of monolith reactors”, Chem. Eng. Sci. vol 38, No. 5 pp. 773-744
106 Cornelius S.J., Collings, N. and Glover, K. (2001): “The role of oxygen storage in NO conversion in automotive catalysts”, Topics in Catalysis Vols. 16/17, Nos. 1–4, 2001, 57 -62
107 Nakatsuji,T., Ruotoistenmäki, J., Komppa, V., Tanaka, T. and Uekusa, T. (2002): “A catalytic NO reduction in periodic lean and rich excursions over Rh supported on oxygen storage capacity materials”, Applied Catalysis B: Environmental Volume 38, Issue 2, Pages 101-116
108Fornasiero, P., Kaspar, J., Montini, T., Graziani, M., Dal Santo, V., Psaro, R.,and Recchia, S. (2003): “Interaction of molecular hydrogen with three-way catalyst model of Pt/Ce0.6Zr0.4O2/Al2O3 type”, Journal of Molecular Catalysis A: Chemical 204–205, 683–691
109 Holles, J. H., Switzer, M.A. and Davis, R.J. (2000): “Influence of Ceria and Lanthana Promoters on the Kinetics of NO and N2O Reduction by CO over Alumina-Supported Palladium and Rhodium”, Journal of Catalysis 190, 247–260
110 Granger, P., Delannoy, L., Lecomte, J. J., Dathy, C., Praliaud, H., Leclercq, L. and Leclercq, G. (2002): “Kinetics of the CO + NO Reaction over Bimetallic Platinum–Rhodium on Alumina: Effect of Ceria Incorporation into Noble Metals”, Journal of Catalysis 207, 202–212
111 Botas, J.A., Gutiérrez-Ortiz, M.A., González-Marcos, M.P., González-Marcos, J.A., González-Velasco, J.R. (2001): “Kinetic considerations of three-way catalysis in automobile exhaust converters”, Applied Catalysis B: Environmental 32, 243–256
112 Konstantas G and Stamatelos A (2004): “Quality assurance of exhaust emissions test data”, Proc. Instn Mech. Engrs Vol. 218 Part D: J. Automobile Engineering, 901-914
113 Montreuil, C. N., Williams, S. C., and Adamczyk, A. A. (1992): “Modeling Current Generation Catalytic Converters: Laboratory Experiments and Kinetic Parameter Optimization - Steady State Kinetics” SAE paper 920096.
114 Balenovic phd, olsson Nox trap, grizzle
115 Hayes, R.E., Mukadi, L.S., Votsmeier, M. and Gieshoff, J. (2004):” Three-way catalytic converter modelling with detailed kinetics and washcoat diffusion”, Topics in Catalysis Vols. 30/31
116 Depcik, C. and Assanis, D. (2005): “One-dimensional automotive catalyst modelling”, Progress in Energy and Combustion Science, Volume 31, Issue 4, 2005, Pages 308-369
117 Presti, M., Pace, L., Hodgson, J., Bella, G., De Maio, A. (2002): “A Computational and Experimental Analysis for Optimization of Cell Shape in High Performance Catalytic Converters”, 2002 – 01 - 0355
118 Aimard, F., Li, S. and Sorine, M. (1996): “Mathematical modelling of automotive three-way catalytic converters with oxygen storage capacity”, Control Eng. Practice, Vol.4, No.8, 1119-1124
119 Koltsakis, G.C., Stamatelos, A.M. (1999): “Modeling dynamic phenomena in 3-way catalytic converters”, Chemical Engineering Science 54, 4567-4578
120 Heck, R.H., Wei, J., Katzer, J.R. (1976). Mathematical modeling of monolithic catalysts. AIChE J, 22 (3), 477–484.

121 Chen, D.K.S, Bisset, E. J., Oh, S. H. and Van Ostrom, D. L. (1988): "A three-dimensional model for the analysis of transient thermal and conversion characteristics of monolithic catalytic converters". SAE paper 880282
122 Zygourakis, K. (1989). Transient operation of monolith catalytic converters: a two-dimensional reactor model and the effects of radially nonuniform flow distributions. Chem. Eng. Sci, 44, 2075–2086.
123 Jahn, R., Snita, D., Kubicek, M., Marek, M. (1997). 3-D modeling of monolith reactors. Catalysis Today, 38, 39–46.
124 Keren, I. and Sheintuch, M. (2000): "Modeling and analysis of spatiotemporal oscillatory patterns during CO oxidation in the catalytic converter". Chemical Engineering Science, 55, 1461-1475,
125 Siemund S.; Leclerc, J.P.; Schweich, D.; Prigent, M.; Castagna, F. (1996). Three Way Monolithic Converter: Simulations versus Experiments. Chem. Eng. Sci., 51 (15), 3709–3720.
126 Young L. C. and Finlayson B. A. (1976): Mathematical models of the monolithic catalytic converter: Part i. development of model and application of orthogonal collocation. American Institute of Chemical Engineers Journal, 22(2):310-343.
127 Hayes, R. E., Kolaczkowski, S. T. (1994). Mass and heat transfer effects in catalytic monolith reactors. Chem. Eng. Sci, 46 (21), 3587–3599.
128 Shinjoh, H. (2006): Rare earth metals for automotive exhaust catalysts Journal of Alloys and Compounds 408–412, 1061–1064
129 Masanobu, T., Tsujimoto,Y., Miyazaki, T., Warashina, M. and Wakamatsu, S. (2001): "Peculiarities of volatile hydrocarbon emissions from several types of vehicles in Japan", Chemosphere - Global Change Science, Volume 3, Issue 2, Pages 185-197
130 Koberstein, E. and Wannemacher, G. (1987). The A/F window with three-way catalysts. Kinetic and surface investigations. CAPOC, International Congress on Catalysis and Automotive Pollution Control, Brussels.
131 Jentoft, F.C.,(2002) Modern Methods in Heterogeneous Catalysis presentation at Berlin University, November 1, 2002
132 degussa NO<->NO2 figure
133 Tuttlies, U., Schmeisser, V. and Eigenberger, G. (2004): "A new simulation model for NOx storage catalyst dynamics", Topics in Catalysis Vols. 30/31, 187-192
134 Rosner, D.E. (1986): "Transport Processes in Chemically Reacting Flow Systems", Butterworth-Heinemann Pubs.
135 J. S. Sterrett, L. F. Brown The application of theoretical diffusion models in the presence of a catalytic reaction AIChE Journal Volume 14, Issue 5, 1968. Pages 696-702
136 Hayes, R.E., Kolaczkowski, S.T., Li, P.K.C., Awdry, S. (2000): "Evaluating the effective diffusivity of methane in the washcoat of a honeycomb monolith", Applied Catalysis B: Environmental 25, 93–104
137 Hayes, R.E., Liu, B., Votsmeier, M. (2005): "Calculating effectiveness factors in non-uniformwashcoat shapes", Chemical Engineering Science 60, 2037 – 2050
138 Dieselnet website: Catalytic Coating and Materials, http://www.dieselnet.com/tech/cat_mat.html, March 2006
139 Hayes, R.E., Kolaczkowski, S.T. (1999): "A study of Nusselt and Sherwood numbers in a monolith reactor", Catalysis Today 47, 295-303
140 West, D.H., Balakotaiah, V., Jovanovic Z. (2003): "Experimental and theoretical investigation of the mass transfer controlled regime in catalytic monoliths", Catalysis Today 88, 3–16
141 Balakotaiah, V., West, D. H. (2002): "Shape normalization and analysis of the mass transfer controlled regime in catalytic monoliths" Chemical Engineering Science 57 1269 – 1286
142 Hawthorn, R.D. AIChE Symp. Ser. 70 (137) (1974) 428-438
143 Marques, R., Darcya, P., Da Costa, P., Mellotte, H., Trichard, J.M., Djega-Mariadassou, G. (2004): "Kinetics and mechanism of steady-state catalytic NO + O2 reactions on Pt/SiO2 and Pt/CeZrO2", Journal of Molecular Catalysis A: Chemical, IN PRESS.
144 Somorjai, G.A.: Introduction to surface chemistry and catalysis, John Wiley and Sons, New York, 1994, (e-book)
145 Chorkendorff, I., Niemantsverdriet, J. W. (2003): Concepts of Modern Catalysis and Kinetics, October 2003
146 Rooney, J.J. (1995): Eyring transition-state theory and kinetics in catalysis Journal of Molecular Catalysis A: Chemical 96, Ll-L3, Letter
147 Rooney, J.J. (1994): An Explanation of the Compensation Effect in Catalysis, JOURNAL OF CATALYSIS 146, 310-312, NOTE

148 González-Velasco, J.R., Gutiérrez-Ortiz, M.A., Marc, J.-L., Botas, J.A., González-Marcos, M. P., Blanchard G. (2000): “Effects of redox thermal treatments and feedstream composition on the activity of Ce/Zr mixed oxides for TWC applications”, Applied Catalysis B: Environmental 25, 19–29
149 Lakis, R.E., Cai, Y., Stenger, H.G. and Lyman, C.E. (1995): “Alumina supported Pt-rh Catalysts. II Kinetic Characterization and Synergistic Effects”, Journal of Catalysis 154, 276-287
150 Hoebink, J. H. B. J., van Gemert R. A., van den Tillaart J. A. A., Marin, G. B. (2000): “Competing reactions in three-way catalytic converters: modelling of the NOx conversion maximum in the light-off curves under net oxidising conditions”, Chemical Engineering Science 55, 1573-1581
151 Olsson, L., Persson, H., Fridell, E., Skoglundh, M. and Andersson, B. (2001): “A Kinetic Study of NO Oxidation and NOx Storage on Pt/Al2O3 and Pt/BaO/Al2O3”, J. Phys. Chem. B 105, 6895-6906
152 Chan SH, Hoang DL. (1999): Modeling of catalytic conversion of CO/HC in gasoline exhaust at engine cold-start. SAE paper 1999-01-0452.
153 Olsson, L., Blint, R.J. and Fridell, E. (2005): “A Global Kinetic Model for Lean NOx Traps” Chem. Eng Sci. 2005
154 Matthess N., Schweich D., Martin B. and Castagna, F. (2001): “From light-off curves to kinetic rate expressions for three-way catalysts”, Topics in Catalysis Vols. 16/17, Nos. 1–4
155 Di Benedetto, A., Marra, F.S., Russo, G. (2003): “Heat and mass fluxes in presence of superficial reaction in a not completely developed laminar flow” Chemical Engineering Science 58, 1079 – 1086
156 Kandylas, I.P., Stamatelos, A.M. and Dimitriadis, S.G., (1999): “Statistical Uncertainty in Automotive Emissions Testing”, Proc. Inst. Mech. Engrs., Vol.213, Part D, J. of Automobile Engineering, 491-502.
157 Klingenberg, H. and Schurmann, D. (1982): “Proposal of New Exhaust Emission Compliance and Testing Procedures Based on Averaging”, SAE Paper 821192.
158 Leventon, W. (2001): “New Test Tools Zero in on Ultra-Low Emissions”, electronically published at http//:www.autotestreport.com, March 2001
159 Siemund, S., Leclerc, J.P., Sweich, D., Prigent, M., Castagna, F. (1996): “Three-Way Monolithic Converer: Simulations Versus Experiments”, Chemical Engineering Science, Vol. 51, No.15, 3709-3720
160 Colvin, A. D. Gierczak, C. A., Siegl, W. O. and Butler, J. W. (1997): “A software program for carrying out multi-purpose exhaust composition calculations”, SAE paper 970749
161 Harringhton, J.A., Shishu, R.C. (1973): “A Single-Cylinder Engine Study of the Effects of Fuel Type, Fuel Stoichiometry, and Hydrogen-to-Carbon Ratio and CO, NO, and HC Exhaust Emissions”, SAE Paper 730476,
162 Chakravarthy, V.K., Conklin, J.C., Daw, C.S. and D’Azevedo, E.F., (2003): “Multi-dimensional Simulations of Cold-startTransients in a Catalytic Converter under Steady Inflow Conditions”, Applied Catalysis A (General), vol. 241, 289-306.
163 Silvis, W. M. (1997): “An algorithm for calculating the air/fuel ratio from exhaust emissions”, SAE paper 970749
164 Heck, R. M. and Farrauto, R.J. (2001): “Automobile exhaust catalysts”, Applied Catalysis A: General 221, 443–457
165 Adomaitis, R. and Heck, R. (1988): “Vehicle Control Strategies Effect on Catalyst Performance”, SAE paper 881597
166 Watson, H.C. (1995): “Effects of a Wide Range of Drive Cycles on the Emissions from Vehicles of Three Levels of Technology”, SAE Paper 950221
167 Heck, R., Farrauto, R. (1995): “Catalytic Air Pollution Control – Commercial Technology”, Van Nostrand Reinhold, New York
168 Adamczyk A.A., Williams S.C., Meneghel M.G., Gandhi H.S. (1999): “Closely coupled exhaust catalyst system and engine strategy associated therewith”, US patent US 5878567, 09.03.1999
169 Lang, A., Druckhammer, J., Schultze, F. (2002): Apparatus and Method for Monitoring NOx storage catalytic Converters US patent US 6499291B2, 31.12.2002
170 Christopher J. Rutland: CLEERS Databases for Aftertreatment Modeling, Third DOE Workshop on Crosscut Lean Emissions Reduction Simulation (CLEERS), October 16-18, 2001
171 Zhang, G., Hirota, T., Hosokawa, Y., Muraki, M., (1997): “Thermally stable Pt/Rh catalysts”, SAE 972909
172 Lucena, P. and Laserna, J.J. (2001): “Three-dimensional distribution analysis of platinum, palladium and rhodium in auto catalytic converters using imaging-mode laser-induced breakdown spectrometry”, Spectrochimica Acta Part B: Atomic Spectroscopy Volume 56, Issue 2, 177-185
173 Theis, J.R. (1996). An engine Test to Measure the Oxygen Storage Capacity of a Catalyst, SAE paper 961900

174 Lindner, D. Lox, E.S., van Yperen, R., Ostgalt, K. Kreuzer, T. (1996): Reduction of exhaust gas emission by using Pd-based three way catalyst", SAE 960802
175 Kirby C. W. (1997): "Catalytic converter having tri precious metal catalysts", US patent US5593647, 14.01.1997
176 Votsmeier et. Al.: Method for determining the instant at which a nitrogen oxide storage catalyst is switched from the storage phase to the regeneration phase and for diagnosing the storage properties of this catalyst. International Patent WO 2005/078254 A1, 25.8.2005
177 Tuttlies, U., Schmeisser, V. and Eigenberger, G. (2004): "A new simulation model for NOx storage catalyst dynamics", Topics in Catalysis Vols. 30/31, 187-192